frontiers | Research Topics

Emerging swine infectious diseases

Edited by
Tao Lin, Qi Wang, Yanhua Li and Shao-Lun Zhai

Published in
Frontiers in Veterinary Science

ISSN 1664-8714
ISBN 978-2-8325-4237-8
DOI 10.3389/978-2-8325-4237-8

About Frontiers

Frontiers is more than just an open access publisher of scholarly articles: it is a pioneering approach to the world of academia, radically improving the way scholarly research is managed. The grand vision of Frontiers is a world where all people have an equal opportunity to seek, share and generate knowledge. Frontiers provides immediate and permanent online open access to all its publications, but this alone is not enough to realize our grand goals.

Frontiers journal series

The Frontiers journal series is a multi-tier and interdisciplinary set of open-access, online journals, promising a paradigm shift from the current review, selection and dissemination processes in academic publishing. All Frontiers journals are driven by researchers for researchers; therefore, they constitute a service to the scholarly community. At the same time, the *Frontiers journal series* operates on a revolutionary invention, the tiered publishing system, initially addressing specific communities of scholars, and gradually climbing up to broader public understanding, thus serving the interests of the lay society, too.

Dedication to quality

Each Frontiers article is a landmark of the highest quality, thanks to genuinely collaborative interactions between authors and review editors, who include some of the world's best academicians. Research must be certified by peers before entering a stream of knowledge that may eventually reach the public - and shape society; therefore, Frontiers only applies the most rigorous and unbiased reviews. Frontiers revolutionizes research publishing by freely delivering the most outstanding research, evaluated with no bias from both the academic and social point of view. By applying the most advanced information technologies, Frontiers is catapulting scholarly publishing into a new generation.

What are Frontiers Research Topics?

Frontiers Research Topics are very popular trademarks of the *Frontiers journals series*: they are collections of at least ten articles, all centered on a particular subject. With their unique mix of varied contributions from Original Research to Review Articles, Frontiers Research Topics unify the most influential researchers, the latest key findings and historical advances in a hot research area.

Find out more on how to host your own Frontiers Research Topic or contribute to one as an author by contacting the Frontiers editorial office: frontiersin.org/about/contact

Emerging swine infectious diseases

Topic editors

Tao Lin — Biocytogen, United States

Qi Wang — National Agricultural Science and Technology Center, Chinese Academy of Agricultural Sciences, China

Yanhua Li — Yangzhou University, China

Shao-Lun Zhai — Department of Swine Diseases, Institute of Animal Health, Guangdong Academy of Agricultural Sciences, China

Citation

Lin, T., Wang, Q., Li, Y., Zhai, S.-L., eds. (2024). *Emerging swine infectious diseases*. Lausanne: Frontiers Media SA. doi: 10.3389/978-2-8325-4237-8

Table of contents

frontiers | Frontiers in Veterinary Science

TYPE Editorial
PUBLISHED 19 December 2023
DOI 10.3389/fvets.2023.1349844

OPEN ACCESS

EDITED AND REVIEWED BY
Michael Kogut,
United States Department of Agriculture,
United States

*CORRESPONDENCE
Shao-Lun Zhai
zhaishaolun@163.com

†These authors have contributed equally to this work

RECEIVED 05 December 2023
ACCEPTED 07 December 2023
PUBLISHED 19 December 2023

CITATION
Gou H, Zhou X and Zhai S-L (2023) Editorial: Emerging swine infectious diseases.
Front. Vet. Sci. 10:1349844.
doi: 10.3389/fvets.2023.1349844

Editorial: Emerging swine infectious diseases

Hongchao Gou[1,2,3†], Xia Zhou[1,2,3†] and Shao-Lun Zhai[1,2,3*]

[1]Institute of Animal Health, Guangdong Academy of Agricultural Sciences, Guangzhou, China, [2]Guangdong Provincial Key Laboratory of Livestock Disease Prevention, Guangzhou, China, [3]Scientific Observation and Experiment Station of Veterinary Drugs and Diagnostic Techniques of Guangdong Province, Guangzhou, China

KEYWORDS

swine emerging infectious diseases, swine emerging viruses, PCV3, PCV4, swine coronavirus

Editorial on the Research Topic
Emerging swine infectious diseases

1 Introduction

As major threats to the global swine industry, swine infectious diseases caused significant economic losses and potential public health issues. During the past three decades, many swine infectious diseases emerged in the field, such as porcine reproductive and respiratory syndrome virus (PRRSV) and its novel isolates with distinct pathogenicity, high pathogenic variants of porcine epidemic diarrhea virus (PEDV) and pseudorabies virus (PRV) and influenza viruses, which lead to tremendous economic losses worldwide. A few novel pathogens identified recently, such as Senecavirus A, atypical porcine pestivirus (APPV), porcine circovirus 3 (PCV3), porcine circovirus 4 (PCV4), porcine deltacoronavirus (PDCoV), swine acute diarrhea syndrome coronavirus (SADS-CoV), influenza D virus (IDV), constitute a new challenge (1–5). This Research Topic is focused on filling in some gaps of emerging swine infectious diseases from diverse aspects, such as the pathogenesis mechanisms, structure and function of viral proteins, protective immunity, viral evolution, and new approaches for prevention and treatment.

2 Organization of the Research Topic

In this Research Topic, we received 20 manuscripts, nine (seven original research, one perspective, one brief research report) were accepted for publication. Among them, nine papers all involved virus research. Stelder et al. designed an experiment in Romania to quantify which species of mosquitoes are attracted to Romanian backyard pigs, which species take blood meals from these, and whether these observed feeding behaviors vary throughout the vector season. PRRSV has caused huge economic losses for the global pig industry, but its origins and evolution remain a mystery. According to the genome sequences of seven arteriviruses isolated from rodents in 2018, Zhao et al. offered new analysis showing that they may be ancestors of PRRSV. Sanchez et al. used a spatial and spatiotemporal kernel density approach to estimate PRRSV relative risk and utilized a Bayesian spatiotemporal hierarchical model to assess the effects of environmental variables, between-farm movement data and on-farm biosecurity features on PRRSV outbreaks in the United States.

In order to effectively monitor swine coronaviruses, a quadruplex reverse transcription-polymerase chain reaction (RT-PCR) method for the simultaneous detection of PEDV, PDCoV, TGEV and SADS-CoV was developed by Niu et al., and TaqMan probe-based multiplex real-time quantitative reverse transcription-polymerase chain reaction (qRT-PCR) was developed by Li et al.. By systematical analysis of all available full-length genomes of TGEVs (n = 43) and porcine respiratory coronaviruses PRCVs ($n = 7$), Wang et al. showed that TGEVs fell into two independent evolutionary phylogenetic clades, GI and GII. Viruses circulating in China (until 2021) clustered with the traditional or attenuated vaccine strains within the same evolutionary clades (GI). To study the cross-reaction and cross-neutralizing activities of antibodies against different genotypes (G) of E2 glycoproteins, ectodomains of G1.1, G2.1, G2.1d, and G3.4 CSFV E2 glycoproteins from a mammalian cell expression system were generated by Chen et al.. To evaluate the virulence reversion potential risk, rPRRSV-E2 had been continuously passaged *in vivo*, the stability of E2 expression and virulence of the passage viruses were analyzed by Jiang et al.. Sirisereewan et al. investigated the genetic diversity of PCV2 strains circulating in Thailand between 2019 and 2020 using 742 swine clinical samples from 145 farms.

3 Conclusion

Since the July of 2022, The Research Topic began to receive the manuscript submission, and invited more than 24 research teams from the world to submit the manuscript, we finally received 20 manuscripts. Although the Topic provides overviews of some swine emerging pathogen and novel strategies for the detection and control, the manuscripts associated with swine emerging pathogen (especially PCV3, PCV4, IDV) were lacking. In the following work, we hope that more scientists pay more attention to emerging swine infectious diseases.

Author contributions

HG: Writing—original draft. XZ: Writing—original draft. S-LZ: Writing—original draft, Writing—review & editing.

Funding

The author(s) declare financial support was received for the research, authorship, and/or publication of this article. This work was supported by grants from the Key Areas of Research and Development Program of Guangdong, China (2023B0202150001), the Special fund for the 14th Five-Year Plan of Guangdong Province (2022SDZG02), the Project of Collaborative Innovation Center of GDAAS (XTXM202202 and XT202207), the grant from Guangzhou Science and Technology Bureau (202206010192), and the grant from the Department of Agriculture and Rural Affairs of Guangdong Province (2023KJ114 and 2023KJ119).

Conflict of interest

The authors declare that the research was conducted in the absence of any commercial or financial relationships that could be construed as a potential conflict of interest.

The author(s) declared that they were an editorial board member of Frontiers, at the time of submission. This had no impact on the peer review process and the final decision.

Publisher's note

References

1. Woo PC, Lau SK, Lam CS, Lau CC, Tsang AK, Lau JH, et al. Discovery of seven novel Mammalian and avian coronaviruses in the genus deltacoronavirus supports bat coronaviruses as the gene source of alphacoronavirus and betacoronavirus and avian coronaviruses as the gene source of gammacoronavirus and deltacoronavirus. *J Virol.* (2012) 86:3995–4008. doi: 10.1128/JVI.06540-11

2. Hause BM, Ducatez M, Collin EA, Ran Z, Liu R, Sheng Z, et al. Isolation of a novel swine influenza virus from Oklahoma in 2011 which is distantly related to human influenza C viruses. *PLoS Pathog.* (2013) 9:e1003176. doi: 10.1371/journal.ppat.1003176

3. Hause BM, Collin EA, Peddireddi L, Yuan F, Chen Z, Hesse RA, et al. Discovery of a novel putative atypical porcine pestivirus in pigs in the USA. *J Gen Virol.* (2015) 96:2994–8. doi: 10.1099/jgv.0.000251

4. Palinski R, Piñeyro P, Shang P, Yuan F, Guo R, Fang Y, et al. A novel porcine circovirus distantly related to known circoviruses is associated with porcine dermatitis and nephropathy syndrome and reproductive failure. *J Virol.* (2016) 91:e01879–16. doi: 10.1128/JVI.01879-16

5. Zhang HH, Hu WQ, Li JY, Liu TN, Zhou JY, Opriessnig T, et al. Novel circovirus species identified in farmed pigs designated as Porcine circovirus 4, Hunan province, China. *Transbound Emerg Dis.* (2020) 67:1057–61. doi: 10.1111/tbed.13446

frontiers | Frontiers in Veterinary Science

TYPE Original Research
PUBLISHED 08 November 2022
DOI 10.3389/fvets.2022.1033864

OPEN ACCESS

EDITED BY
Yuan Wanzhe,
Agricultural University of Hebei, China

REVIEWED BY
Xiaodu Wang,
Zhejiang Agriculture and Forestry University, China
Mengmeng Zhao,
Foshan University, China

*CORRESPONDENCE
Dong-Sheng He
hedongsheng231@126.com
Shao-Lun Zhai
zhaishaolun@163.com
Rui-Ai Chen
chensa727@scau.edu.cn

†These authors have contributed equally to this work

SPECIALTY SECTION
This article was submitted to Veterinary Infectious Diseases, a section of the journal Frontiers in Veterinary Science

RECEIVED 01 September 2022
ACCEPTED 25 October 2022
PUBLISHED 08 November 2022

CITATION
Niu J-W, Li J-H, Guan J-L, Deng K-H, Wang X-W, Li G, Zhou X, Xu M-S, Chen R-A, Zhai S-L and He D-S (2022) Development of a multiplex RT-PCR method for the detection of four porcine enteric coronaviruses. *Front. Vet. Sci.* 9:1033864. doi: 10.3389/fvets.2022.1033864

Development of a multiplex RT-PCR method for the detection of four porcine enteric coronaviruses

Jia-Wei Niu[1†], Jin-Hui Li[1†], Jin-Lian Guan[1], Ke-Hui Deng[1], Xiu-Wu Wang[1], Gen Li[1], Xia Zhou[2], Min-Sheng Xu[2], Rui-Ai Chen[1,3*], Shao-Lun Zhai[2*] and Dong-Sheng He[1,3*]

[1]Key Laboratory of Zoonosis Prevention and Control of Guangdong Province, College of Veterinary Medicine of South China Agricultural University, Guangzhou, China, [2]Ministry of Agriculture of Rural Affairs, Key Laboratory of Animal Disease Prevention of Guangdong Province, Institute of Animal Health, Guangdong Academy of Agricultural Sciences, Scientific Observation and Experiment Station of Veterinary Drugs and Diagnostic Techniques of Guangdong Province, Guangzhou, China, [3]Zhaoqing Branch Center of Guangdong Laboratory for Lingnan Modern Agricultural Science and Technology, Zhaoqing, China

Porcine enteric coronaviruses are pathogens that cause viral diarrhea in pigs and are widely prevalent worldwide. Moreover, studies have shown that some porcine enteric coronaviruses can infect humans and poultry. In order to effectively monitor these viruses, it is necessary to establish a multiple detection method to understand their prevalence and conduct in-depth research. Common porcine enteric coronaviruses include Porcine epidemic diarrhea virus (PEDV), Porcine transmissible gastroenteritis virus (TGEV), Porcine delta coronavirus (PDCoV), and Swine acute diarrhea syndrome coronavirus (SADS-CoV). Pigs infected with these viruses have the common clinical symptoms that are difficult to distinguish. A quadruplex RT-PCR (reverse transcription-polymerase chain reaction) method for the simultaneous detection of PEDV, PDCoV, TGEV and SADS-CoV was developed. Four pairs of specific primers were designed for the PEDV *M* gene, PDCoV *N* gene, TGEV *S* gene and SADS-CoV *RdRp* gene. Multiplex RT-PCR results showed that the target fragments of PDCoV, SADS-CoV, PEDV and TGEV could be amplified by this method. and the specific fragments with sizes of 250 bp, 368 bp, 616 bp and 801 bp were amplified, respectively. This method cannot amplify any fragment of nucleic acids of Seneca Valley virus (SVV), Porcine Reproductive and Respiratory Syndrome Virus (PRRSV) and Atypical Porcine Pestivirus (APPV), and has good specificity. The lowest detection limits of PDCoV, PEDV, TGEV and SADS-CoV were 5.66×10^5 copies/μL, 6.48×10^5 copies/μL, 8.54×10^5 copies/μL and 7.79×10^6 copies/μL, respectively. A total of 94 samples were collected from pig farms were analyzed using this method. There were 15 positive samples for PEDV, 3 positive samples for mixed infection

of PEDV and PDCoV, 2 positive samples for mixed infection of PEDV and TGEV, and 1 positive sample for mixed infection of PEDV, TGEV, and PDCoV. Multiplex RT-PCR method could detect four intestinal coronaviruses (PEDV, PDCoV, TGEV, and SADS-CoV) in pigs efficiently, cheaply and accurately, which can be used for clinical large-scale epidemiological investigation and diagnosis.

KEYWORDS

porcine epidemic diarrhea virus, porcine deltacoronavirus, porcine transmissible gastroenteritis virus, swine acute diarrhea coronavirus, multiplex RT-PCR

Introduction

Viral diarrhea seriously endangers the pig industry throughout the world, and has been one of the problems that has plagued the breeding industry all over the world. It is characterized by acute diarrhea, vomiting, dehydration and high mortality in neonatal piglets, resulting in enormous economic losses (1–3). The pathogens associated with viral diarrhea disease in piglets are mainly coronaviruses, including TGEV, PEDV, PDCoV, and SADS-CoV (4–9). These swine enteric viruses cause similar clinical symptoms in infected pigs, leading to difficulties in diagnosing diarrhea (10).

PEDV and TGEV are two traditional diarrhea pathogens (11). PEDV and TGEV are both unsegmented single-stranded positive-stranded RNA viruses, and both belong to the order *Nidovirales*, the family *Coronaviridae*, and the genus *alpha-coronavirus* (12). Both of two viruses can cause severe diarrheal disease in affected pigs, and the clinical symptoms are mainly acute and severe watery diarrhea, vomiting and dehydration, but the effect of PEDV on 3–4 weeks old piglets is more obvious. In addition, in farms with poor conditions, PEDV and TGEV usually show a trend of mixed infection, and there is the possibility of co-morbidity.

PDCoV and SADS-CoV are two newly discovered coronaviruses in recent years. PDCoV and SADS-CoV are also unsegmented single-stranded positive-stranded RNA viruses. PDCoV belongs to the order *Nidovirales*, the family *Coronaviridae*, and the genus *delta-coronavirus* (13); SADS-CoV belongs to the order *Nidovirales*, the family *Coronaviridae*, and the genus *alpha-coronavirus*. The clinical symptoms caused by PDCoV and SADS-CoV are similar to those caused by other known porcine enteric coronaviruses (12, 14). In 2012, PDCoV was first reported in Hong Kong. It was detected in the feces of diarrhea piglets and sows in the United States in February 2014. Subsequently, the virus was found in the United States, Canada, South Korea, India and Thailand, showing a trend of widespread global spread (15). More notably, research data since 2017 have revealed cross-species transmission and potential zoonotic diseases of swine δ coronavirus from pigs to humans (16). In 2018, SADS-CoV was first reported in Guangdong, China. At present, a large number of piglets have died, and the virus has also been detected in bats in other parts of Guangdong (14).

There are several serological detecting methods currently available for the detection of viruses, such as the immunofluorescence technique, immunochromatography and indirect immunofluorescence assays, but these techniques are time-consuming and unsuitable for testing large-scale samples. Currently, polymerase chain reaction (PCR), real-time PCR, loop-mediated isothermal amplification (LAMP), and enzyme-linked immunosorbent assay (ELISA) methods have been reported for the detection of these viruses (17), these viruses are highly pathogenic in piglets with immature immune systems and few antibodies, so ELISA is less efficient at detecting these viruses than PCR. However, none of the existing RT-PCR methods can simultaneously distinguish between these four viruses. Therefore, in order to diagnose the pathogens quickly and effectively, it is particularly important to establish a rapid and sensitive detection method for the four viruses (18–20). The multiplex RT-PCR method is to detect and identify multiple pathogens at the same time through one RT-PCR reaction (21, 22). The advantages of this method are that it has a wide range of usage environments, excellent specificity and low price. It is more suitable for rapid diagnosis of mixed infections in epidemics, and provides a rapid and accurate diagnostic method for epidemiological investigations and veterinary clinical diagnosis.

TABLE 1 Primer sequences for TGEV, PEDV, PDCoV, and SADS-CoV.

Primer	Sequence (5′-3′)	Gene	Product size
TGEV–F	GTATGAAGCGTAGTGGTTATGGTC	S	801 bp
TGEV–R	AATAGGTTATGACAGGTTCACAATC		
PEDV–F	TTTCACATGGAATATCATACTGAC	M	616 bp
PEDV–R	ATGAAGCACTTTCTCACTATCTGT		
SADS–F	TCCTGAGGAAGAGGTTGAGATGG	RdRp	368 bp
SADS–R	CGTGCTTACCATTGTGTATGAGAC		
PDCoV–F	AGACACTGAGAAGACGGGTATGG	N	250 bp
PDCoV–R	CTTCTTGTCCTTAGTTGGTTTGGT		

TABLE 2 Types of clinical samples and test results.

Sample	One pathogen positive sample				Two pathogens positive sample		Three pathogens positive sample
	PEDV	PDCoV	TGEV	SADS-CoV	PDCoV/PEDV	TGEV/PEDV	PDCoV/PEDV/TGEV
FEC1	-	-	-	-	-	-	-
FEC2	-	-	-	-	-	-	-
FEC3	-	-	-	-	-	-	-
FEC4	-	-	-	-	-	-	-
FEC5	-	-	-	-	-	-	-
FEC6	-	-	-	-	-	-	-
FEC7	-	-	-	-	-	-	-
FEC8	-	-	-	-	-	-	-
FEC9	-	-	-	-	-	-	-
FEC10	-	-	-	-	-	-	-
FEC11	-	+	-	-	-	-	-
FEC12	-	-	-	-	-	-	-
FEC13	-	-	-	-	-	-	-
FEC14	-	-	-	-	-	-	-
FEC15	-	-	-	-	-	-	-
FEC16	-	-	-	-	-	-	-
FEC17	-	-	-	-	-	+	-
FEC18	-	-	-	-	-	-	-
FEC19	-	-	-	-	-	-	-
FEC20	-	-	-	-	-	-	-
FEC21	-	-	-	-	-	-	-
FEC22	-	-	-	-	-	-	-
FEC23	-	-	-	-	-	-	-
FEC24	-	-	-	-	-	-	-
FEC25	-	-	-	-	-	-	-
FEC26	-	-	-	-	-	-	-
FEC27	-	-	-	-	-	-	-
FEC28	-	-	-	-	-	-	-
FEC29	-	-	-	-	-	-	-
FEC30	-	-	-	-	-	-	-
FEC31	-	-	-	-	-	-	-
FEC32	-	-	-	-	-	-	-
FEC33	-	-	-	-	-	-	+
FEC34	+	-	-	-	-	-	-
FEC35	-	+	-	-	-	-	-
FEC36	-	-	-	-	-	-	-
FEC37	+	-	-	-	-	-	-
FEC38	+	-	-	-	-	-	-
FEC39	+	-	-	-	-	-	-
FEC40	-	+	-	-	-	-	-
FEC41	-	-	-	-	-	-	-
FEC42	-	-	-	-	-	-	-
FEC43	-	-	-	-	-	-	-

(Continued)

TABLE 2 (Continued)

Sample	One pathogen positive sample				Two pathogens positive sample		Three pathogens positive sample
	PEDV	PDCoV	TGEV	SADS-CoV	PDCoV/PEDV	TGEV/PEDV	PDCoV/PEDV/TGEV
FEC44	-	-	-	-	-	-	-
FEC45	-	-	-	-	-	-	-
FEC46	-	-	-	-	+	-	-
FEC47	-	-	-	-	+	-	-
FEC48	-	-	-	-	-	-	-
IS1	-	-	-	-	-	-	-
IS2	-	-	-	-	+	-	-
IS3	-	-	-	-	-	-	-
IS4	-	-	-	-	-	-	-
IS5	-	-	-	-	-	-	-
IS6		-	-	-	-	-	-
IS7	+	-	-	-	-	-	-
IS8	-	-	-	-	-	-	-
IS9	-	-	-	-	-	-	-
IS10	-	-	-	-	-	-	-
IS11	-	-	-	-	-	-	-
IS12	-	-	-	-	-	-	-
IS13	+	-	-	-	-	-	-
IS14	+	-	-	-	-	-	-
IS15	-	-	-	-	-	-	-
IS16	+	-	-	-	-	-	-
IS17	-	-	-	-	-	-	-
IS18	-	-	-	-	-	-	-
IS19	+	-	-	-	-	-	-
IS20	-	-	-	-	-	-	-
IS21	+	-	-	-	-	-	-
IS22	+	-	-	-	-	-	-
IS23	-	-	-	-	-	+	-
IS24	-	-	-	-	-	-	-
IS25	-	-	-	-	-	-	-
IS26	-	-	-	-	-	-	-
IS27	-	-	-	-	-	-	-
IS28	-	-	-	-	-	-	-
IS29	+	-	-	-	-	-	-
IS30	-	-	-	-	-	-	-
FEC31	-	-	-	-	-	-	-
FEC32	-	-	-	-	-	-	-
FEC33	-	-	-	-	-	-	-
FEC34	-	-	-	-	-	-	-
FEC35	-	-	-	-	-	-	-
FEC36	-	-	-	-	-	-	-
FEC37	-	-	-	-	-	-	-
FEC38	-	-	-	-	-	-	-

(Continued)

TABLE 2 (Continued)

Sample	One pathogen positive sample				Two pathogens positive sample		Three pathogens positive sample
	PEDV	PDCoV	TGEV	SADS-CoV	PDCoV/PEDV	TGEV/PEDV	PDCoV/PEDV/TGEV
FEC39	-	-	-	-	-	-	-
FEC40	-	-	-	-	-	-	-
FEC41	+	-	-	-	-	-	-
FEC42	-	-	-	-	-	-	-
FEC43	-	-	-	-	-	-	-
FEC44	-	-	-	-	-	-	-
FEC45	+	-	-	-	-	-	-
FEC46	+	-	-	-	-	-	-

Results: "+": Positive; "–": Negative.
Sample types: FEC, Feces specimens; IS, intestine specimens.

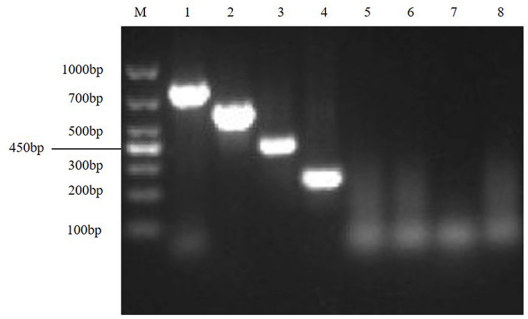

FIGURE 1
Establishment of monoplex RT-PCR reactions for TGEV, PEDV, SADS-CoV and PDCoV. This figure shows the results of monoplex PCR reactions of TGEV, PEDV, SADS-CoV and PDCoV. Among them, lane M is DNA Marker DL1000, lanes 1–4 represent the monoplex RT-PCR results of TGEV, PEDV, SADS-CoV and PDCoV, respectively; lanes 5–8 represent the negative controls of TGEV, PEDV, SADS-CoV, and PDCoV, respectively.

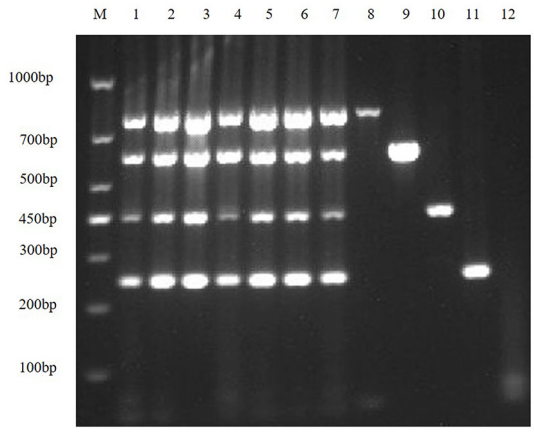

FIGURE 2
Optimize multiplex RT-PCR annealing temperature. This figure shows the optimization results of multiplex RT-PCR annealing temperature, lane M is DNA Marker DL1000, lanes 1–7 represent 7 temperature gradients of 53, 54, 55, 56, 57, 58, 59 °C; lanes 8–11 are the positive controls for TGEV, PEDV, SADS-CoV and PDCoV, respectively; lane 12 is the negative control.

Materials and methods

Construction of plasmid standards

Before establishing the multiplex RT-PCR assay, the single-plex RT-PCR method for each virus was established using the cDNA of each virus as a template. According the following program: 95 °C for 5 min; 95 °C for 30 s, 55 °C for 30 s, 72 °C 1 min for 30 cycles; 72 °C for 10 min. Multiplex RT-PCR consists of the following components: 10 × Buffer, dNTPs (2.5 mM), TaKaRa Taq (5 U/μL), RNAse-free ddH2O, primers and cDNA. Then, these amplified target fragments of were then individually cloned into the pMD19-T vector. Sequencing confirmed that the recombinant plasmids pMD-19-T-PEDV, pMD-19-T-TGEV, pMD-19-T-SADS-CoV and pMD-19-T-PDCoV contained the target fragments.

RNA extraction and reverse transcription

Samples positive for TGEV, PEDV, PDCoV, and SADS-CoV were stored in our laboratory. Clinical samples collected from were stored at −80°C. Then, samples were mixed with supernatant by vortexing and collected after centrifugation at 12,000 × g at 4 °C for 15 min. Viral nucleic acids were extracted using the Viral DNA/RNA Kit (Hangzhou Bioer

Technology Co. Ltd), and the Reverse Transcriptase M-MLV (RNase H-) was used to perform reverse transcription following the manufacturer's instructions.

Primer sequences

TGEV, PEDV, PDCoV and SADS-CoV sequences available in GenBank were analyzed to improve the detection performance of primers. Finally, we designed primers with PEDV *M* gene, PDCoV *N* gene, TGEV *S* gene and SADS-CoV *RdRp* gene as conserved genes. Specific primers for the construction of plasmid standards were designed using primer 5 (Version 5.00) (Table 1).

Reaction condition optimization for multiplex RT-PCR

The optimization was performed on a Biometra TOne 96G PCR instrument based on the following program: 95 °C 5 min; 95 °C 30 s, 55 °C 30 s, 72 °C 1 min 30 cycles; 72 °C 10 min. Multiplex RT-PCR consists of the following components: 10 × Buffer, dNTPs (2.5 mM), TaKaRa Taq (5 U/μL), RNAse-free ddH_2O, primers and positive plasmids for TGEV, PEDV, PDCoV and SADS-CoV. To obtain the best amplification efficiency, the multiple reaction system was optimized by using different concentrations of primers, dNTPs (2.5 mM) and TaKaRa Taq (5 U/μL), and different annealing temperatures.

Sensitivity of the multiplex RT-PCR assay

To analyze the sensitivity of established multiplex RT-PCR, standard plasmids for TGEV, PEDV, SADS-CoV, and PDCoV prepared above were mixed. Then, the mix was diluted by 10 gradients with RNAse-free ddH_2O. The initial concentrations of the four standard plasmids were 8.54 × 10^9 copies/μL, 6.48 × 10^9 copies/μL, 7.79 × 10^9 copies/μL, and 5.66 × 10^9 copies/μL, respectively. The susceptibility of multiplex RT-PCR to the four viruses was assessed using the diluted plasmids as templates.

Specificity of the quadruplex RT-PCR assay

The specificity of multiplex RT-PCR was assessed. RNA was extracted from positive samples of PRRSV, Atypical swine fever virus (APPV), Seneca valley virus (SVV), TGEV, PEDV, PDCoV and SADS-CoV preserved in our laboratory, and the RNA was reverse transcribed into cDNA. Multiplex RT-PCR amplifications were performed using cDNA from these viruses and RNAse-free water as templates.

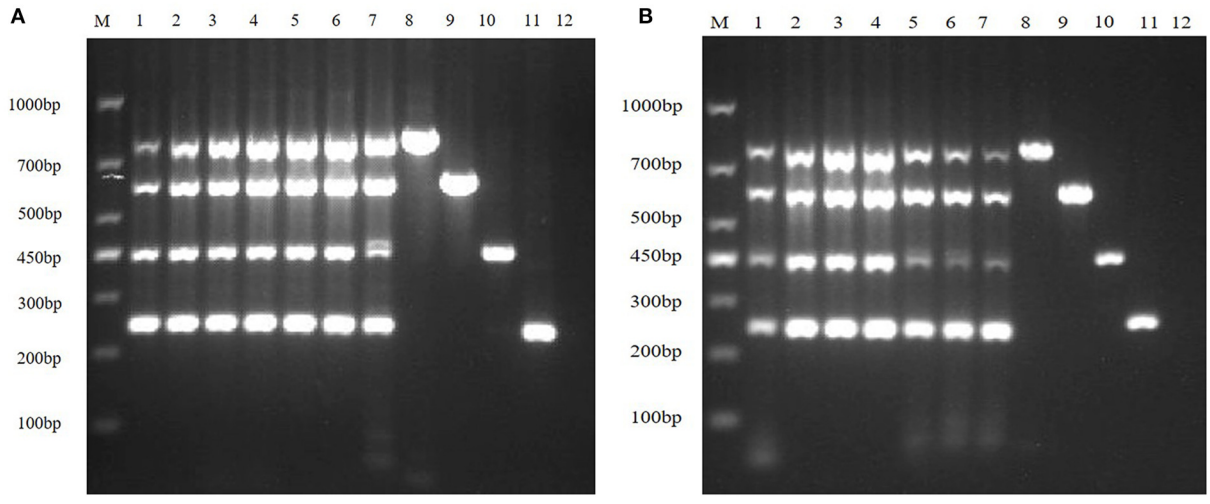

FIGURE 3
Optimizing the concentrations of TaKaRa Taq and dNTPs. **(A)** The optimized electrophoresis result of the optimal TaKaRa Taq concentration; lane M is DNA Marker DL1000, lanes 1–7 represent 0.02 U/μL, 0.04 U/μL, 0.06 U/μL, 0.08 U/μL, 0.10 U/μL, 0.12 U/μL, 0.16 U/μL; Lanes 8–11 are positive controls for TGEV, PEDV, SADS-CoV and PDCoV, respectively; and lane 12 is negative control. **(B)** The electrophoresis result of the optimal dNTPs concentration in multiplex RT-PCR; wherein, lane M is DNA Marker DL1000, and lanes 1–7 represent 0.10, 0.15, 0.20, 0.25, 0.30, 0.35, and 0.40 mM, respectively; lanes 8–11 are positive controls for TGEV, PEDV, SADS-CoV, and PDCoV, respectively; and lane 12 is a negative control.

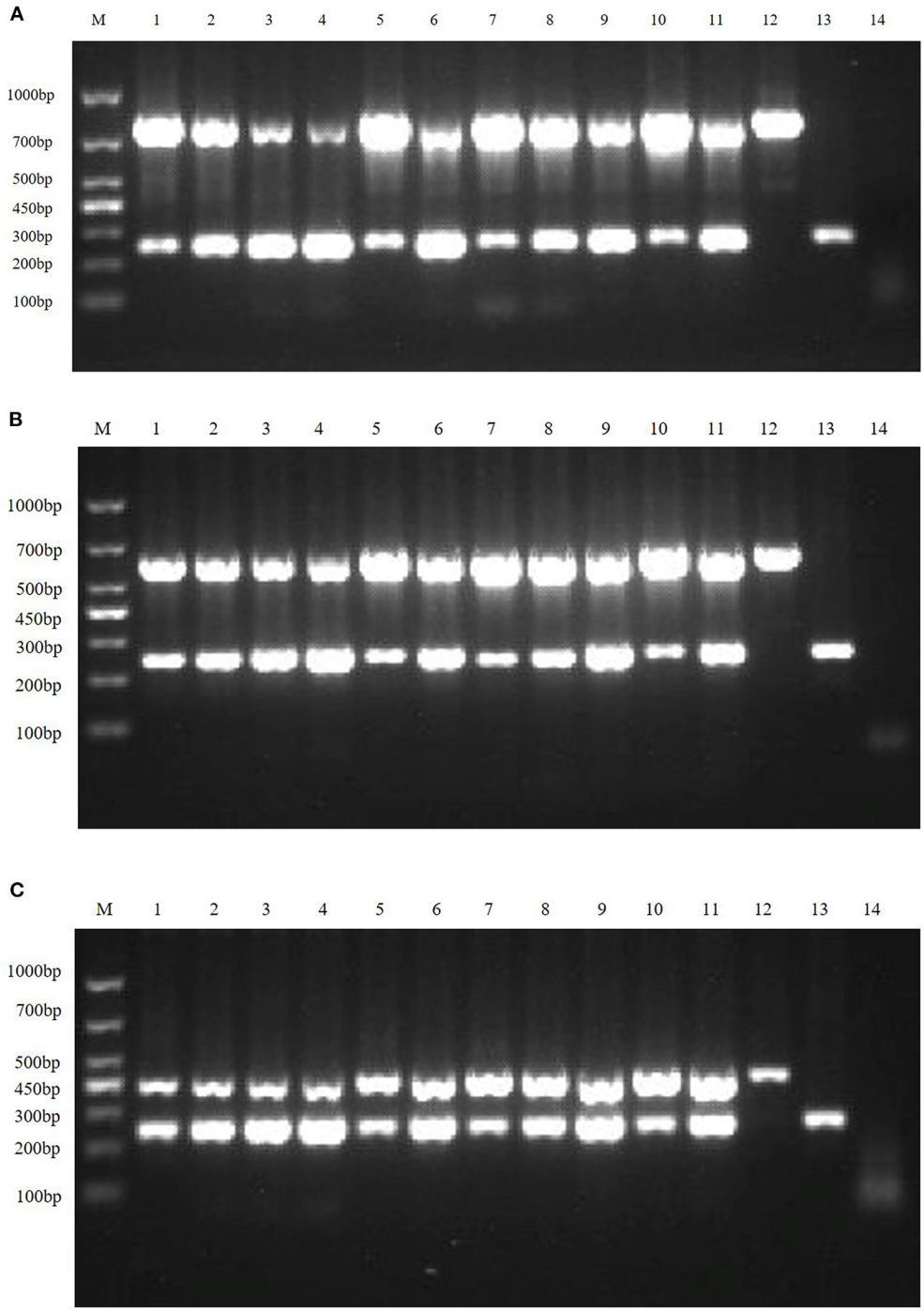

FIGURE 4
Multiplex RT-PCR primers optimization. **(A)** is the electrophoresis results of TGEV and PDCoV duplex RT-PCR with different primer ratios; lane M is DNA Marker DL1000; Lanes 1–11 are the primer ratios of 1: 1, 1: 2, 1: 3, 1: 4, 2: 1, 2: 3, 3: 1, 3: 2, 3: 4, 4: 1, 4: 3; Lanes 12–13 are the positive controls for TGEV and PDCoV; and lane 14 is the negative control. **(B)** The electrophoresis results of PEDV and PDCoV duplex RT-PCR with different primer ratios; lane M is DNA Marker DL1000; Lanes 1–11 are the primer ratios of 1: 1, 1: 2, 1: 3, 1: 4, 2: 1, 2: 3, 3: 1, 3: 2, 3: 4, 4: 1, 4: 3; Lanes 12–13 are the positive controls for PEDV and PDCoV; and lane 14 is the negative control. **(C)** The electrophoresis results of SADS-CoV and PDCoV duplex RT-PCR with different primer ratios; lane M is DNA Marker DL1000; Lanes 1–11 are the primer ratios of 1: 1, 1: 2, 1: 3, 1: 4, 2: 1, 2: 3, 3: 1, 3: 2, 3: 4, 4: 1, 4: 3; Lanes 12–13 are the positive controls for PEDV and PDCoV; and lane 14 is the negative control.

Reproducibility test of the multiplex RT-PCR assay

In this experiment, 10^6 copies/μL recombinant plasmid standard was selected and mixed in equal proportions. The stability and repeatability of the quadruple RT-PCR method were verified by seven repeated tests.

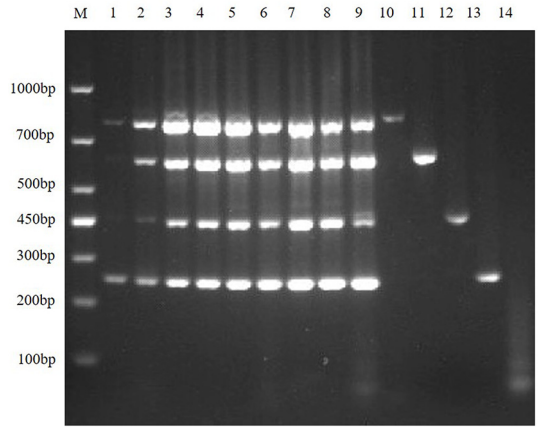

FIGURE 5
Primer concentration electrophoresis results of multiplex RT-PCR of TGEV, PEDV, SADS-CoV, and PDCoV. Lane M is DNA Marker DL1000, lanes 1–9 represent the concentration combination of nine primers in the fixed ratio (3:3:3:4) of TGEV, PEDV, SADS-CoV, and PDCoV; lanes 10–13 represent the positive control of TGEV, PEDV, SADS-CoV, and PDCoV; lane 14 was negative control.

Detection in clinical samples

Ninety four clinical samples (Table 2) collected from pig farms in Guangdong province from 2021 to 2022 were detected. All samples were diluted three-fold with phosphate buffered saline (PBS) using a vortexer and incubated at 4000 ×g for 15 min at 4°C. Total RNA from clinical samples was extracted by the above method. The supernatant was collected and

TABLE 4 Primer concentration combinations at constant ratios.

Experimental group	TGEV (μM)	PEDV (μM)	SADS-CoV (μM)	PDCoV (μM)	Primer ratio
1	0.03	0.03	0.03	0.04	3:3:3:4
2	0.06	0.06	0.06	0.08	3:3:3:4
3	0.09	0.09	0.09	0.12	3:3:3:4
4	0.12	0.12	0.12	0.16	3:3:3:4
5	0.15	0.15	0.15	0.20	3:3:3:4
6	0.18	0.18	0.18	0.24	3:3:3:4
7	0.24	0.24	0.24	0.32	3:3:3:4
8	0.27	0.27	0.27	0.36	3:3:3:4
9	0.30	0.30	0.30	0.40	3:3:3:4

TABLE 3 Ratio of duplex RT-PCR primers combination.

Experimental group	PEDV (μM)	PDCoV (μM)	TGEV (μM)	PDCoV (μM)	SADS-CoV (μM)	PDCoV (μM)	Primer ratio
1	0.20	0.20	0.20	0.20	0.20	0.20	1:1
2	0.20	0.40	0.20	0.40	0.20	0.40	1:2
3	0.20	0.60	0.20	0.60	0.20	0.60	1:3
4	0.20	0.80	0.20	0.80	0.20	0.80	1:4
5	0.40	0.20	0.40	0.20	0.40	0.20	2:1
6	0.40	0.60	0.40	0.60	0.40	0.60	2:3
7	0.60	0.20	0.60	0.20	0.60	0.20	3:1
8	0.60	0.40	0.60	0.40	0.60	0.40	3:2
9	0.60	0.80	0.60	0.80	0.60	0.80	3:4
10	0.80	0.20	0.80	0.20	0.80	0.20	4:1
11	0.80	0.20	0.80	0.20	0.80	0.20	4:3
12	0.20	0	0.20	0	0.20	0	P_1^+
13	0	0.20	0	0.20	0	0.20	P_2^+
14	0.20	0.20	0.20	0.20	0.20	0.20	N

P (positive) represents positive, N (negative) represents negative; P^{1+} represents a positive control for PEDV, TGEV and SADS-CoV; P^{2+} represents the positive control for PDCoV, and N represents the negative control for the ratio of the two primer pairs.

used for RNA extraction and prepared as cDNA using reverse transcription. Then, all cDNA were detected using multiplex RT-PCR of this study. The results of clinical samples detected by the quadruple RT-PCR were repeatedly verified by conventional single RT-PCR to compare the coincidence rate of the two detection methods.

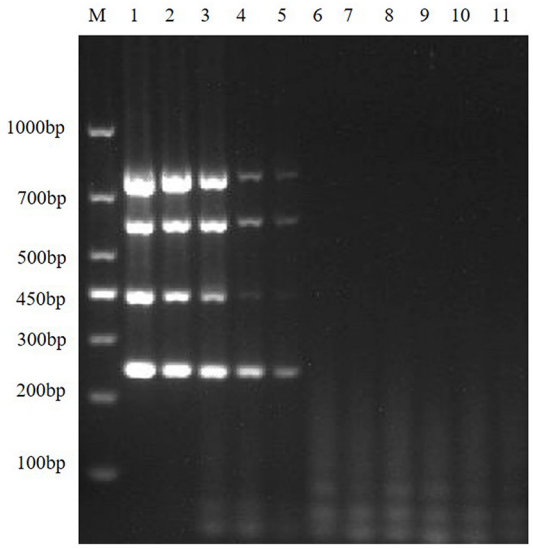

FIGURE 6
Sensitivity of the multiplex RT-PCR assay. This figure shows the results of sensitivity analysis of multiplex RT-PCR for TGEV, PEDV, SADS-CoV and PDCoV. Lane M is DNA Marker DL1000; lanes 1–10 represent the results of TGEV, PEDV, SADS-CoV, and PDCoV mixed plasmids diluted in a gradient of 10^{0}-10^{-9}, with a total of 10 template dilutions; lane 11 is a negative control.

Results

Establishment of monoplex RT-PCR reactions for TGEV, PEDV, SADS-CoV and PDCoV

The results showed that TGEV, PEDV, SADS-CoV and PDCoV showed specific amplification at 801, 616, 368, 263, and 250 bp. The reaction did not produce other miscellaneous bands, indicating that the primer set has good reliability and

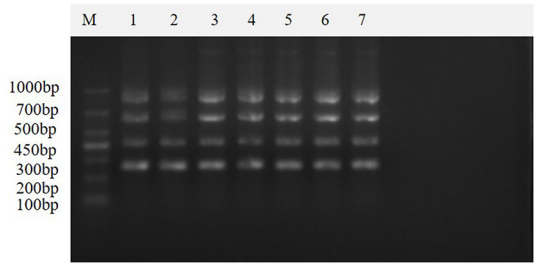

FIGURE 8
Repeatability of the multiplex real-time PCR assay. This figure shows the results of the repeatability assay of this method, which shows that the method is stable and reproducible. Lane M is DNA Marker DL1000; lanes 1–7 are the results of repeated experiments.

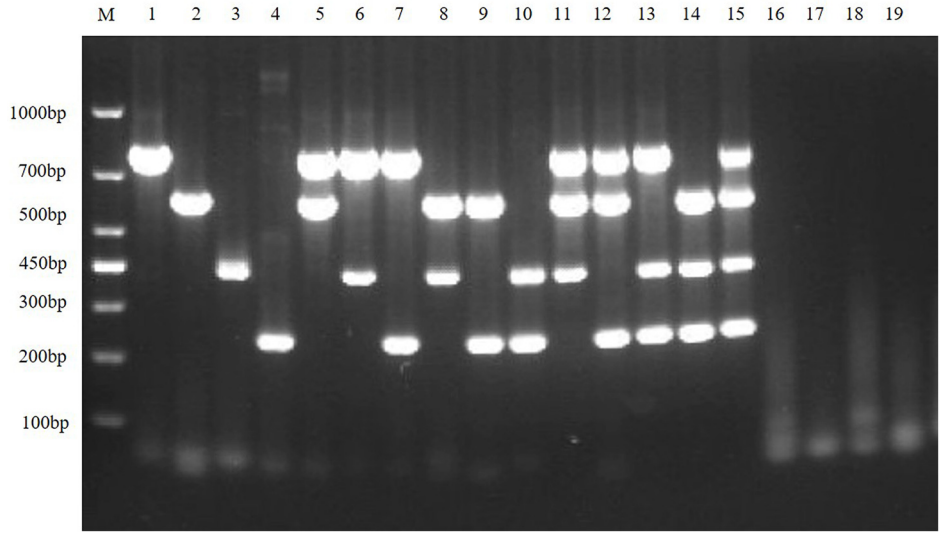

FIGURE 7
Specificity of the multiplex RT-PCR assay. This figure is the specificity analysis result of multiplex RT-PCR of TGEV, PEDV, SADS-CoV and PDCoV; lane M is DNA Marker DL1000, lanes 1–4 represent the monoplex RT-PCR specificity of TGEV, PEDV, SADS-CoV, and PDCoV, respectively; lanes 5–10 represent the duplex RT-PCR specificity of TGEV, PEDV, SADS-CoV and PDCoV, respectively; lanes 11–14 represent the triplex RT-PCR specificity of TGEV, PEDV, SADS-CoV, and PDCoV, respectively; lane 15 represents the quadruplex RT-PCR specificity of TGEV, PEDV, SADS-CoV, and PDCoV, respectively; lanes 16–19 represent SVA, PRRSV, and APPV, respectively; and lane 20 is the negative control.

10.3389/fvets.2022.1033864

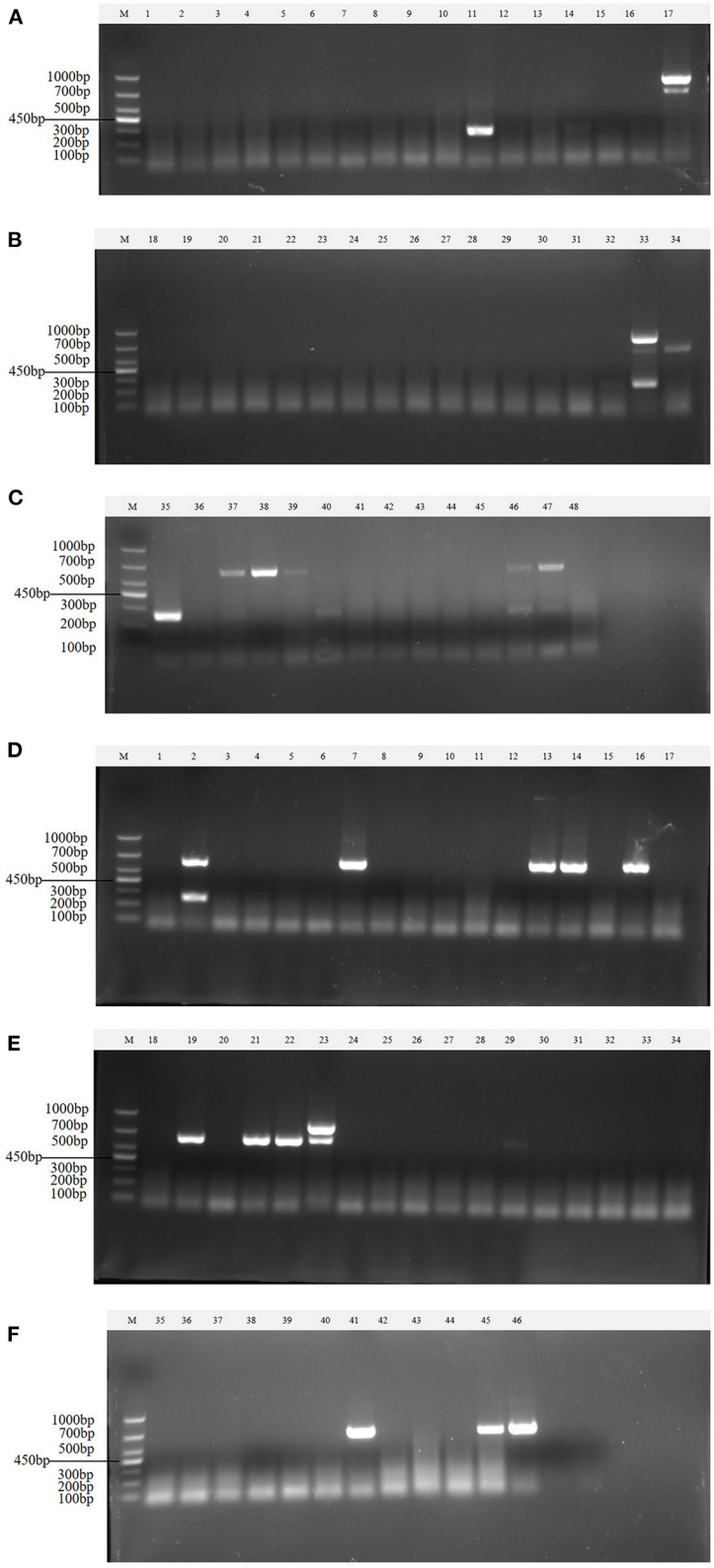

FIGURE 9
Detection in clinical samples. **(A–F)** The agarose gel electrophoresis pattern of the results of 94 clinical samples tested by multiplex RT-PCR. There were 15 positive samples for PEDV, 3 positive samples for mixed infection of PEDV and PDCoV, 2 positive samples for mixed infection of PEDV and TGEV, and 1 positive sample for mixed infection of PEDV, TGEV and PDCoV.

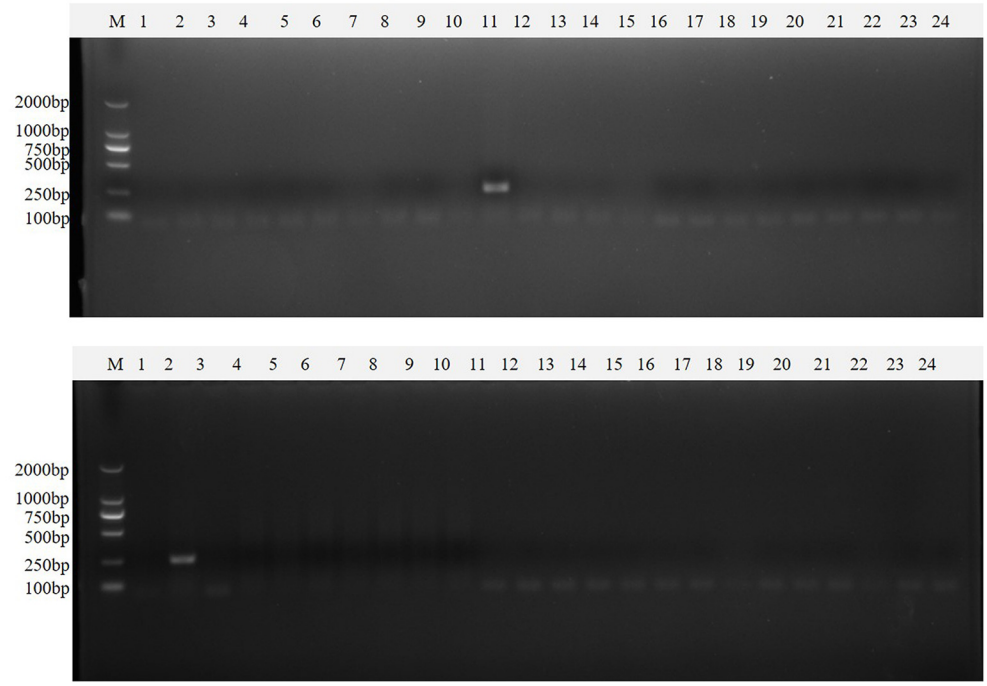

FIGURE 10
Single PT-PCR was used to verify the results of clinical samples. PDCoV **(A–C)** 1–24, PDCoV **(A–C)** 25–48, PDCoV **(D–F)** 1–24, and PDCoV **(D–F)** 25–46 represent agarose gel electrophoresis patterns of single RT-PCR recheck results of clinical samples tested for PDCoV; PEDV **(A–C)** 1–24, PEDV **(A–C)** 25–48, PEDV **(D–F)** 1–24 and PEDV **(D–F)** 25–46 represent agarose gel electrophoresis patterns of single RT-PCR recheck results of clinical samples tested for PEDV; SADS-CoV **(A–C)** 1–24, SADS-CoV **(A–C)** 25–48, SADS-CoV **(D–F)** 1–24 and SADS-CoV **(D–F)** 25–46 represent agarose gel electrophoresis patterns of single RT-PCR recheck results of clinical samples tested for SADS-CoV; TGEV **(A–C)** 1–24, TGEV **(A–C)** 25–48, TGEV **(D–F)** 1–24 and TGEV **(D–F)** 25–46 represent agarose gel electrophoresis patterns of single RT-PCR recheck results of clinical samples tested for TGEV.

specificity. And the accuracy of the amplified product was further confirmed by sequencing analysis (Figure 1).

Optimization of the multiplex reaction system

Optimize multiplex RT-PCR annealing temperature

First, the optimal annealing temperatures for monoplex RT-PCR primers for TGEV, PEDV, SADS-CoV and PDCoV were determined. Then, referring to the optimal annealing temperature of monoplex RT-PCR, and designing seven temperature gradients from 53 to 59°C. Finally, the optimal annealing temperature of multiplex RT-PCR is 55°C (Figure 2).

Optimizing the concentrations of TaKaRa Taq and DNTPs

In order to improve amplification efficiency, the optimal TaKaRa Taq concentration and the optimal dNTPs concentration were obtained by gradient RT-PCR amplification. The result of agarose gel electrophoresis showed that the optimal TaKaRa Taq concentration (Figure 3A) and the optimal dNTPs concentration (Figure 3B) for multiplex RT-PCR of TGEV, PEDV, SADS-CoV and PDCoV were 0.1 U/μL and 0.25 mM, respectively.

Multiplex RT-PCR primers optimization

Then, according to the analysis of the double RT-PCR optimization results, the final concentrations of the optimal primer combinations for each double RT-PCR are respectively: TGEV and PDCoV were 0.24 μM: 0.32 μM (3: 4) (Figure 4A); PEDV and PDCoV were 0.24 μM: 0.32 μM (3: 4) (Figure 4B); SADS-CoV and PDCoV were 0.24 μM: 0.32 μM (3:4) (Figure 4C, Table 3). Final primer concentrations were optimized by quadruplex RT-PCR reactions, ranging from 0.03 μM to 0.4 μM. The optimal final concentrations of primers were 0.24, 0.24, 0.24, 0.32 μM (3:3:3:4) (TGEV, PEDV, SADS-CoV, PDCoV) (Figure 5). Therefore, a primer concentration ratio of 3:3:3:4(TGEV, PEDV, SADS-CoV, PDCoV) was used as a standard to optimize primer concentrations for quadruplex PCR (Table 4).

Sensitivity of the multiplex RT-PCR assay

In order to explore the LOD of the multiplex RT-PCR method, the positive recombinant plasmids of TGEV, PEDV,

TABLE 5 Results of clinical samples detected by the multiplex RT-PCR.

Pathogens	Singleplex RT-PCR			Multiplex RT-PCR			Coincidence rate (%)
	Sample number	Positive	Percentage (%)	Sample number	Positive	Percentage (%)	
PEDV	94	15	15.96	94	15	15.96	100
TGEV	94	0	0	94	0	0	100
PDCoV	94	4	4.26	94	4	4.26	100
SADS-CoV	94	0	0	94	0	0	100
PEDV+TGEV	94	2	2.13	94	2	2.13	100
PEDV+PDCoV	94	3	3.19	94	3	3.19	100
PEDV+PDCoV+TGEV	94	1	1.06	94	1	1.06	100

SADS-CoV and PDCoV were mixed, the standard plasmids were diluted in a gradient of 10^9-10^0, and use the diluted mixture as templates for RT-PCR amplification. The results showed that the sensitivities of multiplex RT-PCR to TGEV, PEDV, SADS-CoV and PDCoV were 8.54×10^5 copies/μL, 6.48×10^5 copies/μL, 7.79×10^6 copies/μL and 5.66×10^5 copies/μL, respectively (Figure 6).

Specificity of the multiplex RT-PCR assay

To exclude potential false-positive results caused by other viruses that may be present in the sample, the quadruplex RT-PCR detection method was used to detect other virus-positive samples stored in our laboratory, including SVA, PRRSV, and APPV. The results showed that the multiplex RT-PCR method had well specificity (Figure 7).

Reproducibility test of the multiplex RT-PCR assay

The results of seven repeated tests showed (Figure 8) that clear and uniform bands could be amplified in all seven tests, indicating that the method was stable and reproducible.

Clinical sample detection

Clinical samples were evaluated using the method established in this study, 94 samples collected from pig farms to validate their performance in clinical applications. After identification, there were 15 positive samples for PEDV, three positive samples for mixed infection of PEDV and PDCoV, 2 positive samples for mixed infection of PEDV and TGEV, and 1 positive sample for mixed infection of PEDV, TGEV and PDCoV (Figure 9). The coincidence rate of the multiplex RT-PCR assay and the conventional single RT-PCR assay in the detection of clinical samples was 100% (Table 5, Figure 10).

Discussion

Porcine viral diarrhea is widespread in the world and spreads rapidly, causing huge economic losses to the global swine industry. These enteroviruses can cause vomiting, diarrhea, and dehydration in infected pigs. In severe cases, a large number of piglets died and the damage was very serious (22). These enteroviruses have similar characteristics after infecting pigs and require laboratory testing to differentiate them. In addition, there are often mixed infections in clinical cases, which brings challenges to the prevention, control and treatment (2). Therefore, establishing a detection method for simultaneous detection of multiple pathogens will greatly improve the diagnosis and prevention and control of swine diarrheal diseases.

Diarrheal virus infection causes diarrhea, high mortality in piglets. Common porcine enteric coronaviruses include TGEV, PEDV, PDCoV, and the SADS-CoV (23, 24) could seriously endanger the development of the pig industry, especially in terms of newborn piglets. The symptoms caused by the above mentioned four viruses are similar, so it is difficult to determine the causative pathogen in clinical diagnosis. Moreover, relatively few studies examine newly-epidemic diseases. Therefore, a rapid, specific, and low-cost detection method is sorely needed for the surveillance of diarrhea viruses.

In recent years, traditional monoplex RT-PCR methods, multiplex RT-PCR methods and multiplex RT-qPCR methods targeting conserved regions have been established for some viruses (21, 24, 25). RT-qPCR-based methods have the disadvantages of high cost and high instrument requirements, and many laboratories cannot obtain relatively expensive qPCR machines. Traditional monoplex RT-PCR requires multiple tests to determine the final result, and the process is cumbersome. The multiplex RT-PCR adds multiple pairs of primers to the same RT-PCR reaction system to detect multiple target genes at the same time, which improves the detection efficiency, and has the sensitivity and specificity of a single RT-PCR; compared with qPCR, it is extensively used, and inexpensive. Therefore, we developed multiplex RT-PCR to detect and differentially diagnose four diarrheal viruses in swine herds. In this study, a multiplex RT-PCR assay was established. For the best amplification efficiency, the final concentrations of multiple pairs of primers, TaKaRa Taq enzyme and dNTP Mixture in the reaction system were optimized, and the annealing temperature of the reaction program was optimized

(21). Compared with traditional monoplex PCR primers, four viruses can be detected in a single reaction. The specificity of this method showed that each pair of primers could only detect the target gene itself, but could not detect the non-specific fragment. The sensitivity results showed that the samples with the mixture of four kinds of positive plasmid still had excellent sensitivity.

According to the virus detection and source analysis of positive samples in this study, the results show that PEDV, TGEV, and PDCoV are still the main causes of pig diarrhea in South China, which is consistent with previous research results (26). Porcine viral diarrheal disease may be caused by a single virus or a combination of multiple viruses, and coinfection of porcine enteroviruses has been reported to be common in pig farm. The results of these clinical samples confirmed the cases of mixed infection of the viruses in pigs. During the epidemiological investigation, our laboratory found that among mixed infections, the co-infection rate of PEDV and PDCoV was the highest at 9.39%, followed by PEDV and SADS-CoV at 7.18% (24). Epidemiological surveys showed that SADS-CoV was only found in Guangdong and Fujian provinces, and not in other areas. Therefore, it is necessary to strengthen the surveillance of SADS-CoV to prevent its spread to other areas. The latest research shows that coronaviruses can spread across species. According to research, mixed infection may lead to recombination between viruses and changes in virus virulence. This highlights the importance of identifying multiple viral infections simultaneously.

In conclusion, the established multiplex RT-PCR method has excellent specificity, well detection efficiency and can be applied to laboratory diagnosis, epidemiological research and monitoring of SADS-CoV, TGEV, PEDV, and PDCoV. In addition, the established method can be applied to the clinical differential diagnosis of clinical mixed infection, and realize the early diagnosis of clinical cases.

Data availability statement

The original contributions presented in the study are included in the article/supplementary material, further inquiries can be directed to the corresponding author.

Author contributions

D-SH, S-LZ, and R-AC were involved in the experimental design and provided guidance on the experimental operation. J-WN, J-HL, J-LG, K-HD, X-WW, GL, XZ, and M-SX performed the experiments and data analysis. All authors contributed to writing the manuscript and have read and approved the final version of the manuscript.

Funding

This study was supported by the following grants: Key Laboratory of Zoonosis Prevention and Control of Guangdong Province (No. P20211154-0302), the Guangdong Province Pig Industrial System Innovation Team (No. 2018LM1103), Key-Area R&D Program of GuangDong Province (No. 2021B0707010009), Major Program of Zhaoqing Branch Center of Guangdong Laboratory for Lingnan Modern Agricultural Science and Technology (No. P20211154-0101), Guangdong Department of Science and Technology (No. 2020B0202080004), Guangzhou Science and Technology Bureau (Nos. 202103000096 and 202206010192), Guangdong Provincial Science and Technology Planning Project (No. P20211154-030), and the grant (No. 2021TDQD002) from Maoming Branch Center of Guangdong Laboratory for Lingnan Modern Agricultural Science and Technology.

Conflict of interest

The authors declare that the research was conducted in the absence of any commercial or financial relationships that could be construed as a potential conflict of interest.

Publisher's note

References

1. Zhang J, Tsai YL, Lee PY, Chen Q, Zhang Y, Chiang CJ, et al. Evaluation of two singleplex reverse transcription-Insulated isothermal PCR tests and a duplex real-time RT-PCR test for the detection of porcine epidemic diarrhea virus and porcine deltacoronavirus. *J Virol Methods*. (2016) 234:34–42. doi: 10.1016/j.jviromet

2. Liu Q, Wang HY. Porcine enteric coronaviruses: an updated overview of the pathogenesis, prevalence, and diagnosis. *Vet Res Commun*. (2021) 45:75–86. doi: 10.1007/s11259-021-09808-0

3. Sun L, Tang Y, Yan K, Chen H, Zhang H. Inactivated Pseudomonas PE(ΔIII) exotoxin fused to neutralizing epitopes of PEDV S proteins produces a specific immune response in mice. *Anim Dis*. (2021) 1:22. doi: 10.1186/s44149-021-00021-9

4. Niederwerder MC, Hesse RA. Swine enteric coronavirus disease: a review of 4 years with porcine epidemic diarrhoea virus and porcine deltacoronavirus in the United States and Canada. *Transbound Emerg Dis*. (2018) 65:660–75. doi: 10.1111/tbed.12823

5. Wang H, Qin Y, Zhao W, Yuan T, Yang C, Mi X, et al. Genetic characteristics and pathogenicity of a novel porcine deltacoronavirus southeast asia-like strain found in China. *Front Vet Sci.* (2021) 8:701612. doi: 10.3389/fvets.2021.701612

6. Puente H, Argüello H, Mencía-Ares Ó, Gómez-García M, Rubio P, Carvajal A. Detection and genetic diversity of porcine coronavirus involved in diarrhea outbreaks in spain. *Front Vet Sci.* (2021) 8:651999. doi: 10.3389/fvets.2021.651999

7. Yuan D, Yan Z, Li M, Wang Y, Su M, Sun D. Isolation and characterization of a porcine transmissible gastroenteritis coronavirus in Northeast China. *Front Vet Sci.* (2021) 8:611721. doi: 10.3389/fvets.2021.611721

8. Guo YY, Wang PH, Pan YQ, Shi RZ Li YQ, Guo F, et al. The characteristics of Spike glycoprotein gene of swine acute diarrhea syndrome coronavirus strain CH/FJWT/2018 isolated in China. *Front Vet Sci.* (2021) 8:687079. doi: 10.3389/fvets.2021.687079

9. Wang L, Su S, Bi Y, Wong G, Gao GF. Bat-origin coronaviruses expand their host range to pigs. *Trends Microbiol.* (2018) 26:466–70. doi: 10.1016/j.tim.2018.03.001

10. Wang Q, Vlasova AN, Kenney SP, Saif LJ. Emerging and re-emerging coronaviruses in pigs. *Curr Opin Virol.* (2019) 34:39–49. doi: 10.1016/j.coviro.2018.12.001

11. Jung K, Saif LJ, Wang Q. Porcine epidemic diarrhea virus (PEDV): an update on etiology, transmission, pathogenesis, and prevention and control. *Virus Res.* (2020) 286:198045. doi: 10.1016/j.virusres.2020.198045

12. Zhou Z, Qiu Y, Ge X. The taxonomy, host range and pathogenicity of coronaviruses and other viruses in the Nidovirales order. *Anim Dis.* (2021) 1:5. doi: 10.1186/s44149-021-00005-9

13. Zhao Y, Qu H, Hu J, Fu J, Chen R, Li C, et al. Characterization and pathogenicity of the porcine deltacoronavirus isolated in Southwest China. *Viruses.* (2019) 11:1074. doi: 10.3390/v11111074

14. Yang YL Yu JQ, Huang YW. Swine enteric alphacoronavirus (swine acute diarrhea syndrome coronavirus): an update three years after its discovery. *Virus Res.* (2020) 285:198024. doi: 10.1016/j.virusres.2020.198024

15. Duan C. An updated review of porcine deltacoronavirus in terms of prevalence, pathogenicity, pathogenesis and antiviral strategy. *Front Vet Sci.* (2022) 8:811187. doi: 10.3389/fvets.2021.811187

16. Callebaut P, Pensaert MB, Hooyberghs J. A competitive inhibition ELISA for the differentiation of serum antibodies from pigs infected with transmissible gastroenteritis virus (TGEV) or with the TGEV-related porcine respiratory coronavirus. *Vet Microbiol.* (1989) 20:9–19. doi: 10.1016/0378-1135(89)90003-5

17. Zhai SL, Sun MF, Zhang JF, Zheng C, Liao M. Spillover infection of common animal coronaviruses to humans. *Lancet Microbe.* (2022) S2666-5247(22)00198-7. doi: 10.1016/S2666-5247(22)00198-7

18. Lednicky JA, Tagliamonte MS, White SK, Elbadry MA, Alam MM, Stephenson CJ, et al. Emergence of porcine delta-coronavirus pathogenic infections among children in Haiti through independent zoonoses and convergent evolution. *medRxiv.* (2021) 25:2021.03.19.21253391. doi: 10.1101/2021.03.19.21253391

19. Boley PA, Alhamo MA, Lossie G, Yadav KK, Vasquez-Lee M, Saif LJ, et al. Porcine deltacoronavirus infection and transmission in poultry, United States1. *Emerg Infect Dis.* (2020) 26:255–65. doi: 10.3201/eid2602.190346

20. Luo Y, Chen Y, Geng R, Li B, Chen J, Zhao K, et al. Broad cell tropism of SADS-CoV in vitro implies its potential cross-species infection risk. *Virol Sin.* (2021) 36:559–63. doi: 10.1007/s12250-020-00321-3

21. Ding G, Fu Y, Li B, Chen J, Wang J, Yin B, et al. Development of a multiplex RT-PCR for the detection of major diarrhoeal viruses in pig herds in China. *Transbound Emerg Dis.* (2020) 67:678–85. doi: 10.1111/tbed.13385

22. Turlewicz-Podbielska H, Pomorska-Mól M. Porcine Coronaviruses: overview of the state of the art. *Virol Sin.* (2021) 36:833–51. doi: 10.1007/s12250-021-00364-0

23. Bevins SN, Lutman M, Pedersen K, Barrett N, Gidlewski T, Deliberto TJ, et al. Spillover of swine coronaviruses, United States. *Emerg Infect Dis.* (2018) 24:1390–92. doi: 10.3201/eid2407.172077

24. Si G, Niu J, Zhou X, Xie Y, Chen Z, Li G, et al. Use of dual priming oligonucleotide system-based multiplex RT-PCR assay to detect five diarrhea viruses in pig herds in South China. *AMB Express.* (2021) 11:99. doi: 10.1186/s13568-021-01255-z

25. Huang X, Chen J, Yao G, Guo Q, Wang J, Liu G. A TaqMan-probe-based multiplex real-time RT-qPCR for simultaneous detection of porcine enteric coronaviruses. *Appl Microbiol Biotechnol.* (2019) 103:4943-4952. doi: 10.1007/s00253-019-09835-7

26. Li ZL, Zhu L, Ma JY, Zhou QF, Song YH, Sun BL, et al. Molecular characterization and phylogenetic analysis of porcine epidemic diarrhea virus (PEDV) field strains in south China. *Virus Genes.* (2012) 45:181–5. doi: 10.1007/s11262-012-0735-8

frontiers | Frontiers in Veterinary Science

TYPE Original Research
PUBLISHED 04 January 2023
DOI 10.3389/fvets.2022.1046263

OPEN ACCESS

EDITED BY
Shao-Lun Zhai,
Guangdong Academy of Agricultural Sciences, China

REVIEWED BY
Edward D. Walker,
Michigan State University, United States
John Bosco Keven,
University of California, Irvine, United States

*CORRESPONDENCE
Jonno Jorn Stelder
✉ jonno.stelder@sund.ku.dk

SPECIALTY SECTION
This article was submitted to Veterinary Infectious Diseases, a section of the journal Frontiers in Veterinary Science

RECEIVED 16 September 2022
ACCEPTED 08 December 2022
PUBLISHED 04 January 2023

CITATION
Stelder JJ, Mihalca AD, Olesen AS, Kjær LJ, Boklund AE, Rasmussen TB, Marinov M, Alexe V, Balmoş OM and Bødker R (2023) Potential mosquito vector attraction to- and feeding preferences for pigs in Romanian backyard farms.
Front. Vet. Sci. 9:1046263.
doi: 10.3389/fvets.2022.1046263

Potential mosquito vector attraction to- and feeding preferences for pigs in Romanian backyard farms

Jonno Jorn Stelder[1]*, Andrei Daniel Mihalca[2], Ann Sofie Olesen[3], Lene Jung Kjær[1], Anette Ella Boklund[1], Thomas Bruun Rasmussen[3], Mihai Marinov[4], Vasile Alexe[4], Oana Maria Balmoş[2] and René Bødker[1]

[1]Section for Animal Welfare and Disease Control, Department of Veterinary and Animal Sciences, Copenhagen University, Copenhagen, Denmark, [2]Department of Parasitology and Parasitic Diseases, University of Agricultural Sciences and Veterinary Medicine of Cluj-Napoca, Cluj-Napoca, Romania, [3]Department of Virus and Microbiological Special Diagnostics, Statens Serum Institut, Copenhagen, Denmark, [4]Department of Biodiversity Conservation and Sustainable Use of Natural Resources, Danube Delta National Institute for Research and Development, Tulcea, Romania

Introduction: Mosquitoes either biologically or mechanically transmit various vector-borne pathogens affecting pigs. Mosquito species display a wide variety of host preference, as well as host attraction and behaviours. Mosquito species attraction rates to- and feeding rates on pigs or other potential hosts, as well as the seasonal abundance of the mosquito species affects their pathogen transmission potential.

Methods: We caught mosquitoes in experimental cages containing pigs situated in Romanian backyard farms. The host species of blood meals were identified with PCR and sequencing.

Results: High feeding preferences for pigs were observed in *Aedes vexans* (90%), *Anopheles maculipennis* (80%) and *Culiseta annulata* (72.7%). However, due to a high abundance in the traps, *Culex pipiens/torrentium* were responsible for 37.9% of all mosquito bites on pigs in the Romanian backyards, despite low feeding rates on pigs in the cages (18.6%). We also found that other predominantly ornithophilic mosquito species, as well as mosquitoes that are already carrying a blood meal from a different (mammalian) host, were attracted to backyard pigs or their enclosure.

Discussion: These results indicate that viraemic blood carrying, for instance, African swine fever virus, West-Nile virus or Japanese encephalitis virus could be introduced to these backyard pig farms and therefore cause an infection, either through subsequent feeding, via ingestion by the pig or by environmental contamination.

KEYWORDS

blood meal, african swine fever virus, mechanical transmission, west-nile virus, japanese encephalitis virus, insect vectors

1. Introduction

Flying hematophagous insects that are known to feed on wild boar and domestic pigs have been described as vectors of a wide variety of pathogens (1–4), with some of these affecting pigs (Suidae) (5). In terms of vector-borne transmission of pathogens, two distinct mechanisms are described, namely biological- and mechanical transmission (6). With biological transmission, a pathogen is able to replicate within the body of a vector before it is delivered to a new host, whereas with mechanical transmission, the pathogen cannot replicate and is eventually digested or shed, thus requiring transmission to a new host while still infectious (6). An example of pathogens transmitted by biological vector transmission is Japanese encephalitis virus [mosquitoes (7)], while examples of pathogens transmitted by mechanical vector transmission are porcine reproductive and respiratory syndrome (8), Ross River Virus [mosquitoes (9)], *Mycoplasma suis* [mosquitoes and *Stomoxys calcitrans* (10)], and classical swine fever [mosquitoes (11), *S. calcitrans* (12), and tabanids (13)].

Mosquitoes can act as vectors between vertebrate species for pathogens of increasing societal concern. Mosquitoes infected with West-Nile virus (WNV) or Japanese encephalitis virus (JEV) after feeding on an infected bird can act as bridge-vectors to pigs (7, 14, 15), and pigs can then act as important amplification hosts for the virus (5). As different mosquito species can show varying host preferences (16), it is necessary to determine the host-preferences of each mosquito species to evaluate its transmission potential for various pathogens.

Hematophagous insects are potential mechanical vectors of African swine fever virus (ASFV) (17), and in the Baltic countries a seasonal pattern is observed in outbreaks in domestic pigs coinciding with the summer peak abundance pattern observed in many hematophagous insect species (18, 19). Various studies suggest that mechanical transmission by vectors can occur in an experimental setting (20), for instance through ingestion (21), environmental contamination (22) or subsequent blood feeding (23), and may occur in a natural setting (24, 25). Insect species frequently attracted to, and feeding on, pigs are particularly interesting when exploring the risk of introducing pathogens to domestic pig farms by contaminated insects. Other studies have indicated that ASFV contaminated trucks (26) or professional farm visitors (27) could be a source of ASFV introduction to commercial pig farms, although the exact transmission mechanism behind these two risk factors is not yet fully understood. From this, we can hypothesise that the introduction of viraemic blood into a pig farm through hematophagous insects, if carrying a sufficient viral load, could potentially cause an outbreak. It is therefore important to identify which hematophagous insect species would potentially feed on an ASFV infected pig host outside of a farm, before they could be attracted to domestic pigs and thus introduce virus into a pig farm.

Studies show that throughout the vector season in Europe (in Sweden, Italy and the Netherlands), *Culex* spp. are significantly more abundant than any other mosquito genus, particularly *Culex pipiens*, while *Aedes* spp. also takes up a significant proportion of the total number of mosquitoes throughout the year (28). Differences in overall abundance are important as, while host preferences can vary between species (29), it is not necessarily the species with the strongest preference towards a certain host that is the most relevant in terms of vector potential of a certain pathogen (14, 30).

Spread of pathogens by hematophagous insects could be influenced by differences in seasonal activity patterns, species abundance, locality, host-diversity or host-preference, insect species size, digestion as well as reproductive behaviour and strategies. We designed an experiment in Romania to quantify which species of mosquitoes are attracted to Romanian backyard pigs, which species take blood meals from these, and whether these observed feeding behaviours vary throughout the vector season. The findings from this experiment could provide more evidence for the introduction of pathogens in blood meals by flying vectors.

2. Methodology

We selected two backyard pig farm locations in Tulcea County (Somova and Sălcioara, Southeast Romania, GPS coordinates: 45°11′41"N 28°38′52"E & 44°47′57"N 28°53′49"E) and another two in Satu Mare County (Ambud and Odoreu, Northwest Romania, GPS coordinates: 47°45′59"N 22°56′22"E & 47°47′54"N 22°58′59"E) (Figure 1). We selected the specific localities based on availability and suitability for our experimental purposes, as well as there being ASFV outbreaks in these regions.

2.1. Cages and pigs

Domestic pigs were kept outside in modified dog puppy cages (~120 cm height × 160 cm length × 160 cm depth) fitted with fine stainless-steel mesh (mesh size: 0.6 mm) sheets on the walls and fine mesh on the roof. For this, we obtained an animal experiment ethical permit, registration number: 216, issued 12-06-2020 by the Bioethics Commission of USAMV Cluj-Napoca, Romania. We conducted animal care and maintenance in accordance with EU legislation on animal experimentation (EU Directive 2010/63/EU). We applied an

entry-trap design, which allowed flying insects to fly into the cages through a ∼5 cm cage-wide slit on two sides of the cages (Figure 2). In each of the 4 locations, we kept 2 pigs weighing between 7.5 and 10 kg each at the onset of their respective sampling period.

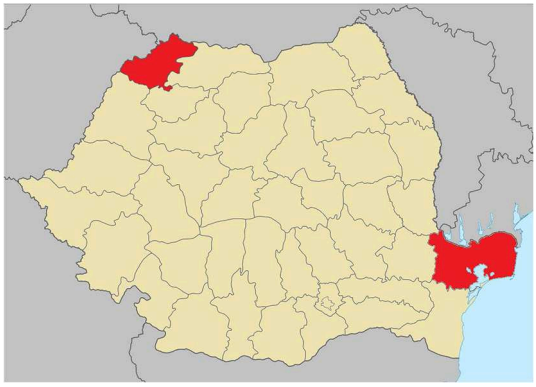

FIGURE 1
Map of Romania with Satu Mare County (locations Ambud and Odoreu) highlighted in red in the Northwest and Tulcea County (locations Somova and Sălcioara) highlighted in red in the Southeast.

FIGURE 2
One of the pig cages used in the experiment (pigs not yet included). The entry trap slit can be seen on the front right panel. Collectors entered the cage through a small door, as can be seen on the front left panel, by carefully opening it and closing it immediately upon entry, so no insects would fly out.

2.2. BG-Pro traps

In each of the 4 locations, we also set up a BG-Pro mosquito trap (BioGents AG). We baited each of these traps with CO_2 (0.5 kg of CO_2 per 24 h) and BG-Lure mosquito attractants (which emit lactic- and caproic acid as well as ammonia). We placed the traps within the vicinity of the cages to catch mosquitoes continuously throughout the season, and we collected the mosquitoes once a week. These 7-day catches allowed us to quantify abundance of mosquitoes as well as correlate it to the proportion of mosquitoes with pig blood in mosquitoes collected from the pig cages.

2.3. Sampling periods

We carried out sampling during June to October 2021. For the cages, we aimed at 3 sampling periods of 4 weeks each, whereas the BG-Pro mosquito traps ran continuously throughout the study. For each sampling period, we replaced the pigs with new pigs, leading to 24 pigs in total during the study. The first collection period started on the 14th of June 2021 and ended on the 7th of July. In Satu Mare, the start of the second period was delayed due to logistical issues and the collection was extended beyond the original collection schedule for this period from the 16th of August until the 8th of September. In Tulcea, the second collection period started on the 1st of August and was also extended until the 8th of September to align with the collections in Satu Mare. The third collection period in both regions started on the 20th of September and ended on the 13th of October 2021.

2.4. Sampling procedure

We cleaned the cages once per week, after which we placed the mesh roofs on top of the cages, which indicated the start of that week's collection. We entered the cages 24 h later. Using aspirators, we collected all hematophagous insects present inside the cages and stored them at −20°C. Another 24 h later, we would repeat this process, after which we removed the roofs of the cages for the remainder of the week. For each of the four locations, we therefore had two 24 h consecutive collections of hematophagous insects from the cages per week for a total of 12 weeks.

2.5. Species identification

In the high containment laboratory (OIE3/4, BSL2) at Statens Serum Institut (Denmark), we identified each sample from the cages to species level using the Moskeytool identification tool

(https://www.medilabsecure.com/moskeytool.html). We then visually screened each mosquito for the presence of a blood meal according to the Sella score (1–7) where Sella score 1 and 7 indicate no blood in the abdomen, and Sella score 2–6 indicates varying amounts of blood present (31).

Due to large numbers of mosquitoes collected in the BG-Pro traps, we subsampled collections when necessary and identified the mosquitoes only to genus level. We subsampled collections using a divider in a Petri dish until a single subsample contained <350 mosquitoes. We then extrapolated the results from the selected subsample to the original sample. We did not screen these mosquitoes any further or analyse them for the presence of blood meals.

2.6. Lab procedure

After species identification, we placed each mosquito with blood in the abdomen (Sella score between 2 and 6) individually in a 1.5 ml Eppendorf tube and added 1 ml MagNA Pure Lysis/Binding Buffer (Roche). We homogenised the samples using two 3 mm stainless steel beads (Dejay Distribution Ltd.) in a TissueLyser II (Qiagen) for 3 min at 25 Hz, after which we centrifuged the sample homogenates for 2 min at 10.000 RCF to collect supernatants for nucleic acid extraction. We purified the nucleic acids from the homogenised sample supernatants as previously described by Olesen et al. (32) and analysed for the presence of a porcine blood meal (i.e. MT-CYTB from Suidae) applying a TaqMan assay (33) using the CFX Opus Real-Time PCR System (BioRad). We determined a positive result (Suid blood present) in this qPCR by identification of the threshold cycle value (Cq) at which FAM dye emission appeared above background within 35 cycles.

Samples testing negative for porcine blood were tested using the TaqMan assay (No Cq value or Cq value above 35) for the presence of a mammalian blood meal (i.e. MT-CYTB of mammalian origin) using a Resolight (Roche) approach with primer sequences obtained from Andrejevic et al. (34), with minor modifications. The slightly modified primer sequences were 5′ GACGGCCAGTGAAACAGGATCCAACAACCC 3′ (forward) and 5′ GCTATGACCGGTGTAGTTGTCTGGGTCTCC 3′ (reverse). We performed the amplification using the CFX Opus Real-Time PCR System (Bio-Rad). We determined a positive result (mammalian blood present) in this qPCR by identification of the Cq value at which SYBR dye emission appeared above background within 30 cycles. We chose this threshold of 30 based on prior validation using templates of different mammalian, avian and invertebrate origin. During this validation, samples with Cq values above 30 were of avian and invertebrate origin.

We selected samples in which we detected a blood meal of mammalian origin, using the mammalian MT-CYB assay, for Sanger sequencing. For sequencing, we purified PCR products using the GeneJET PCR Purification Kit (Thermo Scientific) according to the manufacturer's instructions. We performed cycle sequencing of the PCR products using the Veriti^{TM} 96-Well Thermal Cycler (Applied Biosystems). We performed the sequencing of the reverse and forward strand using 10 μM of the primers and the BigDye Terminator v. 1.1. Cycle Sequencing Kit (Applied BioSystems). For capillary electrophoresis, we purified the sequencing products using the SigmaSpin Post-Reaction columns (Sigma-Aldrich). We carried out capillary electrophoresis out using an ABI3500 Genetic Analyzer (Applied BioSystems). Ultimately, we analysed the results using Sequence Scanner Software v1.0 (Applied BioSystems) and the blood meal source identified using BLAST (https://blast.ncbi.nlm.nih.gov/Blast.cgi).

3. Results

In total, we identified 356 mosquitoes and 1 tabanid from the cages in the 4 locations. From the Satu Mare region, this includes 204 mosquitoes from Ambud and 96 mosquitoes from Odoreu, while from the Tulcea region this includes 38 mosquitoes and 1 tabanid samples from Sălcioara and 18 mosquito samples from Somova. Unfortunately, some of the samples from Tulcea turned unidentifiable upon arrival to the high containment laboratory, as unforeseen leakage of a number of sample containers in the same shipment necessitated use of decontamination (disinfection) upon arrival to the laboratory. This caused disinfectant to seep into some of the containers. This caused the mosquitoes inside 12 out of 20 (60%) 24 h collections from Sălcioara and 15 out of 20 (75%) 24 h collections from Somova to become unidentifiable, while it was still possible to count the numbers of mosquitoes in most collections excluding 6 collections from Somova, where we estimated the numbers visually.

From the Tulcea region (Somova and Sălcioara), and in particular Somova, we caught larger numbers of mosquitoes in the cages throughout the experiment, compared to the Satu Mare region (Ambud and Odoreu) (Figure 3). We can also see that mosquito activity likely already started prior to the start of the experiment due to the high numbers already observed in week 24. Activity gradually declined, particularly in the Tulcea region, until there were only more or less sporadic catches left after week 36.

3.1. Mosquito species feeding on pigs

Of the 356 mosquito (and 1 tabanid) samples that we successfully identified, a total of 130 showed visual traces of blood meals (Table 1). Of these, 116 (89.2%) tested positive for porcine blood (Cq values from 22.5 to 34.8 in the Suid

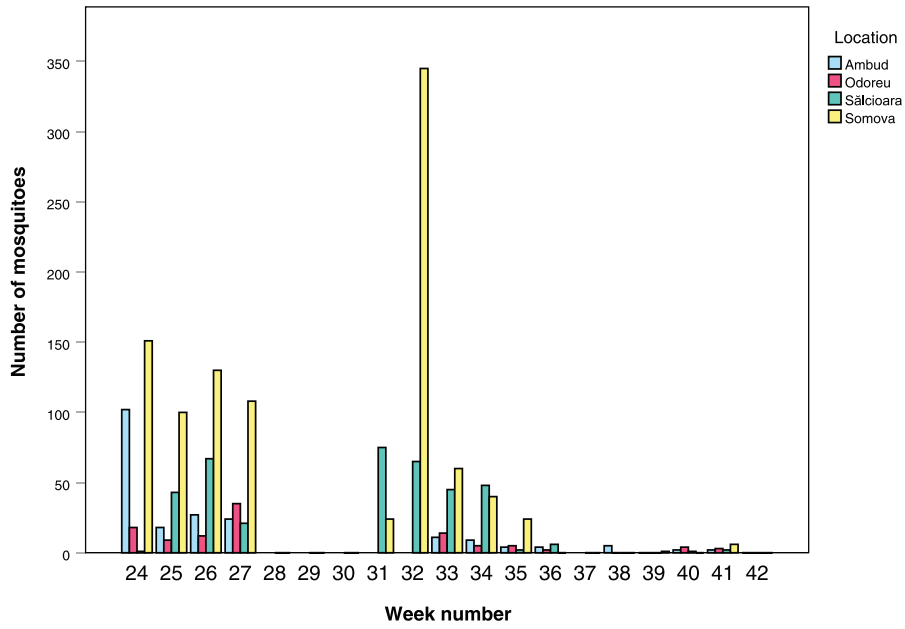

FIGURE 3
Number of mosquitoes caught inside the pig cages per week for all four locations. Note that there were no pigs inside the cages, and thus no collections, in week 28, 29, 30 (+ 31, 32 for Satu Mare's Ambud and Odoreu locations) and week 37.

assay). Upon testing for the presence of mammalian blood in the remaining 14 mosquito samples, one *Aedes caspius* caught in Sălcioara tested positive for bovine blood (*Bos taurus*) (Cq-value of 29 in the mammalian assay,). The remaining 13 samples tested negative for any mammalian blood in the analysis, despite the visual trace of blood. The one horsefly tested negative for any blood.

While only 18.6% of the collected *Culex pipiens/torrentium* carried a porcine blood meal (44 out 236), this species still constituted the largest number of mosquitoes carrying pig blood due to their high abundance (44 positive *Culex pipiens/torrentium* out of 116 positive mosquitoes in total, or 37.9%) (Table 1). Among the other species of which we caught at least five specimen, *Aedes vexans* (18 out of 20, i.e. 90 or 15.5% of all porcine blood meals), *Anopheles maculipennis* (12 out of 15, i.e. 80 or 10.3% of all porcine blood meals) and *Culiseta annulata* (16 out of 22, i.e. 72.7 or 13.8% of all porcine blood meals) showed the highest proportions feeding on domestic pig. These four species combined comprised 77.5% of all porcine blood meals. Other (non-sporadic, i.e. >5) species were *Aedes geniculatus* (12 out of 25, i.e. 48 or 10.3% of all porcine blood meals), and *Aedes caspius* (8 out of 24, i.e. 33.3 or 6.9% of all porcine blood meals). Note that *Aedes caspius* was only caught in cages from the Tulcea region.

3.2. Seasonality vs. proportion of mosquitoes with pig blood

We plotted the overall mosquito seasonal abundance data from our subsampled BG-Pro trap collections for each genera together with the number of mosquitoes with pig blood in the cages (Figure 4). *Culex* spp. was significantly more abundant than the other genera. Collections tended to be more numerous in Odoreu compared to Ambud for all genera. Overall, vector seasonal abundance increased the first 2 weeks from the onset of our BG-Pro trap collections and decreased towards the end of the collection period to almost zero. While peak activity in Ambud occurred in week 32 and 33 for all genera, both *Aedes* spp. and *Culex* spp. activity peaked in week 27 in Odoreu, while *Culiseta* spp. peak activity was later in week 31.

For all four mosquito genera and for both Ambud and Odoreu, we tested for a correlation between the seasonal abundance (i.e. BG-Pro trap results) and the proportion of blood fed mosquitoes of that genus in our cages using Spearman's correlation test. None of these tests found a significant correlation between seasonal abundance and the proportion of mosquitoes having fed on pigs.

TABLE 1 Overview of the number of mosquitoes and horseflies (*N*) caught in the pig cages of each species in total and per location, as well as the number (Npos) and percentage (%pos) of porcine-blood PCR positive samples per species.

		Location																		
						Satu Mare								Tulcea						
		Total				Ambud				Odoreu				Sălcioara				Somova			
Genus	Species	*N*	Npos	%pos	Σpos	*N*	Npos	%pos	Σpos	*N*	Npos	%pos	Σpos	*N*	Npos	%pos	Σpos	*N*	Npos	%pos	Σpos
Aedes	*caspius*	24	8	33.3	6.9	0	0	0	0	0	0	0	0	15	8	53.3	47.1	9	0	0	0
	flavescens	1	1	100	0,9	0	0	0	0	0	0	0	0	1	1	100	5.9	0	0	0	0
	geniculatus	25	12	48	10.3	11	6	54.5	9.2	13	5	38.5	17.2	1	1	100	5.9	0	0	0	0
	riparius	1	0	0	0	0	0	0	0	0	0	0	0	1	0	0	0	0	0	0	0
	vexans	20	18	90	15.5	16	15	93.8	23.1	4	3	75	10.3	0	0	0	0	0	0	0	0
Anopheles	*hyrcanus*	4	2	50	1.7	0	0	0	0	0	0	0	0	3	2	66.7	11.8	1	0	0	0
	maculipennis s.l.	15	12	80	10.3	4	4	100	6.2	2	2	100	6.9	2	1	50	5.9	7	5	71.4	100
	plumbeus	2	1	50	0.9	1	1	100	1.5	0	0	0	0	1	0	0	0	0	0	0	0
Culex	*modestus*	4	2	50	1.7	0	0	0	0	4	2	50	6,9	0	0	0	0	0	0	0	0
	pipiens/ torrentium	236	44	18.6	37.9	169	37	21.9	56.9	53	3	5.7	10.3	14	4	28.6	23.5	0	0	0	0
Culiseta	*annulata*	22	16	72.7	13.8	3	2	66.7	3.1	19	14	73.7	48.3	0	0	0	0	0	0	0	0
	longiareolata	1	0	0	0	0	0	0	0	1	0	0	0	0	0	0	0	0	0	0	0
	morsitans	1	0	0	0	0	0	0	0	0	0	0	0	0	0	0	0	1	0	0	0
Haematopota	*pluvialis/ subcylindrica*	1	0	0	0	0	0	0	0	0	0	0	0	1	0	0	0	0	0	0	0
Total		357	116	32.5	100	204	65	31.9	100	96	29	30.2	100	39	17	43.6	100	18	5	27.8	100

Σpos indicates the percentage that each species contributes to the total number of porcine-blood PCR positive samples, in total as well as per location. Mosquitoes without visual blood in abdomen (Sella score of 1 and 7) have been excluded from PCR-analysis. The *Haematopota pluvialis/subcylindrica* could not be Sella scored, but was still included for PCR-analysis.

10.3389/fvets.2022.1046263

10.3389/fvets.2022.1046263

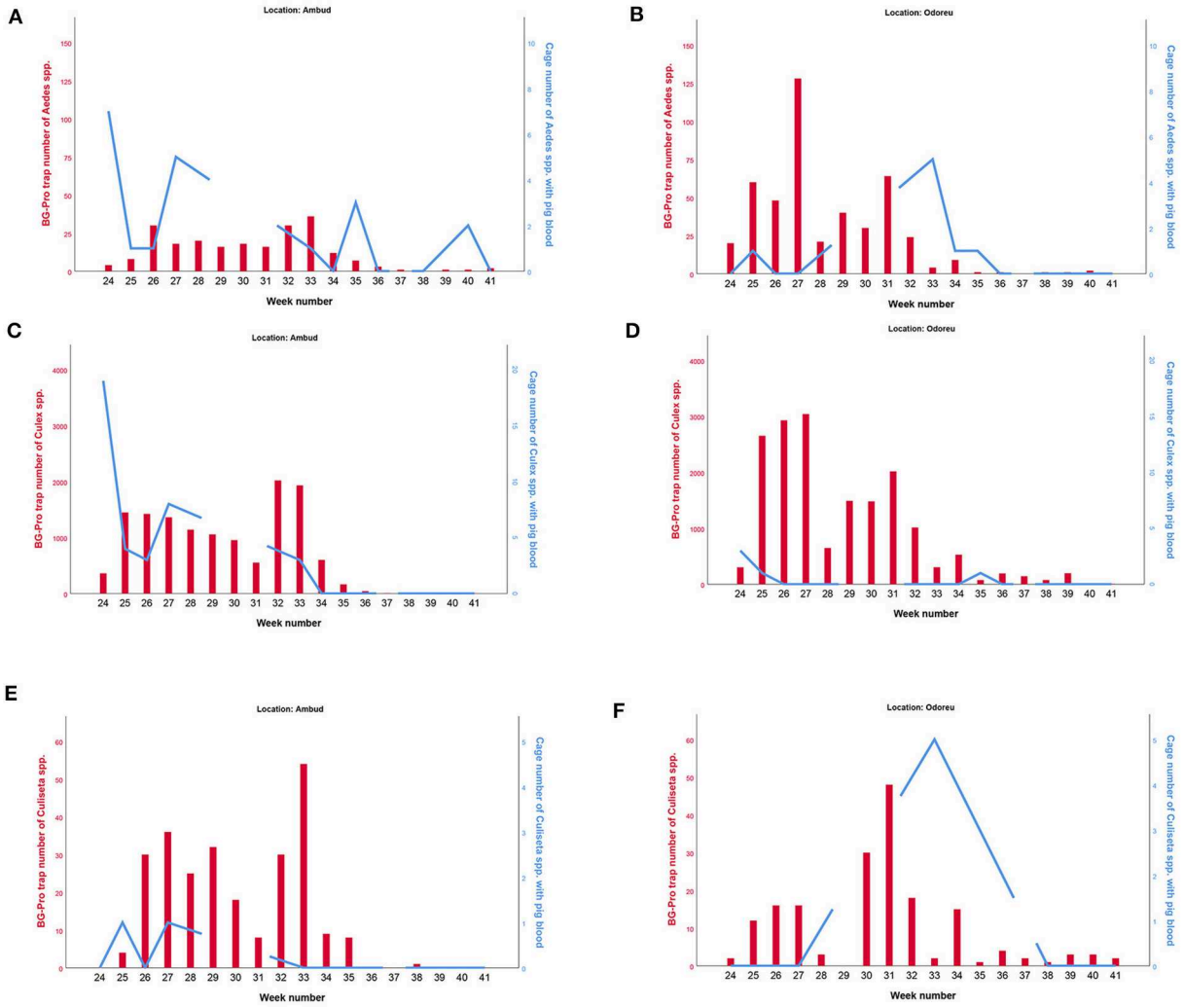

FIGURE 4
Seasonal abundance of the different genera of mosquitoes caught in our BG traps (red bars and the left Y-axis), as well as the number of mosquitoes with pig blood of the specific mosquito genera in our cages (blue lines and the right Y-axis). *Aedes spp.* is shown in **(A,B)**, *Culex spp.* is shown in **(C,D)**, *Culiseta spp.* is shown in **(E,F)**. Ambud is shown in the left **(A,C,E)** and Odoreu is shown in the right **(B,D,F)**, both locations are situated in northwestern Romania. Note that the proportion of mosquitoes with pig blood are based on the sum of all the individual species caught for each genera, and only porcine-blood PCR-positive cases are included. Left and right Y-axes scales are not identical, and axes scales between the different genera are not identical. Anopheles are not included as we had too few observations to make any meaningful plots.

4. Discussion

Of the 356 successfully identified mosquitoes caught in the cages, 116 carried a porcine blood meal, while one *Aedes caspius* in Sălcioara carried a bovine blood meal (*Bos taurus*) and the remaining 239 did not carry any identifiable blood meals. The bovine blood meal finding indicates that blood from different hosts is occasionally introduced to backyard pig farms and that blood fed mosquitoes are still attracted to backyard pigs or their enclosures. Given this finding, we argue that a mosquito carrying an ASFV blood meal, obtained from a nearby infected domestic pig or wild boar, could potentially introduce ASFV to a farm. To cause an outbreak, virus transmission from the mosquito to domestic pigs is needed, for example by the mosquito taking a consecutive blood meal from the backyard pig, as has been shown possible in previous studies using *S. calcitrans* (23). Additional modes of transmission could for example be through the pig ingesting the mosquito, as has been shown sufficient for *S. calcitrans* (21), or environmental contamination of the pig enclosure. However, there are significant differences in the volume of a blood meal taken between potential vectors. *S. calcitrans* is known to take blood meals between 11.2 and 15.1 µl (35), while horseflies can take blood meals ranging from 20 µl (*Chrysops* spp.) to

almost 700 μl (*Tabanus attratus*) (36), as they can consume more than their own weight in blood (37). Mosquito blood meals are significantly smaller, ranging, for example, between 1.3 μl and 5.4 μl in *Anopheles stephensi* (38), or 1.86–3.74 μl in *Aedes aegypti* (39). Previous studies have identified close proximity to outbreaks in domestic farms to be a risk factor for ASF occurrence in Romanian farms (27). Our findings support that mosquitoes do bring exogenous blood meals in close contact with backyard pigs.

Some mosquitoes that we caught inside the cages, are species known to be predominantly ornithophilic (i.e. *Culiseta longiareolata* and *Culiseta morsitans*) (Appendix I). These mosquitoes did not show any signs of blood meals. Conversely, some mosquitoes that we caught inside the cages are species known to be primarily ornithophilic (i.e. *Culex pipiens/torrentium* and *Culiseta annulata*) (Appendix I). Some of these mosquitoes from the pig cages did carry visual blood meals but tested negative for both porcine and mammalian blood. Catching these mosquitoes in the cages indicates that the predominantly ornithophilic mosquitoes are still attracted to the pigs or their enclosures, despite not feeding on the pigs. It also shows that the occasional ornithophilic species, despite already carrying a (non-mammalian) blood meal, are attracted to the pigs or their enclosures. *Culex pipiens* could therefore have taken a WNV or JEV viraemic blood meal before coming into contact with domestic pigs. The finding of these mosquito species next to pigs suggests that these mosquitoes may introduce JEV to pig stables without being biological vectors, which we argue could potentially still transmit the virus either by being ingested by a pig or through environmental contamination.

Despite having one of the lowest proportions of porcine-blood meals in the cages, the predominantly ornithophilic *C. pipiens/torrentium* still accounted for the highest number of the identified porcine blood meals (44 out of 116). This is due to their higher abundance compared to the other species caught (236 out of 356). Kilpatrick et al. (14) coined this phenomenon the Bridge Vector Paradigm. This paradigm describes the phenomenon where a potential vector is deemed unimportant for a particular pathogen from a qualitative perspective, conversely becomes a key vector species when studied in a quantitative manner. Their findings show that *Culex pipiens* and *Culex restuans*, two species previously considered unimportant in humans infections due to their predominantly ornithophilic feeding behaviour, are actually responsible for up to 80% of WNV infections in humans in the northeast United States due to their abundance compensating for the proportional feeding preference for mammalian blood. We argue that, assuming random selection of host species between individual *C. pipiens/torrentium* mosquitoes, the vast majority of *C. pipiens/torrentium* that take a second or third blood meals will at some point likely have fed on bird blood, which in turn could make them important bridge vectors for WNV and JEV. However, the abundance of *C. pipiens/torrentium* could be exacerbated due to the (semi-) urban settings we used for our collection, as *C. pipiens* is known to prefer (semi-) urban habitats over rural/wild habitats (40).

The use of *C. pipiens/torrentium* in this study, which is a combination of the *C. pipiens* complex (i.e. *C. pipiens pipiens* and *C. pipiens molestus*) and *C. torrentium*, was due to the females of these species/biotypes being very difficult to reliably distinguish (16). This however limits the conclusions that can be drawn from the study, as *C. pipiens pipiens* and *C. pipiens molestus* exhibit different feeding behaviours, with *C. pipiens pipiens* being primarily ornithophilic and *C. pipiens molestus* feeding on both birds and mammals (41), with humans representing 20% of blood meal hosts of *C. pipiens molestus* in Romania (42). Because of this difference, *C. pipiens pipiens* are believed to play only a minor role in the spread of arboviruses in Europe (16), although *C. pipiens* (in combination with *C. restuans*) are reported to account for over 80% of WNV infections in the north-eastern United States (14). As for *C. pipiens* and *C. torrentium*, *C. pipiens* is reported to be the dominant species in southern Europe, with *C. torrentium* rarely being reported. In northern Europe, *C. torrentium* is the dominant species while in central Europe similar proportions of *C. pipiens* and *C. torrentium* are observed (41). Nicolescu reported that, in Romania, *C. pipiens s.l.* is more abundant in urban areas compared to *C. pipiens molestus*, while in rural areas, they are abundant in animal shelters along with *Anopheles* spp. (43). Tiron et al. (42) however reported that, in southeastern Romania, *C. pipiens pipiens* has a preference for "green areas," while *C. pipiens molestus* prefers human settings and animal farmland. Given the location of our study sites (i.e. animal shelters in rural southeastern Europe) and the described differences in feeding behaviour, the blood fed *C. pipiens/torrentium* in our study (44 out of 236 contained pig blood) are likely to *C. pipiens molestus*, although we cannot state this for certain. *C. pipiens* is considered the main vector of WNV in southern Romania, while *Anopheles* spp. could also play a role in rural environments (43). *Aedes vexans*, the second-most frequent feeder on pig blood caught in the cages (18 out of 20 contained pig blood), is a predominantly mammalophilic species most abundant around floodplains or lakes (16, 44), that can take multiple blood meals (16). *Culiseta annulata*, the third-most frequent feeder on pig blood caught in the cages, also displays a strong preference for mammals (16) and frequently enter animal enclosures or houses to feed on humans or domestic animals during the summer months (16).

While the vast majority of mosquitoes with visual signs of a blood meal also tested positive for porcine blood (89.1%), 14 samples (10.9%) did not. Besides one sample with *Bos taurus* blood, we were unable to state for certain that the remaining 13 samples did not carry blood of mammalian origin. Most likely, the blood meals within the remaining 13 samples were

too degraded, the amount of blood within the samples were too low, or they were of non-mammalian origin.

We did not observe any clear correlation between the proportion of mosquitoes with pig blood (i.e. pig blood fed mosquitoes in the cages) and seasonal abundance (i.e. BG-Pro trap mosquitoes) of the various mosquito genera we caught (Figure 4). Throughout the sampling period, *Culex* spp. were significantly more abundant in the BG-Pro traps than the other genera ($\bar{x}$ = 92.3%, max = 99.2%, min = 60%). Other studies on mosquito abundance also indicate that *Culex* is the most abundant mosquito genus throughout Europe, particularly *Culex pipiens* (28).

We observed two seasonal peaks in *Culex* spp. (Figure 4) in both locations (Ambud and Odoreu). Although we cannot say what the vector activity was prior to week 24, personal communication with people at both locations tells us mosquito activity was very low before the onset of our collection period. Interestingly, for both *Aedes* spp. and *Culex* spp., the cage collections with the highest number of mosquitoes with pig blood occurred in the first week of the experiment (week 24). This was several weeks before the observed seasonal peak of these two genera in the BG-Pro traps (week 32 + 33). Furthermore, personal communication also tells us that the region was sprayed with insecticide from a helicopter right after our collection in week 27, from which it appears we can see the effect particularly in Odoreu. While the most abundant species of the *Culex* genus, *Culex pipiens*, is known to go through up to 7 generations in a single year (16), the insecticide sprayed over the region by helicopter following the collection in week 27 could also potentially explain the apparent double peaks.

Since insects were collected once every 24 h, after we fitted the roof on the cages, any mosquito taking a blood meal directly after the roof placement would have up to 24 h to digest the blood meal before collection. According to the digestion times given by Detinova et al. (31), a mosquito could digest enough blood within these 24 h to reach a Sella score of up to 4 (i.e. practically half full and half empty with dark blood). Interestingly, 25 out of 28 samples with a Sella score of 5, and 7 out of 9 with a Sella score of 6 tested positive for pig blood, which indicates that these blood meals either came from other pigs in the vicinity or were only partial/interrupted blood meals. It should be noted however, that the rate of blood meal digestion in mosquitoes, being poikilotherms, varies according to the temperature in the surrounding environment (45). We initially assumed that a higher Sella score (i.e. the blood meal being in a later state of digestion) would correlate to higher Cq-values for our PCR assays. However, a scatterplot comparing Cq-values to Sella scores provided an R^2 correlation coefficient of 0.0004, indicating a negligible correlation between the two variables (data not shown).

Our findings contribute to our understanding of which mosquito species are relevant when studying vector-borne pathogens that involve pigs. *Culex pipiens*, despite not preferentially feeding on pigs, should be the mosquito species of primary focus when looking at mosquito-borne pathogens, due to its high abundance. Other mosquito species, that do not tend to feed on pigs, could still be relevant vectors in terms of the introduction of viraemic blood from other host species, such WNV, as these ornithophilic mosquito species are still attracted to pigs or their enclosures. Future studies are needed to assess, which specific pathogens are introduced by mosquitoes to backyard pigs or their enclosures, and in what quantities. It is also important to gain more insights into the flight distance of these blood fed mosquitoes, to understand the possible range of transmission from viraemic blood-carrying vectors.

Data availability statement

The raw data supporting the conclusions of this article will be made available by the authors, without undue reservation.

Ethics statement

The animal study was reviewed and approved by Bioethics Commission of USAMV Cluj-Napoca.

Author contributions

JS, AM, RB, LK, and AB: conceptualisation. JS, AM, OB, MM, and VA: field data collection. JS, AO, and TR: sample processing. JS: data analysis and draft writing. JS, RB, AM, AO, LK, AB, TR, MM, and VA: draft review. All authors contributed to the article and approved the submitted version.

Funding

This study was supported by the University of Copenhagen.

Acknowledgments

We would like to thank Emanuel Albu and Razvan Blaga for their assistance in collecting the samples. We thank Philippe Weissenberg, Noureddine Mechouk, Gheorghe Bucur, and Mircea Coroian for their logistical support and Fie Fisker Brønnum Christiansen for her help processing the samples in the laboratory.

Conflict of interest

The authors declare that the research was conducted in the absence of any commercial or financial relationships that could be construed as a potential conflict of interest.

Publisher's note

All claims expressed in this article are solely those of the authors and do not necessarily represent those of their affiliated organizations, or those of the publisher, the editors and the reviewers. Any product that may be evaluated in this article, or claim that may be made by its manufacturer, is not guaranteed or endorsed by the publisher.

Supplementary material

The Supplementary Material for this article can be found online at: https://www.frontiersin.org/articles/10.3389/fvets.2022.1046263/full#supplementary-material

References

1. Craigo JK, Montelaro RC. Equine infectious anemia virus. *Evol Viruses.* (2008) 167–74. doi: 10.1016/B978-012374410-4.00395-2

2. Vloet RPM, Vogels CBF, Koenraadt CJM, Pijlman GP, Eiden M, Gonzales JL, et al. Transmission of Rift Valley fever virus from European-breed lambs to Culex pipiens mosquitoes. *PLoS Negl Trop Dis.* (2017) 11:e0006145. doi: 10.1371/journal.pntd.0006145

3. Fischer EA, Boender GJ, Nodelijk G, De Koeijer AA, Van Roermund HJ. The transmission potential of Rift valley fever virus among livestock in the Netherlands: a modelling study. *Vet Res.* (2013) 44:58. doi: 10.1186/1297-9716-44-58

4. Mellor PS, Carpenter S, White DM. Bluetongue virus in the insect host. *Bluetongue.* (2009) 295:320. doi: 10.1016/B978-012369368-6.50018-6

5. Zimmerman JJ, Karriker LA, Ramirez A, Schwartz KJ, Stevenson GW, Zhang J. *Diseases of Swine*. Hoboken, NJ: Wiley-Blackwell (2019).

6. EFSA. *Vector-borne Diseases*. EFSA (2022). Available online at: https://www.efsa.europa.eu/en/topics/topic/vector-borne-diseases (accessed October 9, 2022).

7. Auerswald H, Maquart PO, Chevalier V, Boyer S. Mosquito vector competence for japanese encephalitis virus. *Viruses.* (2021) 13:1154. doi: 10.3390/v13061154

8. Otake S, Dee SA, Rossow KD, Moon RD, Pijoan C. Mechanical transmission of porcine reproductive and respiratory syndrome virus by mosquitoes, *Aedes vexans* (Meigen). *Can J Vet Res.* (2002) 66:191–5.

9. Harley D, Sleigh A, Ritchie S. Ross river virus transmission, infection, and disease: a cross-disciplinary review. *Clin Microbiol Infect.* (2001) 14:909–32. doi: 10.1128/CMR.14.4.909-932.2001

10. Prullage JB, Williams RE, Gaafar SM. On the transmissibility of *Eperythrozoon suis* by *Stomoxys calcitrans* and *Aedes aegypti*. *Vet Parasitol.* (1993) 50:125–35. doi: 10.1016/0304-4017(93)90013-D

11. Stewart WC, Carbrey EA, Jenney EW. Transmission of hog cholera virus by mosquitoes. *Am J Vet Res.* (1975) 36:611–4.

12. Morgan NO, Miller DM. Muscidae (diptera): experimental vectors of hog cholera virus. *J Medi.* (1976) 12:657–60. doi: 10.1093/jmedent/12.6.657

13. Tidwell MA, Dean WD, Tidwell MA, Combs GP, Anderson DW, Cowart WO, et al. Transmission of hog cholera virus by horseflies (*Tabanidae: Diptera*). *Am J Vet Res.* (1972) 33:615–22.

14. Kilpatrick AM, Kramer LD, Campbell SR, Alleyne EO, Dobson AP, Daszak P. West nile virus risk assessment and the bridge vector paradigm. *Emerg Infect Dis.* (2005) 11:425–9. doi: 10.3201/eid1103.040364

15. Molaei G, Andreadis TG. Identification of avian- and mammalian-derived bloodmeals in *Aedes vexans* and *Culiseta melanura* (*Diptera: Culicidae*) and its implication for West Nile virus transmission in connecticut, U.S.A. *J Med Entomol.* (2006) 43:1088–93. doi: 10.1093/jmedent/43.5.1088

16. Becker N, Petric D, Zgomba M, Boase C, Dahl C, Madon M, et al. *Mosquitoes and Their Control*. 2nd edition. Heidelberg; Dordrecht; London; New York, NY: Springer (2010). doi: 10.1007/978-3-540-92874-4

17. EFSA, Miteva A, Papanikolaou A, Gogin A, Boklund A, Bøtner A, et al. Epidemiological analyses of African swine fever in the European Union (November 2018 to October 2019). *EFSA J.* (2020) 18:5996. doi: 10.2903/j.efsa.2020.5996

18. Resh VH, Carde RT. *Encyclopedia of Insects*. Vol. 7. Amsterdam: Elsevier; Academic Press. (2015) 37–72p.

19. EFSA, Desmecht D, Gerbier G, Schmidt CG, Grigaliuniene V, Helyes G, et al. Epidemiological analysis of African swine fever in the European Union (September 2019 to August 2020). *EFSA J.* (2021) 19:6572. doi: 10.2903/j.efsa.2021.6572

20. Olesen AS, Hansen MF, Rasmussen TB, Belsham GJ, Bødker R, Bøtner A. Survival and localization of African swine fever virus in stable flies (Stomoxys calcitrans) after feeding on viremic blood using a membrane feeder. *Vet Microbiol.* (2018) 222:25–9. doi: 10.1016/j.vetmic.2018.06.010

21. Olesen AS, Lohse L, Hansen MF, Boklund A, Halasa T, Belsham GJ, et al. Infection of pigs with African swine fever virus via ingestion of stable flies (Stomoxys calcitrans). *Transbound Emerg Dis.* (2018) 65:1152–7. doi: 10.1111/tbed.12918

22. Olesen AS, Lohse L, Boklund A, Halasa T, Belsham GJ, Rasmussen TB, et al. Short time window for transmissibility of African swine fever virus from a contaminated environment. *Transbound Emerg Dis.* (2018) 65:1024–32. doi: 10.1111/tbed.12837

23. Mellor PS, Kitching RP, Wilkinson PJ. Mechanical transmission of capripox virus and African swine fever virus by *Stomoxys calcitrans*. *Res Vet Sci.* (1987) 43:109–12. doi: 10.1016/S0034-5288(18)30753-7

24. Balmoş OM, Supeanu A, Tamba P, Cazan CD, Ionică AM, Ungur A, et al. Entomological survey to study the possible involvement of arthropod vectors in the transmission of African swine fever virus in Romania. *EFSA Supp Public.* (2021) 18:6460E. doi: 10.2903/sp.efsa.2021.EN-6460

25. Mazur-Panasiuk N, Zmudzki J, Wozniakowski G. African swine fever virus - persistence in different environmental conditions and the possibility of its indirect transmission. *J Vet Res.* (2019) 63:303–10. doi: 10.2478/jvetres-2019-0058

26. Mur L, Martínez-López B, Sánchez-Vizcaíno JM. Risk of African swine fever introduction into the European Union through transport-associated routes: returning trucks and waste from international ships and planes. *BMC Vet Res.* (2012) 8:149. doi: 10.1186/1746-6148-8-149

27. Boklund A, Dhollander S, Vasile C, Abrahantes J, Bøtner A, Gogin A, et al. Risk factors for African swine fever incursion in Romanian domestic farms during (2019). *Sci Rep.* (2020) 10:10215. doi: 10.1038/s41598-020-66381-3

28. Möhlmann TWR, Wennergren U, Tälle M, Favia G, Damiani C, Bracchetti L, et al. Community analysis of the abundance and diversity of mosquito species (*Diptera: Culicidae*) in three European countries at different latitudes. *Parasit Vect.* (2017) 10:510. doi: 10.1186/s13071-017-2481-1

29. Shahhosseini N, Frederick C, Racine T, Kobinger GP, Wong G. Modeling host-feeding preference and molecular systematics of mosquitoes in different ecological niches in Canada. *Acta Trop.* (2021) 213:105734. doi: 10.1016/j.actatropica.2020.105734

30. Boyer S, Durand B, Yean S, Brengues C, Maquart PO, Fontenille D, et al. Host-feeding preference and diel activity of mosquito vectors of the Japanese encephalitis virus in rural Cambodia. *Pathogens.* (2021) 10:376. doi: 10.3390/pathogens10030376

31. Detinova TS. *Age-Grouping Methods in Diptera of Medical Importance: With Special Reference to Some Vectors of Malaria*. Geneva: WHO (1962). doi: 10.2307/3275215

32. Olesen AS, Lohse L, Boklund A, Halasa T, Gallardo C, Pejsak Z, et al. Transmission of African swine fever virus from infected pigs by direct contact and aerosol routes. *Vet Microbiol.* (2017) 211:92–102. doi: 10.1016/j.vetmic.2017.10.004

33. Forth JH. Standardisierung eines nicht-invasiven *Beprobungssystems zur* infektionsüberwachung bei wildschweinen (*Sus scrofa*). *Ernst Moritz Arndt Universität Greifswald*. (2015)

34. Andrejevic M, Markovic MK, Bursac B, Mihajlovic M, Tanasic V, Kecmanovic M, et al. Identification of a broad spectrum of mammalian and avian species using the short fragment of the mitochondrially encoded cytochrome b gene. *For Sci Med Pathol.* (2019) 15:169–77. doi: 10.1007/s12024-019-00096-4

35. Schowalter T, Klowden M. *Blood Meal Size of the Stable Fly, Stomoxys calcitrans, Measured by the HICN Method*. Vol. 39. Mosquito News. Athens, GA: Department of Entomology, University of Georgia, (1979).

36. Mullens BA. Horse flies and deer flies (*Tabanidae*). *Med Vet Entomol.* (2019) 3:327–43. doi: 10.1016/B978-0-12-814043-7.00016-9

37. Leprince DJ, Foil LD. Relationships among body size, blood meal size, egg volume, and egg production of *Tabanus fuscicostatus* (*Diptera: Tabanidae*). *J Med Entomol.* (1993) 30:865–71. doi: 10.1093/jmedent/30.5.865

38. Graumans W, Heutink R, Van Gemert GJ, Van De Vegte-Bolmer M, Bousema T, Collins KA. A mosquito feeding assay to examine plasmodium transmission to mosquitoes using small blood volumes in 3D printed nano-feeders. *Parasit Vect.* (2020) 13:401. doi: 10.1186/s13071-020-04269-x

39. Knaus RM, Foil LD, Issel CJ, Leprince DJ. Insect blood meal studies using radiosodium 24Na and 22Na. *J Am Mosq Control Assoc.* (1993) 9:264–8.

40. González MA, Prosser SW, Hernández-Triana LM, Alarcón-Elbal PM, Goiri F, López S, et al. Avian feeding preferences of *Culex pipiens* and *Culiseta spp*. Along an urban-to-wild gradient in Northern Spain. *Front Ecol Evol.* (2020) 8:568835. doi: 10.3389/fevo.2020.568835

41. Brugman VA, Hernández-Triana LM, Medlock JM, Fooks AR, Carpenter S, Johnson N. The role of *Culex pipiens* L. (*Diptera: Culicidae*) in virus transmission in Europe. *Int J Environ Res Public Health*. (2018) 15:389. doi: 10.3390/ijerph15020389

42. Tiron GV, Stancu IG, DInu S, Prioteasa FL, Falcuta E, Ceianu CS, et al. Characterization and host-feeding patterns of *Culex pipiens* s.l. Taxa in a West Nile virus-endemic area in Southeastern Romania. *Vector Borne Zoonotic Dis.* (2021) 21:713–9. doi: 10.1089/vbz.2020.2739

43. Nicolescu G. A general characterisation of the mosquito fauna (*Diptera: Culicidae*) in the epidemic area for West Nile vims in the south of Romania. *Eur Mosq Bull.* (1998) 2:13–8.

44. Kurucz K, Kepner A, Bosiljka K, Hederics D, Földes F, Zana B, et al. Blood-meal analysis and avian malaria screening of mosquitoes collected from human-inhabited areas in Hungary and Serbia. *J Eur Mosq Control Assoc.* (2018) 36: 3–13.

45. Reinhold JM, Lazzari CR, Lahondère C. Effects of the environmental temperature on aedes aegypti and aedes albopictus mosquitoes: a review. *Insects.* (2018) 9:158. doi: 10.3390/insects9040158

frontiers | Frontiers in Veterinary Science

TYPE Original Research
PUBLISHED 07 March 2023
DOI 10.3389/fvets.2023.1128863

OPEN ACCESS

EDITED BY
Tao Lin,
New Hope Group, United States

REVIEWED BY
Yanhua Li,
Yangzhou University, China
Lang Gong,
South China Agricultural University, China

*CORRESPONDENCE
Guoxin Li
✉ guoxinli@shvri.ac.cn
Guangzhi Tong
✉ gztong@shvri.ac.cn

†These authors have contributed equally to this work

SPECIALTY SECTION
This article was submitted to Veterinary Infectious Diseases, a section of the journal Frontiers in Veterinary Science

RECEIVED 21 December 2022
ACCEPTED 08 February 2023
PUBLISHED 07 March 2023

CITATION
Jiang Y, Gao F, Li L, Zhou Y, Tong W, Yu L, Zhang Y, Zhao K, Zhu H, Liu C, Li G and Tong G (2023) The rPRRSV-E2 strain exhibited a low level of potential risk for virulence reversion. *Front. Vet. Sci.* 10:1128863. doi: 10.3389/fvets.2023.1128863

The rPRRSV-E2 strain exhibited a low level of potential risk for virulence reversion

Yifeng Jiang[1,2†], Fei Gao[1,2†], Liwei Li[1], Yanjun Zhou[1,2], Wu Tong[1,2], Lingxue Yu[1], Yujiao Zhang[1], Kuan Zhao[1], Haojie Zhu[1], Changlong Liu[1], Guoxin Li[1,2*] and Guangzhi Tong[1,2*]

[1]Department of Swine Infectious Diseases, Shanghai Veterinary Research Institute, Chinese Academy of Agricultural Sciences, Shanghai, China, [2]Jiangsu Co-Innovation Center for the Prevention and Control of Important Animal Infectious Disease and Zoonosis, Yangzhou University, Yangzhou, China

Porcine Reproductive and Respiratory Syndrome Virus (PRRSV) and Classical Swine Fever Virus (CSFV) are two important pathogens, which cause serious impact on swine industry worldwide. In our previous research, rPRRSV-E2, the recombinant PRRSV expressing CSFV E2 protein, could provide sufficient protection against the lethal challenge of highly pathogenic PRRSV and CSFV, and could maintained genetically stable *in vitro*. Here, to evaluate the virulence reversion potential risk, rPRRSV-E2 had been continuously passaged *in vivo*, the stability of E2 expression and virulence of the passage viruses were analyzed. The results showed that no clinical symptoms or pathological changes could be found in the inoculated groups, and there were no significant differences of viraemia among the test groups. Sequencing and IFA analysis showed that the coding gene of exogenous CSFV E2 protein existed in the passaged viruses without any sequence mutations, deletions or insertions, and could expressed steadily. It could be concluded that the foreign CSFV E2 gene in the genome of rPRRSV-E2 could be maintained genetically stable *in vivo*, and rPRRSV-E2 strain had relatively low level of potential risk for virulence reversion.

KEYWORDS

rPRRSV-E2, virulence reversion, genetic stability, *in vivo* passage, CSFV E2

1. Introduction

Porcine reproductive and respiratory syndrome (PRRS) is characterized by late-term reproductive failure in sows and severe pneumonia in neonatal pigs (1–3). PRRSV is the causative pathogen of PRRS, which seriously affects the swine herds and causes huge economic losses to the pig industry worldwide (4–6). PRRSV is a positive-sense single-stranded RNA virus, belonging to the family *Arteriviridae* and genus *Arterivirus*. The 15-kb genome encoded at least 10 open reading frames (ORFs), which expressed at least 12 non-structural proteins (Nsps) and eight structural proteins (7–11). Although the level of bio-safety elevated since the ASF outbreak in 2018, PRRS is still one of the most significant threats to pig production in China (12–16).

Immunization is an effective measure to prevent and control PRRS, in which inactivated vaccines and subunit vaccines could not provide effective protection against PRRSV (17, 18). Live PRRS vaccines could stimulate cellular and humoral immune responses and provide respectable immune efficacy against heterologous PRRSV strains (19–23). In China, many live vaccines have been developed and used for PRRS control and contributed to the development of the pig industry (24, 25). However, the risk of virulence reversion of live vaccines has attracted extensive concerns and became one of the most important preclinical results in the innovation and development of a new vaccine (26–28).

Based on reverse genetic manipulation, several regions of the PRRSV genome could be used to insert foreign genes, to perform basic research or vaccine innovation (29–32). In the previous study, rPRRSV-E2-expressing CSFV E2 protein with the backbone of vaccine strain HuN4-F112 was engineered, and its genetic stability could be maintained *in vitro* for at least 25 consecutive cell passages (32). In this study, an *in vivo* trial was designed, and the potential risk for virulence reversion of rPRRSV-E2 was evaluated.

2. Materials and methods

2.1. Cells and viruses

African green monkey kidney cells (MARC-145 cells) were cultured in minimum essential medium (MEM; Invitrogen Corporation, Carlsbad, CA, USA) and supplemented with 10% fetal bovine serum (FBS; Life Technologies Inc., Gibco/Brl Division, Grand Island, NY, USA). It was maintained in MEM supplemented with 2% FBS at 37°C in a humidified atmosphere of 5% CO_2, as described previously (33). The virus titer of recombinant strain rPRRSV-E2 was determined by performing standard median tissue culture infective dose ($TCID_{50}$) assays in 96-well-plates. According to the Reed and Muench method (34), rPRRSV-E2 for experimental usage in this study is the fifth passage, and the virus titer is $10^{6.0}TCID_{50}$/mL.

2.2. Immunofluorescence assays

The expression of PRRSV N protein and CSFV E2 protein in the experimental samples was determined by immunofluorescence assays (IFAs). MARC-145 cells grew to 70% confluence in six-well-plates and were infected with rPRRSV-E2 samples and mock controls, as reported. After 48 h of infection, cell monolayers were fixed with ice-cold methanol at room temperature for 10 min, blocked with 0.1% bovine serum albumin for 30 min, and incubated with 1:600 anti-PRRSV N (SR30A, Rural Technologies) or 1:1000 anti-E2 monoclonal antibody (prepared and preserved by our laboratory) at 37°C for 2 h. After washing with PBS five times, cells were incubated at 37°C for 1 h with Alexa Fluor 594-labeled goat anti-mouse IgG (H+L) (Invitrogen Corporation). After washing with PBS, fluorescence was visualized using an inverted fluorescence microscope (model IX741; Olympus Corporation, Tokyo, Japan), as previously mentioned (35).

2.3. Animal experiments

All pig experimental programs follow the guidelines for the Care and Use of Experimental Animals and are approved by the Ethics Committee of the Shanghai Veterinary Research Institute, Chinese Academy of Agricultural Sciences, with the number SHvri-pi-20190067. Fifty piglets at 30 days of age, which were PRRSV-free, CSFV-free, PCV2-free, and PRV-free, were purchased and bred. In the first generation, the recombinant vaccine strain rPRRSV-E2 was inoculated intramuscularly at a dose of $10^{5.0}TCID_{50}$, and the serum samples with the highest viral load were selected to be inoculated with the second-generation to the fifth-generation virus at a dose of 2 mL. Five piglets per generation were inoculated with virus/serum samples (named R1–R5 groups, respectively, and each generation of pigs was one-to-one corresponded during the experiment). Another three piglets per generation served as the control group. When the virus was transmitted to the fifth generation, the serum samples of each pig in the fifth generation at the highest level of viremia were mixed, and then five piglets were inoculated. The original generation virus was inoculated at the same time, and the clinical manifestations were observed and recorded. After vaccination, the clinical manifestations of pigs were observed and recorded every day, such as feed intake, mental state, and abnormal conditions of the ears, eyelids, and body surfaces. After feeding, rectal temperature measurement was performed every morning until necropsy. Clinical anatomy observation: The experimental pigs were killed and necropsied on the 21st day after inoculation, and the pathological changes in inguinal lymph nodes, spleen, lung, kidney, and other tissues and organs were observed. Histopathological observation: The tissues of the inguinal lymph nodes, spleen, lung, and kidney of inoculated pigs were collected and their histopathological examination was carried out.

2.4. Analysis of viremia by real-time RT-qPCR

Blood samples and serum samples were collected 0, 7, 14, and 21 days after immunization, and the serum was split into four centrifuge tubes. RNA was extracted from one tube for real-time RT-qPCR from a blood sample using the QIAprep viral RNA Kit (Qiagen, Hilden, Germany) according to the manufacturer's instructions, as previously described. The other three test tubes were immediately frozen in a refrigerator at −70°C. RT-qPCR was used to detect and analyze the viremia of serum samples. Viral RNA was extracted from 140 μL of pig serum sample. Primers PNPF/PNPR and the NP probe were used for PRRSV RT-qPCR, and the sequences of primer pairs and probes are listed in Table 1.

Re-isolation of virus: The first–fifth generation pig sera were taken and filtrated using a 0.22-μm filter, then inoculated with single-layer MARC-145 cells and adsorbed in an incubator at 37°C for 1 h. The inoculated serum was discarded, and DMEM culture solution containing 2% FBS was replaced and cultured at 37°C. The virus was collected when 60–70% CPE occurred, and RT-PCR amplification and the whole genome sequence determination were performed with PRRSV primers, of which sequences were listed in Table 1.

2.5. Statistical analysis

SPSS 14.0 software and GraphPad Prism 6.0 were used to perform all the data analysis and charting.

TABLE 1 Oligonucleotides used for RT-PCR and qRT-PCR.

Name[a]	Sequence[b]	Position[c]	Application
HF11559	5′-TCATACATCCGAGTTCCTGTT-3′	11,559–11,579	PCR mutagenesis
HR13090	5′-GAAATATTGTCATGGCGAGGC-3′	13,070–13,090	PCR mutagenesis
HF11805	5′-TTTGAATCGGATACAGCGTATC-3′	11,805–11,826	Nucleotide sequencing
HR12100	5′-CCAAACAAAATGGCCAAAAATAT-3′	12,078–12,100	Nucleotide sequencing
PNPF	5′-CCCTAGTGAGCGGCAATTGT-3′	15,002–15,021	qRT-PCR primer (PRRSV)
PNPR	5′-TCCAGCGCCCTGATTGAA-3′	15,045–15,062	qRT-PCR primer (PRRSV)
NP-probe	FAM-TCTGTCGTCGATCCAGA-MGB	15,023–15,039	qRT-PCR probe (PRRSV)

[a]Abbreviations in primer names: F, forward PCR primer; R, reverse PCR primer.
[b]Italic lowercase represents sequences different from HuN4 (EF635006).
[c]Numbers in the primer names denote the nucleotide positions in the parental HuN4 (EF635006) and the CSFV Shimen strain (AF092448).

Results: It was considered that there was a significant difference when the $p < 0.05$, and an extremely significant difference when the $p < 0.01$ or < 0.001 (26).

2.6. Detection of the *in vivo* passage stability of exogenous gene

The rPRRSV-E2 strain isolated *in vivo* was passaged on MARC-145 cells to detect the stability of foreign genes in the process of virus passage. The stability of the marker gene CSFV E2 during the passage of the virus was determined. The MARC-145 cells infected by the virus were detected by IFA, and the expression of the CSFV E2 gene was observed.

3. Results

3.1. Clinical manifestations of experimental piglets showed normal conditions

After the inoculation of each generation of virus/serum samples, the feed intake and mental state of the test pigs were normal, and there was no significant difference between the test and the mock control groups. There were no clinical symptoms such as anorexia, cough, diarrhea, congestion, or ulcer spots in the ears and body surface, no swelling of eyelids, and no obvious increase of eye secretion in pigs. After inoculation, all the pigs showed no symptoms of persistent hyperthermia (the body temperature was over 40.5°C, which was determined as persistent hyperthermia for 3 days). The temperature changes of the tested pigs are shown in Figure 1A. The serum samples were collected on the 7th, 14th, and 21st days after inoculation, which was used to determine the viral load in serum. The results showed that the virus load in pig serum of each group reached a peak in 7–14 days after inoculation (Figure 1B). However, the viremia level of R1–R5 groups gradually decreased, especially R5 group, their viremia levels were all below the negative value. In addition, viral shedding was also conducted to assess the risk. The results showed that the viral shedding levels were all below the negative threshold line (data not shown).

3.2. No obvious pathological changes were found in the clinical anatomy of piglets inoculated with rPRRSV-E2 at different generations

On the 21st day after inoculation, the experimental piglets were killed and necropsied. The dissection observation results showed that there were no visible pathological changes in the internal organs of each piglet of the rPRRSV-E2 *in vivo* passage group, and there was no significant difference compared with the blank control group (mock group) (Figure 1C). Histopathological examination was carried out on each group of organs, and the results showed that there was no obvious pathological damage to all kinds of parenchymal organs (spleen, lung, kidney, and lymph nodes) (Figure 1D).

3.3. Foreign CSFV E2 gene in the genome of rPRRSV-E2 was intact in the genetic stability analysis *in vitro* and *in vivo*

The genetic stability analysis for rPRRSV-E2 was carried out in MARC-145 cells *in vitro*, and P5, P10, P15, and P20 viruses were sequenced. The sequencing results of the samples showed that the inserted CSFV E2 protein gene could exist stably in the viral genome, and no nucleotide variation occurred. The results of IFA showed that the E2 gene of CSFV could be expressed normally (Figure 2A). The whole genome of each generation of the virus during *in vivo* passage was sequenced. The results of stability analysis of the CSFV E2 gene showed that compared with its parental strain, the virus isolated *in vivo* (R1–R5) had no nucleotide mutation in the E2 insertion region (Figure 2B). Only a few base mutations were scattered in the whole genome. Neither base insertion nor deletion was found. IFA for CSFV E2 protein of the isolated virus showed that E2 protein was stably and abundantly expressed (Figure 2C).

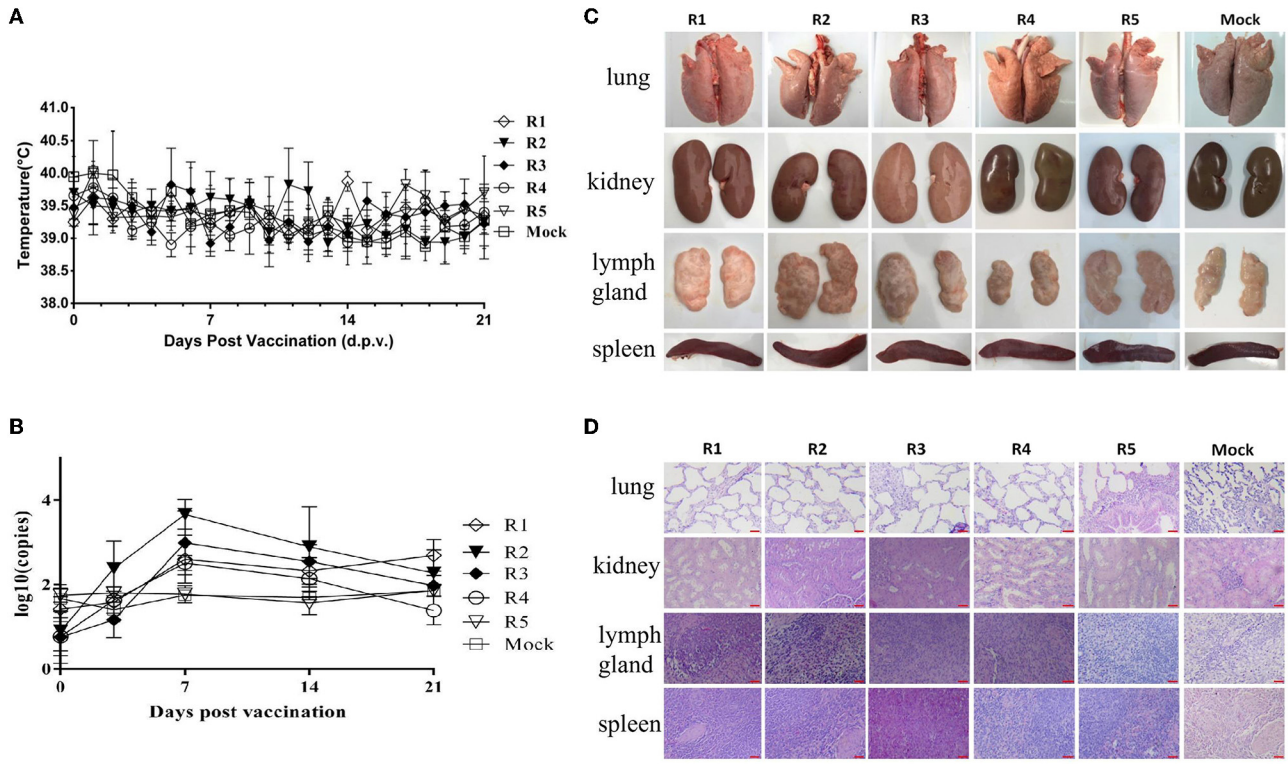

FIGURE 1
Safety identification of rPRRSV-E2 vaccination group and pig–pig *in vivo* serial passage sera inoculation group. The values of mock groups of each generation were indicated together. **(A)** Daily rectal temperature record of the rPRRSV-E2 inoculation group and the *in vivo* passage groups. **(B)** Viral RNA replication in serum samples detection for the rPRRSV-E2 inoculation group and the pig–pig *in vivo* generation sera inoculation group. Five piglets in each generation were inoculated with virus/serum samples, named R1–R5 groups, respectively, and each generation of pigs was one-to-one corresponded during the experiment. **(C)** Gross pathological changes of organs and tissues (spleen, lung, kidney, and lymph node) of rPRRSV-E2 inoculation group and *in vivo* passage sera inoculation group after necropsy. **(D)** Histopathological observation of organs and tissues (spleen, lung, kidney, and lymph node) of rPRRSV-E2 inoculation group and *in vivo* serial passage sera inoculation group after necropsy. Scale bar = 200 μm.

3.4. High degree of safety could be proved in the comparative evaluation between *in vivo* passage serum mixture inoculated group and the original virus inoculated group

After inoculation, there was no redness and inflammation in the inoculated parts of piglets in the fifth-generation virus inoculation group and the original virus inoculation group. The feed intake and mental state of the experimental piglets inoculated with the fifth-generation virus were normal, and there was no significant difference between the blank control group and the fifth-generation virus inoculation group. There was no congestion or ulcer spots on the ears and body surfaces of inoculated piglets, no swelling of eyelids, and no obvious increase in the secretions of eyes. All the piglets did not show symptoms of persistent hyperthermia after inoculation (Figure 3A). Autopsy results showed that no visible pathological changes were found in the parenchymal organs and the lymph nodes of the piglets in each group (Figure 3B). Histopathological observation showed that there was no obvious pathological damage to the spleen, lung, kidney, lymph nodes, and other parenchymal organs of the pigs in each group (Figure 3C).

4. Discussion

Since it emerged in the late 1980's, many kinds of vaccines have been developed for PRRS control, including inactive, subunit, and attenuated live vaccines. However, only live vaccines showed sufficient immune protection and are used in major pig breeding areas all over the world (17, 18, 20, 23). Although PRRS spreads and evolves rapidly, immunization still plays a very positive role in the prevention and control of PRRS (36, 37). On the other hand, live vaccines still have many defects to be improved, including the risk of virulence reversion, which has been reported by many studies and has become one of our foremost concerns of PRRSV vaccine innovation and development (26–28).

In this study, the recombinant PRRSV live vector vaccine rPRRSV-E2 strain was concerned. The E2 gene, an important protective antigen of CSFV, was inserted into the intergenic region of ORF1b and ORF2 of PRRSV by reverse genetic manipulation. Previous studies had proved that the vaccine could provide good immune protection for both HP-PRRSV and CSFV (32). The potential risk of virulence reversion for rPRRSV-E2 was assessed in this study. The results of this study showed that during the observation period, piglets inoculated P1–P5 rPRRSV-E2/serum did not show any PRRS-related clinical symptoms or visible

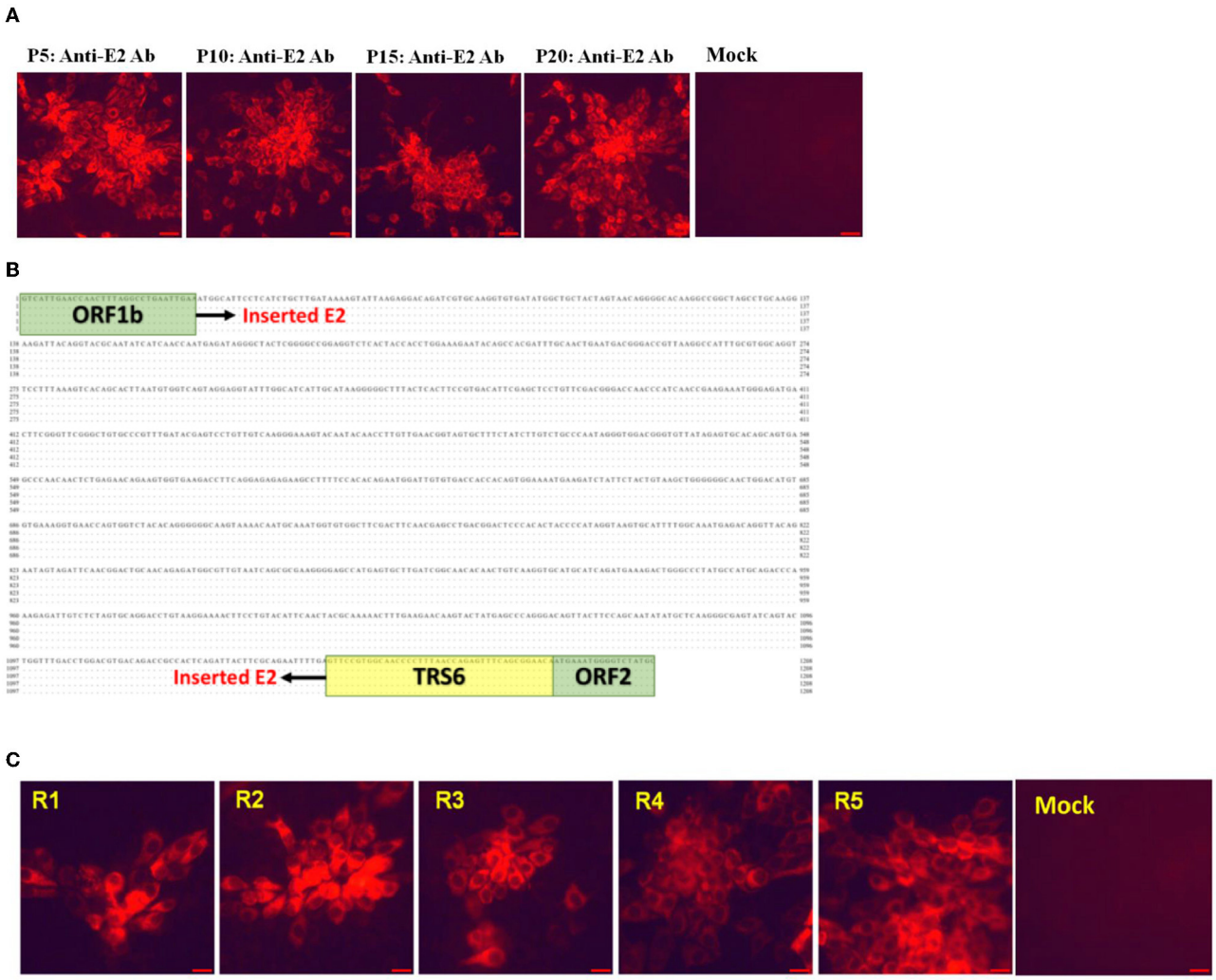

FIGURE 2
The genetic stability of foreign genes in rPRRSV-E2 *in vitro* and *in vivo*. **(A)** Indirect immunofluorescence results of CSFV E2 protein of *in vitro* generation of P5, P10, P15, and P20 viruses. **(B)** Sequence alignments of CSFV E2 protein insertion region of the isolated virus of various passages *in vivo*. **(C)** Indirect immunofluorescence assay of CSFV E2 protein expression of the isolated virus after passage *in vivo*. Scale bar = 20 μm.

pathological lesions in the lungs, kidneys, lymph nodes, and spleens, which demonstrated the safety of the passaged viruses and indicated that rPRRSV-E2 had no virulence reversion of *in vivo*, at least in these five passage processes. The stability of the PRRSV genome was very important for virulence. In the evolution history of PRRSV, the virulence change is always accompanied by great changes in the genome (38–40). The results showed that the coding gene of exogenous CSFV E2 protein existed in the passage viruses, without any sequence mutations, deletions, or insertions, and it could be stably expressed. Combined with the previous study, full-length sequencing of P5, P10, P15, P20, and P25 rPRRSV-E2 virus stocks of MARC-145 cells showed that there were no mutations in the region where foreign genes were expressed, and they remained stable at least for 25 consecutive cell passages (32). The genome of rPRRSV-E2 was stable *in vivo* and *in vitro*, and this will reduce the possibility of virulence reversion.

For live PRRSV vaccine, most studies consider that there are high risks of virulence reversion. The causes for this phenomenon should be considered from the following aspects: 1. Genetic stability of gene sequences; 2. Horizontal transmission capability of vaccine; and 3. The level and duration of viremia. In this study, the potential risk of virulence reversion of the rPRRSV-E2 strain was evaluated, and the results showed that the risk was relatively low. First, the genetic stability test *in vitro* and *in vivo* confirmed that the virus sequences of the rPRRSV-E2 strain, especially the sequences of foreign genes, were stable. In addition, rPRRSV-E2 had passed the transgenic safety evaluation. The experiment of horizontal transmission confirmed that the pigs immunized with the rPRRSV-E2 strain were kept in the same house as normal piglets and could not infect other non-immunized piglets (data not shown). There is no ability and risk of horizontal transmission. Moreover, compared with the parental vaccine strain vHuN4-F112, the rPRRSV-E2 strain has a shorter duration and a lower viremia level, because the insertion of the exogenous CSFV E2 gene makes it further weakened and has higher safety characteristics. In addition, previous studies also found that the virus shedding and virus

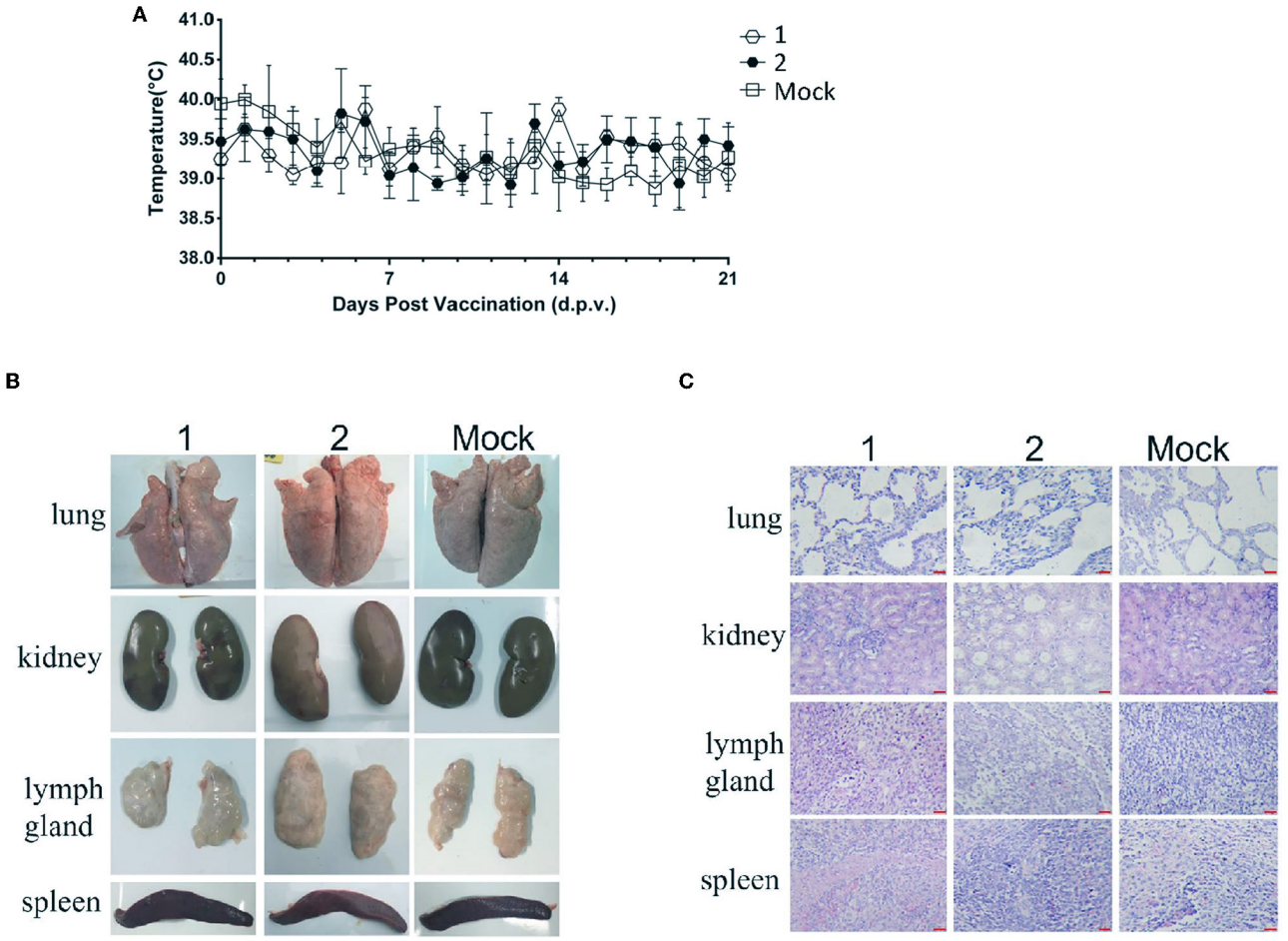

FIGURE 3
Safety comparison test between *in vivo* passage serum mixture inoculated group and original virus inoculated group. The changes in rectal temperature of pigs in each group after inoculation, autopsy results, and histopathological observation. **(A)** Daily rectal temperature record of rPRRSV-E2 inoculation group compared with *in vivo* passage sera inoculation group. **(B)** Gross pathological changes of organs and tissues (spleen, lung, kidney, and lymph node) of rPRRSV-E2 inoculation group (1) and *in vivo* passage mixed-sera inoculation group (2) after necropsy. **(C)** Histopathological observation of organs and tissues (spleen, lung, kidney, and lymph node) of rPRRSV-E2 inoculation group (1) and *in vivo* passage mixed sera inoculation group (2) after necropsy. Scale bar = 200 μm.

load levels of rPRRSV-E2 in tissues were low. All these causes and factors determined that rPRRSV-E2 showed little potential risk in the assessment of virulence reversion. Furthermore, it is worth noting that the reverse genetic manipulation platform for full-length infectious cDNA clone of pHuN4-F112 is stable and convenient, and it exhibits a strong ability to accommodate foreign genes. Thus, far, we have found that multiple sites and foreign genes can be stably inserted based on this platform, and the maximum foreign gene size can reach 2,100 bp. Multiple foreign genes can be simultaneously and stably expressed. Therefore, stability is essential for PRRSV to be used as a platform for the development to develop new genetic engineering live vaccines. This may also be one of the reasons for the good performance of rPRRSV-E2 in the risk assessment of virulence reversion.

Virulence reversion is determined by many factors, including the frequency, correct use of the vaccine, selection of generation to be used as vaccines, and the characteristic of the candidate vaccine strain. This vaccine strain, which was reported with virulence reversion, mainly used the virus that has been passaged on MARC-145 cells for <100 generations (26–28). rPRRSV-E2 was generated by the full-length infectious clone of the vaccine strain HuN4-F112, which was made from the serial passage of wild-type HuN4 on MARC-145 cells for 112 generations (24, 41). HuN4-F112 was proved to be safe, and the genome was stable from generations 112–130, which increases the safety of rPRRSV-E2. We already exhibited the stability of the rPRRSV-E2 genome and the virulence of *in vivo* passage viruses. A previous study also demonstrated that there was no virus shedding after rPRRSV-E2 inoculation and no horizontal transmission among the co-inhabited piglets, which also indicated the safety of rPRRSV-E2 (32). Virulence reversion was determined by many factors, although the safety of rPRRSV-E2 is demonstrated, the scientific and rational usage of the vaccine still needs more attention, and the PRRS vaccine needs to be upgraded continuously.

In conclusion, rPRRSV-E2 is a candidate vaccine strain that is safe for immunization. The genome was observed to be stable

in vivo and *in vitro*, and the level of potential risk for virulence reversion was relatively quite low.

Data availability statement

The original contributions presented in the study are included in the article/supplementary material, further inquiries can be directed to the corresponding authors.

Ethics statement

The animal study was reviewed and approved by Ethics Committee of the Shanghai Veterinary Research Institute, Chinese Academy of Agricultural Sciences.

Author contributions

This study was conceived and designed by GL and GT. YJ and FG performed the experiments and prepared the figures. FG, LL, and YZho wrote the main manuscript text. WT and LY analyzed the data. YZha, KZ, and HZ prepared the manuscript. GT made constructive comments on the experiments. All authors participated in the experiments, contributed to the article, and approved the submitted version.

Funding

We gratefully acknowledge support from the National Key Research and Development Program of China (2022YFD1800800 and 2021YFD1801401), Natural Science Foundation of Shanghai (21ZR1476900 and 21ZR1477200), Shanghai Municipal Agriculture Science and Technology Project (2022-02-08-00-12-F01115), External Collaborative Scientific Research Program (2022YJXTGCWQSX5006), the National Natural Science Foundation of China (31941017), and Central Public-interest Scientific Institution Basal Research Fund (Y2020YJ15, 2021JB01, and 2020JB01).

Conflict of interest

The authors declare that the research was conducted in the absence of any commercial or financial relationships that could be construed as a potential conflict of interest.

Publisher's note

All claims expressed in this article are solely those of the authors and do not necessarily represent those of their affiliated organizations, or those of the publisher, the editors and the reviewers. Any product that may be evaluated in this article, or claim that may be made by its manufacturer, is not guaranteed or endorsed by the publisher.

References

1. Meulenberg JJ. PRRSV the virus. *Vet Res.* (2000) 31:11–21. doi: 10.1051/vetres:2000103

2. Wensvoort G, de Kluyver EP, Pol JM, Wagenaar F, Moormann RJ, Hulst MM, et al. Lelystad virus, the cause of porcine epidemic abortion and respiratory syndrome: a review of mystery swine disease research at lelystad. *Vet Microbiol.* (1992) 33:185–93. doi: 10.1016/0378-1135(92)90046-V

3. Snijder EJ, Horzinek MC, Spaan WJ. The coronaviruslike superfamily. *Adv Exp Med Biol.* (1993) 342:235–44. doi: 10.1007/978-1-4615-2996-5_37

4. Holtkamp DJ, Kliebenstein JB, Neumann EJ, Zimmerman JJ, Rotto HF, Yoder TK, et al. Assessment of the economic impact of porcine reproductive and respiratory syndrome virus on United States pork producers. *J Swine Health Product.* (2013) 21:72–84. doi: 10.31274/ans_air-180814-28

5. Zhou L, Yang H. Porcine reproductive and respiratory syndrome in China. *Virus Res.* (2010) 154:31–7. doi: 10.1016/j.virusres.2010.07.016

6. Collins JE, Benfield DA, Christianson WT, Harris L, Hennings JC, Shaw DP, et al. Isolation of swine infertility and respiratory syndrome virus (isolate ATCC VR-2332) in North America and experimental reproduction of the disease in gnotobiotic pigs. *J Vet Diagn Invest.* (1992) 4:117–26. doi: 10.1177/104063879200400201

7. Bautista EM, Meulenberg JJ, Choi CS, Molitor TW. Structural polypeptides of the American (VR-2332) strain of porcine reproductive and respiratory syndrome virus. *Arch Virol.* (1996) 141:1357–65. doi: 10.1007/BF01718837

8. Snijder EJ, Meulenberg JJ. The molecular biology of arteriviruses. *J Gen Virol.* (1998) 79:961–79. doi: 10.1099/0022-1317-79-5-961

9. Firth AE, Zevenhoven-Dobbe JC, Wills NM, Go YY, Balasuriya UB, Atkins JF, et al. Discovery of a small arterivirus gene that overlaps the gp5 coding sequence and is important for virus production. *J Gen Virol.* (2011) 92:1097–106. doi: 10.1099/vir.0.029264-0

10. Li Y, Treffers EE, Napthine S, Tas A, Zhu L, Sun Z, et al. Transactivation of programmed ribosomal frameshifting by a viral protein. *Proc Natl Acad Sci U S A.* (2014) 111:E2172–81. doi: 10.1073/pnas.1321930111

11. van Aken D, Snijder EJ, Gorbalenya AE. Mutagenesis analysis of the Nsp4 main proteinase reveals determinants of arterivirus replicase polyprotein autoprocessing. *J Virol.* (2006) 80:3428–37. doi: 10.1128/JVI.80.7.3428-3437.2006

12. Zhao D, Liu R, Zhang X, Li F, Wang J, Zhang J, et al. Replication and virulence in pigs of the first african swine fever virus isolated in China. *Emerg Microbes Infect.* (2019) 8:438–47. doi: 10.1080/22221751.2019.1590128

13. Zhu Z, Yuan L, Hu D, Lian Z, Yao X, Liu P, et al. Isolation and genomic characterization of a Chinese NADC34-like PRRSV isolated from Jiangsu province. *Transbound Emerg Dis.* (2022) 69:e1015–e27. doi: 10.1111/tbed.14392

14. Xu Y, Ji X, Fu C, Hu D, Pang H, Wang T, et al. Evolution characterization and pathogenicity of a porcine reproductive and respiratory syndrome virus isolate from a pig farm in Shandong Province, China. *Viruses.* (2022) 14:1194. doi: 10.3390/v14061194

15. Xu H, Xiang L, Tang YD, Li C, Zhao J, Gong B, et al. Genome-wide characterization of QYYZ-like PRRSV during 2018-2021. *Front Vet Sci.* (2022) 9:945381. doi: 10.3389/fvets.2022.945381

16. Yu F, Liu L, Tian X, Chen L, Huang X, Sun Y, et al. Genomic analysis of porcine reproductive and respiratory syndrome virus 1 revealed extensive recombination and potential introduction events in China. *Vet Sci.* (2022) 9:450. doi: 10.3390/vetsci9090450

17. Prieto C, Martinez-Lobo FJ, Diez-Fuertes F, Aguilar-Calvo P, Simarro I, Castro JM. Immunisation of pigs with a major envelope protein sub-unit vaccine against porcine reproductive and respiratory syndrome virus (PRRSV) results in enhanced clinical disease following experimental challenge. *Vet J.* (2011) 189:323–9. doi: 10.1016/j.tvjl.2010.07.010

18. Scortti M, Prieto C, Alvarez E, Simarro I, Castro JM. Failure of an inactivated vaccine against porcine reproductive and respiratory syndrome to protect gilts against a heterologous challenge with PRRSV. *Vet Rec.* (2007) 161:809–13. doi: 10.1136/vr.161.24.809

19. Martinez-Lobo FJ, Diez-Fuertes F, Simarro I, Castro JM, Prieto C. The ability of porcine reproductive and respiratory syndrome virus isolates to induce broadly

reactive neutralizing antibodies correlates with in vivo protection. *Front Immunol.* (2021) 12:691145. doi: 10.3389/fimmu.2021.691145

20. Rawal G, Angulo J, Linhares DCL, Mah CK, Van Vlaenderen I, Poulsen Nautrup B. The efficacy of a modified live virus vaccine fostera(R) PRRS against heterologous strains of porcine reproductive and respiratory syndrome virus: a meta-analysis. *Res Vet Sci.* (2022) 150:170–8. doi: 10.1016/j.rvsc.2022.06.026

21. Proctor J, Wolf I, Brodsky D, Cortes LM, Frias-De-Diego A, Almond GW, et al. Heterologous vaccine immunogenicity, efficacy, and immune correlates of protection of a modified-live virus porcine reproductive and respiratory syndrome virus vaccine. *Front Microbiol.* (2022) 13:977796. doi: 10.3389/fmicb.2022.977796

22. Duerlinger S, Knecht C, Sawyer S, Balka G, Zaruba M, Ruemenapf T, et al. Efficacy of a modified live porcine reproductive and respiratory syndrome virus 1 (PRRSV-1) vaccine against experimental infection with PRRSV Aut15-33 in weaned piglets. *Vaccines.* (2022) 10:934. doi: 10.3390/vaccines10060934

23. Zuckermann FA, Garcia EA, Luque ID, Christopher-Hennings J, Doster A, Brito M, et al. Assessment of the efficacy of commercial porcine reproductive and respiratory syndrome virus (PRRSV) vaccines based on measurement of serologic response, frequency of Gamma-Ifn-producing cells and virological parameters of protection upon challenge. *Vet Microbiol.* (2007) 123:69–85. doi: 10.1016/j.vetmic.2007.02.009

24. Tian ZJ, An TQ, Zhou YJ, Peng JM, Hu SP, Wei TC, et al. An attenuated live vaccine based on highly pathogenic porcine reproductive and respiratory syndrome virus (HP-PRRSV) protects piglets against HP-PRRS. *Vet Microbiol.* (2009) 138:34–40. doi: 10.1016/j.vetmic.2009.03.003

25. Leng X, Li Z, Xia M, He Y, Wu H. Evaluation of the efficacy of an attenuated live vaccine against highly pathogenic porcine reproductive and respiratory syndrome virus in young pigs. *Clin Vaccine Immunol.* (2012) 19:1199–206. doi: 10.1128/CVI.05646-11

26. Jiang YF, Xia TQ, Zhou YJ, Yu LX, Yang S, Huang QF, et al. Characterization of three porcine reproductive and respiratory syndrome virus isolates from a single swine farm bearing strong homology to a vaccine strain. *Vet Microbiol.* (2015) 179:242–9. doi: 10.1016/j.vetmic.2015.06.015

27. Yu LX, Wang X, Yu H, Jiang YF, Gao F, Tong W, et al. The emergence of a highly pathogenic porcine reproductive and respiratory syndrome virus with additional 120aa deletion in Nsp2 region in Jiangxi, China. *Transbound Emerg Dis.* (2018) 65:1740–8. doi: 10.1111/tbed.12947

28. Wang J, Zhang M, Cui X, Gao X, Sun W, Ge X, et al. Attenuated porcine reproductive and respiratory syndrome virus regains its fatal virulence by serial passaging in pigs or porcine alveolar macrophages to increase its adaptation to target cells. *Microbiol Spectr.* (2022) 10:e0308422. doi: 10.1128/spectrum.03084-22

29. Wang Y, He W, Li Q, Xie X, Qin N, Wang H, et al. Generation of a porcine reproductive and respiratory syndrome virus expressing a marker gene inserted between ORF4 and ORF5a. *Arch Virol.* (2020) 165:1803–13. doi: 10.1007/s00705-020-04679-3

30. Li Y, Ren C, Li C, Xiao Y, Zhou Y. A recombinant porcine reproductive and respiratory syndrome virus stably expressing a Gaussia luciferase for antiviral drug screening assay and luciferase-based neutralization assay. *Front Microbiol.* (2022) 13:907281. doi: 10.3389/fmicb.2022.907281

31. Xu YZ, Zhou YJ, Zhang SR, Jiang YF, Tong W, Yu H, et al. Stable expression of foreign gene in nonessential region of nonstructural protein 2 (Nsp2) of porcine reproductive and respiratory syndrome virus: applications for marker vaccine design. *Vet Microbiol.* (2012) 159:1–10. doi: 10.1016/j.vetmic.2012.03.015

32. Gao F, Jiang Y, Li G, Zhou Y, Yu L, Li L, et al. Porcine reproductive and respiratory syndrome virus expressing E2 of classical swine fever virus protects pigs from a lethal challenge of highly-pathogenic PRRSV and CSFV. *Vaccine.* (2018) 36:3269–77. doi: 10.1016/j.vaccine.2018.04.079

33. Gao F, Yao H, Lu J, Wei Z, Zheng H, Zhuang J, et al. Replacement of the heterologous 5' untranslated region allows preservation of the fully functional activities of type 2 porcine reproductive and respiratory syndrome virus. *Virology.* (2013) 439:1–12. doi: 10.1016/j.virol.2012.12.013

34. Pizzi M. Sampling variation of the fifty percent end-point, determined by the reed-muench (Behrens) method. *Hum Biol.* (1950) 22:151–90.

35. Li L, Wei Z, Zhou Y, Gao F, Jiang Y, Yu L, et al. Host Mir-26a suppresses replication of porcine reproductive and respiratory syndrome virus by upregulating type I interferons. *Virus Res.* (2015) 195:86–94. doi: 10.1016/j.virusres.2014.08.012

36. Jiang Y, Li G, Yu L, Li L, Zhang Y, Zhou Y, et al. Genetic diversity of porcine reproductive and respiratory syndrome virus (PRRSV) from 1996 to 2017 in China. *Front Microbiol.* (2020) 11:618. doi: 10.3389/fmicb.2020.00618

37. Corzo CA, Mondaca E, Wayne S, Torremorell M, Dee S, Davies P, et al. Control and elimination of porcine reproductive and respiratory syndrome virus. *Virus Res.* (2010) 154:185–92. doi: 10.1016/j.virusres.2010.08.016

38. Zhou YJ, Hao XF, Tian ZJ, Tong GZ, Yoo D, An TQ, et al. Highly virulent porcine reproductive and respiratory syndrome virus emerged in China. *Transbound Emerg Dis.* (2008) 55:152–64. doi: 10.1111/j.1865-1682.2008.01020.x

39. Wang Y, Liang Y, Han J, Burkhart KM, Vaughn EM, Roof MB, et al. Attenuation of porcine reproductive and respiratory syndrome virus strain Mn184 using chimeric construction with vaccine sequence. *Virology.* (2008) 371:418–29. doi: 10.1016/j.virol.2007.09.032

40. Brockmeier SL, Loving CL, Vorwald AC, Kehrli ME, Baker RB, Nicholson TL, et al. Genomic sequence and virulence comparison of four type 2 porcine reproductive and respiratory syndrome virus strains. *Virus Res.* (2012) 169:212–21. doi: 10.1016/j.virusres.2012.07.030

41. Zhang S, Zhou Y, Jiang Y, Li G, Yan L, Yu H, et al. Generation of an infectious clone of HuN4-F112, an attenuated live vaccine strain of porcine reproductive and respiratory syndrome virus. *Virol J.* (2011) 8:410. doi: 10.1186/1743-422X-8-410

frontiers | Frontiers in Veterinary Science

TYPE Original Research
PUBLISHED 16 March 2023
DOI 10.3389/fvets.2023.1158585

OPEN ACCESS

EDITED BY
Xiangdong Li,
Yangzhou University, China

REVIEWED BY
Lang Gong,
South China Agricultural University, China
Bin Li,
Jiangsu Academy of Agricultural Sciences (JAAS), China

*CORRESPONDENCE
Chun-Ling Li
✉ lclclare@163.com
Ming Liao
✉ mliao@scau.edu.cn
Shao-Lun Zhai
✉ zhaishaolun@163.com

†These authors have contributed equally to this work

SPECIALTY SECTION
This article was submitted to Veterinary Infectious Diseases, a section of the journal Frontiers in Veterinary Science

RECEIVED 04 February 2023
ACCEPTED 27 February 2023
PUBLISHED 16 March 2023

CITATION
Li Y, Niu J-W, Zhou X, Chu P-P, Zhang K-L, Gou H-C, Yang D-X, Zhang J-F, Li C-L, Liao M and Zhai S-L (2023) Development of a multiplex qRT-PCR assay for the detection of porcine epidemic diarrhea virus, porcine transmissible gastroenteritis virus and porcine Deltacoronavirus. *Front. Vet. Sci.* 10:1158585. doi: 10.3389/fvets.2023.1158585

Development of a multiplex qRT-PCR assay for the detection of porcine epidemic diarrhea virus, porcine transmissible gastroenteritis virus and porcine Deltacoronavirus

Yan Li[1†], Jia-Wei Niu[1†], Xia Zhou[1†], Pin-Pin Chu[1], Kun-Li Zhang[1], Hong-Chao Gou[1], Dong-Xia Yang[1], Jian-Feng Zhang[1], Chun-Ling Li[1*], Ming Liao[1,2*] and Shao-Lun Zhai[1*]

[1]Guangdong Provincial Key Laboratory of Livestock Disease Prevention, Institute of Animal Health Guangdong Academy of Agricultural Sciences, Scientific Observation and Experiment Station of Veterinary Drugs and Diagnostic Techniques of Guangdong Province, Guangzhou, Guangdong, China, [2]Maoming Branch Center of Guangdong Laboratory for Lingnan Modern Agricultural Science and Technology, Maoming, China

Currently, porcine coronaviruses are prevalent in pigs, and due to the outbreak of COVID-19, porcine coronaviruses have become a research hotspot. porcine epidemic diarrhea virus (PEDV), Transmissible Gastroenteritis Virus (TGEV), and Porcine Deltacoronavirus (PDCoV) mentioned in this study mainly cause diarrhea in pigs. These viruses cause significant economic losses and pose a potential public health threat. In this study, specific primers and probes were designed according to the *M* gene of PEDV, the *S* gene of TGEV, and the *M* gene of PDCoV, respectively, and TaqMan probe-based multiplex real-time quantitative reverse transcription-polymerase chain reaction (qRT-PCR) was developed for the simultaneous detection of PEDV, TGEV, and PDCoV. This method has high sensitivity and specificity, and the detection limit of each virus can reach 2.95 $\times$ 10^0 copies/μl. An assay of 160 clinical samples from pigs with diarrhea showed that the positive rates of PEDV, TGEV, and PDCoV were 38.13, 1.88, and 5.00%; the coinfection rates of PEDV+TGEV, PEDV+PDCoV, TGEV+PDCoV, PEDV+TGEV+PDCoV were 1.25, 1.25, 0, 0.63%, respectively. The positive coincidence rates of the multiplex qRT-PCR and single-reaction qRT-PCR were 100%. This method is of great significance for clinical monitoring of the porcine enteric diarrhea virus and helps reduce the loss of the breeding industry and control the spread of the disease.

KEYWORDS

porcine epidemic diarrhea virus, Transmissible Gastroenteritis Virus, Porcine Deltacoronavirus, porcine coronaviruses, multiplex real-time qRT-PCR

Introduction

Coronaviruses belonging to the family Coronaviridae, the order Nidovirales, are single-stranded, positive-sense RNA viruses with the largest genome among known RNA viruses (1–3). Within swine enteric viruses, coronaviruses are the most devastating pathogens responsible for acute diarrhea, vomiting, dehydration, and high mortality in neonatal and suckling piglets (4–6).

According to the genetic and antigenic characteristics, all coronaviruses were divided into four genera: Alphacoronaviruses, Betacoronaviruses, Gammacoronaviruses, and Deltacoronaviruses (7). Novel coronavirus whole genome sequencing analysis showed that alpha-coronaviruses and beta-coronaviruses infected mammals; gamma-coronaviruses and delta-coronaviruses mainly infected birds, but some viruses could also infect mammals (6).

Coronaviruses, including PEDV, TGEV, and PDCoV, can cause diarrhea in piglets. PEDV and TGEV are alphacoronaviruses, while PDCoV is delta coronavirus.

PEDV was first isolated from porcine intestinal contents in the United Kingdom in 1978. Since then, PEDV has spread worldwide and isolated in many countries, including the USA, the UK, Argentina, Russia, and China, resulting in heavy economic losses to the porcine industry (8–10).

TGEV was first reported in 1946 in the United States, followed by outbreaks in many countries in the Americas, Asia, and Europe. TGEV has the greatest impact on piglets, especially those under 2 weeks of age, who are most susceptible to infection. Piglets often excrete feces containing undigested curds, with mortality rates often reaching 100% (11–13).

PDCoV was identified in pigs in Hong Kong in late 2012 (14). To date, PDCoV has been detected in at least 20 states in the United States, as well as in Canada, South Korea, China, Thailand, Lao People's Democratic Republic, Vietnam, and Mexico, posing a significant threat to the global swine industry (11, 15–19). In addition, PDCoV has been detected in poultry and humans, reflecting the potential for cross-species transmission (20, 21).

The clinical symptoms of the intestinal diseases caused by these swine coronaviruses are highly similar, and it can be challenging to distinguish them. It is important to note that coronaviruses tend to interspecies transmission, as exemplified by SARS-CoV-2 and PDCoV (22–27). By monitoring the epidemiology of coronaviruses in pigs, the potential for cross-species transmission of these viruses and the trend of cross-regional transmission of viruses can be well studied.

So far, PEDV, TGEV, and PDCoV have caused huge economic losses to the pig industry worldwide. In addition, some viruses' cross-species transmission ability may threaten public health. Therefore, developing a simple, rapid, accurate, and high-throughput detection method is necessary to distinguish porcine enteric coronaviruses. A multiplex qRT-PCR detection method based on TaqMan probes was established to detect three viruses, PEDV, TGEV, and PDCoV. This method will improve the virus's detection efficiency and accuracy while reducing the detection cost.

TABLE 1 Primer and probe sequences.

Target genes	Sequences (5′-3′)	Product size (bp)
PEDV-M	F: ATCACYCTTATGCTGTGG ATAATGT	112
	R: CAGAAGTAGTGAGAAGCGCGT	
	Probe: Cy5-CGGTTGTGGCGCAGGACA CATT-BHQ1	
TGEV-S	F: TGAATGGCTCAATAGAA TTGAAAC	120
	R: CAACCTGTRCTACAACAGC AAAATAG	
	Probe: ROX-ATGGCCYTGGTATGTGT GGCTAC-BHQ2	
PDCoV-M	F: CACGCGTAAYCGTGTGATCTA	143
	R: CGGCAAAAVTTATGGACACA	
	Probe: FAM-TGGCTGCTCCAACCC TTCACCC-BHQ1	

The capital letters marked in red represent degenerate bases.

TABLE 2 Multiplex qRT-PCR reaction system.

Reagent	Volume (μl)
2×One Step RT-PCR Buffer III	12.5
TaKaRa Ex Taq HS (5 U/ μl)	0.5
PrimeScript RT Enzyme Mix II	0.5
Primer-F (TGEV/PEDV/PDCoV)	0.8
Primer-R (TGEV/PEDV/PDCoV)	0.8
Probe (TGEV/PEDV/PDCoV)	0.3
Template	1
RNase Free dH_2O	4.8
Total volume	25

Experimental section

Primers and probes

To ensure the detection performance of the primers used in the multiplex qRT-PCR method, all available PEDV, TGEV, and PDCoV sequences were obtained and analyzed from GenBank. The primers and probes of PEDV, TGEV, and PDCoV were designed according to the *M* gene of PEDV, the *S* gene of TGEV, and the *M* gene of PDCoV. Three primer pairs and probes were designed using Oligo 6 (Version 6.44) software (Table 1). TaqMan probes for PEDV, TGEV, and PDCoV were labeled at the 5′-end with the reporter molecule: X-Rhodamine maleimide (ROX), pentamethylene cyanine (CY5) and 5(6)-carboxyfluorescein (FAM), respectively. The 3′-end of TaqMan probes were labeled with the quenchers: 8-Bromo-7-hydroxyquinoline 1 (BHQ1), 8-Bromo-7-hydroxyquinoline 2

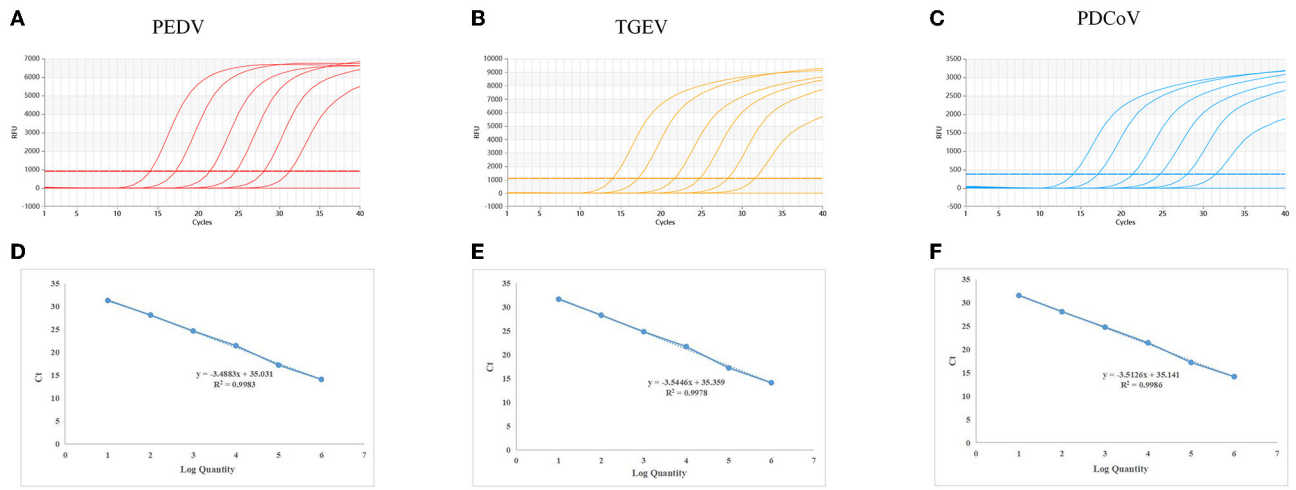

FIGURE 1
Dynamic curves and standard curves of the multiplex qRT-PCR: The dynamic curves were generated using the recombinant standard plasmids p-PEDV-TGEV-PDCoV for PEDV, TGEV, and PDCoV. The standard curves **(D–F)** were generated from the dynamic curves. In **(A–C)**, the plasmid concentrations of curves 1 to 6 ranged from 2.95×10^7 to 2.95×10^2 copies/μl; 7: Negative control.

(BHQ2), 8-Bromo-7-hydroxyquinoline 2 (BHQ2). Primers and probes were synthesized by Sangon Biotechnology (Shanghai) Co., Ltd. Primers were also used to construct plasmid standards.

Virus strains and field samples

RNA extraction and reverse transcription treat intestinal tissue or stool samples with 3 to 5 times PBS, vortex to mix, and collect supernatant after centrifugation at 12,000 × g for 15 min at 4°C. Nucleic acids were extracted using the E.Z.N.A.® Total RNA Kit (Omega Bio-Tek, China) following the manufacturer's instructions. Reverse transcription was performed using the HiScript III RT SuperMix for qPCR (+gDNAwiper) kit (Nanjing Vazyme Biotechnology Co., Ltd.).

Construction of plasmid standards

The target fragments of PEDV, TGEV, and PDCoV were amplified by PCR using PrimeScript™ High-Fidelity RT-PCR Kit [Bao Biomedical Technology (Beijing) Co., Ltd]. The PCR fragment was then cloned into a pUC57 vector [Takara Biomedical Technology (Beijing) Co., Ltd.] by TA colony and confirmed by DNA sequencing, p-PEDV-TGEV-PDCoV. The plasmid copy number was calculated, diluting the plasmids from 2.95×10^7 to 2.95×10^0 copies/μl. Single-reaction qRT-PCR was performed for each virus using the 10-fold diluted plasmids to generate standard curves.

Reaction conditions of the single-plex qRT-PCR

As shown in Table 2, the total volume of the single-reaction qRT-PCR reaction was 25 μl. Amplification was carried out on Gentier 96R (Xi'an Tianlong Science and Technology) using the following program: 95°C 10 s; 40 cycles of 95°C 5 s, 60°C 30 s. The fluorescence signal was automatically collected at the end of each cycle, 35°C 30 s.

Optimization of the multiplex qRT-PCR

The multiplex reaction system was optimized using different volumes of primers (10 μM) and probes (10 μM). In the optimization stage, the number of primers added to the system was 0.4, 0.6, 0.8, 1.0, and 1.2 μl, respectively. The number of probes added to the system was 0.1, 0.2, 0.3, 0.4, 0.5, and 0.6 μl, respectively. The recombinant plasmid (2.95×10^7 copies/μl) was used as the standard plasmid. Finally, each primer and probe concentration's fluorescence intensity and cycle threshold (Ct) value were compared. The same instrument and qRT-PCR program were used as described above. To obtain the best amplification efficiency, the annealing temperature was optimized. Twelve annealing temperature gradients were set up from 44 to 64°C, and each annealing temperature's fluorescence intensity and Ct values were compared.

Sensitivity of the multiplex qRT-PCR assay

The standard plasmids were serially diluted 10-fold from 2.95×10^7 to 0.295×10^0 copies/μl (final concentration) for the standard plasmid and used as templates to evaluate the sensitivity of the developed assay, and the reaction does three repetitions at a time.

Specificity of the multiplex qRT-PCR assay

To verify the specificity of the assay, positive samples for PEDV, TGEV, PDCoV, SADS-CoV, porcine rotavirus (PoRV), porcine pseudorabies virus (PRV), porcine circovirus 2 (PCV-2), porcine

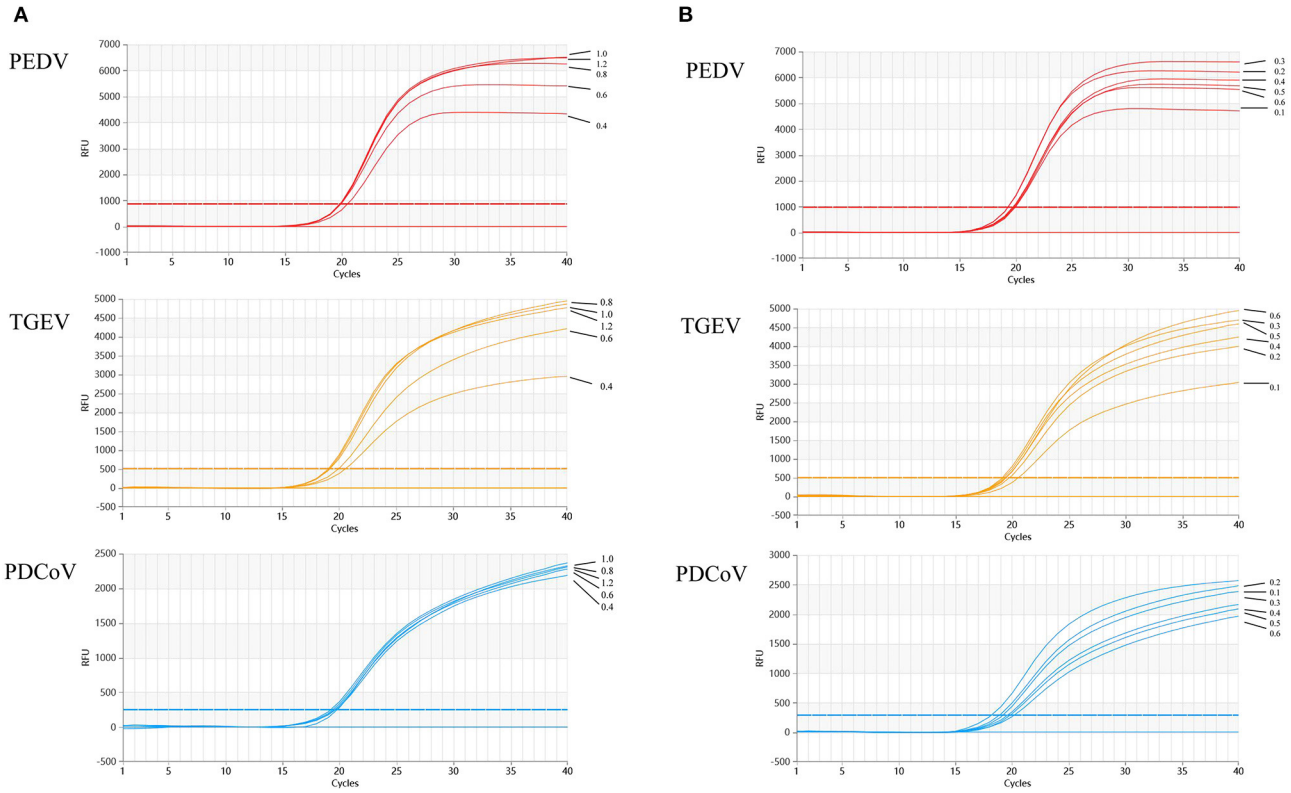

FIGURE 2
Optimization of multiplex qRT-PCR system. **(A)** shows the results of primers optimization in the reaction system, which showed that the optimal addition amount of upstream and downstream primers for TGEV and PEDV are 0.8 μl; the optimal addition amount of upstream and downstream primers for PDCoV is 0.6 μl. Optimization of multiplex qRT-PCR system. **(B)** Multiplex qRT-PCR probe volume optimizations. Probes optimization in the reaction system showed that the optimal addition number of probes for TGEV and PEDV is 0.3 μl; the optimal amount of probes for PDCoV is 0.2 μl.

reproductive and respiratory syndrome (PRRSV) were used for detection by the developed multiplex qRT-PCR. All the samples were previously stored in our laboratory.

Repeatability of the multiplex qRT-PCR assay

The assay was repeated three times with a 7-days interval, using 10-fold dilutions of the standard plasmid of each pathogen ranging from 2.95×10^7 to 2.95×10^2 copies/μl with three replicates per reaction. The coefficient of variation (CV) of the Ct values of the samples at each concentration in the three experiments was calculated to estimate repeatability.

Clinical sample detection

To test the clinical application effect of the developed method, a total of 160 clinical samples collected from pigs with symptoms of diarrhea, including 70 small intestinal tissues and 90 anal swabs, were used for detection. At the same time, a single-plex qRT-PCR was used to verify the results, and the results were compared and analyzed.

Results

Establish a standard curve

The standard plasmids, ranging from 2.95×10^7 to 2.95×10^2 copies/μl, were used to create standard curves. The standard curves showed an acceptable amplification efficiency and correlation coefficient: PEDV, $R^2 = 0.9983$; TGEV, $R^2 = 0.9986$ and PDCoV, $R^2 = 0.9978$, and these results showed that the designed primers and probes were effective (Figure 1).

Optimization of the multiplex reaction system

The standard plasmids p-PEDV-TGEV-PDCoV carrying the target fragments were used as templates to optimize the reaction conditions of the multiplex qRT-PCR. The optimal annealing temperature and the concentrations of primers and probes were acquired based on orthogonal experiments.

The results show that the optimal volume of probe and primer for PEDV and TGEV are 0.3 and 0.8 μl, respectively. The optimal volume of probes and primers

10.3389/fvets.2023.1158585

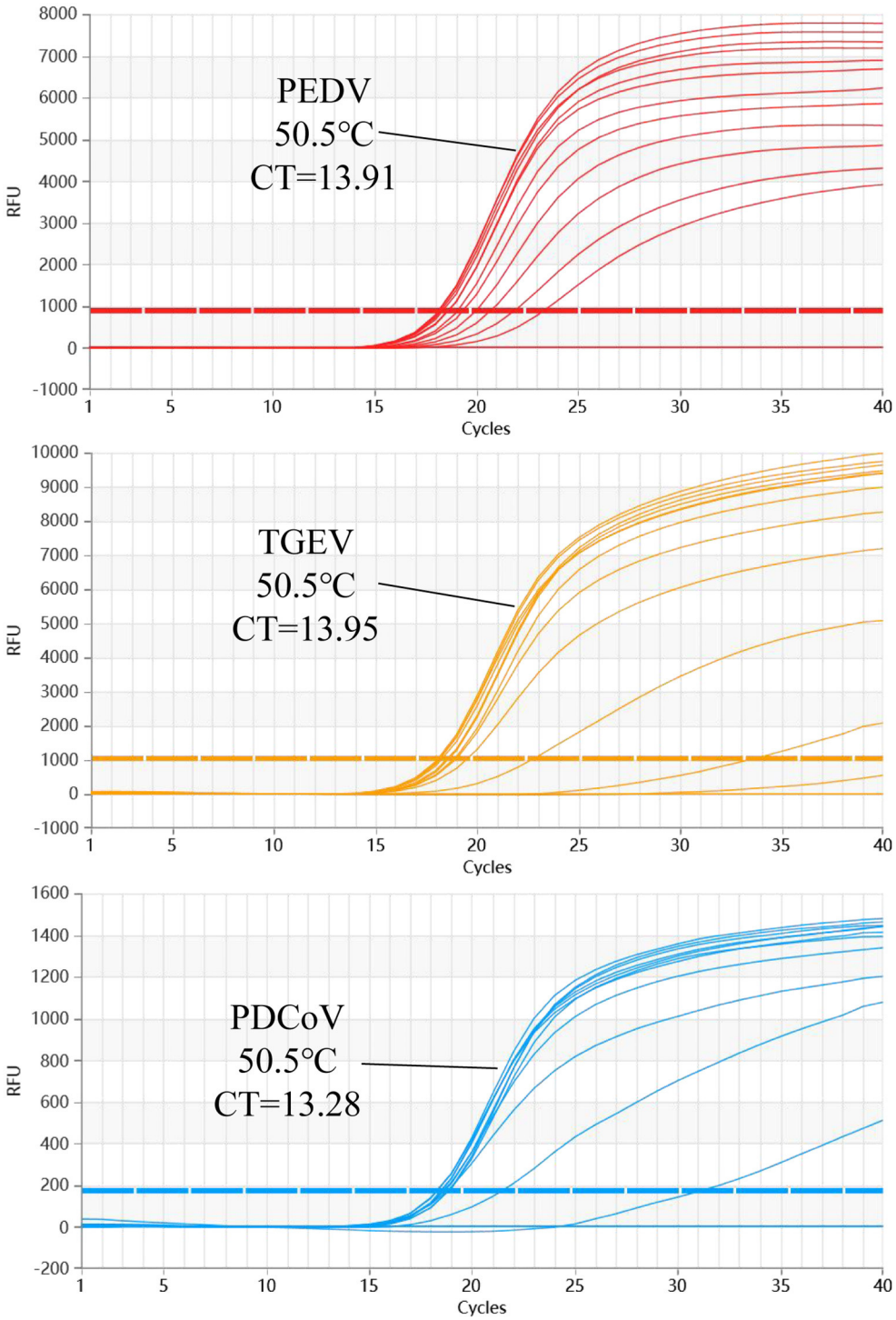

FIGURE 3
The multiplex qRT-PCR amplification curves of different Tm values. The annealing temperature optimization results of multiplex qRT-PCR. The results show that the amplification efficiency of this reaction is the highest when Tm = 50.5°C.

for PDCoV were 0.2 and 0.6 μl, respectively (Figure 2). The results of annealing temperature optimization showed that 50.5°C was the optimal annealing temperature and the reaction had the best amplification efficiency (Figure 3).

Sensitivity of the multiplex qRT-PCR assay

The sensitivity results showed that the detection limit of the developed multiplex qRT-PCR assay was 2.95×10^0 copies/μl of the standard plasmid (Figure 4).

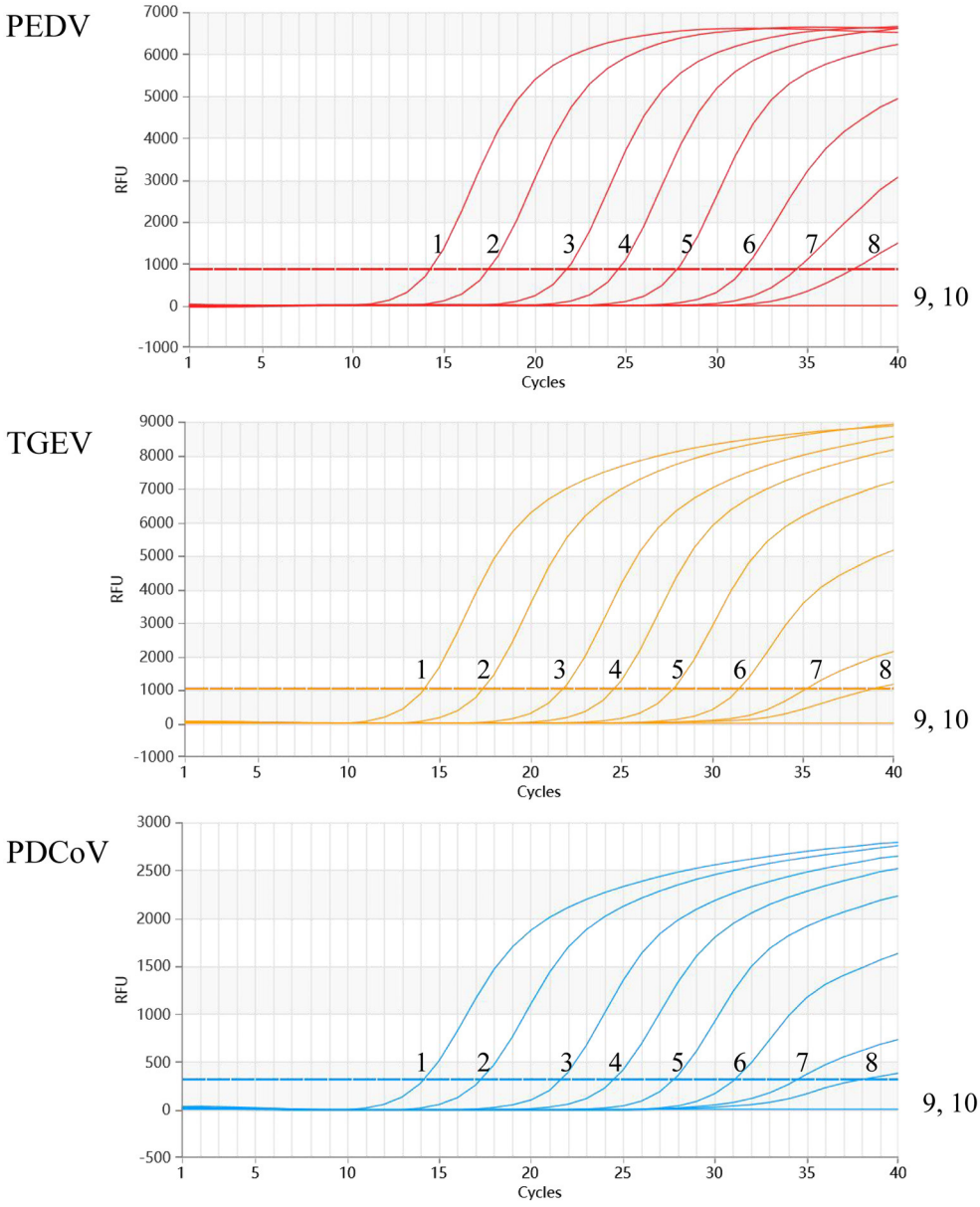

FIGURE 4
Sensitivity of the multiplex qRT-PCR assay. The dynamic curves were generated by using the recombinant standard plasmid p-PEDV-TGEV-PDCoV. 1-9: 2.95 × 107-0.219 × 100 copies/μl (final concentration); 10: Negative control.

Specificity of the multiplex qRT-PCR assay

As shown in Figure 5, the positive samples for PEDV, TGEV, and PDCoV could be detected, while no amplification curve was observed with other viruses of pigs used in the assay.

Repeatability of the multiplex qRT-PCR assay

The repeatability experiment was carried out with the serially diluted standard plasmids (2.95×10^7 to 2.95×10^2 copies/μl) as templates, and the Ct value of the experiment was calculated. As shown in Table 3, the coefficients of variation (CVs) of the intra- and inter-assay ranged from 0.12 to 1.22% and 0.38–1.34%, respectively, <2%. The experimental results showed that the developed multiplex method was stable.

Clinical sample detection

A total of 160 clinical samples, including 70 intestinal tissue samples and 90 anal swab samples from pig farms where diarrhea occurred in southern China, were tested by the developed multiplex qRT-PCR. The results of clinical sample tests showed that the positive rates of PEDV, TGEV, and PDCoV were 38.13% (61/160),

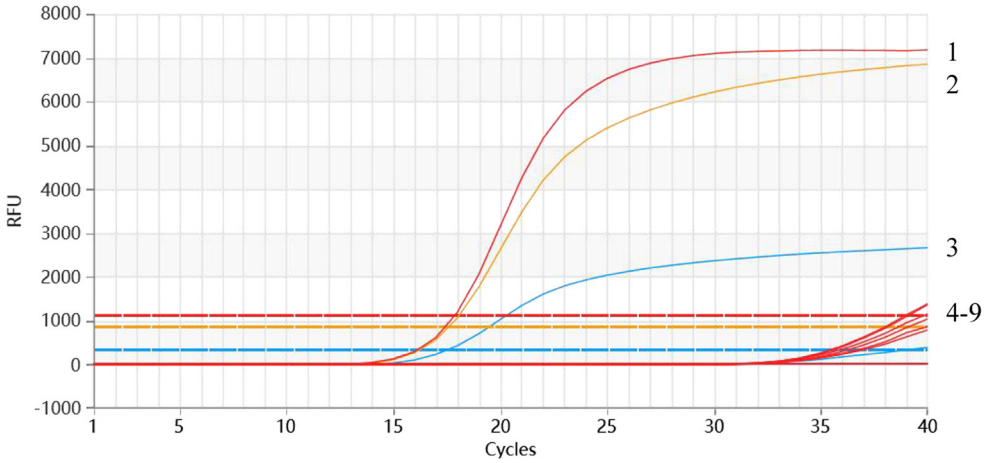

FIGURE 5
Specificity analysis of the multiplex qRT-PCR. 1-3: p-PEDV-TGEV-PDCoV (2.95 × 106 copies/μl); 4: PRRSV; 5: SADS; 6: PRV; 7: PoRV; 8: PCV2; 9: Negative control.

TABLE 3 Repeatability results of the multiplex qRT-PCR assay.

Plasmid	Concentration (copies/μl)	Ct values of intra-assay			Ct value of inter-assay		
		$\bar{x}$	SD	CV (%)	$\bar{x}$	SD	CV (%)
PEDV	2.95×10^7	14.25	0.05	0.36%	14.17	0.17	1.17%
	2.95×10^6	17.52	0.02	0.12%	17.49	0.12	0.67%
	2.95×10^5	21.96	0.25	1.14%	21.90	0.27	1.22%
	2.95×10^4	24.77	0.11	0.45%	24.74	0.09	0.38%
	2.95×10^3	28.03	0.17	0.59%	28.03	0.14	0.51%
	2.95×10^2	31.49	0.19	0.62%	31.44	0.27	0.87%
TGEV	2.95×10^7	14.22	0.04	0.25%	14.16	0.18	1.26%
	2.95×10^6	17.49	0.02	0.09%	17.53	0.16	0.89%
	2.95×10^5	22.02	0.23	1.04%	22.06	0.27	1.22%
	2.95×10^4	24.80	0.12	0.46%	24.82	0.14	0.56%
	2.95×10^3	28.10	0.16	0.56%	28.15	0.14	0.51%
	2.95×10^2	31.45	0.12	0.37%	31.57	0.27	0.85%
PDCoV	2.95×10^7	14.22	0.11	0.74%	14.06	0.19	1.33%
	2.95×10^6	17.38	0.06	0.32%	17.34	0.08	0.45%
	2.95×10^5	21.79	0.27	1.22%	21.77	0.29	1.34%
	2.95×10^4	24.73	0.16	0.63%	24.67	0.20	0.79%
	2.95×10^3	27.97	0.14	0.51%	27.93	0.16	0.57%
	2.95×10^2	31.32	0.21	0.67%	31.28	0.32	1.01%

1.88% (3/160), and 5.00% (8/160), respectively. Additionally, the results also showed that 2 (1.25%) samples were coinfected by PEDV and PDCoV; 2 (1.25%) samples were coinfected by PEDV and TGEV; no coinfection of TGEV and PDCoV, and 1 (0.63%) sample was coinfected with PEDV, TGEV, and PDCoV. To verify the accuracy of the developed method, the clinical samples were detected by single-plex qRT-PCR, and the results of single-plex and multiplex qRT-PCR were compared and analyzed. The coincidence rate of the two methods was 100%, which confirmed that the results of the developed method were accurate and reliable (Table 4).

Discussion

In recent years, the viral diarrhea of piglets has still seriously threatened the development of the pig industry, causing major

TABLE 4 Detection of clinical samples by the multiple and single-reaction qRT-PCR methods.

Pathogens	Triple qRT-PCR			Single-reaction qRT-PCR			Coincidence rate
	Sample number	Positive	Percentage	Sample number	Positive	Percentage	
PEDV	160	61	38.13	160	61	38.13	100%
TGEV	160	3	1.88	160	3	1.88	100%
PDCoV	160	8	5.00	160	8	5.00	100%
PEDV+ TGEV	160	2	1.25	160	2	1.25	100%
PEDV+ PDCoV	160	2	1.25	160	2	1.25	100%
TGEV+ PDCoV	160	0	0	160	0	0	100%
PEDV+ TGEV+ PDCoV	160	1	0.63	160	1	0.63	100%

economic losses to global pig farmers. Clinically, PEDV, TGEV, and PDCoV are piglets' main pathogens causing viral diarrhea (28, 29). The epidemiological survey of pig diarrhea viruses showed that PEDV, TGEV, and PDCoV exhibited a trend of hybrid infection, including PEDV and PDCoV hybrid infections, PEDV and TGEV hybrid infections, and PEDV, TGEV, and PDCoV mixed infections (12, 30). The cause of the intestinal disease of piglets with hybrid infection of these viruses is becoming increasingly complicated. The clinical symptoms caused by PEDV, TGEV, and PDCoV exhibited high similarities, leading to the difficulty of determining the pathogens through clinical symptoms. Studies have shown that hybrid infections of multiple viruses may accelerate the common evolution of single and hybrid viruses or the reorganization of multiple viruses into new viruses, as reported by TGEV and PEDV reorganized strains in 2016 (31–34). Reorganization may produce intestinal virus strains or new viruses, which may cause potential outbreaks or popularity of pig viral diarrhea. Due to the global prevalence of SARS-CoV-2, coronavirus has attracted the great attention of scientists. It is worth noting that the newly discovered pork intestine coronavirus PDCoV has been detected in the infection cases of other species (including humans), indicating the great species crossing potential of PDCoV and a great threat to human public health (20).

Real-time quantitative fluorescent PCR is more sensitive, faster, and more accurate for detecting viral pathogens (35, 36). The multiplex RT-qPCR can detect and differentiate more than one pathogen in a single assay, which is particularly suitable for detecting mixed infection of multiple pathogens. In this study, a real-time multiplex PCR based on three pairs of specific primers and probes was developed for the differential detection of PEDV, TGEV, and PDCoV in one reaction. The developed multiplex qRT-PCR could specifically detect PEDV, TGEV, and PDCoV with the LOD of 2.95×10^0 copies/μl for each pathogen. In multiplex qRT-PCR systems, the primers and probes must have good specificity. Because multiplex groups of oligonucleotides in the system will increase the possibility of non-specific amplification, it is necessary for probes and primers with excellent specificity.

The developed multiplex assay was also used to detect clinical diarrhea samples of piglets from southern China. Among the 160 samples, 61 samples were positive for PEDV, 3 samples for TGEV, and 8 samples for PDCoV, indicating that PEDV was still the major pathogen of piglet diarrhea, while the sporadic infections of PDCoV should also be highly concerned, as the increased detection rate of PDCoV in recent clinical samples. Furthermore, coinfection of PEDV, TGEV, and PDCoV had existed in certain pig herds, confirmed by the detection results that coinfection rates of PEDV/TGEV, PEDV/PDCoV, PEDV/TGEV/PDCoV were 1.25, 1.25, and 0.63%, respectively. Based on the results mentioned above, the developed multiplex real-time PCR could be a useful tool for rapid differentiation of PEDV, TGEV, and PDCoV in clinical samples from piglets with diarrhea and warning the infection of PDCoV.

Conclusion

In conclusion, an excellent detection method should accurately reflect the pathogen's epidemiological data and help researchers monitor and prevent the virus more effectively. Although multiplex qRT-PCR has the advantages of saving time and capital costs, due to the high requirements for primers and probes, it still needs to be improved to develop effective multiplex qRT-PCR, often accompanied by many challenges. The development method can quickly and accurately detect three kinds of porcine diarrhea viruses, PEDV, TGEV, and PDCoV, simultaneously, effectively saving time and cost. The prevalence of different diarrhea viruses in piglets will increase the complexity of diarrhea and make it difficult to prevent and control. As a potential zoonotic pathogen, the prevalence of PDCoV in piglets should also attract continuous attention. Above all, more attention should be given to the molecular prevalence of PEDV, TGEV, and PDCoV, guiding precise prevention and control more effectively in the field.

Data availability statement

The original contributions presented in the study are included in the article/supplementary material, further inquiries can be directed to the corresponding authors.

Author contributions

YL, J-WN, and XZ performed the experiments and drafted the manuscript. J-WN, P-PC, and D-XY prepared materials for the experiments. YL and J-WN participated in the experiments. K-LZ, H-CG, C-LL, and S-LZ contributed to the data analysis. J-FZ, ML,

and S-LZ conceived the study. All authors read and approved the final manuscript.

Funding

We are supported by the grants from Guangzhou Science and Technology Bureau (202206010192), Natural Science Foundation of China (No. U22A20520), Guangdong Academy of Agricultural Sciences (XTXM202202, R2020PY-JC001, and 202122TD), Guangdong Provincial Department of Science and Technology (2021B1212050021), Department of Agriculture and Rural Affairs of Guangdong Province (2022KJ114), and the open competition program of top ten critical priorities of Agricultural Science and Technology Innovation for the 14th Five-Year Plan of Guangdong Province (No. 2022SDZG02).

Conflict of interest

The authors declare that the research was conducted in the absence of any commercial or financial relationships that could be construed as a potential conflict of interest.

Publisher's note

References

1. Brian DA, Baric RS. *Coronavirus Genome Structure and Replication*. Berlin, Heidelberg: Springer Berlin Heidelberg (2005). p. 1–30.

2. Kroneman A, Cornelissen LAHM, Horzinek MC, de Groot RJ, Egberink HF. Identification and characterization of a porcine Torovirus. *J Virol.* (1998) 72:3507–11. doi: 10.1128/JVI.72.5.3507-3511.1998

3. Liao ME, Xie Y, Shi M, Cui J. Over two decades of research on the marine RNA virosphere. *iMeta.* (2022). doi: 10.1002/imt2.59

4. Huang X, Chen J, Yao G, Guo Q, Wang J, Liu G, et al. TaqMan-probe-based multiplex real-time RT-qPCR for simultaneous detection of porcine enteric coronaviruses. *Appl Microbiol Biotechnol.* (2019) 103:4943–52. doi: 10.1007/s00253-019-09835-7

5. Li G, Wu M, Li J, Cai W, Xie Y, Si G, et al. Rapid detection of porcine deltacoronavirus and porcine epidemic diarrhea virus using the duplex recombinase polymerase amplification method. *J Virol Methods.* (2021) 292:114096. doi: 10.1016/j.jviromet.2021.114096

6. Woo PCY, Huang Y, Lau SKP, Yuen K. Coronavirus genomics and bioinformatics analysis. *Viruses.* (2010) 2:1804–20. doi: 10.3390/v2081803

7. Wang Q, Vlasova AN, Kenney SP, Saif LJ. Emerging and re-emerging coronaviruses in pigs. *Curr Opin Virol.* (2019) 34:39–49. doi: 10.1016/j.coviro.2018.12.001

8. Ma L, Lian K, Zhu M, Tang Y, Zhang M. Visual detection of porcine epidemic diarrhea virus by recombinase polymerase amplification combined with lateral flow dipstrip. *BMC Vet Res.* (2022) 18:140. doi: 10.1186/s12917-022-03232-5

9. Pensaert MB, de Bouck P. A new coronavirus-like particle associated with diarrhea in swine. *Arch Virol.* (1978) 58:243–47. doi: 10.1007/BF01317606

10. Yang Y, Yu J, Huang Y. Swine enteric alphacoronavirus (swine acute diarrhea syndrome coronavirus): An update three years after its discovery. *Virus Res.* (2020) 285:198024. doi: 10.1016/j.virusres.2020.198024

11. Hu X, Li N, Tian Z, Yin X, Qu L, Qu J. Molecular characterization and phylogenetic analysis of transmissible gastroenteritis virus HX strain isolated from China. *Bmc Vet Res.* (2015) 11:72. doi: 10.1186/s12917-015-0387-8

12. Liu Q, Wang H. porcine enteric coronaviruses: an updated overview of the pathogenesis, prevalence, and diagnosis. *Vet Res Commun.* (2021) 45:75–86. doi: 10.1007/s11259-021-09808-0

13. Xia L, Yang Y, Wang J, Jing Y, Yang Q. Impact of TGEV infection on the pig small intestine. *Virol J.* (2018) 15:102. doi: 10.1186/s12985-018-1012-9

14. Woo PCY, Lau SKP, Lam CSF, Lau CCY, Tsang AKL, Lau JHN, et al. Discovery of seven novel mammalian and avian coronaviruses in the genus deltacoronavirus supports bat coronaviruses as the gene source of alphacoronavirus and betacoronavirus and avian coronaviruses as the gene source of gammacoronavirus and deltacoronavirus. *J Virol.* (2012) 86:3995–4008. doi: 10.1128/JVI.06540-11

15. Liu C, Zhang X, Zhang Z, Chen R, Zhang Z, Xue Q. Complete genome characterization of novel Chinese porcine deltacoronavirus strain SD. *Genome Announcements.* (2017) 5:17. doi: 10.1128/genomeA.00930-17

16. Madapong A, Saeng-chuto K, Lorsirigool A, Temeeyasen G, Srijangwad A, Tripipat T, et al. Complete genome sequence of porcine deltacoronavirus isolated in Thailand in 2015. *Genome Announcements.* (2016) 4:16. doi: 10.1128/genomeA.00408-16

17. Pérez Rivera C, Ramírez Mendoza H, Mendoza Elvira S, Segura Velázquez R, Sánchez Betancourt JI. First report and phylogenetic analysis of porcine deltacoronavirus in Mexico. *Transbound Emerg Dis.* (2019) 66:1436–41. doi: 10.1111/tbed.13193

18. Wang L, Byrum B, Zhang Y. Detection and genetic characterization of deltacoronavirus in Pigs, Ohio, USA, 2014. *Emerg Infect Dis.* (2014) 20:1227–30. doi: 10.3201/eid2007.140296

19. Woo PCY, Lau SKP, Yip CCY, Huang Y, Tsoi H, Chan K, et al. Comparative analysis of 22 coronavirus HKU1 genomes reveals a novel genotype and evidence of natural recombination in coronavirus HKU1. *J Virol.* (2006) 80:7136–45. doi: 10.1128/JVI.00509-06

20. Boley PA, Alhamo MA, Lossie G, Yadav KK, Vasquez-Lee M, Saif LJ, et al. porcine delta coronavirus infection and transmission in poultry, United States1. *Emerg Infect Dis.* (2020) 26:255–65. doi: 10.3201/eid2602.190346

21. Lednicky JA, Tagliamonte MS, White SK, Elbadry MA, Alam MM, Stephenson CJ, et al. Emergence of porcine delta-coronavirus pathogenic infections among children in Haiti through independent zoonoses and convergent evolution. *medRxiv.* (2021). doi: 10.1101/2021.03.19.21253391

22. Gralinski LE, Menachery VD. Return of the coronavirus: 2019-nCoV. *Viruses.* (2020) 12:135. doi: 10.3390/v12020135

23. Li G, Zhai SL, Zhou X, Chen TB, Niu JW, Xie YS, et al. Phylogeography and evolutionary dynamics analysis of porcine delta-coronavirus with host expansion to humans. *Transbound Emerg Dis.* (2022) 69:14503. doi: 10.1111/tbed.14503

24. Pekar JE, Magee A, Parker E, Moshiri N, Izhikevich K, Havens JL, et al. The molecular epidemiology of multiple zoonotic origins of SARS-CoV-2. *Science.* (2022) 377:960–66. doi: 10.1126/science.abp8337

25. Sun J, He W, Wang L, Lai A, Ji X, Zhai X, et al. COVID-19: epidemiology, evolution, and cross-disciplinary perspectives. *Trends Mol Med.* (2020) 26:483–95. doi: 10.1016/j.molmed.2020.02.008

26. Zhai SL Li CL, Sun MF, Zhang JF, Zheng C, Liao M. Natural infections of SARS-CoV-2 increased in animals: how should humans interact with animals? *J Med Virol.* (2022) 94:3503–05. doi: 10.1002/jmv.27772

27. Zhai SL, Sun MF, Zhang JF, Zheng C, Liao M. Spillover infection of common animal coronaviruses to humans. *Lancet Microbe.* (2022) 3:e808. doi: 10.1016/S2666-5247(22)00198-7

28. Bevins SN, Lutman M, Pedersen K, Barrett N, Gidlewski T, Deliberto TJ, et al. Spillover of Swine Coronaviruses, United States. *Emerg Infect Dis.* (2018) 24:1390–92. doi: 10.3201/eid2407.172077

29. Zhao Y, Qu H, Hu J, Fu J, Chen R, Li C, et al. Characterization and pathogenicity of the porcine delta coronavirus isolated in Southwest China. *Viruses.* (2019) 11:1174. doi: 10.3390/v11111074

30. Si G, Niu J, Zhou X, Xie Y, Chen Z, Li G, et al. Use of dual priming oligonucleotide system-based multiplex RT-PCR assay to detect five diarrhea viruses in pig herds in South China. *AMB Express.* (2021) 11:99. doi: 10.1186/s13568-021-01255-z

31. Akimkin V, Beer M, Blome S, Hanke D, Höper D, Jenckel M, et al. New chimeric porcine coronavirus in swine feces, Germany, 2012. *Emerg Infect Dis.* (2016) 22:1314–15. doi: 10.3201/eid2207.160179

32. Belsham GJ, Rasmussen TB, Normann P, Vaclavek P, Strandbygaard B, Bøtner A. Characterization of a novel chimeric swine enteric coronavirus from diseased pigs in central eastern Europe in 2016. *Transbound Emerg Dis.* (2016) 63:595–601. doi: 10.1111/tbed.12579

33. Ding G, Fu Y, Li B, Chen J, Wang J, Yin B, et al. Development of a multiplex RT-PCR for the detection of major diarrhoeal viruses in pig herds in China. *Transbound Emerg Dis.* (2020) 67:678–85. doi: 10.1111/tbed.13385

34. Zhao P, Bai J, Jiang P, Tang T, Li Y, Tan C, et al. Development of a multiplex TaqMan probe-based real-time PCR for discrimination of variant and classical porcine epidemic diarrhea virus. *J Virol Methods.* (2014) 206:150–55. doi: 10.1016/j.jviromet.2014.06.006

35. Boniotti MB, Papetti A, Lavazza A, Alborali G, Sozzi E, Chiapponi C, et al. porcine epidemic diarrhea virus and discovery of a recombinant swine enteric coronavirus, Italy. *Emerg Infect Dis.* (2016) 22:83–7. doi: 10.3201/eid2201.150544

36. Cao S, Lu H, Wu Z, Zhu S, A. duplex fluorescent quantitative PCR assay to distinguish the genotype I and II strains of African swine fever virus in Chinese epidemic strains. *Front Vet Sci.* (2022) 9:998874. doi: 10.3389/fvets.2022.998874

frontiers | Frontiers in Veterinary Science

TYPE Original Research
PUBLISHED 03 April 2023
DOI 10.3389/fvets.2023.1174031

OPEN ACCESS

EDITED BY
Yanhua Li,
Yangzhou University, China

REVIEWED BY
Zuzhang Wei,
Guangxi University, China
Fangfeng Yuan,
Massachusetts Institute of Technology, United States

*CORRESPONDENCE
Yao-Wei Huang
✉ yhuang@zju.edu.cn
Bin Wang
✉ hlab-wangbin@zju.edu.cn

SPECIALTY SECTION
This article was submitted to Veterinary Infectious Diseases, a section of the journal Frontiers in Veterinary Science

RECEIVED 25 February 2023
ACCEPTED 21 March 2023
PUBLISHED 03 April 2023

CITATION
Zhao Z-Y, Yu D, Ji C-M, Zheng Q, Huang Y-W and Wang B (2023) Comparative analysis of newly identified rodent arteriviruses and porcine reproductive and respiratory syndrome virus to characterize their evolutionary relationships. *Front. Vet. Sci.* 10:1174031. doi: 10.3389/fvets.2023.1174031

Comparative analysis of newly identified rodent arteriviruses and porcine reproductive and respiratory syndrome virus to characterize their evolutionary relationships

Zhuang-Yan Zhao[1], De Yu[1], Chun-Miao Ji[2], Qiankun Zheng[3], Yao-Wei Huang[1,2]* and Bin Wang[2]*

[1]Department of Veterinary Medicine, Zhejiang University, Hangzhou, Zhejiang, China, [2]Guangdong Laboratory for Lingnan Modern Agriculture, College of Veterinary Medicine, South China Agricultural University, Guangzhou, China, [3]DELISI GROUP Co., LTD., Delisi Industrial Park, Weifang, China

Porcine reproductive and respiratory syndrome virus (PRRSV) has caused huge economic losses for the global pig industry, but its origins and evolution remain a mystery. In 2018, the genome sequences of seven arteriviruses isolated from rodents were determined, and here we publish new analysis showing that they may be ancestors of PRRSV. The sequence similarity of these viruses to PRRSV was ~60%, with shared genome organization and other characteristics, such as slippery sequences and C-rich motifs in nsp2, and a transactivated protein sequence in nsp1β. Codon usage basis analysis showed that PRRSV was closer to these rodent arteriviruses than lactate dehydrogenase-elevating virus (LDV) and they were both under pressure of natural selection. Evolutionary analysis revealed that four of the rodent arteriviruses shared the same genus with PRRSV, and were more closely related to PRRSV-2 than PRRSV-1. In addition to this, they all appeared earlier than PRRSV according to evolutionary modeling, and we speculate that they represent an intermediate step in the origin of PRRSV by arterivirus transmission from rodents to swine. Our in-depth analysis furthers our understanding of arteriviruses, and will serve as the basis for subsequent exploration of the evolution of PRRSV and other arteriviruses.

KEYWORDS

rodent arterivirus, porcine reproductive and respiratory syndrome virus (PRRSV), genome, origin, evolution

Introduction

Arteriviruses can infect domestic and wild animals, causing a variety of diseases (1). Arteriviruses (order *Nidovirales*; family *Arteriviridae*) have a positive-sense, single-stranded RNA genome that ranges from 12 to 16 kb (2). Among them, equine arteritis virus (EAV), lactate dehydrogenase-elevating virus (LDV) and simian hemorrhagic fever virus (SHFV) were first isolated separately in 1953, 1960, and 1964, respectively, while porcine reproductive and respiratory syndrome virus (PRRSV) was first recognized in the late 1980s (3–6). Emerging arteriviruses have been discovered in recent years, such as the highly divergent wobbly possum disease virus (WPDV) in New Zealand and some rodent arteriviruses in China (7, 8).

PRRSV has had the greatest economic impact of all arteriviruses, causing reproductive problems in pregnant sows including abortion, stillbirth and mummified fetuses as well as respiratory disease such as pneumonia and dyspnea in piglets (9, 10). PRRSV is divided into two genotypes that share only 60% sequence similarity: PRRSV-1 is mainly distributed in European countries; PRRSV-2 is mainly distributed in North America and Asia (11, 12). Their prototypes, Lelystad virus and VR-2332, respectively, were isolated separately in the Netherlands and the United States almost simultaneously (13, 14). Subsequently, outbreaks of severe disease occurred in the United States in 1996 and 2001, and in China in 2006 (6, 15–17).

Though the exact ancestor of PRRSV is still unknown, some have speculated it to be LDV; however, several strains of arterivirus have recently been isolated from rodents in China, with a much closer evolutionary relationship to PRRSV than LDV, leading to speculation that they are likely the original ancestor of PRRSV (8). Therefore, the aim of this study was to investigate this newly discovered evolutionary relationship by comparing the genome organization and codon usage bias in details, providing further insight into the origin of PRRSV.

Materials and methods

Genetic material

The complete sequences of 43 arteriviruses were downloaded from GenBank (http://www.ncbi.nlm.nih.gov); detailed information about the viruses is listed in Supplementary Table S1.

Codon usage analysis

Different aspects of codon usage in the arterivirus coding sequences (CDS) were analyzed: the frequency of nucleotides (A%, C%, U%, and G%); G+C content (GC); G+C content at the first, second or third position, (GC1, GC2, GC3, respectively); the frequency of nucleotides G+C at the third synonymous codon positions (GC3s); codon adaptation index (CAI), representing the fitness coefficient of all codons encoding the protein in the case of using optimal codons; effective number of codons (ENC), reflecting the degree to which codons deviate from random selection (usually low-expressed genes have a weaker codon usage bias and a larger ENC value).

The nucleotide content of each arterivirus coding sequence was calculated using the CAI calculator website (http://genomes.urv.es/CAIcal/), and CAI and ENC values were calculated using the program CodonW 1.4.2.

Neutrality plot analysis

Neutrality plot analysis is an analytical method for evaluating the use of codons, and it reflects the factors that affect codon usage bias. A scatter plot was drawn with GC12 as the vertical coordinate and GC3 as the abscissa coordinate of each gene, and the correlation between the two was analyzed. If the regression coefficient was >0 and the correlation coefficient >0.75, it meant that GC3 was significantly related to GC12, further illustrating that the codons in three positions have the same variation pattern and mutation is the main factor of codon usage bias. Conversely, if the correlation between GC3 and GC12 was not significant, it indicated that the variation patterns of the codons in three positions are quite different, i.e., the codon usage bias is mainly affected by natural selection. The scatter plot was drawn by Graphpad Prism 8.0.2.

TABLE 1 The marginal likelihoods estimated of molecular clock models and coalescent models.

Model of rate variation	Coalescent tree prior	Log marginal likelihood	Rank
Strict clock	Constant size	−21643.0146	4
Strict clock	Bayesian skyline	−21641.4570	3
Uncorrelated lognormal relaxed clock	**Constant size**	**−21485.3313**	**1**
Uncorrelated lognormal relaxed clock	Bayesian skyline	−21488.8779	2

The best-fitting combination of molecular clock models and coalescent tree prior are indicated in bold font.

ENC-GC3s plot analysis

The ENC-GC3s plot was drawn with the ENC values plotted against the GC3s values, and the theoretical ENC values of each gene were calculated according to the formula for drawing the standard curves, with GC3s as the abscissa and the theoretical ENC values as the ordinate. A gene lying on or near the standard curve indicates that the codon usage bias is only affected by mutation and has no selection pressure, whereas distribution far away from the standard curve means the codon usage bias is mainly affected by natural selection factors. The standard ENC values were calculated using the formula:

$$ENC_{expected} = 2 + S + \frac{29}{(S^2 + (1 - S)^2)}$$

where "s" represents the given GC3s value.

Parity rule 2 plot (PR2-plot) analysis

In this plot, G3/(G3 + C3) was compared to A3/(A3 + U3) to analyze the base composition on the nucleotide of the third codon, so as to explore the influence of mutation and natural selection on the codon usage bias. The midpoint 0.5 in Figure 3C represents A = U and G = C, indicating no bias toward mutation or selection effect between the two complementary strands of a gene; the vector from the center point to other site shows the degree and direction of bias in the gene. The neutral theory proves that if codon usage bias is only affected by genetic mutations, then the usage frequency of the four bases will be equal, and a relatively equal distribution is expected to be shown in the plot. The scatter plot was drawn by Graphpad Prism 8.0.2.

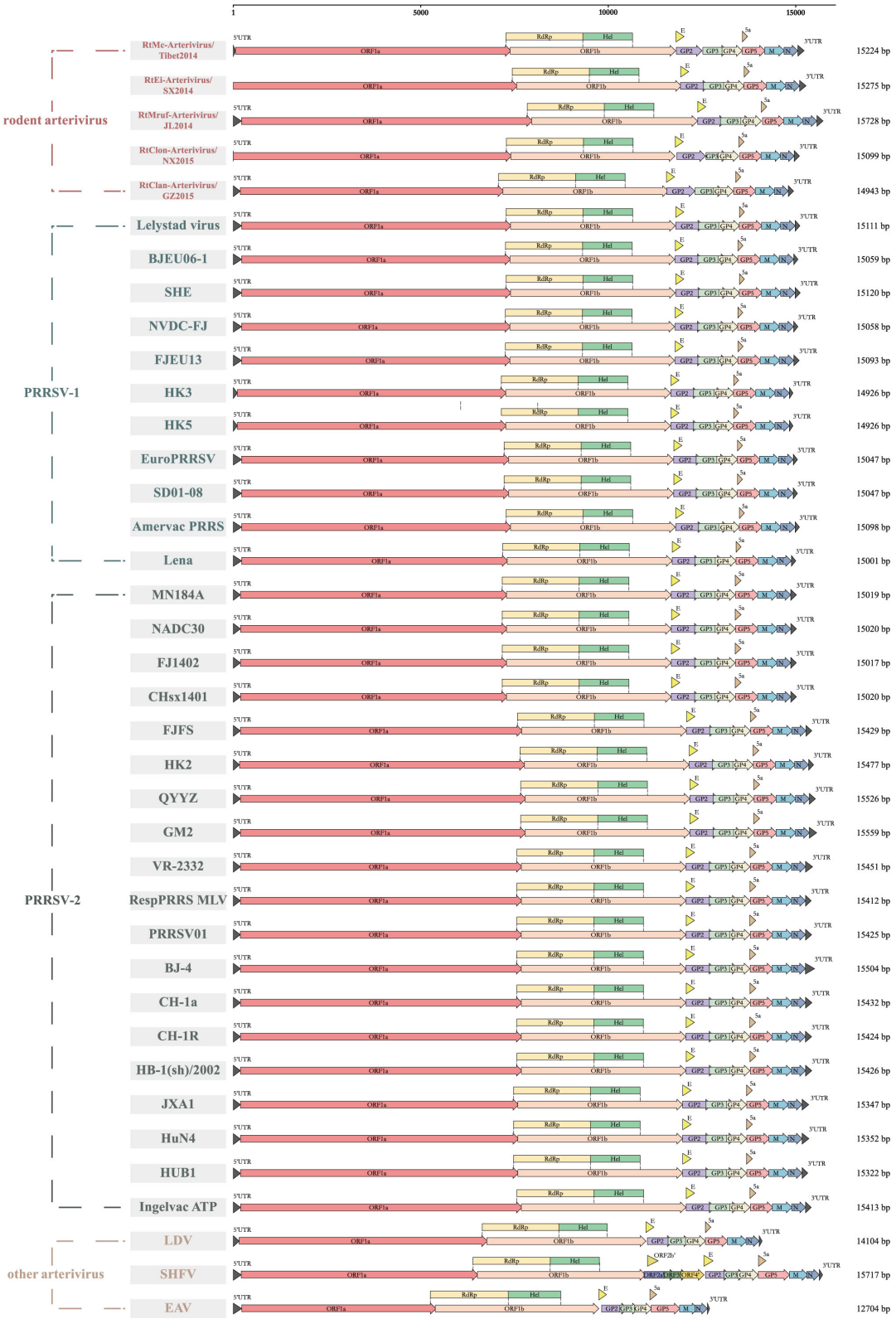

FIGURE 1
Genome organization of different arteriviruses. Every ORF is marked to show the genomic differences among them. ORF1a, ORF1b, GP2, envelope (E), GP3, GP4, 5a, GP5, membrane (M), nucleocapsid (N) are represented by boxes of different colors.

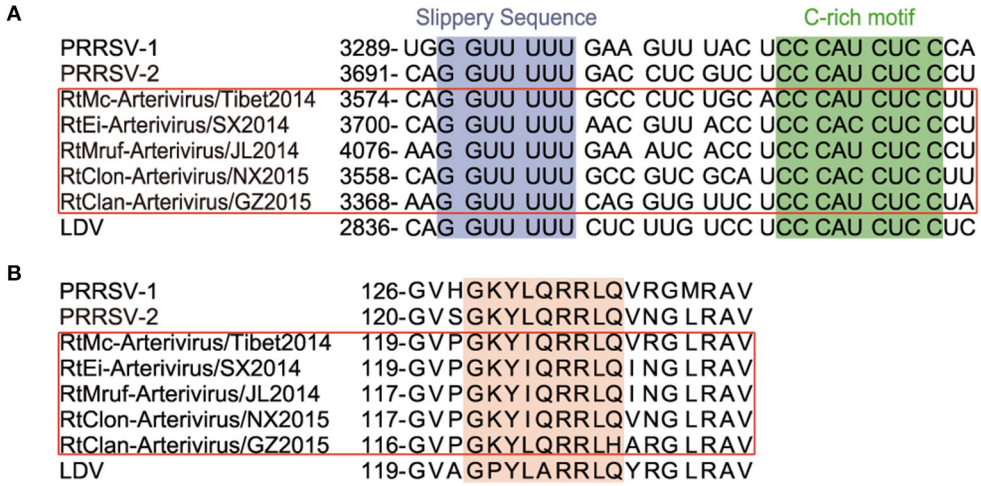

FIGURE 2
−2 PRF-related elements of arterivirus. The conserved "slippery sequence" and C-rich motif in nsp2 are highlighted in purple and green, respectively **(A)**, and the transactivated protein sequence in nsp1β is highlighted in orange **(B)**.

Relative synonymous codon usage (RSCU) analysis

RSCU represents the ratio of the actual usage value of the codon to the theoretical use value. When RSCU is <1 or >1, it means the usage frequency of the codon is lower or higher, respectively, than that of other synonymous codons; RSCU = 1 considers that the codon has no preference. The codon usage pattern heatmap was drawn by TBtools (18), and RSCU values were calculated as follows:

$$RSCU = \frac{x_{ij}}{\sum_{j}^{ni} x_{ij}} n_i$$

Phylogenetic analysis

Sequence alignment of the complete genomes and selected genes including RNA-dependent RNA polymerase (RdRp), helicase (Hel), 3C-like protease (3CLpro) and nucleocapsid (N) was performed using MAFFT v 7.475 (19). Maximum-likelihood (ML) phylogenetic tree construction was performed with 1,000 bootstraps using IQ-tree v 1.6.12 (20), and the best-fitting nucleotide substitution model was calculated automatically by the program. Finally, the results were visualized using iTOL (http://itol.embl.de/).

Origin and evolutionary analysis

In order to investigate the relationship between the rodent arteriviruses and PRRSV, a time-scaled phylogenetic tree of the Hel gene was constructed. The evolutionary rate was estimated using BEAST v 1.10.4 with a separate GTR+F+G4 nucleotide substitution model analyzed by PhyloSuite v 1.2.2, and the uncorrelated lognormal relaxed constant clock model selected by both path sampling and stepping-stone sampling procedures (Table 1) (21–23). We operated MCMC duplicate runs of 1 billion states each with sampling every 100,000 steps, and then examined the result using Tracer v1.6 to ensure the effective sample size (ESS) values of all estimated parameters was >200. The final maximum clade credibility (MCC) tree was generated by TreeAnnotator v 1.10.4 and visualized in Figtree v1.4.4 after discarding the first 10% of the samples.

Results

Genome organization and characteristics

Rodent arteriviruses have single-stranded, positive-sense polycistronic RNA genomes with similar organization to the other arteriviruses (Figure 1). Their genomes encode at least 11 known open reading frames (ORF) with a 5′ cap and a 3′ poly-A tail, in the order of 5′-polyprotein (pp) 1a, pp1b, GP2, envelope (E), GP3, GP4, 5a, GP5, membrane (M) and N-3′. The first two ORFs occupy two-thirds of the genomes and use a −1 programmed ribosomal frameshifting (-1PRF) strategy to encode at least 13 non-structural proteins (nsps). The size and the GC content of the genomes of seven rodent arterivirus are shown in Supplementary Table S1, where two of them, RtDs-Arterivirus-4/IM2014 and RtDs-Arterivirus-1/IM2014, did not detect the full length.

All members of arterivirus except EAV use a −2 programmed ribosomal frameshifting (−2PRF) mechanism and produce a transframe (TF) protein (nsp2TF) at an efficiency of about 20% of nsp2. This protein, comprising the N-terminal two thirds of nsp2 fused to a 169-aa fragment encoded by the TF ORF, is stimulated by a highly conserved "slippery sequence" (G_GUU_UUU) and a C-rich motif (CCCANCUCC) 11 nt-downstream. Moreover, it was identified that a subunit of viral protein nsp1β (GKYLQRRLQ) is a transactivator of efficient −2 PRF expression (24). We found that

10.3389/fvets.2023.1174031

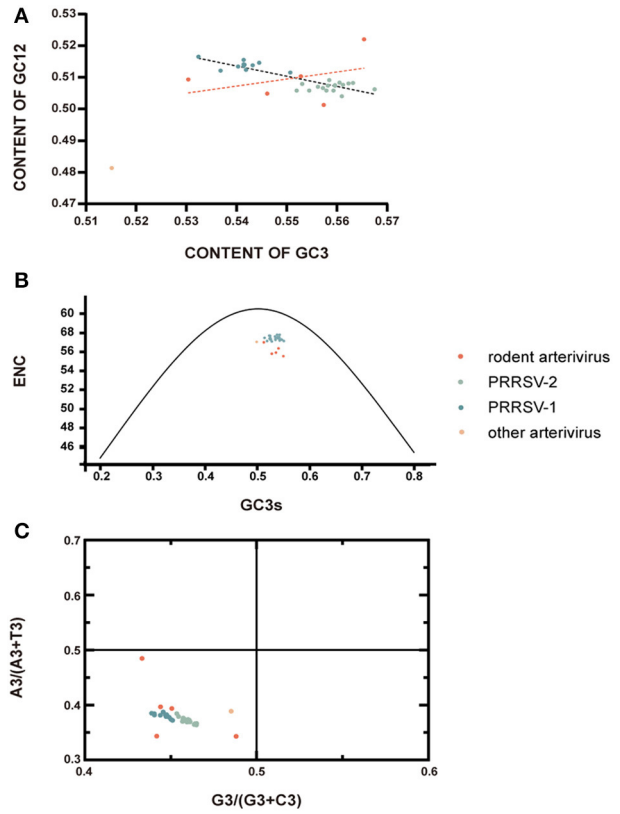

FIGURE 3
Selection pressure analysis. **(A)** Neutrality plot analysis. GC12 plotted against GC3. The dashed black line is fitted by the scatter points of GC12 and GC3 of PRRSV, and the black formula next to it illustrates the relationships between them; rodent arterivirus is represented by the orange line. **(B)** ENC plotted against GC3s. The black curve represents the theoretical ENC values when the codon usage was only determined by the GC3s composition. **(C)** PR2-plot analysis. A3/(A3 + U3) is plotted against G3/(G3 + C3); the midpoint represents A = U and G = C.

the nsp2 of rodent arteriviruses also has the conserved slippery sequence as well as the C-rich motif mentioned above, and also contains the transactivation protein sequence in nsp1β, which is assumed to be able to perform −2PRF for production of nsp2TF (Figure 2).

The TRS (transcription regulatory sequence) is particularly important for viral transcription and replication, especially in the process of discontinuous transcription of subgenomic mRNA. The genomic TRS of rodent arterivirus can be summarized as [U/A]UAACC, which is similar to the UUAACC of PRRSV and UAUAACC of LDV (Supplementary Table S2). Although the base composition of the first four positions in the TRS varies to some extent, the highly conserved CC at the last two positions is critical for complementary base pairing during discontinuous transcription. We also found that although these TRS sequences differ between the ORFs, they all have a certain degree of conservation in the same ORF, except for RtClan-Arterivirus/GZ2015 in ORF5 and RtMc-Arterivirus/Tibet2014 in ORF6.

Codon usage bias

Analysis of codon usage of the rodent arterivirus genomes revealed a slightly lower proportion of A (21.62%) compared with U (26.09%), G (25.69%), and C (26.60%) (Supplementary Table S3). The ENC values of all 43 arteriviruses were >45, which implies that their codon usage bias is weak (Supplementary Table S3). CAI can be used to assess the expression level of genes, generally between 0 and 1, with larger values indicating a stronger preference for codon use, and the CAI of these 43 arteriviruses were all below 0.23, again indicating that their codon usage bias is weak (Supplementary Table S3).

Neutrality plot analysis showed that the regression coefficient between GC3 and GC12 of rodent arterivirus is 0.2217, with a correlation coefficient of 0.3740, meaning the correlation was not significant (Figure 3A). Their coefficient of determination was 0.1399; i.e. only 13.99% change of GC3 resulted in a change of GC2 (Figure 3A). All in all, these data show that the base composition of the codon at the first and second position is quite different from that of the third position. Moreover, the codon usage bias of the rodent arteriviruses is more affected by the pressure of directional mutations of external natural selection than the pressure of their own non-directional mutations. The regression coefficient and the correlation coefficient between GC3 and GC12 of PRRSV were −0.3235 and −0.8703, respectively, a significant inverse correlation that indicates the base composition of the codon at the first and second position is also quite different from the third. However, the overall GC content was relatively stable, and the own non-directional mutation pressure has a great impact on codon usage bias (Figure 3A).

The mean ENC values for rodent arterivirus and PRRSV were 56.14 and 57.42, respectively, which indicates the codon usage bias in these viruses is a little low. All of the rodent arteriviruses and PRRSV fell far below the standard curve in the ENC-GC3s plots, demonstrating that the codon usage patterns of the two viruses are also affected by external natural selection pressure and other factors (Figure 3B).

PRRSV and the rodent arteriviruses were all distributed in the lower left area of the PR2-plot analysis, indicating that the frequency of nucleotide U and C at the third positions is greater than A and G, evidence of a clear preference (Figure 3C). Therefore, it can be inferred that the usage patterns of these codons are not only affected by their self-mutations, but also by factors such as natural selection.

As shown in Figure 4, the codon usage pattern of rodent arterivirus is very similar to that of other arteriviruses. RtClan-Arterivirus/GZ2015, Arterivirus/NX2015 and RtMc-Arterivirus/Tibet2014 clustered with PRRSV-2, RtMruf-Arterivirus/JL2014 clustered with PRRSV-1, and RtEi-Arterivirus/SX2014 was similar to LDV (Figure 4).

Phylogenetic analysis and evolutionary analysis

Phylogenetic trees of the rodent arteriviruses, PRRSV and other arteriviruses were constructed based on nucleotide sequences of

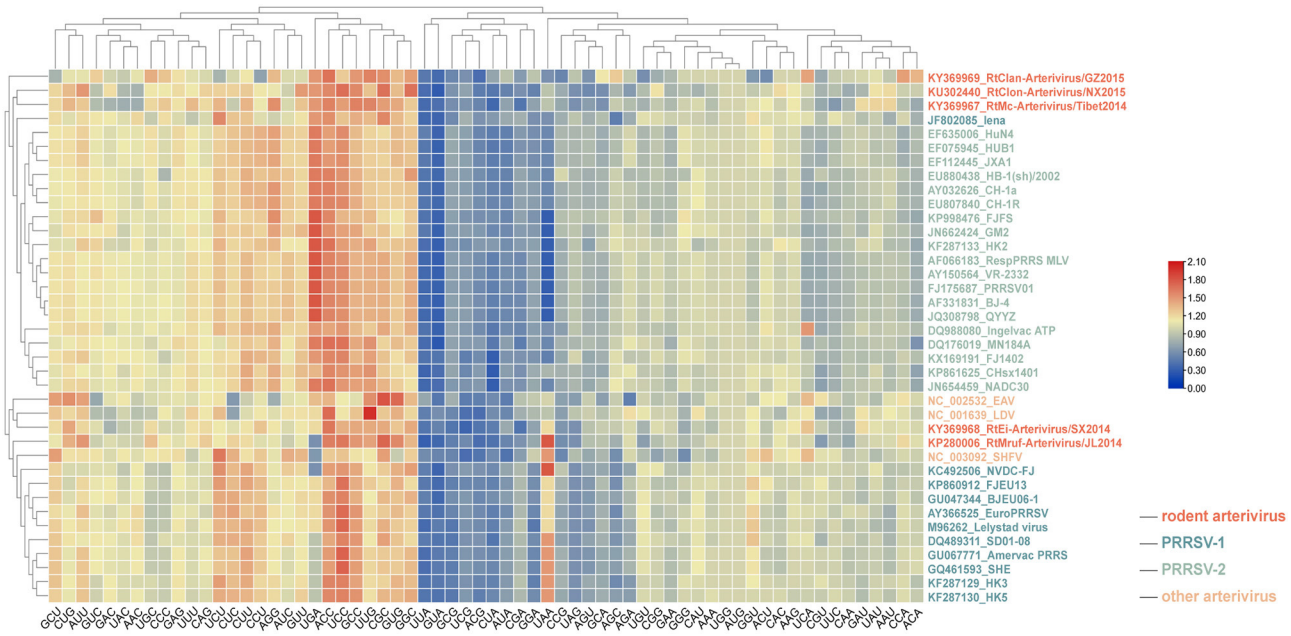

FIGURE 4
Relative synonymous codon usage (RSCU) comparisons between different arteriviruses. Frequently used codons with higher RSCU values are in red, moderately used codons are in yellow, while the less frequently used codons are represented in blue.

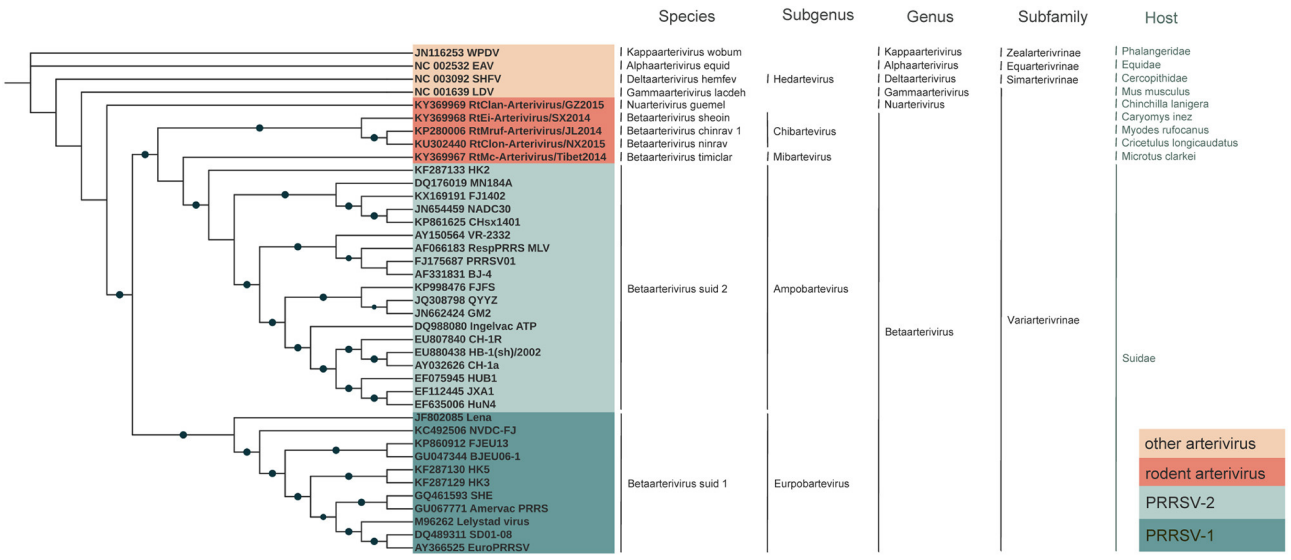

FIGURE 5
Phylogenetic analyses of arterivirus. Whole genome trees were constructed by using the maximum-likelihood (ML) method and bootstrap values calculated from 1,000 trees.

the full genome or RdRp, Hel, 3CLpro, and N genes. In the full genome-based phylogenetic tree, RtMc-Arterivirus/Tibet2014, RtEi-Arterivirus/SX2014, RtMruf-Arterivirus/JL2014, and RtClon-Arterivirus/NX2015 clustered together with PRRSV-2 and were closer than PRRSV-1, while RtClan-Arterivirus/GZ2015 was outside these strains (Figure 5).

RtMruf-Arterivirus/JL2014, RtEi-Arterivirus/SX2014, RtClon-Arterivirus/NX2015, RtMc-Arterivirus/Tibet2014 and PRRSV all belong to *Betaarterivirus*, while RtClan-Arterivirus/GZ2015 belongs to another genus, *Nuarterivirus* (Figure 5). In trees based on the three highly conserved RdRp, Hel and 3CLpro genes, it can be seen that RtMc-Arterivirus/Tibet2014, RtEi-Arterivirus/SX2014,

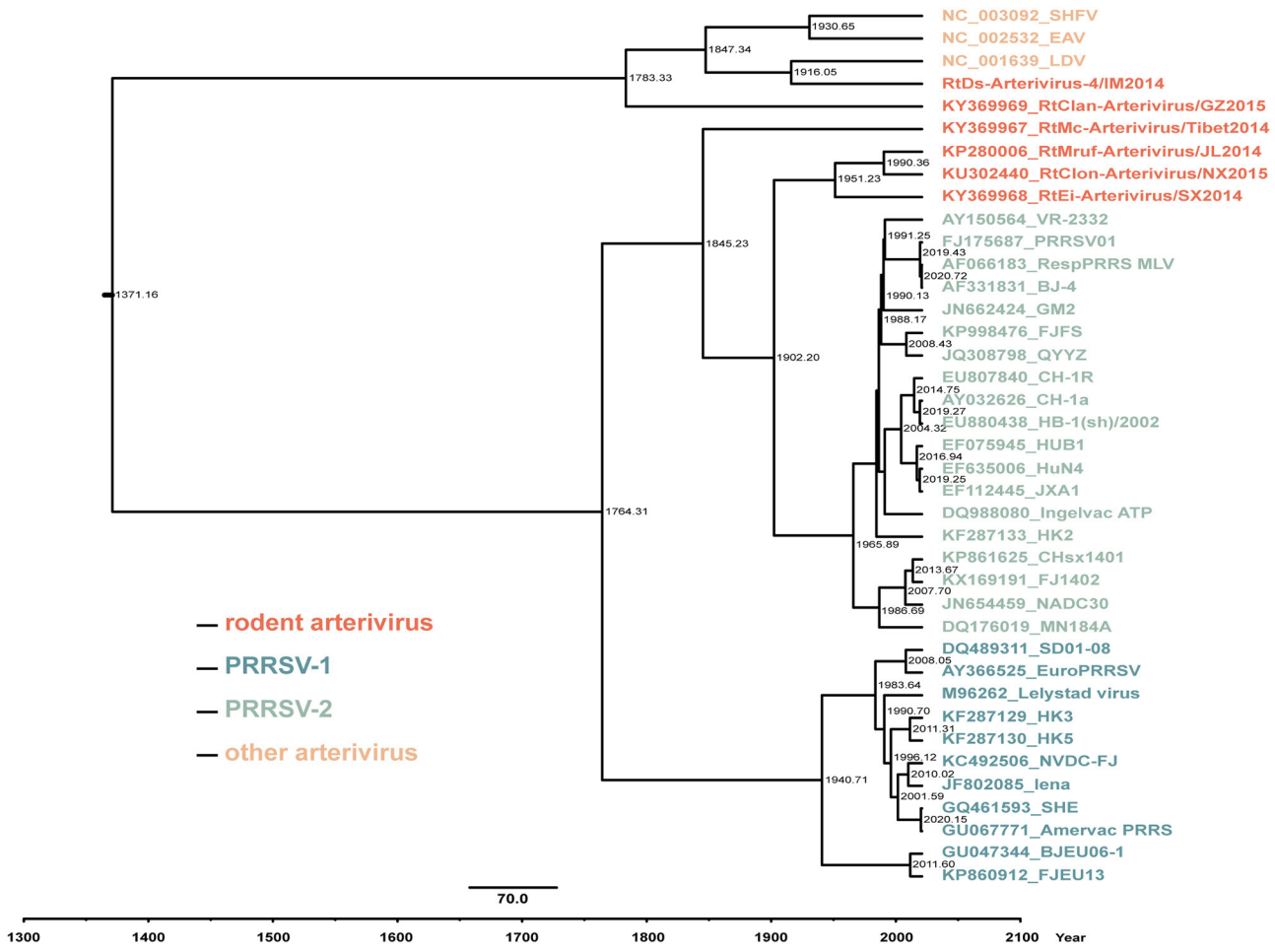

FIGURE 6
Estimation of the mean time to the most recent common ancestor (tMRCA) for arterivirus based on the helicase (Hel) gene. The time-scaled phylogeny was summarized from all Markov chain Monte Carlo (MCMC) phylogenies of the Hel gene data set analyzed under the GTR + F + G4 nucleotide substitution model and the uncorrelated lognormal relaxed constant clock model in BEAST v1.10.4. The numbers near the internal node indicate the estimated time of divergence.

RtMruf-Arterivirus/JL2014, Arterivirus/NX2015 were closer to PRRSV-2 than PRRSV-1, but RtClan-Arterivirus/GZ2015 and RtDs-Arterivirus-4/IM2014 were always on the periphery (Supplementary Figures S1A–C). However, these strains were relatively close to PRRSV-1 in the N-based tree (Supplementary Figure S1D).

The results of molecular clock analysis using the Hel gene were consistent with the phylogenetic tree, with RtEi-Arterivirus/SX2014, RtMruf-Arterivirus/JL2014, and RtClon-Arterivirus/NX2015 closest to PRRSV-2, followed by RtMc-Arterivirus/Tibet2014, RtClan-Arterivirus/GZ2015 and RtDs-Arterivirus-4/IM2014 at the periphery of PRRSV (Figure 6). In addition, we found that the mean time to the most recent common ancestor (tMRCA) of RtEi-Arterivirus/SX2014 was March 1951 [95% highest posterior density (HPD), April 1853 to July 2006], that of RtMruf-Arterivirus/JL2014 and RtClon-Arterivirus/NX2015 was May 1990 (95% HPD, October 1930 to February 2018), that of RtMc-Arterivirus/Tibet2014 was March 1845 (95% HPD, April 1614 to October 1957), that of LDV and RtDs-Arterivirus-4/IM2014 was January 1916 (95% HPD, April 1643 to February 2014), and that of RtClan-Arterivirus/GZ2015 was April 1783 (95% HPD, December 1406 to November 1982) (Figure 6). It can be seen that RtEi-Arterivirus/SX2014, RtMruf-Arterivirus/JL2014, and RtClon-Arterivirus/NX2015 appeared earlier than PRRSV and later than LDV, and not only was RtClan-Arterivirus/GZ2015 in the periphery of PRRSV, but it also appeared much earlier than LDV.

Nucleotide, amino acid identity and codon usage analysis

The nucleotide and amino acid identity of PRRSV relative to RtClan-Arterivirus/GZ2015, LDV and other rodent arteriviruses in RdRp, Hel, 3CLpro and N is shown in Figure 7. The identity of PRRSV was clearly more similar to the rodent arteriviruses than to LDV, and the average difference in identity values was about

10.3389/fvets.2023.1174031

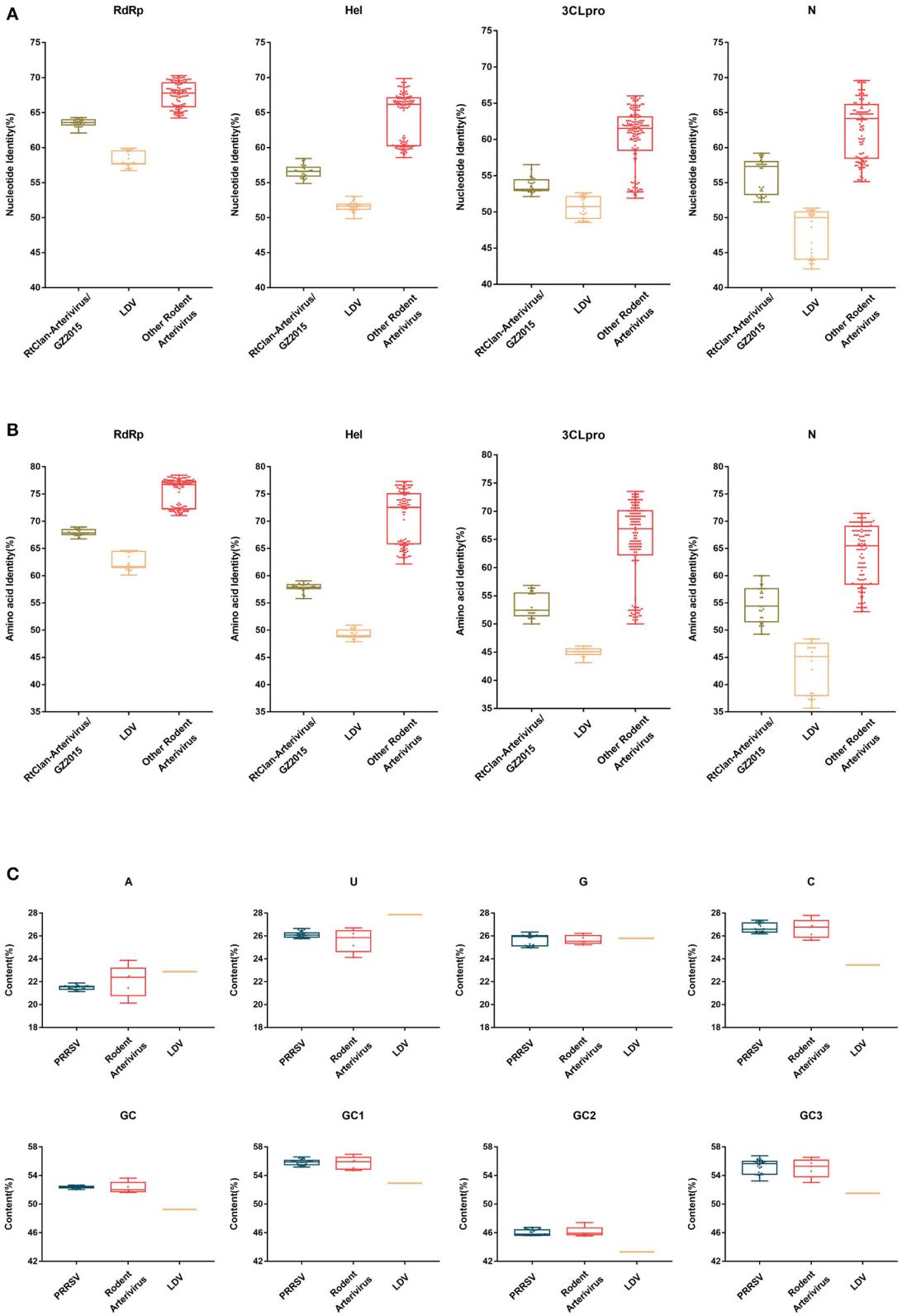

FIGURE 7
Nucleotide, amino acid identity and codon usage bias of PRRSV and rodent arterivirus. The nucleotide identity **(A)** and putative amino acid identity **(B)** compared to PRRSV of RNA-dependent RNA polymerase (RdRp), helicase (Hel), 3C-like protease (3CLpro) and nucleocapsid (N) genes were analyzed by BioAider v 1.314. The A%, U%, G%, C%, GC1, GC2, GC3, and GC of arterivirus **(C)** were calculated using the CAI calculator website (http://genomes.urv.es/CAIcal/). Each dot represents the corresponding value of each strain. The box size represents the interquartile range (IQR), which is equal to the difference between the upper quartile and the lower quartile. The middle horizontal line of the box represents the median of the samples.

10–21% (Figures 7A, B), indicating that rodent arteriviruses have a closer evolutionary relationship with PRRSV than LDV. However, RtClan-Arterivirus/GZ2015, which has a more distant evolutionary relationship, is more similar than LDV to PRRSV, inconsistent with the evolutionary tree and molecular clock analysis.

Since RtClan-Arterivirus/GZ2015 was closer to rodent arterivirus at the nucleotide level, we analyzed codon usage of all the rodent arteriviruses. Based on the analysis, the GC content of codons in three positions is different, and the average GC content at each position (high to low) was GC1, GC3, GC2.We can also see that PRRSV and rodent arteriviruses are very similar, but there is a gap with LDV, indicating that the codon usage bias of PRRSV and rodent arterivirus is more similar than LDV (Figure 7C).

Discussion

In this article, we collected sequences from 7 rodent arteriviruses, 33 PRRSV isolates, and three other representative arteriviruses (LDV, SHFV and EAV) and conducted in-depth analysis of their genomes, codons, and phylogenies. The newly discovered rodent arteriviruses have a genome size and organization similar to other arteriviruses, and share other conserved features such as slippery sequences and C-rich motifs in the nsp2, and the transactivated protein sequence in nsp1β. In addition, the TRS of these viruses is very similar to that of PRRSV and LDV, indicating a common transcription regulatory strategy and supporting their close evolutionary relationship.

We found all 43 arteriviruses studied to have weak codon usage bias and are under greater pressure from external natural selection than from their own non-directional mutations. Although the primary structure of proteins obtained after translation from synonymous codons is the same, codon usage bias may affect gene expression, as reflected in the effects on mRNA secondary structure and protein abundance (25, 26). Therefore, the similarity of codon usage bias between PRRSV and rodent arteriviruses suggests that there are similar gene expression patterns between them, further evidence of a close evolutionary relationship.

From evolutionary analysis, it can be concluded that PRRSV diverged from other arteriviruses more than 100 years ago, and PRRSV likely existed in swine prior to its discovery in the late 1980s (6). Previous studies speculated that because LDV is older and closest to PRRSV in the *Arteriviridae*, some LDV-like rodent virus might spread to wild boars in Asia and Europe through wounds and other routes, making them intermediate hosts (27, 28). According to this theory, PRRSV-1 was transmitted from European wild boars to European domestic swine, and PRRSV-2 would have been transmitted to American domestic pigs through wild boars imported into America (27). However, no strong evidence has been found for the presence of this type of LDV-like rodent virus in wild boars until now, making the origin of PRRSV untraceable (29) until now.

Through phylogenetic and origin analysis combined with the tMRCA of these arteriviruses, we speculate that an early RtClan-Arterivirus/GZ2015 was likely transmitted from *Chinchilla lanigera* to *Microtus clarkei* in Tibet to form RtMc-Arterivirus/Tibet2014, then might spread to the *Circetidae* in Shanxi, Jilin and Ningxia to form several similar strains. Finally, these *Circetidae* were possibly transported to Europe and the Americas to infect domestic pigs, forming the two types of PRRSV. It is worth noting that in the 20th century, many countries worldwide had not form a large-scale pig industry, pigs were usually kept free-range; therefore, rats or other rodent species could circulate freely in the pigsty. Pig feed might be contaminated with rodent feces containing certain rodent arteriviruses, which was then eaten by pigs, thus leading to arterivirus cross-species transmission from rodents to pigs. This explanation of PRRSV origin is distinct from other theories (that LDV-infected European wild boars transmitted virus to domestic pigs in Europe and the Americas).

The similarity between PRRSV and rodent arteriviruses is not very high, so there must have been other viruses involved in the evolution of PRRSV, but sequences are currently unavailable for any such intermediate ancestor.

In summary, based on an in-depth evolutionary analysis of the genomes and codon usage bias of the newly discovered rodent arteriviruses, we propose them as novel ancestors of PRRSV. The results fill the gaps in knowledge about the origin and evolution of PRRSV and rodent arteriviruses, and elucidate important insights for monitoring potential interspecies transmission between wild rodents and pigs in the future.

Data availability statement

The original contributions presented in the study are included in the article/Supplementary material, further inquiries can be directed to the corresponding authors.

Author contributions

Y-WH, BW, and Z-YZ conceived and designed the study and wrote the paper. Z-YZ, DY, C-MJ, and QZ performed the experiments and analyzed the data. All authors contributed to the article and approved the submitted version.

Funding

This work was supported by the Laboratory of Lingnan Modern Agriculture Project (NG2022001).

Acknowledgments

We thank the professional editing service NB Revisions for technical preparation of the text prior to submission.

Conflict of interest

QZ was employed by DELISI GROUP Co., LTD.

The remaining authors declare that the research was conducted in the absence of any commercial or financial

relationships that could be construed as a potential conflict of interest.

Publisher's note

All claims expressed in this article are solely those of the authors and do not necessarily represent those of their affiliated organizations, or those of the publisher, the editors and the reviewers. Any product that may be evaluated in this article, or claim that may be made by its manufacturer, is not guaranteed or endorsed by the publisher.

Supplementary material

The Supplementary Material for this article can be found online at: https://www.frontiersin.org/articles/10.3389/fvets.2023.1174031/full#supplementary-material

References

1. Archambault D, Balasuriya UB, Rowland RR, Yang H, Yoo D. Animal arterivirus infections. *Biomed Res Int.* (2014) 2014:303841. doi: 10.1155/2014/303841

2. Brinton MA, Gulyaeva AA, Balasuriya UBR, Dunowska M, Faaberg KS, Goldberg T, et al. Ictv virus taxonomy profile: arteriviridae 2021. *J Gen Virol.* (2021) 102:001632. doi: 10.1099/jgv.0.001632

3. Riley V, Lilly F, Huerto E, Bardell D. Transmissible agent associated with 26 types of experimental mouse neoplasms. *Science.* (1960) 132:545–7. doi: 10.1126/science.132.3426.545

4. Bryans JT, Doll ER, Knappenberger RE. An outbreak of abortion caused by the equine arteritis virus. *Cornell Vet.* (1957) 47:69–75.

5. Tauraso NM, Shelokov A, Palmer AE, Allen AM. Simian hemorrhagic fever. 3. Isolation and characterization of a viral agent. *Am J Trop Med Hyg.* (1968) 17:422–31. doi: 10.4269/ajtmh.1968.17.422

6. Shi M, Lam TT-Y, Hon C-C, Hui RK-H, Faaberg KS, Wennblom T, et al. Molecular epidemiology of prrsv: a phylogenetic perspective. *Virus Res.* (2010) 154:7–17. doi: 10.1016/j.virusres.2010.08.014

7. Mackintosh CG, Crawford JL, Thompson EG, McLeod BJ, Gill JM, O'Keefe JS. A newly discovered disease of the brushtail possum: wobbly possum syndrome. *New Zeal Vet J.* (1995) 43:126. doi: 10.1080/00480169.1995.35869

8. Wu Z, Lu L, Du J, Yang L, Ren X, Liu B, et al. Comparative analysis of rodent and small mammal viromes to better understand the wildlife origin of emerging infectious diseases. *Microbiome.* (2018) 6:178. doi: 10.1186/s40168-018-0554-9

9. Rossow KD. Porcine reproductive and respiratory syndrome. *Vet Pathol.* (1998) 35:1–20. doi: 10.1177/030098589803500101

10. Neumann EJ, Kliebenstein JB, Johnson CD, Mabry JW, Bush EJ, Seitzinger AH, et al. Assessment of the economic impact of porcine reproductive and respiratory syndrome on swine production in the United States. *J Am Vet Med Assoc.* (2005) 227:385–92. doi: 10.2460/javma.2005.227.385

11. Nelsen CJ, Murtaugh MP, Faaberg KS. Porcine reproductive and respiratory syndrome virus comparison: divergent evolution on two continents. *J Virol.* (1999) 73:270–80. doi: 10.1128/JVI.73.1.270-280.1999

12. Murtaugh MP, Elam MR, Kakach LT. Comparison of the structural protein coding sequences of the Vr-2332 and lelystad virus strains of the Prrs virus. *Arch Virol.* (1995) 140:1451–60. doi: 10.1007/BF01322671

13. Collins JE, Benfield DA, Christianson WT, Harris L, Hennings JC, Shaw DP, et al. Isolation of swine infertility and respiratory syndrome virus (isolate Atcc Vr-2332) in North America and experimental reproduction of the disease in gnotobiotic pigs. *J Vet Diagn Invest.* (1992) 4:117–26. doi: 10.1177/104063879200400201

14. Wensvoort G, Terpstra C, Pol JMA, ter Laak EA, Bloemraad M, de Kluyver EP, et al. Mystery swine disease in the netherlands: the isolation of lelystad virus. *Vet Quart.* (1991) 13:121–30. doi: 10.1080/01652176.1991.9694296

15. Zhou L, Yang H. Porcine reproductive and respiratory syndrome in China. *Virus Res.* (2010) 154:31–7. doi: 10.1016/j.virusres.2010.07.016

16. Blaha T. The "colorful" epidemiology of Prrs. *Vet Res.* (2000) 31:77–83. doi: 10.1051/vetres:2000109

17. Tian K, Yu X, Zhao T, Feng Y, Cao Z, Wang C, et al. Emergence of fatal prrsv variants: unparalleled outbreaks of atypical prrs in china and molecular dissection of the unique hallmark. *PLoS ONE.* (2007) 2:e526. doi: 10.1371/journal.pone.0000526

18. Chen C, Chen H, Zhang Y, Thomas HR, Frank MH, He Y, et al. Tbtools: an integrative toolkit developed for interactive analyses of big biological data. *Mol Plant.* (2020) 13:1194–202. doi: 10.1016/j.molp.2020.06.009

19. Katoh K, Standley DM. Mafft multiple sequence alignment software version 7: improvements in performance and usability. *Mol Biol Evol.* (2013) 30:772–80. doi: 10.1093/molbev/mst010

20. Nguyen LT, Schmidt HA, von Haeseler A, Minh BQ. Iq-tree: a fast and effective stochastic algorithm for estimating maximum-likelihood phylogenies. *Mol Biol Evol.* (2015) 32:268–74. doi: 10.1093/molbev/msu300

21. Zhang D, Gao F, Jakovlić I, Zou H, Zhang J, Li WX, et al. Phylosuite: an integrated and scalable desktop platform for streamlined molecular sequence data management and evolutionary phylogenetics studies. *Mol Ecol Resourc.* (2020) 20:348–55. doi: 10.1111/1755-0998.13096

22. Suchard MA, Lemey P, Baele G, Ayres DL, Drummond AJ, Rambaut A. Bayesian phylogenetic and phylodynamic data integration using beast 1.10. *Virus Evol.* (2018) 4:vey016. doi: 10.1093/ve/vey016

23. Drummond AJ, Rambaut A, Shapiro B, Pybus OG. Bayesian coalescent inference of past population dynamics from molecular sequences. *Mol Biol Evol.* (2005) 22:1185–92. doi: 10.1093/molbev/msi103

24. Li Y, Firth AE, Brierley I, Cai Y, Napthine S, Wang T, et al. Programmed−2/-1 ribosomal frameshifting in simarteriviruses: an evolutionarily conserved mechanism. *J Virol.* (2019) 93:e00370–19. doi: 10.1128/JVI.00370-19

25. Parvathy ST, Udayasuriyan V, Bhadana V. Codon usage bias. *Mol Biol Rep.* (2022) 49:539–65. doi: 10.1007/s11033-021-06749-4

26. Roth JR, Silbert DF, Fink GR, Voll MJ, Antón D, Hartman PE, et al. Transfer RNA and the control of the histidine operon. *Cold Spring Harbor Symposia Quant Biol.* (1966) 31:383–92. doi: 10.1101/SQB.1966.031.01.050

27. Plagemann PGW. Porcine reproductive and respiratory syndrome virus: origin hypothesis. *Emerg Infect Dis.* (2003) 9:903–8. doi: 10.3201/eid0908.030232

28. Albina E, Mesplède A, Chenut G, Le Potier MF, Bourbao G, Le Gal S, et al. A serological survey on classical swine fever (Csf), Aujeszky's disease (Ad) and porcine reproductive and respiratory syndrome (Prrs) virus infections in french wild boars from 1991 to 1998. *Vet Microbiol.* (2000) 77:43–57. doi: 10.1016/S0378-1135(00)00255-8

29. Reiner G, Fresen C, Bronnert S, Willems H. Porcine reproductive and respiratory syndrome virus (Prrsv) infection in wild boars. *Vet Microbiol.* (2009) 136:250–8. doi: 10.1016/j.vetmic.2008.11.023

frontiers | Frontiers in Veterinary Science

TYPE Perspective
PUBLISHED 17 April 2023
DOI 10.3389/fvets.2023.1146648

OPEN ACCESS

EDITED BY
Tomomi Takano,
School of Veterinary Medicine, Kitasato University, Japan

REVIEWED BY
Tereza Cristina Cardoso,
Universidade Estadual de São Paulo, Brazil
Long Liu,
Hubei University of Medicine, China

*CORRESPONDENCE
Li Xing
✉ xingli107@gmail.com

†These authors have contributed equally to this work

SPECIALTY SECTION
This article was submitted to Veterinary Infectious Diseases, a section of the journal Frontiers in Veterinary Science

RECEIVED 17 January 2023
ACCEPTED 29 March 2023
PUBLISHED 17 April 2023

CITATION
Wang P-H, Nawal Bahoussi A, Tariq Shah P, Guo Y-Y, Wu C and Xing L (2023) Genetic comparison of transmissible gastroenteritis coronaviruses. *Front. Vet. Sci.* 10:1146648. doi: 10.3389/fvets.2023.1146648

Genetic comparison of transmissible gastroenteritis coronaviruses

Pei-Hua Wang[1†], Amina Nawal Bahoussi[1†], Pir Tariq Shah[1†], Yan-Yan Guo[1], Changxin Wu[1,2,3,4] and Li Xing[1,2,3,4*]

[1]Institutes of Biomedical Sciences, Shanxi University, Taiyuan, China, [2]Shanxi Provincial Key Laboratory of Medical Molecular Cell Biology, Shanxi University, Taiyuan, China, [3]Shanxi Provincial Key Laboratory for Prevention and Treatment of Major Infectious Diseases, Taiyuan, China, [4]The Key Laboratory of Chemical Biology and Molecular Engineering of Ministry of Education, Shanxi University, Taiyuan, China

Transmissible gastroenteritis virus (TGEV) is a porcine coronavirus that threatens animal health and remains elusive despite years of research efforts. The systematical analysis of all available full-length genomes of TGEVs (a total of 43) and porcine respiratory coronaviruses PRCVs (a total of 7) showed that TGEVs fell into two independent evolutionary phylogenetic clades, GI and GII. Viruses circulating in China (until 2021) clustered with the traditional or attenuated vaccine strains within the same evolutionary clades (GI). In contrast, viruses latterly isolated in the USA fell into GII clade. The viruses circulating in China have a lower similarity with that isolated latterly in the USA all through the viral genome. In addition, at least four potential genomic recombination events were identified, three of which occurred in GI clade and one in GII clade. TGEVs circulating in China are distinct from the viruses latterly isolated in the USA at either genomic nucleotide or antigenic levels. Genomic recombination serves as a factor driving the expansion of TGEV genomic diversity.

KEYWORDS

coronavirus, transmissible gastroenteritis virus (TGEV), porcine respiratory coronavirus (PRCV), phylogeographic network, phylogenetic tree, China, USA, recombination

Introduction

Porcine transmissible gastroenteritis virus (TGEV) is a member of the *Coronaviridae* family that was first identified in the United States of America (USA) in 1946 (1) and was reported subsequently in countries of Europe, Asia, Africa, and America (2). In China, TGEV infection was first detected in Guangdong province in 1956, and since then, sporadic outbreaks have been reported in multiple swine-producing provinces, including Heilongjiang, Jilin, Henan, Gansu, Shanghai, and Guangxi (3–7).

TGEV is a rapidly spreading pathogen that infects swine of all ages and species and causes enteritis with a mortality rate >90%, inversely correlated with the age of pigs (8–10). TGEV has a single-stranded positive-sense RNA genome of ~28.6 kb in length (11) and belongs to the subgenus *Tegacovirus* of the *Alphacoronavirus* genus (12). The viral genome encompasses at least nine open reading frames (ORFs). The 5' two-thirds of the virus genome contains ORF1a and ORF1b, encoding the polyprotein 1a (pp1a) and polyprotein 1b (pp1b), respectively, proteolytically processed by virus-encoded proteases into 16 nonstructural proteins (Nsps 1–16) during the translation (13). The 3' one-third of the virus genome encodes four viral structural proteins, including the spike glycoprotein (S), the envelope protein (E), the membrane protein (M), the nucleocapsid protein (N), and three accessory proteins (NS3A, NS3B, and NS7) (14).

The S glycoprotein of TGEV is a large type 1 membrane protein composed of 1448 amino acids (GenBank: KX499468.1, TGEV AHHF strain) (15) and containing five domains: N-terminal domain (NTD, aa 1–248) with a short peptide signal (aa 1–16) (16), S1 domain (aa 249–670), S2 domain (aa 832–1372) (15), the transmembrane domain (TM, aa 1388–1410), and C-terminal cytoplasmic tail (aa 1411–1448). S glycoprotein of coronaviruses is the main structural protein of the viral envelope, which mediates the entry of virions into the host cell and induces the generation of neutralizing antibodies (17). S glycoprotein of TGEV binds the sialic acid or the porcine aminopeptidase N (pAPN) to ensure the entry of virion into host cells (18). The cysteine-rich motif (CRM) at the TGEV S glycoprotein carboxy-terminus is palmitoylated, which facilitates the assembly of S glycoprotein during the maturation of viral particles (19). Mutational analysis of NTD of S glycoprotein revealed a mild effect on viral virulence (20–22).

A previous study of S glycoprotein of TGEV strain PUR46-MAD (GenBank: M94101.1; Protein ID: AAA47109.1) has identified four major epitope sites within the N-terminal first 543 amino acids in the order of C, B, D, and A (17). Sites A and B contain conformational epitopes that depend on glycosylation (23). The amino acid residues 538K, 591R, and 543G are essential to forming the antigen subsites Aa, Ab and Ac of site A, respectively. Site B also consists of at least three subsites, two of which are overlapped and include tryptophan. The amino acid residues 97W and 144S contribute to the formation of epitopes in site B. However, sites C and D contain glycosylation-independent linear epitopes located at aa 48–52 and aa 373–398, respectively (17, 24).

The non-enteropathogenic porcine respiratory coronavirus (PRCV) is a naturally occurring mutant of TGEV with the deletion of an N terminal segment of S glycoprotein (25). PRCV preferentially infects non-ciliated epithelial cells of the porcine respiratory tract (26).

Vaccination and immunoprophylaxis represent the most effective means to contain and prevent TGEV, in addition to biosecurity measures (27). Since coronaviruses are an ongoing threat to humans, animals and the global economy, this study aimed to review the evolution and molecular characteristics of the full-length genomes of TGEV and PRCV during past decades to help promote the control and surveillance strategies.

TGEV and PRCV fall into two major genogroups GI and GII

The full-length genomes of all available TGEVs, including 19 strains isolated in China between 1973–2021 and 24 strains isolated in the USA between 1952–2014, in addition to 7 PRCV viruses isolated in the USA and UK between 1986 to 2016 (Supplementary Table 1), were retrieved from the NCBI GenBank and aligned with the ClustalW using the MEGA11 software. The maximum likelihood (ML) phylogenetic trees based on the full-length genome sequences or genomic fragments containing different ORFs were inferred using the best-fitting models in the IQ-TREE multicore version 1.6.12 (28) with 1000 bootstraps. As shown in Figure 1A, the complete genome-based phylogenetic tree identified two main clades GI and GII. All viruses isolated in China fell into the GI clade, together with the eight earliest strains from the USA, including attenuated Purdue P115 (GenBank ID: DQ811788.1), Virulent Purdue (GenBank ID: DQ811789.2), virulent Miller-M6 (GenBank ID: DQ811785.1), attenuated Miller-M60 (GenBank ID: DQ811786.2), TGEV/USA/HB/1988 (GenBank ID: KX900394.1), TGEV/USA/Z/1986 (GenBank ID: KX900393.1), Purdue (GenBank ID: AJ271965.2), and TGEV/Mex/145/2008 (GenBank ID: KX900402.1). The remaining 16 viruses from the USA fell independently into a separate, distinct clade referred to as the GII clade (Figure 1A). To deeply understand the virus evolution, we further constructed phylogenetic trees based on different genomic fragments. In the phylogenetic trees based on ORF1a (Supplementary Figure 1A), and ORF1b (Supplementary Figure 1B), ORF2 (encoding spike glycoprotein of TGEV and PRCV) (Supplementary Figure 1C), and genomic fragment containing ORFs of E, M, and N proteins (Supplementary Figure 1D), all viruses isolated in China and the aforementioned relatively earliest or attenuated vaccine viruses identified in the USA clustered in GI clade, corroborating results of the full-length genome-based phylogenetic analysis (Figure 1). In addition, the phylogenetic tree based on the ORF2 (Supplementary Figure 1C) or genomic fragment containing ORFs of E, M, and N proteins (Supplementary Figure 1D) revealed that the PRCV strains, known as a natural mutant of TGEV with a segmental deletion in the ORF2, clustered independently according to their geographical regions. The two PRCV strains identified in the UK clustered into GI, whereas the five identified in the USA clustered genetically closer to each other into GII, within different sub-lineage (Figure 1, Supplementary Figures 1A, B), demonstrating a complex evolutionary relationship between TGEV and PRCV strains (29).

Before this report, all constructed phylogenetic trees based on the full-length genomes of 30 TGEV isolates (30), 23 isolates (8), or based on the ORF2 of 11 isolates (3), displayed two major clades. Herein, our study: (1) included all available full-length genomic sequences of TGEV and PRCV, (2) showed that the GII clade contains all viruses from the USA, whereas the GI clade encompasses the nine relatively old TGEVs or attenuated vaccine strains from the USA in addition to all TGEVs from China. These findings indicate that the genetic distance of TGEVs from China is relatively far from that of the strains from the USA in the GII clade.

To further determine the genetic relatedness of TGEV genomes, we conducted a genomic similarity analysis using SimPlot software (31) and involving nine representative TGEV isolates from each clade: GI clade (Supplementary Figures 2A, B) and GII clade (Supplementary Figures 2A, C), separately. The Virulent-Purdue TGEV (GenBank ID: DQ811789.2) was included as a query. The nucleotide sequences of China viruses revealed a great similarity (>97%) with the query strain for most parts of the viral genome (Supplementary Figures 2A, B). In contrast, the similarity between viral isolates of the GII clade and the query strain is significantly reduced to <97% for most parts of the viral genome (Supplementary Figures 2A, C). Notably, the sequence similarity plot revealed that the ORF2 region shows the lowest similarity for viral isolates in both GI and GII clades (Supplementary Figures 2B, C, respectively). The genomic similarity plot results are consistent with the phylogenetic trees in that TGEVs isolated in China and USA belong to two distinct evolutionary branches. The low

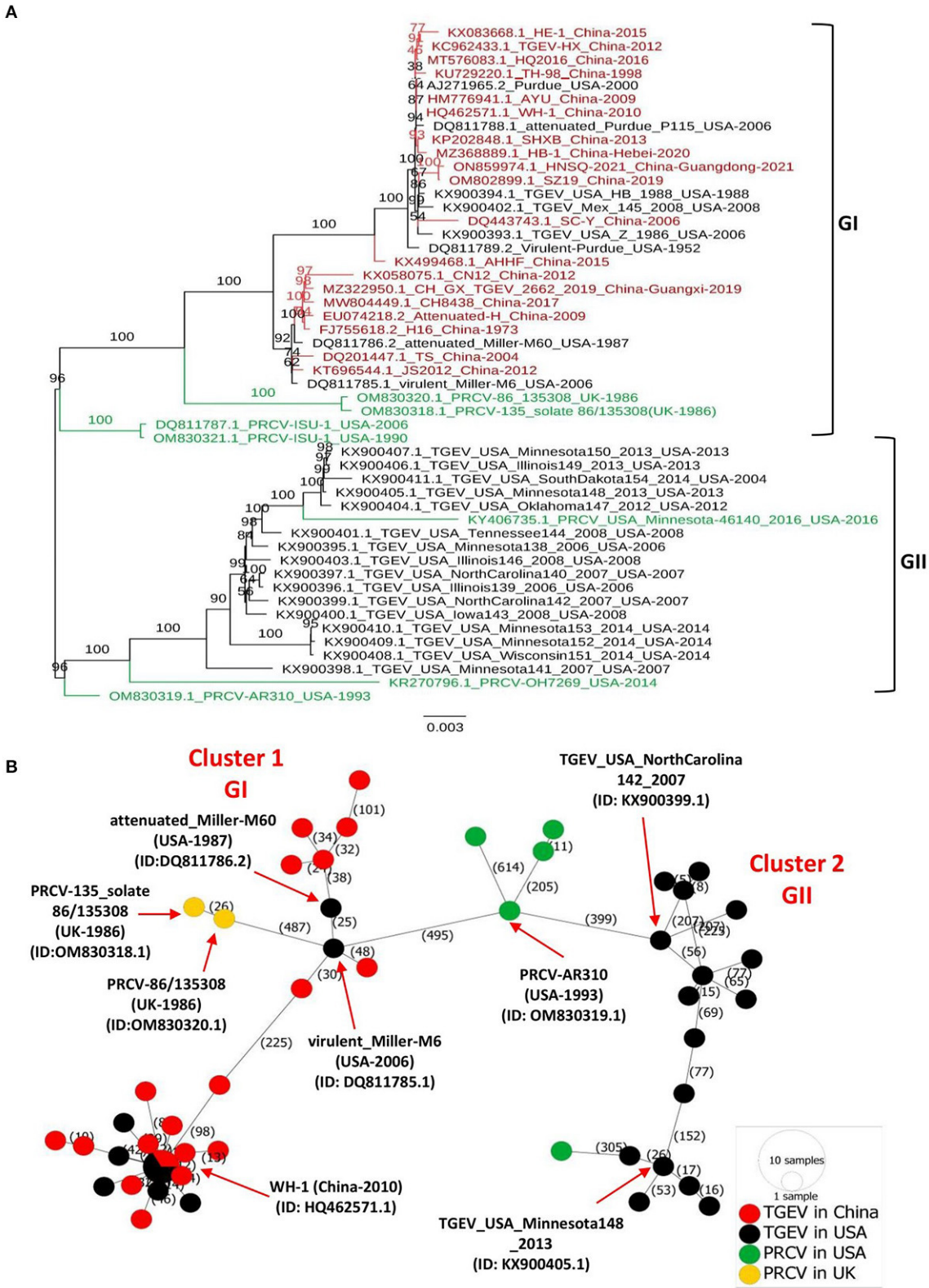

FIGURE 1
Phylogenetic tree and phylogeographic network of TGEV and PRCV strains. **(A)** Complete genome sequence-based ML tree. All complete genome nucleotide sequences were aligned using the MEGA11 software (37) and edited with the BioEdit v7.2.5. The ML phylogenetic trees were inferred using the IQ-TREE multicore version 1.6.12 (28) with 1000 bootstraps and the best-fitting model TIM + F + I + G4. The numbers on each branch are the bootstrap values (%). The scale bar represents a length corresponding to 0.003 nucleotide substitutions per site. Virus strains are formatted as GenBank accession number: virus name (country-year of collection). The red indicates TGEV from China, and the black indicates TGEV from the USA. The green color indicates PRCVs. **(B)** Phylogeographic network. The complete genome sequences of TGEV and PRCV were used to infer the Minimum Spanning Network (MSN) implemented by PopArt v1.7 (38). The network included 50 TGEV/PRCV strains, where 24 TGEV strains were from the USA, 19 TGEV strains from China, 5 PRCV strains from the USA and 2 PRCV strains from the UK. The mutation numbers are shown.

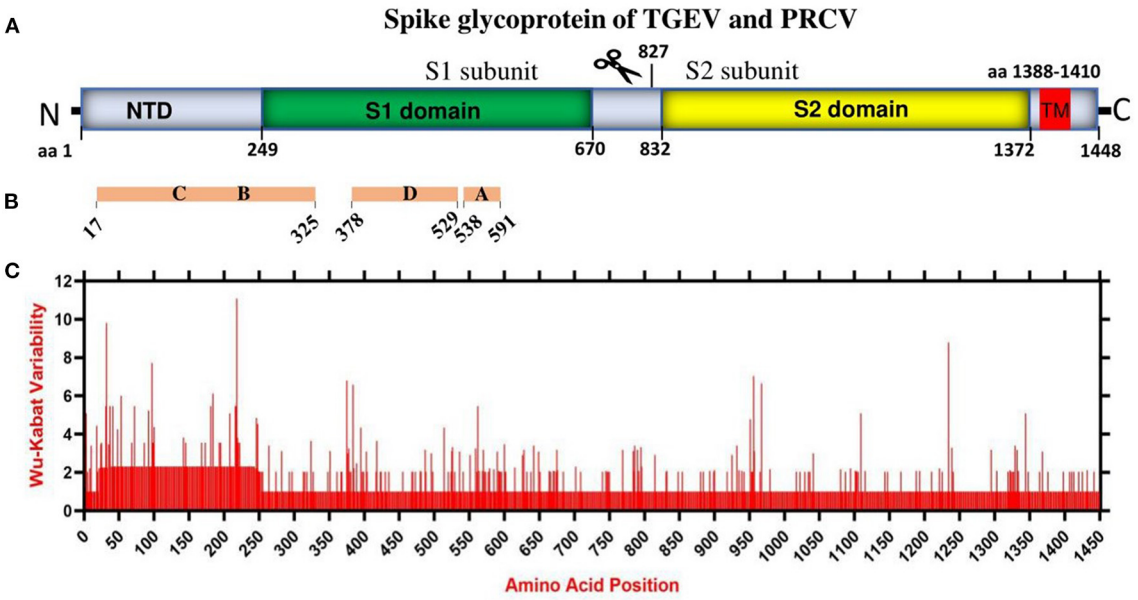

FIGURE 2
The amino acid variation landscape of TGEV and PRCV spike glycoprotein. **(A)** Domain structure of TGEV S glycoprotein, including NTD (aa 1–248), S1 domain (aa 249–670), S2 domain (aa 832–1,372), TM (aa 1,388–1,410) and C-terminal cytoplasmic tail (aa 1,411–1,448). **(B)** The brown blocks represent the relative positions of known sites containing neutralizing epitopes in the spike glycoprotein of TGEV (17). **(C)** Amino acid variation landscape. The amino acid sequences of all available complete spike proteins (a total of 58, Supplementary Table 1) of TGEV and PRCV were separately retrieved from the NCBI database and were aligned with ClustalW using the MEGA11 software (37). The protein variability was determined using the Wu-Kabat variability coefficient offered by the Protein Variability Server (PVS) (39). The Wu-Kabat variability coefficient describes the susceptibility of an amino acid position to evolutionary replacements and is computed using the following formula: variability coefficient = N*k/n, where N is the number of sequences in the alignment, k is the number of different amino acids at a given position and n is the frequency of the most common amino acid at that position. Y-axes represent the Wu-Kabat variability coefficient values, where the estimation limit is set as "1". Above the limit of ">1" represents variations. X-axes represent the amino acid positions.

similarity of ORF2 region in the genome (Supplementary Figure 2) indicates that the spike glycoprotein is highly variable.

Phylogeographic network of TGEV and PRCV

To map the regional spread and genetic relationships of TGEV and PRCV strains, we performed a phylogenetic network using all available complete genome sequences isolated from 1952 to 2021 (Supplementary Table 1). The analysis showed that strains within the GI and GII clades cluster into two separate Network Clusters (Figure 1B). The first Network Cluster (Cluster 1) consists of GI strains, while the second (Cluster 2) comprises GII strains (Figure 1B). These results support our ML phylogenetic classification of the complete genomes. Further, TGEV and PRCV strains seem to be radiated from strains isolated in the USA. The TGEV WH-1 (GenBank ID: HQ462571.1, China-2010) is identified sharing its genetic ancestor with the USA TGEV strains and connecting most of the GI strains to it through short mutational branches (Figure 1B). The remaining China TGEV strains are connected to the virulent_Miller-M6 (GenBank ID: DQ811785.1, USA-2006) within the same Network Cluster (Cluster 1). Interestingly, both the PRCV strains isolated in the UK, e.g., PRCV-86_135308 (GenBank ID: OM830320.1, UK-1986) and PRCV-135_solate 86/135308 (GenBank ID: OM830318.1, UK-1986) that were identified to be more distanced within GI clade of the full-length phylogenetic, are also connected to the virulent_Miller-M6 in the Network Cluster 1 (Figure 1B).

Recombination of TGEV

Genomic recombination is a relatively common phenomenon for coronaviruses, which have also been reported to occur in TGEVs. Zhang et al. reported that the TGEV AHHF strain (GenBank: KX499468.1) is a natural recombinant (32). The ORF1a gene of AHHF resulted from the recombination between SC-Y (GenBank: DQ443743.1) and H16 (GenBank: FJ755618.2), while the spike gene of AHHF was produced by recombination between the virulent Purdue (GenBank: DQ811789.2) and the attenuated H strain (GenBank: EU074218.2). TGEV JS2012 (GenBank: KT696544.1) strain is another natural recombinant between Miller M6 (GenBank: DQ811785.1) and Purdue 115 (GenBank: DQ811788.1) (8). Thus, we performed further recombination analysis of the entire TGEV and PRCV genome sequences (from the USA and China) using the seven algorithms of the recombination detection program 4 (RDP, GENECONV, BootScan, MaxChi, Chimera, SiScan, and 3Seq) (33). The analysis identified the occurrence of at least four potential recombination events (Supplementary Table 2), three of which (Events 1–3) occurred within the GI clade, and one event (Event 4) occurred between

strains in GII clade. The recombination among the USA strains (Event 4) is identified for the first time. In consistence with the previous reports (8, 32), the beginning and ending breakpoints of the identified recombination events are mainly located in ORF1a (Events 1 and 4) and ORF2-containg spike gene (Events 2 and 3) (Supplementary Figure 3). Zhang et al. report analyzed the occurrence of recombination among TGEV AHHF and 14 other strains and identified potential recombination at two locations (ORF1a and ORF2) (32). Consistent with those results, our analysis detected AHHF strain as a recombinant in two events (Events 1 and 2). In Event 2, the AHHF strain was recombined by CN12 and attenuated Purdue P115 in the ORF2, a new possibility of recombination for the AHHF virus. A previous report indicated that TGEV JS2012, a highly pathogenic strain isolated in newborn piglets faces in Jiangsu Province, China, resulted from natural recombination between Miller M6 and Purdue 115 and preserved the genetic integrity and characteristics of virulent strain, despite the recombination breakpoints in the ORF2 (8). Consistent with this report, TGEV JS2012 in our analysis was also identified as a recombinant strain, but between H16 (major parent) and the attenuated Purdue P115 (minor parent) in the ORF2, indicating the existence of alternative recombination. Interestingly, the identified recombination events occurred only between viruses in the same clade (intra-clade). None of the inter-clade recombinations have been found so far.

The landscape of amino acid variation of the spike glycoprotein

Coronaviruses enter the host cells by interaction between the S glycoprotein and the cellular receptor. S glycoprotein represents the chief immunogenic protein that elicits neutralizing antibody production (34) and the main antigen for vaccine research (35, 36). The virulence and antigenicity of TGEV S protein were shown to be sensitive to amino acid (aa) changes (3, 8). The mutation at aa 585 of TGEV HQ2016 engenders a serine-to-alanine change, affecting receptor binding and antigenicity (8). Here, the genome similarity and recombination analysis identified a low similarity of ORF2 (encoding spike glycoprotein) (Supplementary Figure 2) with potential recombination events (Supplementary Figure 3). In addition, the S1 subunit of TGEV spike glycoprotein has been shown to contain the neutralizing epitopes (17) (Figures 2A, B). Thus, we evaluated the amino acid variation patterns of TGEV and PRCV spike proteins by applying the Wu-Kabat variability coefficient provided by the Protein Variability Server (PVS). The method was used to acquire the consensus sequences of spike protein that consists of 1449 aa in TGEV (Figure 2C). The N terminal region, including both NTD and S1 domain, is the most variable, especially the aa positions 1–100, aa 200–250, aa 370–400, and aa 500–600, where the neutralizing epitopes have been identified (17).

Overall, China TGEV isolates are found to keep genetic features similar to that of older or attenuated vaccine strains so far, but distinct from that of the USA strains isolated latterly, which has implications in the monitoring, prevention, and control of TGEV. Furthermore, mutation is the modification of a gene resulted from insertion, deletion, or substitution of a single or multiple base units. Recombination occurs when the larger genetic fragments from at least two genomes are exchanged. The highly variable regions of spike proteins of TGEV and PRCV (Figure 2) and the recombination events (Supplementary Figure 3) demonstrate that both mutation and recombination are driving the expansion of genetic diversity and transmission of TGEV and PRCV, which need attention for the surveillance and vaccine development.

Data availability statement

The original contributions presented in the study are included in the article/Supplementary material, further inquiries can be directed to the corresponding author.

Author contributions

P-HW and LX conceived the study. P-HW, PT, and AN performed analysis. Y-YG provided resources in data analysis. P-HW and AN wrote the manuscript. CW and LX carried out administration. AN, PT, and LX revised the manuscript. All authors have read and approved the final manuscript.

Funding

This work was supported by the Programme of Introducing Talents of Discipline to Universities (D21004).

Acknowledgments

We thank all the persons who contributed to the collection and production of TGEV and PRCV genomic sequences in NCBI GenBank.

Conflict of interest

The authors declare that the research was conducted in the absence of any commercial or financial relationships that could be construed as a potential conflict of interest.

Publisher's note

Supplementary material

The Supplementary Material for this article can be found online at: https://www.frontiersin.org/articles/10.3389/fvets.2023.1146648/full#supplementary-material

References

1. Doyle LP, Hutchings LM. A transmissible gastroenteritis in pigs. *J Am Vet Med Assoc.* (1946) 108:257–9.

2. Pineyro PE, Lozada MI, Alarcon LV, Sanguinetti R, Cappuccio JA, Perez EM, et al. First retrospective studies with etiological confirmation of porcine transmissible gastroenteritis virus infection in Argentina. *BMC Vet Res.* (2018) 14:292. doi: 10.1186/s12917-018-1615-9

3. Hu X, Li N, Tian Z, Yin X, Qu L, Qu J. Molecular characterization and phylogenetic analysis of transmissible gastroenteritis virus HX strain isolated from China. *BMC Vet Res.* (2015) 11:72. doi: 10.1186/s12917-015-0387-8

4. Li JQ, Cheng J, Lan X, Li XR, Li W, Yin XP, et al. Complete genomic sequence of transmissible gastroenteritis virus TS and 3' end sequence characterization following cell culture. *Virol Sin.* (2010) 25:213–24. doi: 10.1007/s12250-010-3108-2

5. Wang L, Ge C, Wang D, Li Y, Hu J. The survey of porcine teschoviruses, porcine circovirus and porcine transmissible gastroenteritis virus infecting piglets in clinical specimens in China. *Trop Anim Health Prod.* (2013) 45:1087–91. doi: 10.1007/s11250-012-0329-4

6. Weiwei H, Qinghua Y, Liqi Z, Haofei L, Shanshan Z, Qi G, et al. Complete genomic sequence of the coronavirus transmissible gastroenteritis virus SHXB isolated in China. *Arch Virol.* (2014) 159:2295–302. doi: 10.1007/s00705-014-2080-9

7. Yuan D, Yan Z, Li M, Wang Y, Su M, Sun D. Isolation and characterization of a porcine transmissible gastroenteritis coronavirus in Northeast China. *Front Vet Sci.* (2021) 8:611721. doi: 10.3389/fvets.2021.611721

8. Guo R, Fan B, Chang X, Zhou J, Zhao Y, Shi D, et al. Characterization and evaluation of the pathogenicity of a natural recombinant transmissible gastroenteritis virus in China. *Virology.* (2020) 545:24–32. doi: 10.1016/j.virol.2020.03.001

9. Li X, Li P, Cao L, Bai Y, Chen H, Liu H, et al. Porcine IL-12 plasmid as an adjuvant improves the cellular and humoral immune responses of DNA vaccine targeting transmissible gastroenteritis virus spike gene in a mouse model. *J Vet Med Sci.* (2019) 81:1438–44. doi: 10.1292/jvms.18-0682

10. Yuan X, Lin H, Fan H. Efficacy and immunogenicity of recombinant swinepox virus expressing the a epitope of the TGEV S protein. *Vaccine.* (2015) 33:3900–6. doi: 10.1016/j.vaccine.2015.06.057

11. Hubert L, Denis R, Bernard D, Murielle G, Jacqueline G, Bernard C. *Molecular Biology of Transmissible Gastroenteritis Virus.* Amsterdam: Elsevier (1990), p. 23. doi: 10.1016/0378-1135(90)90144-K

12. Wong ACP, Li X, Lau SKP, Woo PCY. Global epidemiology of bat coronaviruses. *Viruses.* (2019) 11:174. doi: 10.3390/v11020174

13. Gorbalenya A, Enjuanes L, Zi Eb Uhr J, Snijder EJ. Nidovirales: evolving the largest RNA virus genome. *Virus Res.* (2006) 117:17–37. doi: 10.1016/j.virusres.2006.01.017

14. Penzes Z, González JM, Calvo E, Izeta A, Smerdou C, Méndez A, et al. Complete genome sequence of transmissible gastroenteritis coronavirus PUR46-MAD clone and evolution of the purdue virus cluster. *Virus Genes.* (2001) 23:105–18. doi: 10.1023/A:1011147832586

15. Marchler-Bauer A, Bo Y, Han L, He J, Lanczycki CJ, Lu S, et al. CDD/SPARCLE: functional classification of proteins via subfamily domain architectures. *Nucleic Acids Res.* (2017) 45:D200–3. doi: 10.1093/nar/gkw1129

16. Laude H, Godet M, Bernard S, Gelfi J, Duarte M, Delmas B. Functional domains in the spike protein of transmissible gastroenteritis virus. *Adv Exp Med Biol.* (1995) 380:299–304. doi: 10.1007/978-1-4615-1899-0_48

17. Gebauer F, Posthumus WP, Correa I, Suñé C, Smerdou C, Sánchez CM, et al. Residues involved in the antigenic sites of transmissible gastroenteritis coronavirus *S glycoprotein. Virology.* (1991) 183:225–38. doi: 10.1016/0042-6822(91)90135-X

18. Ballesteros ML, Sánchez CM, Enjuanes L. Two amino acid changes at the N-terminus of transmissible gastroenteritis coronavirus spike protein result in the loss of enteric tropism. *Virology.* (1997) 227:378–88. doi: 10.1006/viro.1996.8344

19. Sandra G, Bastian T, Kathrin E, Michael V, Christel S-W. Palmitoylation of the Alphacoronavirus TGEV spike protein S is essential for incorporation into virus-like particles but dispensable for S-M interaction. *Virology.* (2014) 464:397–405. doi: 10.1016/j.virol.2014.07.035

20. Sánchez CM, Izeta A, Sánchez-Morgado JM, Alonso S, Sola I, Balasch M, et al. Targeted recombination demonstrates that the spike gene of transmissible gastroenteritis coronavirus is a determinant of its enteric tropism and virulence. *J Virol.* (1999) 73:7607–18. doi: 10.1128/JVI.73.9.7607-7618.1999

21. Sanchez CM, Pascual-Iglesias A, Sola I, Zuniga S, Enjuanes L. Minimum determinants of transmissible gastroenteritis virus enteric tropism are located in the N-Terminus of spike protein. *Pathogens.* (2019) 9:2. doi: 10.3390/pathogens9010002

22. Wang G, Liang R, Liu Z, Shen Z, Shi J, Shi Y, et al. The N-Terminal domain of spike protein is not the enteric tropism determinant for transmissible gastroenteritis virus in piglets. *Viruses.* (2019) 11:313. doi: 10.3390/v11040313

23. Reguera J, Ordoño D, Santiago C, Enjuanes L, Casasnovas JM. Antigenic modules in the N-terminal S1 region of the transmissible gastroenteritis virus spike protein. *J Gen Virol.* (2011) 92:1117–26. doi: 10.1099/vir.0.027607-0

24. Enjuanes L, Suñé C, Gebauer F, Smerdou C, Camacho A, Antón IM, et al. Antigen selection and presentation to protect against transmissible gastroenteritis coronavirus. *Vet Microbiol.* (1992) 33:249–62. doi: 10.1016/0378-1135(92)90053-V

25. Pensaert M, Callebaut P, Vergote J. Isolation of a porcine respiratory, non-enteric coronavirus related to transmissible gastroenteritis. *Vet Q.* (1986) 8:257–61. doi: 10.1080/01652176.1986.9694050

26. Peng JY, Punyadarsaniya D, Shin DL, Pavasutthipaisit S, Beineke A, Li G, et al. The cell tropism of porcine respiratory coronavirus for airway epithelial cells is determined by the expression of porcine aminopeptidase N. *Viruses.* (2020) 12:1211. doi: 10.3390/v12111211

27. Gerdts V, Zakhartchouk A. Vaccines for porcine epidemic diarrhea virus and other swine coronaviruses. *Vet Microbiol.* (2017) 206:45–51. doi: 10.1016/j.vetmic.2016.11.029

28. Trifinopoulos J, Nguyen L-T, von Haeseler A, Minh BQ. W-IQ-TREE: a fast online phylogenetic tool for maximum likelihood analysis. *Nucleic Acids Res.* (2016) 44:W232–5. doi: 10.1093/nar/gkw256

29. Chen F, Knutson TP, Rossow S, Saif LJ, Marthaler DG. Decline of transmissible gastroenteritis virus and its complex evolutionary relationship with porcine respiratory coronavirus in the United States. *Sci Rep.* (2019) 9:3953. doi: 10.1038/s41598-019-40564-z

30. Cheng S, Wu H, Chen Z. Evolution of transmissible gastroenteritis virus (TGEV): a codon usage perspective. *Int J Mol Sci.* (2020) 21:7898. doi: 10.3390/ijms21217898

31. Lole KS, Bollinger RC, Paranjape RS, Gadkari D, Kulkarni SS, Novak NG, et al. Full-length human immunodeficiency virus type 1 genomes from subtype C-infected seroconverters in India, with evidence of intersubtype recombination. *J Virol.* (1999) 73:152–60. doi: 10.1128/JVI.73.1.152-160.1999

32. Zhang X, Zhu Y, Zhu X, Shi H, Chen J, Shi D, et al. Identification of a natural recombinant transmissible gastroenteritis virus between Purdue and Miller clusters in China. *Emerg Microbes Infect.* (2017) 6:e74. doi: 10.1038/emi.2017.62

33. Martin DP, Murrell B, Golden M, Khoosal A, Muhire B. RDP4: Detection and analysis of recombination patterns in virus genomes. *Virus Evol.* (2015) 1: vev003. doi: 10.1093/ve/vev003

34. Turlewicz-Podbielska H, Pomorska-Mól M. Porcine coronaviruses: overview of the state of the art. *Virol Sin.* (2021) 36:833–51. doi: 10.1007/s12250-021-00364-0

35. Meng F, Zhao Z, Li G, Suo S, Shi N, Yin J, et al. Bacterial expression of antigenic sites A and D in the spike protein of transmissible gastroenteritis virus and evaluation of their inhibitory effects on viral infection. *Virus Genes.* (2011) 43:335–41. doi: 10.1007/s11262-011-0637-1

36. Mou C, Zhu L, Xing X, Lin J, Yang Q. Immune responses induced by recombinant Bacillus subtilis expressing the spike protein of transmissible gastroenteritis virus in pigs. *Antiviral Res.* (2016) 131:74–84. doi: 10.1016/j.antiviral.2016.02.003

37. Sievers F, Wilm A, Dineen D, Gibson TJ, Karplus K, Li W, et al. Fast, scalable generation of high-quality protein multiple sequence alignments using Clustal Omega. *Mol Syst Biol.* (2011) 7:539. doi: 10.1038/msb.2011.75

38. Leigh JW, Bryant D. POPART: full-feature software for haplotype network construction. *Methods Ecol Evolut.* (2015) 6:1110–6. doi: 10.1111/2041-210X.12410

39. Garcia-Boronat M, Diez-Rivero CM, Reinherz EL, Reche PA. PVS: a web server for protein sequence variability analysis tuned to facilitate conserved epitope discovery. *Nucleic Acids Res.* (2008) 36:W35–41. doi: 10.1093/nar/gkn211

frontiers | Frontiers in Veterinary Science

TYPE Original Research
PUBLISHED 27 April 2023
DOI 10.3389/fvets.2023.1169766

OPEN ACCESS

EDITED BY
Shao-Lun Zhai,
Guangdong Academy of Agricultural Sciences, China

REVIEWED BY
Semmannan Kalaiyarasu,
ICAR-National Institute of High Security Animal Diseases (ICAR-NIHSAD), India
Elisabetta Razzuoli,
Experimental Zooprophylactic Institute for Piedmont, Liguria and Valle d'Aosta (IZSTO), Italy

*CORRESPONDENCE
Hui-Wen Chang
huiwenchang@ntu.edu.tw

†These authors have contributed equally to this work

RECEIVED 20 February 2023
ACCEPTED 10 April 2023
PUBLISHED 27 April 2023

CITATION
Chen W-T, Liu H-M, Chang C-Y, Deng M-C, Huang Y-L, Chang Y-C and Chang H-W (2023) Cross-reactivities and cross-neutralization of different envelope glycoproteins E2 antibodies against different genotypes of classical swine fever virus.
Front. Vet. Sci. 10:1169766.
doi: 10.3389/fvets.2023.1169766

Cross-reactivities and cross-neutralization of different envelope glycoproteins E2 antibodies against different genotypes of classical swine fever virus

Wei-Tao Chen[1,2†], Hsin-Meng Liu[1,2,3†], Chia-Yi Chang[1], Ming-Chung Deng[3], Yu-Liang Huang[3], Yen-Chen Chang[1,2] and Hui-Wen Chang[1,2*]

[1]School of Veterinary Medicine National Taiwan University, Taipei, Taiwan, [2]School of Veterinary Medicine, Graduate Institute of Molecular and Comparative Pathobiology, National Taiwan University, Taipei, Taiwan, [3]College of Bioresources and Agriculture, Animal Health Research Institute, Tamsui, Taiwan

Classical swine fever (CSF) is a highly contagious swine disease caused by the classical swine fever virus (CSFV), wreaking havoc on global swine production. The virus is divided into three genotypes, each comprising 4–7 sub-genotypes. The major envelope glycoprotein E2 of CSFV plays an essential role in cell attachment, eliciting immune responses, and vaccine development. In this study, to study the cross-reaction and cross-neutralizing activities of antibodies against different genotypes (G) of E2 glycoproteins, ectodomains of G1.1, G2.1, G2.1d, and G3.4 CSFV E2 glycoproteins from a mammalian cell expression system were generated. The cross-reactivities of a panel of immunofluorescence assay-characterized serum derived from pigs with/without a commercial live attenuated G1.1 vaccination against different genotypes of E2 glycoproteins were detected by ELISA. Our result showed that serum against the LPCV cross-reacted with all genotypes of E2 glycoproteins. To evaluate cross-neutralizing activities, hyperimmune serum from different CSFV E2 glycoprotein-immunized mice was also generated. The result showed that mice anti-E2 hyperimmune serum exhibited better neutralizing abilities against homologous CSFV than heterogeneous viruses. In conclusion, the results provide information on the cross-reactivity of antibodies against different genogroups of CSFV E2 glycoproteins and suggest the importance of developing multi-covalent subunit vaccines for the complete protection of CSF.

KEYWORDS

classical swine fever, E2 glycoprotein, cross-reaction, cross-neutralizing activity, genotypes

1. Introduction

Classical swine fever (CSF) is a highly contagious World Organization for Animal Health (WOAH) notifiable disease that causes significant economic losses. A devastating CSF has been reported in Central and South America, Europe, Asia, and Africa (1–5). Even though areas can be declared CSF-free, the re-emergence of CSF and emergence of new sub-genotypes of classical

swine fever virus (CSFV) have been reported (6). In Japan, outbreaks of G2.1d CSFV in pig farms and wild boars in Gifu City in 2018 were re-emerged after 26 years of CSF-free status (6–8) indicating the difficulty in eradication of the disease.

Clinical signs of CSF are determined by the virulence of the viral strain, age, health condition, and immune responses of pigs and can be divided into peracute, acute, subacute, chronic, and subclinical (3, 9, 10). The common pathological findings in the acute phase are hemorrhage and petechiae in multiple organs with necrotizing tonsillitis and enteritis (11, 12). The most prominent histopathological changes in chronic CSF are lymphoid depletion and lymph node necrosis (13). Subclinical CSF, resembling a persistent infection, is caused by a transplacental transmission during mid-gestation periods (14, 15). Infected piglets can be asymptomatic but persistently shed the virus, becoming a source of virus (11, 16).

Classical swine fever virus, belonging to the family *Flaviviridae* and genus *Pestivirus*, is a single positive-strand RNA virus. CSFV carries a genome of ~12.3 kbp, encoding one continuous open reading frame (ORF) flanked by two non-translated regions (NTR) on both sides. The ORF encodes a polypeptide precursor of approximately 3,898 amino acids (aa) that can be cleaved into 12 mature proteins, including four structural proteins, namely nucleocapsid protein (C), enveloped glycoproteins (E) E^{rns}, E1, and E2, and eight non-structural (NS) proteins, namely N-terminal protease (N^{pro}), p7, NS2, NS3, NS4A, NS4B, NS5A, and NS5B (17–19). Among the CSFV proteins, the E2 protein is the most immunogenic and essential for inducing neutralizing antibodies and protecting against lethal challenge (20). It has been demonstrated that the removal of certain glycosylation sites of the E2 protein significantly reduced the immunogenicity of the protein and increased its virulence (21, 22). There are four immunogenic domains at the C-terminus of the E2 protein, which can be divided into a less conservative B/C domain (690–779 a.a.) and a conservative A/D domain (780–859 a.a.). Several linear epitopes were identified in these domains (23), such as ^{772}LFDGTNP^{778} at the tail of domain B/C (24) and ^{829}TAVSPTTLR^{837} recognized by the monoclonal antibody (mAb) WH303 (25). At the N-terminus of the B/C domain, four residues at positions ^{709}P, ^{713}E, ^{725}G, and ^{738}I/V have been identified as important for antigen–antibody interactions (26).

Substitutions can cause dramatic topology changes and might abolish antibody binding (27). It has been shown that specific glycosylation or the lack of E2 glycoprotein through point mutation and deglycosylation of the highly virulent Shimen strain at position 986 could result in a lower virulence (22). In this study, deglycosylation of the E2 protein at the ^{986}NYA^{988} glycosylation site resulted in a decrease in E2 dimerization, which affected viral interactions with cell surface attachment factors, virion stability, and virus replication (22, 28, 29).

Classical swine fever virus can be divided into three genotypes (G1, G2, and G3). Each genotype comprises four to seven sub-genotypes according to the 5'NTR and E2 sequences (17, 18, 30, 31). Among the different genotypes, the nucleotide sequence identities genetically range from 80 to 86%. In the same genotype, there is 86–91% similarity among various sub-genotypes (18). Only the original reference strain, G1, has been reported in North America. The G2 CSFV emerged in Europe in the 1980s. The G3 CSFV has only been identified in Asia (11, 32). Regarding the historical distribution of sub-genotypes, the G1.1 CSFVs were identified in Argentina, Brazil, Colombia, and Mexico. The G1.3 strains were identified in Honduras and Guatemala. The G1.2 and G1.4 strains were identified in Cuba (32–35). Currently, genotype 2, |originating in Central Europe, is the predominant strain. G2.1 CSFV is a moderately virulent genotype compared with high-virulence G1 strains. The G2.1, 2.2, and 2.3 CSFV strains have been reported in Nepal, China, Japan, Korea, and the Middle East. G3 CSFV has only been reported in Asia, with G3.2 isolated in Korea between 1988 and 1999 (36), G3.3 in Thailand between 1988 and 1996 (1), and G3.4 in Japan and Taiwan (37). In Taiwan, the G3.4 strain was gradually replaced by the G2.1 CSFV. This was suggestively due to the superior replication and infectivity of the G2 virus compared with the G3 CSFV (1). However, the mechanism responsible for genotype switching has not been completely investigated.

Extensive vaccination programs have been used to control CSF in endemic regions, with varying degrees of success. Live attenuated vaccine (LAV) generally performs well against homologous strain CSFV infections. However, conflicting results of various degrees of protection against heterologous strains have been debated (38–40). Even after extensive vaccination with C-strain LAV, frequent CSF outbreaks have been reported in China. The reported strains include G1.1, G2.1, G2.2, G2.3, and the newly emerged sub-genotypes G2.1b, G2.1c, and G2.1d (41–44). The newly emerged clades of subgenotype G2.1 are moderately virulent and more dominant, arguing the efficacy of the C-strain G1-based vaccine.

To study the cross-reaction and cross-neutralizing activities of antibodies against different genotypes of E2 glycoproteins, ectodomains of G1.1, G2.1, G2.1d, and G3.4 CSFV E2 glycoproteins derived from the HEK293 mammalian expression system were generated to mimic the integrity of E2 glycoproteins. These E2 glycoprotein-based in-house ELISAs were developed to evaluate the cross-reactivity of a panel of immunofluorescence assay (IFA)-characterized sera derived from Lapinized Philippines Coronel strain live attenuated vaccine (LPCV) immunized pigs. These ELISA performances were compared with that of a commercialized CSFV ELISA. Hyperimmune mouse serum against these CSFV E2 glycoproteins was generated to detect the neutralizing activity against different genogroups of CSFV.

2. Materials and methods

2.1. Cells and virus

Sequences of the E2 encoded region from G1.1 (GenBank Accession No. AAS20416.1), G2.1a (GenBank Accession No. LC425854.1), G2.1d (GenBank Accession No. AY554397.1), and G3.4 (GenBank Accession No. AY646427.1), modified by truncation of the transmembrane domains and addition of the human tissue plasminogen activator sequence at the 5′-end with two restriction enzyme sites, NotI and BamHI, at the 3′ and 5′ ends, respectively, were synthesized by Genscript Corporation (Piscataway, NJ, United States). The modified sequences were digested and ligated into the pcDNA 3.1/V5-His TOPO TA mammalian expression vector (Invitrogen, Carlsbad, CA, United States) at BamHI and NotI restriction sites (Figure 1).

The plasmids obtained were transfected into HEK 293 cells with PolyJet (SignaGen Laboratories, Frederick, MD, United States) and selected by culturing in DMEM high-glucose culture medium (Gibco, USA) containing 1.5% geneticin (G418) (Gibco) and 10% FBS (Gibco). Once stable cell lines were developed, the cells were placed

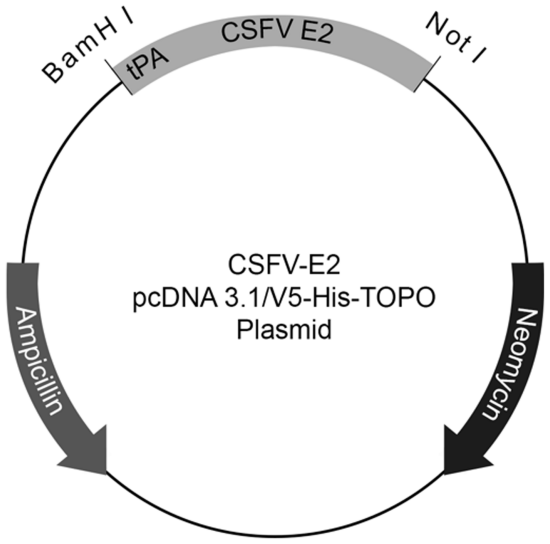

FIGURE 1
Schematic plasmid map of the recombinant CSFV E2 construct. Sequences of E2 modified by truncation of the transmembrane domains and addition of the human tissue plasminogen activator (tPA) sequence at 5′-end with two restriction enzyme sites, NotI and BamHI, at 3′ and 5′ end of the sequences, respectively, were cloned onto the pcDNATM 3.1/V5-His TOPO® TA mammalian expression vector.

into 175 T flasks and cultured with Freestyle 293 expression medium (Gibco) for five days for supernatant collection.

2.2. Immunocytochemistry staining for E2 detection

The expression of E2 glycoproteins was detected by fixing the cells in a 96-well-plate with 80% acetone (Avantor, PA, United States) for 20 min on ice. After air-drying and washing with 200 µL of PBS, 100 µL of anti-V5 antibody (Invitrogen; 1:1,000 dilution) was added to each well and incubated at room temperature (RT) for 1 h. Each well was washed six times using 200 µL PBS. In each well, 100 µL of Dako REAL EnVision antirabbit/mouse horseradish peroxidase (HRP)-conjugated antibody (Dako, CA, United States; 1:10 dilution) was added and incubated at RT for 1 h. The signals were detected using 3,3′-diaminobenzidine (DAB) (Dako) following the manufacturer's instructions. Results were evaluated using an inverted light microscope.

2.3. Sodium dodecyl sulfate–polyacrylamide gel electrophoresis and western blot

The E2 glycoproteins were mixed with NuPAGE LDS sample buffer (Thermo Fisher Scientific, Waltham, MA, United States). For the denatured samples, NuPAGE Sample Reducing agent (Thermo Fisher Scientific) was added and incubated at 95°C for 10 min. The samples were then separated by SDS-PAGE using a Bio-Rad Mini-PROTEIN electrophoresis system (Bio-Rad, Hercules, CA, United States) with a 10% separating gel and 17% stacking gel, following the manufacturer's recommendations. The proteins were transferred to a polyvinylidene fluoride (PVDF) membrane (Bio-Rad) and blocked with 5% skim milk (Beckton, Dickson and Company, MD, United States) in 5% tris-buffered saline and polysorbate 20 (Tween 20) (TBS-T) (Genestar, Beijing, China) at RT for 1 h. followed by 1 h. of WH303 (APHA Scientific, United Kingdom; 1:1,000 dilution) or anti-V5 (Novex, Invitrogen; 1:5,000 dilution), and 1 h. of Goat-anti-mouse HRP conjugated secondary antibody (Jackson ImmunoResearch, PA, United States; 1:10,000 dilution) with three washes of TBS-T between each incubation. The results were visualized using Clarity Western ECL Blotting Substrates (Bio-Rad) and a ChemiDoc XSR+ Imaging System (Bio-Rad).

2.4. Protein affinity-based purification

The collected expression medium was filtered through a 0.22 µm filter to remove any cell debris. The filtered expression medium was then incubated at 4°C overnight with HisPur cobalt resin (10 mL/1 L) (Thermo Fisher Scientific). The resin was collected in a column and washed with 10 resin-bed volumes of sodium-phosphate-based wash buffer. The proteins were eluted by passing five resin-bed volumes of 300 mM imidazole elution buffer through a column. The eluates were concentrated using Amicon Ultra-15 10 kDa concentration tubes (Millipore, Merck, Ireland). The concentration was determined by measuring the UV absorbance at 280 nm using a Take 3 BioTek microplate (Cytation 7, Agilent, Santa Clara, CA, United States).

2.5. Indirect immunofluorescent assay of swine serum antibody

PK-15 cells were seeded in a flat bottom 96-well-plate at 80% confluence and infected with the attenuated LPCV (AHRI) virus at a multiplicity of infection of 10. After 72 h of inoculation, the cells were fixed by adding 100 µL of 10% formaldehyde, incubated at RT for 1 h, and air-dried. One hundred microliters of 10% goat serum (Dako) were used as a blocking buffer and were incubated at RT for 1 h. The sera collected from pigs submitted to Veterinary Medicine Diagnostic Center at School of Veterinary Medicine in National Taiwan University for diagnostic needs with or without LPCV immunization history was diluted 80 folds and incubated at RT for 1 h. After washing with PBS six times, fluorescein isothiocyanate (FITC)-conjugated AffiniPure goat anti-swine IgG antibody (Jackson ImmunoResearch; 1:100 dilution) was applied to the microplates for 1 h at RT. After washing with PBS, the cells were mounted with a mounting medium containing DAPI (Abcam, Cambridge, United Kingdom). Fluorescence was observed using an inverted fluorescence microscope.

2.6. Commercial and in-house CSFV enzyme-linked immunosorbent assay

A CSFV antibody ELISA kit (BioChek, Berkshire, UK) was used to detect CSFV antibodies in swine serum, following the manufacturer's recommendations. For different in-house CSFV E2 ELISA, 100 µL purified E2 proteins diluted to 1 ng/microliter in coating buffer (KPL, SeraCare, Milford, United States) was added onto 96-well-plates, following manufacturer's instructions, and incubated overnight at

4°C. Following removal of the coating buffer, each well was washed six times with 200 µL of wash buffer (KPL, SeraCare). One hundred microliters of blocking buffer (KPL, SeraCare) were added to each well and incubated at RT for 30 min. Swine or mouse blood serum was diluted 80-fold with PBS before adding to each well. After washing with wash buffer, 100 µL of HRP-conjugated goat anti-swine IgG (Jackson ImmunoResearch; 1:1,000 dilution in blocking buffer) or HRP conjugated goat-anti-mouse secondary antibody (Jackson ImmunoResearch; 1:1,000 dilution in blocking buffer) was added and incubated at RT. After 1 h, the plates were washed six times. Fifty microliter ABTS peroxidase substrate (KPL, SeraCare) was added for 3 min following the manufacturer's instructions. The reaction was halted by adding a 50 µL stopping buffer (KPL, SeraCare). The results were evaluated by measuring the optical density at 405 nm (OD 405) on an EMax Plus microplate reader (Molecular Device, Crawly, United Kingdom). Cutoff values were determined by adding two standard deviations of all IFA-negative samples to the average of IFA-negative samples. Higher OD values were considered to be positive and vice versa.

2.7. Mice immunization

Twelve eight-week-old BALB/c mice were randomly separated into three groups. Each group was administered 50 µg of G1.1, 2.1d, or 3.4 CSFV E2 proteins in 0.2 mL of Montanide Gel 01 (Seppic, France) intraperitoneally and boosted with the same dosage at 14, 28, 42, and 56 days post-immunization (dpi). Hyperimmune mouse serum samples of different E2 levels were collected retro-orbitally and at 70 dpi, per the Institutional Animal Care and Use Committee (IACUC) guidelines. All procedures involving animals were performed following the regulations and with permission of the IACUC protocol (No. A10008) at the Animal Health Research Institute (AHRI, Council of Agriculture, Executive Yuan, Taiwan).

2.8. Serum neutralizing assay

The serum neutralizing assay was performed as described in previous studies (45). All serum samples were first inactivated at 56°C. Starting from 1:40 dilution, twofold serial diluted sera were incubated with equal amount of100 $TCID_{50}$ of different CSFV genotypes, including LPC/AHRI strain (G1.1) (46), TD/96/TWN strain (G2.1a) (47), and 94.4/IL/94/TWN (G3.4) (32) at 37°C for 1 h, and subsequently added into PK-15 seeded 96-well microplates. At 72 h post-infection, the cells were fixed with 10% formalin for CSFV antigen detection by IFA staining, as previously described (45). The neutralizing titer in the $\log_2$ of the Ab dilution factor was recorded.

2.9. Translational alignment and statistical analysis

Translational alignment of all four E2 sequences were carried out using Geneious 9 (Version 9.1.8).[1] Data were analyzed using software GraphPad Prism (version 8.4.0) (GraphPad Software Inc., San Diego, CA, United States) and differences were considered significant by p-value ($^*p < 0.05$; $^{**}p < 0.01$).

3. Results

3.1. Expression and detection of different CSFV E2 glycoproteins

After G418 selection, the expression of each CSFV E2 glycoprotein was successfully detected in HEK293 cells using an anti-V5 antibody. In each CSFV E2 plasmid-transfected cell line, more than 90% of cells were stained positive by ICC (Figures 2A,B). The expression medium collected contained 3–4.5 mg of E2 glycoprotein/L after purification. After protein purification of the supernatant of these CSFV E2 glycoprotein-expressing stable cell lines, proteins migrated to 100 kDa under non-reduction conditions and were suspected as homodimers. Proteins migrated to 50 kDa under reduction conditions corresponding to the predicted size of E2 monomer were confirmed by using an anti-V5 antibody (Figure 2C) and the anti-CSF E2 specific antibodies, WH303 (Figure 2D).

3.2. Cross-reactivity of LPCV-induced antibody responses in pigs against different genotypes of CSFV E2 proteins

To investigate the cross-reactivity of the LPC-induced porcine IgG against different genotypes of CSFV E2 proteins, a panel of 177 porcine serum samples from farms with and without an LPC-vaccination history was used. The binding activity of porcine sera against CSFV was first evaluated using IFA on LPC virus-infected PK-15 cells. Under fluorescent microscopic examination, a total of 78 serum samples were positive for IgG against LPC-infected PK-15 cells. Ninety-nine sera were negative.

Using the IFA-characterized porcine sera, the cross-reactivity of these porcine sera against different genotypes of CSFV E2 proteins was investigated by ELISAs (Figure 3). The S/P ratio of the commercially available ELISA was calculated following the manufacturer's recommendations. Using the mean value of the negative samples plus two standard deviations (mean + 2SD) as the cut-off values for in-house CSFV G1.1 E2-based ELISA had a cut-off O.D. of 0.71; the in-house CSFV G2.1a E2-based ELISA had a cut-off value of 0.71; the in-house CSFV 2.1d-based E2 glycoprotein ELISA had a cut-off value of 0.70; and the in-house CSFV 3.4 E2-based glycoprotein ELISA had a cut-off value of 0.66. After evaluating four in-house E2 glycoprotein-based ELISA of the 177 serum samples, all glycoproteins showed comparable sensitivity and specificity to the commercially available CSFV E2 ELISA (Table 1).

3.3. Virus cross-neutralizing test for different CSFV E2 immunized mice

After immunization, elevated anti-CSFV E2 IgG levels in the sera of different CSFV E2 immunized mice were detected. There

1 http://www.geneious.com

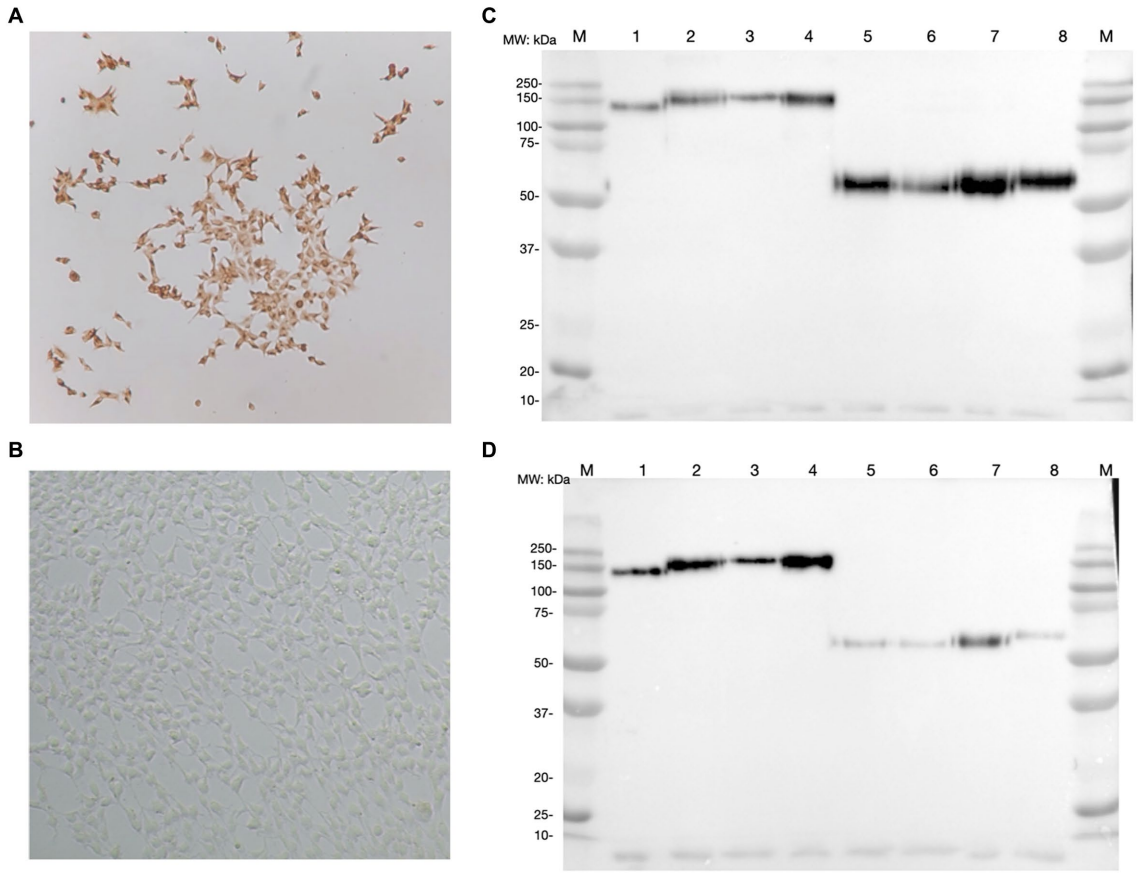

FIGURE 2
Detection of classical swine fever virus (CSFV) E2 expression by immunocytochemistry staining (ICC) and western blot (WB). **(A)** The result of ICC in detecting the expression of CSFV E2 glycoprotein using anti-V5 antibody. **(B)** The ICC result of mock transfected HEK 293 cells **(C)** Western blot result of different CSFV genotypes of E2 glycoproteins detected by anti-V5 antibody. **(D)** Western blot result of different CSFV genotypes of E2 glycoproteins detected by WH303 antibody. The ICC were performed 7days after the transfection in HEK 293 cells fixed with 80% acetone for the immunostaining. Proteins after purification with HisPurTM cobalt resin and separated by SDS-PAGE in both naïve and reduced gels were analyzed by WB detected with anti-V5 or anti-WH303 antibodies. The positions of markers are as indicated. 1, CSFV G 1.1 E2 naïve form; 2, CSFV G 2.1a E2 naïve form; 3, CSFV G 2.1d E2 naïve form; 4, CSFV G 3.4 E2 naïve form; 5, CSFV G 1.1 E2 reduced form; 6, CSFV G 2.1a E2 reduced form; 7, CSFV G 2.1d E2 reduced form; 8, CSFV G 3.4 E2 reduced form; M, Marker.

were no differences in the IgG-binding abilities of these sera against homologous and heterologous CSFV E2 proteins (Figure 4). Antibody neutralizing (NA) in the sera of CSFV E2-immunized mice generally exhibited a better NA against the homologous genotype virus than against the heterologous viruses (Figure 5). Mice immunized with CSFV G1.1 E2 glycoprotein presented significantly higher NA titers (average 1:10,240 dilution) against LPC/AHRI strain (G 1.1) infection than the TD/96/TWN strain (G 2.1a) (average dilution 1:640) and 94.4/IL/94/TWN strain (G 3.4) (average dilution 1:640) in sera. In contrast, CSFV G2.1d E2 protein-immunized sera also exhibited significantly higher NA against the homologous TD/96/TWN strain challenge (G2.1a; average dilution 1:14,480) than LPC/AHRI strain (CSFV G1.1; average dilution 1:1810) and higher NA against the 94.4/IL/94/TWN strain (G 3.4) (average dilution 1:2,560). CSFV G3.4 E2 protein-immunized sera exhibited higher NA titer against 94.4/IL/94/TWN strain (G 3.4) (average dilution 1:17,220) than the LPC/AHRI strain (G 1.1) (average dilution 1:7,240) and significantly higher NA against the TD/96/TWN strain (G 2.1a) (average dilution 1:1,810). No detectable NA was detected in any of the sera collected before protein immunization.

3.4. The deduced amino acid alignments of different E2 sequences

The alignment result revealed several variations in known epitope regions of E2 glycoproteins (Figure 6). As compared to the G 1.1 E2, the G 2.1a E2 had substitutions of L709P, G713E, D725G, V738T, T745I, K761R, and N777S in domain B/C, R786T, A795T, V789L, R848K, D850E, K851R, M857V, N858D, T863I, and N866K in domain A/D; the G 2.1d E2 had substitutions of Y697H, L709P, G713E, D725G, V738I, K761R, and N777S in domain B/C,R786T, A795T, V789L, R848K, D850E, K851R, M857V, N858D, T863I, and N866K in domain A/D. The G 3.4 E2 had substitutions of G713E, K720R, D725N, V738T, K760N, K761R, N777R in domain B/C, R786S, A795T, V789L, D850E, M857G, N858E, T863M, and N866D in domain A/D. Also, substitution of

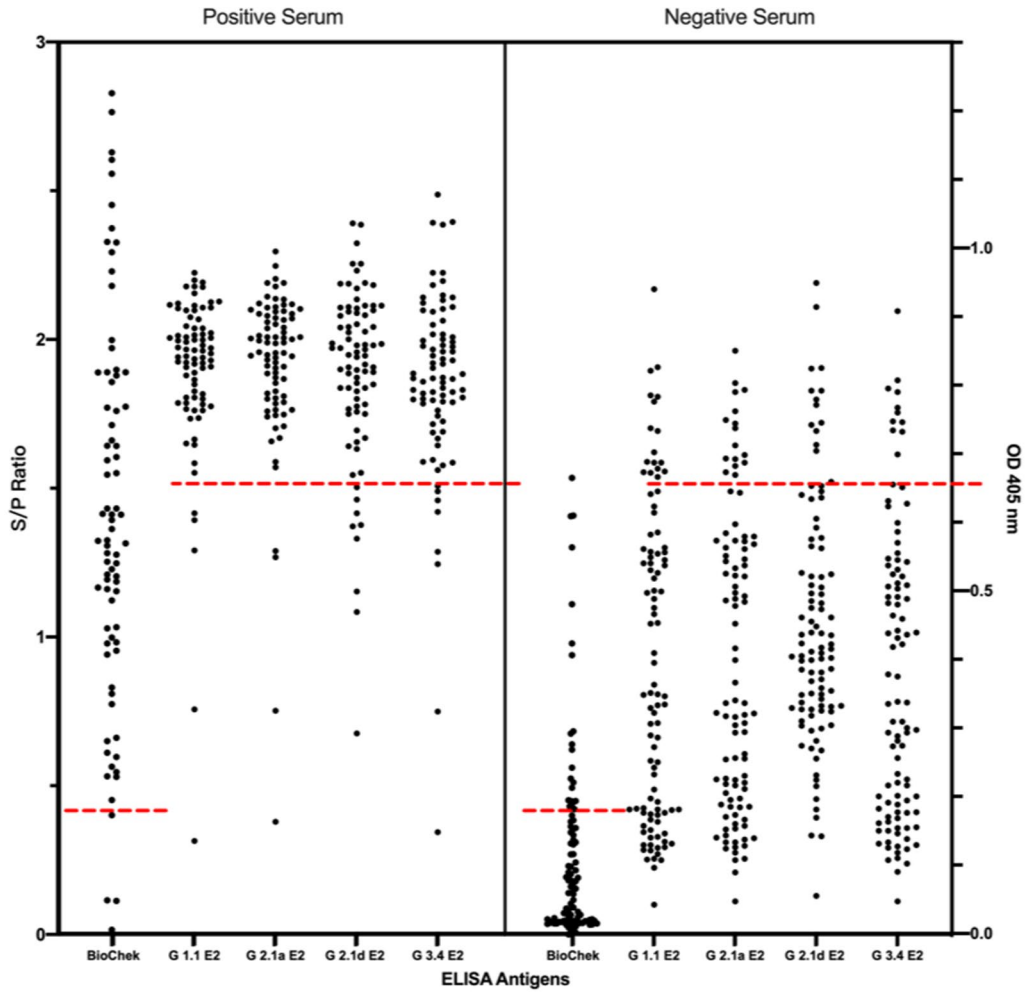

FIGURE 3
Comparison of cross-reactivities of serums derived from pigs with/without LPC vaccine-immunization among the commercial CSFV E2 ELISA and different four different in-house E2 glycoproteins-based ELISA. Results of the commercial CSFV E2 ELISA and in-house E2-based ELISAs are represented as in S/P ratio and OD 405, respectively. Black round dots on the right column are IFA-confirmed negative serums and dots on the left column are the IFA-confirmed serums. Cut-off values are calculated according to the manufacture's guideline or the mean value of the negative samples plus two standard deviations (mean+2SD) for in-house ELISA presented as red dotted lines.

A988T present in G 2.1a, G 2.1d and G 3.4 result in an extra glycosylation site compared to G 1.1 of LPC strain (Figure 6; Supplementary Table 1).

4. Discussion

Historically, CSF has been controlled by extensive vaccination and complete stamp-out programs. However, outbreaks of G2.1d CSF occurred in a large number of C-strain-vaccinated pig farms in China, highlighting the importance of investigating the cross-reaction and cross-neutralizing activity of immune responses against different genotypes of CSFVs (23, 43). In this study, ectodomains of G1.1, G2.1a, G2.1d, and G3.4 CSFV E2 glycoproteins were successfully generated in a mammalian expression system. Antibodies derived from the G1.1 LPCV-immunized animals were demonstrated to recognize all genotypes of E2 glycoproteins. We also demonstrated that different E2 antibodies exhibited better neutralizing abilities against homologous CSFV than heterogeneous viruses. The results provide information on the cross-reactivity of antibodies against different genogroups of CSFV E2 glycoproteins and suggest the importance of developing multivalent E2 subunit vaccines for CSF protection.

TABLE 1 Summarized results of in-house E2 glycoproteins-based ELISAs and the commercial ELISA in detection of IFA-confirmed positive (+) and negative (–) serums against the classical swine fever virus (CSFV) Lapinized Philippines Coronel (LPC) strain in PK-15 cells.

	ELISA result	BioChek	CSFV 1.1 E2	CSFV 2.1 E2	CSFV 2.1d E2	CSFV 3.4 E2
IFA (+) ($N=78$)	Positive	73	70	72	67	70
	Negative	5	8	6	11	8
IFA (–) ($N=99$)	Positive	14	8	9	13	11
	Negative	85	91	90	86	88
Sensitivity		0.936	0.828	0.860	0.828	0.860
Specificity		0.859	0.919	0.909	0.869	0.889
Accuracy		0.893	0.875	0.885	0.849	0.875

In this study, the high cross-reactivity of LPC-induced porcine IgG against different genotypes of CSFV E2 proteins was confirmed by ELISA. Our results also indicated that the HEK293 cell-derived E2 glycoprotein-based ELISA developed, exhibited comparable sensitivity and specificity to the commercially available CSFV E2 ELISA. Several CSFV E2- and E^{rns}-based ELISAs have been developed to evaluate CSFV exposure and immunity in animals with E2 being the most widely adopted and commercially successful ELISA (48–50). Similar to our results, the indirect ELISA based on the Shimen strain (G1.1) E2 expressed by lentivirus-infected Chinese hamster ovary (CHO) cells has been reported to have 92.9% agreement with the viral neutralizing test and 92.2% agreement with the IDEXX blocking ELISA (48). In *Spodoptera frugiperda* (SF21) cells expression system, it has been demonstrated that the Brescia (G1.2) strain, Paderborn (G2.1) strain, and Kanagawa (G3.4) strain E2-based ELISA derived had high Ab binding activities against homologous strain-immunized swine hyperimmune serum (51). However, the E2 protein-based ELISA derived from the *E. coli* expression system had a relative sensitivity of 90.2% and a relative specificity of 55.3% compared with the IDEXX blocking ELISA kit with an overall concordance rate of 80.3% (52). The low specificity of the *E. coli*-expressed E2 protein-based ELISA argues the accuracy of the method.

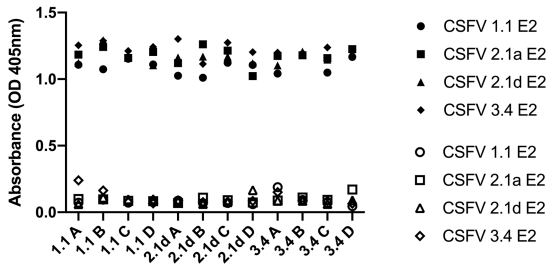

FIGURE 4
Cross-reactivity of IgG before and after G 1.1, 2.1d, and 3.4 E2 immunization in mice against different E2 glycoproteins detected by ELISA. Sera sample were collected retro-orbitally before immunization and at 70days post immunization with different E2 glycoproteins and anti-E2 antibody levels were measured by ELISA coated with G 1.1, G 2.1a, G 2.1d, and G 3.4 E2 and read at OD 405nm. The hollow icons represent serum samples collected prior to immunization and solid icons are at 70days post immunization. Circular shape is against G 1.1 in-house E2-based ELISA, square shape is against G 2.1a in-house E2-based ELISA, triangular shape is against G 2.1d in-house E2-based ELISA, and diamond shape is against G 3.4 in-house E2-based ELISA.

Regarding cross-protectivity of CSFV vaccines, it has been shown that the C-strain vaccine and the LPC G1-based vaccines could prevent the circulation of most G1 CSFVs in the world and reduce the incidences of G3.2 CSFV in Korea, G3.3 CSFV in Thailand, and G3.4 CSFV in Japan and Taiwan (36, 37, 53). The tissue-adapted version of the C-stain vaccine Riemser vaccine has also been demonstrated to provide complete protection against G2.1 and G3.3, and G2.1c CSFVs (8, 38). However, we have demonstrated herein that hyperimmune serum from CSFV E2 glycoprotein-immunized mice exhibited better neutralizing

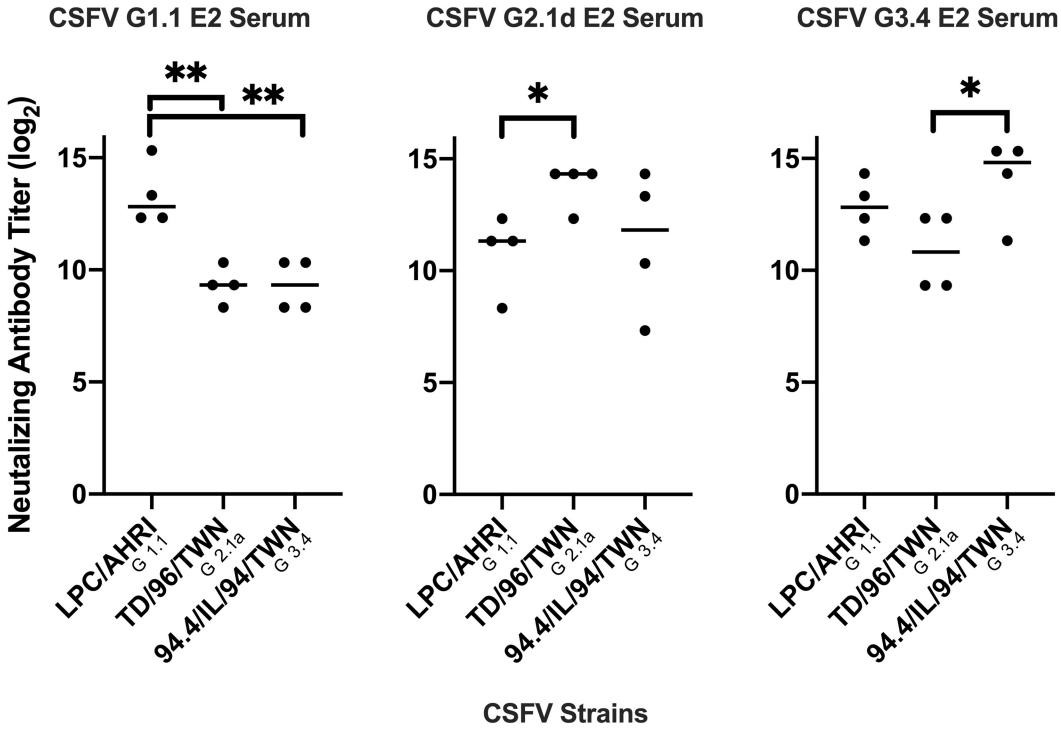

FIGURE 5
Comparison of different mice serum neutralizing antibody titer against different CSFV genotypes. Mice sera at 70days after immunization with G 1.1, G 2.1d, or G 3.4 glycoproteins were collected, inactivated at 56°C, incubated with 100 TCID50 of LPC/AHRI strain (G 1.1), TD/96/TWN strain (G 2.1a), or 94.4/IL/94/TWN strain (G 3.4) of CSFV for 1h at 37°C, and infected PK-15 cells. The highest dilution that is able to stop 50 percent of the cell from infection were recorded. *p<0.05; **p<0.01.

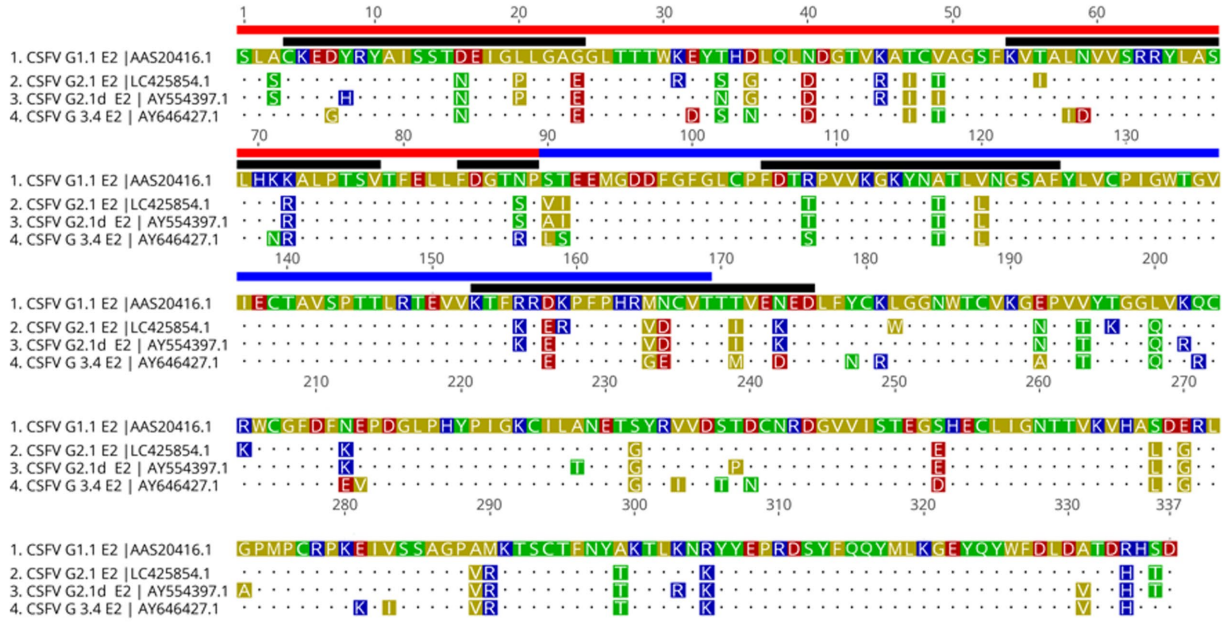

FIGURE 6
Translational alignment of different genotypes of CSFV E2 sequences. The G 1.1 sequence is used as the reference sequence. The B/C domain are underlined in red and A/D domain in blue. Known epitope region are indicated by black line. The extra predicted glycosylation site of G 2.1a, G 2.1d, and G3.4 are marked by the red box.

abilities against homologous CSFV than heterogeneous viruses. Notably, sera derived from mice immunized with the LPC strain E2 (G1.1) had a lower neutralizing antibody titer against G2.1 and G3.4 CSFVs. This is consistent with the previous findings (23, 45). Our results might also explain, at least partially, occasional cases of the new G2.1b and G2.1d sub-genotypes of CSFV infection in a large number of C-strain-vaccinated pig farms in China (54, 55) and the findings of C-strain-based vaccination could provide clinical but not pathological and virological protection against the G2.1d CSFV emerging in China (39). According to our results, we speculated that the antibody induced by the monovalent G1.1 E2 subunit vaccine might not be able to completely neutralize heterogeneous viruses. Since the above-mentioned vaccines are LAVs, further animal experiments to evaluate the cross-protectivity of different genotype E2 proteins against different genotype CSFVs to understand the immune efficacy and protectivity of E2 subunit vaccines are needed.

To investigate potential mutations responsible for the reduction of neutralizing abilities of E2 antibodies against heterogeneous CSFVs, amino acid sequence alignment was performed. Several amino acid substitutions, D705N, L709P, G713E, N723S, and S779A, in the G2.1a and G2.1d E2 sequences reported as antigenic domains responsible for a decrease in the neutralizing ability of heterologous strains (23, 26), were noted. Importantly, these mutations were demonstrated to lead to conformational changes in the antigenic epitope domain covering ^{773}FDGTNP^{778} of the E2 protein predicted by SWISS-MODEL as compared with the CSFV G1.1 E2 protein in the present study (Supplementary Figure 1). This domain is a conserved linear B-cell epitope composed of three essential residues ^{773}F, ^{775}G, and ^{778}P, with ^{774}D and ^{777}N contributing to most of the epitope activity. Replacing of these residues has been demonstrated to abolish or remarkably reduce the reactivity of the epitope (56). We propose that the substitutions and structural alteration of the epitope domains of the E2 protein might be responsible for the differences in the lower neutralizing ability of the G1.1 LPC strain virus against the G2.1a and G2.1d CSFVs. Further investigations, such as mutagenesis assays of E2 proteins, to map critical mutations responsible for the viral neutralization are also needed.

Live attenuated vaccines have been widely used to control CSFV. Among the currently used vaccines to combat CSFV, LAVs are the most common, with worldwide adaptation to region-specific strains or genotypes. However, LAVs have several disadvantages, including acceptance of maternal-derived Ab titer interference (57), lack of DIVA ability, the requirement for low-temperature transportation, and the possibility of virulence reversion (58). Combined with the progress in molecular biology and insight into the pathogenesis of CSFV infections, methods to distinguish vaccinated and clinically infected pigs can be developed using subunit E2 DIVA vaccines. However, variable results of vaccination-challenge experiments and transmission studies on E2 subunit vaccines (59, 60) suggest limited capacity of monovalent CSFV E2 subunit vaccines to provide sterilizing immunity against heterogeneous field CSFV-strains in pigs (59–61). For CSFV subunit vaccine development, multivalent subunit vaccines should be essential based on the reduction in neutralizing ability against heterogeneous CSFV observed in the present study. Using the mammalian expression system of HEK-293 could provide unique opportunities for E2 proteins to process complex multi-dimensional folding and post-translational modifications. Four CSFV E2 proteins covering G1-G3 CSFV with proper mammalian glycosylation and able to elicit neutralizing antibodies against G1–G3 CSFVs generated in this study could be multi-covalent CSFV subunit vaccine candidates.

Data availability statement

The original contributions presented in the study are included in the article/Supplementary material, further inquiries can be directed to the corresponding author.

Ethics statement

The animal study was reviewed and approved by IACUC protocol (No. A10008) at the Animal Health Research Institute.

Author contributions

W-TC and H-ML contributed to the data acquisition, analysis, and interpretation. W-TC drafted and revised the manuscript. C-YC, M-CD, Y-LH, Y-CC, and H-WC contributed to the conception, design, and data acquisition. H-WC contributed to the conception and design, revised the manuscript critically for important intellectual content, and approved the final version to be published. All authors agreed to be accountable for all aspects of this work, ensuring that questions related to the accuracy and integrity of any part of this work were appropriately investigated and resolved.

Funding

This work was supported by the Ministry of Science and Technology, Taiwan, R.O.C. (MOST 109-2313-B-002-016-MY3) and the National Taiwan University (Grant no. 112L894802).

Acknowledgments

The authors expressed deep gratitude toward the lab of molecular pathobiology of the Graduate Institute of Molecular and Comparative Pathobiology for providing infrastructure and facilities. It was a collaborative work among Graduate Institute of Molecular and Comparative Pathobiology, School of Veterinary Medicine, National Taiwan University (Taiwan), Classical Swine Fever group of Animal Health Research Institute (Taiwan) and Institute of Biological Chemistry, Academia Sinica (Taiwan).

Conflict of interest

The authors declare that the research was conducted in the absence of any commercial or financial relationships that could be construed as a potential conflict of interest.

Publisher's note

All claims expressed in this article are solely those of the authors and do not necessarily represent those of their affiliated organizations, or those of the publisher, the editors and the reviewers. Any product that may be evaluated in this article, or claim that may be made by its manufacturer, is not guaranteed or endorsed by the publisher.

Supplementary material

The Supplementary material for this article can be found online at: https://www.frontiersin.org/articles/10.3389/fvets.2023.1169766/full#supplementary-material

References

1. Artois M, Depner K, Guberti V, Hars J, Rossi S, Rutili D. Classical swine fever (hog cholera) in wild boar in Europe. *Rev Sci Tech*. (2002) 21:287–303. doi: 10.20506/rst.21.2.1332

2. Edwards S, Fukusho A, Lefèvre PC, Lipowski A, Pejsak Z, Roehe P, et al. Classical swine fever: the global situation. *Vet Microbiol*. (2000) 73:103–19. doi: 10.1016/S0378-1135(00)00138-3

3. Ganges L, Crooke HR, Bohórquez JA, Postel A, Sakoda Y, Becher P, et al. Classical swine fever virus: the past, present and future. *Virus Res*. (2020) 289:198151. doi: 10.1016/j.virusres.2020.198151

4. Hanson R. Origin of hog cholera. *J Am Vet Med Assoc*. (1957) 131:211–8.

5. Liess B. Pathogenesis and epidemiology of hog cholera. *Ann Rech Vet*. (1987) 18:139–45.

6. Postel A, Nishi T, Kameyama KI, Meyer D, Suckstorff O, Fukai K, et al. Reemergence of classical swine fever, Japan, 2018. *Emerg Infect Dis*. (2019) 25:1228–31. doi: 10.3201/eid2506.181578

7. Shimizu Y, Hayama Y, Murato Y, Sawai K, Yamaguchi E, Yamamoto T. Epidemiology of classical swine fever in Japan—a descriptive analysis of the outbreaks in 2018–2019. *Front Vet Sci*. (2020) 7:573480–0. doi: 10.3389/fvets.2020.573480

8. Wang FI, Chang CY. Classical swine fever: a truly classical swine disease. *Pathogens*. (2020) 9:745. doi: 10.3390/pathogens9090745

9. Ganges L, Núñez JI, Sobrino F, Borrego B, Fernández-Borges N, Frías-Lepoureau MT, et al. Recent advances in the development of recombinant vaccines against classical swine fever virus: cellular responses also play a role in protection. *Vet J*. (2008) 177:169–77. doi: 10.1016/j.tvjl.2007.01.030

10. Van Oirschot JT, Terpstra C. Hog cholera virus In: . *Virus infections of porcines*. eds. Straw, B. E., D'Allaire, S., Mengeling, W. L., Taylor, D. J. Amsterdam: Elsevier (1989). 113–31.

11. Blome S, Staubach C, Henke J, Carlson J, Beer M. Classical swine fever—an updated review. *Viruses*. (2017) 9:86. doi: 10.3390/v9040086

12. Moennig V, Floegel-Niesmann G, Greiser-Wilke I. Clinical signs and epidemiology of classical swine fever: a review of new knowledge. *Vet J*. (2003) 165:11–20. doi: 10.1016/S1090-0233(02)00112-0

13. Choi C, Chae C. Localization of classical swine fever virus from chronically infected pigs by in situ hybridization and immunohistochemistry. *Vet Pathol*. (2003) 40:107–13. doi: 10.1354/vp.40-1-107

14. Bohórquez JA, Muñoz-González S, Pérez-Simó M, Muñoz I, Rosell R, Coronado L, et al. Foetal immune response activation and high replication rate during generation of classical swine fever congenital infection. *Pathogens*. (2020) 9:285. doi: 10.3390/pathogens9040285

15. Van Oirschot JT, Terpstra C. A congenital persistent swine fever infection. I. Clinical and virological observations. *Vet Microbiol*. (1977) 2:121–32. doi: 10.1016/0378-1135(77)90003-7

16. Muñoz-González S, Ruggli N, Rosell R, Pérez LJ, Frías-Leuporeau MT, Fraile L, et al. Postnatal persistent infection with classical swine fever virus and its immunological implications. *PLoS One*. (2015) 10:e0125692. doi: 10.1371/journal.pone.0125692

17. Postel A, Schmeiser S, Bernau J, Meindl-Boehmer A, Pridotkas G, Dirbakova Z, et al. Improved strategy for phylogenetic analysis of classical swine fever virus based on full-length E2 encoding sequences. *Vet Res*. (2012) 43:50. doi: 10.1186/1297-9716-43-50

18. Rios L, Coronado L, Naranjo-Feliciano D, Martínez-Pérez O, Perera CL, Hernandez-Alvarez L, et al. Deciphering the emergence, genetic diversity and evolution of classical swine fever virus. *Sci Rep*. (2017) 7:17887. doi: 10.1038/s41598-017-18196-y

19. Wang FI, Deng MC, Huang YL, Chang CY. Structures and functions of pestivirus glycoproteins: not simply surface matters. *Viruses*. (2015) 7:3506–29. doi: 10.3390/v7072783

20. Hulst M, Westra D, Wensvoort G, Moormann R. Glycoprotein E1 of hog cholera virus expressed in insect cells protects swine from hog cholera. *J Virol.* (1993) 67:5435–42. doi: 10.1128/jvi.67.9.5435-5442.1993

21. Gavrilov BK, Rogers K, Fernandez-Sainz IJ, Holinka LG, Borca MV, Risatti GR. Effects of glycosylation on antigenicity and immunogenicity of classical swine fever virus envelope proteins. *Virology*. (2011) 420:135–45. doi: 10.1016/j.virol.2011.08.025

22. Li Y, Yuan M, Han Y, Xie L, Ma Y, Li S, et al. The unique glycosylation at position 986 on the E2 glycoprotein of classical swine fever virus is responsible for viral attenuation and protection against lethal challenge. *J Virol.* (2022) 96:e01768–21. doi: 10.1128/JVI.01768-21

23. Chen N, Tong C, Li D, Wan J, Yuan X, Li X, et al. Antigenic analysis of classical swine fever virus E2 glycoprotein using pig antibodies identifies residues contributing to antigenic variation of the vaccine C-strain and group 2 strains circulating in China. *Virol J.* (2010) 7:378. doi: 10.1186/1743-422X-7-378

24. Tong C, Chen N, Liao X, Xie W, Li D, Li X, et al. The epitope recognized by monoclonal antibody 2B6 in the B/C domains of classical swine fever virus glycoprotein E2 affects viral binding to Hyperimmune sera and replication. *J Microbiol Biotechnol.* (2015) 25:537–46. doi: 10.4014/jmb.1407.07073

25. Lin M, Lin F, Mallory M, Clavijo A. Deletions of structural glycoprotein E2 of classical swine fever virus strain alfort/187 resolve a linear epitope of monoclonal antibody WH303 and the minimal N-terminal domain essential for binding immunoglobulin G antibodies of a pig hyperimmune serum. *J Virol.* (2000) 74:11619–25. doi: 10.1128/JVI.74.24.11619-11625.2000

26. Huang YL, Meyer D, Postel A, Tsai KJ, Liu HM, Yang CH, et al. Identification of a common conformational epitope on the glycoprotein E2 of classical swine fever virus and border disease virus. *Viruses*. (2021) 13:1655. doi: 10.3390/v13081655

27. Li X, Wang L, Zhao D, Zhang G, Luo J, Deng R, et al. Identification of host cell binding peptide from an overlapping peptide library for inhibition of classical swine fever virus infection. *Virus Genes.* (2011) 43:33–40. doi: 10.1007/s11262-011-0595-7

28. Carbaugh DL, Lazear HM, Gack MU. Flavivirus envelope protein glycosylation: impacts on viral infection and pathogenesis. *J Virol.* (2020) 94:e00104–20. doi: 10.1128/JVI.00104-20

29. Leifer I, Ruggli N, Blome S. Approaches to define the viral genetic basis of classical swine fever virus virulence. *Virology*. (2013) 438:51–5. doi: 10.1016/j.virol.2013.01.013

30. Lowings P, Ibata G, Needham J, Paton D. Classical swine fever virus diversity and evolution. *J Gen Virol.* (1996) 77:1311–21. doi: 10.1099/0022-1317-77-6-1311

31. Vilček Š, Herring AJ, Herring JA, Nettleton PF, Lowings JP, Paton DJ. Pestiviruses isolated from pigs, cattle and sheep can be allocated into at least three genogroups using polymerase chain reaction and restriction endonuclease analysis. *Arch Virol.* (1994) 136:309–23. doi: 10.1007/BF01321060

32. Paton DJ, McGoldrick A, Greiser-Wilke I, Parchariyanon S, Song JY, Liou PP, et al. Genetic typing of classical swine fever virus. *Vet Microbiol.* (2000) 73:137–57. doi: 10.1016/S0378-1135(00)00141-3

33. de Arce H, Frias M, Baireras M, Ganges L, Núnez J, Sobrino F. Analysis of genomic differences between Cuban classical swine fever virus isolates. In: OIE Symposium on Classical Swine Fever. Birmingham. (1998).

34. de Arce HD, Ganges L, Barrera M, Naranjo D, Sobrino F, Frías MT, et al. Origin and evolution of viruses causing classical swine fever in Cuba. *Virus Res.* (2005) 112:123–31. doi: 10.1016/j.virusres.2005.03.018

35. Pereda A, Greiser-Wilke I, Schmitt B, Rincon M, Mogollon J, Sabogal Z, et al. Phylogenetic analysis of classical swine fever virus (CSFV) field isolates from outbreaks in south and Central America. *Virus Res.* (2005) 110:111–8. doi: 10.1016/j.virusres.2005.01.011

36. Cha SH, Choi EJ, Park JH, Yoon SR, Kwon JH, Yoon KJ, et al. Phylogenetic characterization of classical swine fever viruses isolated in Korea between 1988 and 2003. *Virus Res.* (2007) 126:256–61. doi: 10.1016/j.virusres.2007.01.017

37. Sakoda Y, Ozawa S, Damrongwatanapokin S, Sato M, Ishikawa K, Fukusho A. Genetic heterogeneity of porcine and ruminant pestiviruses mainly isolated in Japan. *Vet Microbiol.* (1999) 65:75–86. doi: 10.1016/S0378-1135(98)00284-3

38. Graham SP, Everett HE, Haines FJ, Johns HL, Sosan OA, Salguero FJ, et al. Challenge of pigs with classical swine fever viruses after C-strain vaccination reveals remarkably rapid protection and insights into early immunity. *PLoS One.* (2012) 7:e29310. doi: 10.1371/journal.pone.0029310

39. Luo Y, Ji S, Lei JL, Xiang GT, Liu Y, Gao Y, et al. Efficacy evaluation of the C-strain-based vaccines against the subgenotype 2.1d classical swine fever virus emerging in China. *Vet Microbiol.* (2017) 201:154–61. doi: 10.1016/j.vetmic.2017.01.012

40. Wang Q, Liu H, Xu L, Li J, Wu H, Yang C, et al. Different clinical presentations of subgenotype 2.1 strain of classical swine fever infection in weaned piglets and adults, and long-term cross-protection conferred by a C-strain vaccine. *Vet Microbiol.* (2021) 253:108915. doi: 10.1016/j.vetmic.2020.108915

41. Hao G, Zhang H, Chen H, Qian P, Li X. Comparison of the pathogenicity of classical swine fever virus subgenotype 2.1c and 2.1d strains from China. *Pathogens*. (2020) 9:821. doi: 10.3390/pathogens9100821

42. Jiang DL, Gong WJ, Li RC, Liu GH, Hu YF, Ge M, et al. Phylogenetic analysis using E2 gene of classical swine fever virus reveals a new subgenotype in China. *Infect Genet Evol.* (2013) 17:231–8. doi: 10.1016/j.meegid.2013.04.004

43. Luo Y, Ji S, Liu Y, Lei JL, Xia SL, Wang Y, et al. Isolation and characterization of a moderately virulent classical swine fever virus emerging in China. *Transbound Emerg Dis.* (2017) 64:1848–57. doi: 10.1111/tbed.12581

44. Zhang H, Leng C, Feng L, Zhai H, Chen J, Liu C, et al. A new subgenotype 2.1d isolates of classical swine fever virus in China, 2014. *Infect Genet Evol.* (2015) 34:94–105. doi: 10.1016/j.meegid.2015.05.031

45. Huang YL, Tsai KJ, Deng MC, Liu HM, Huang CC, Wang FI, et al. *In vivo* demonstration of the superior replication and infectivity of genotype 2.1 with respect to genotype 3.4 of classical swine fever virus by dual infections. *Pathogens*. (2020) 9:261. doi: 10.3390/pathogens9040261

46. Deng MC, Huang CC, Huang TS, Chang CY, Lin YJ, Chien MS, et al. Phylogenetic analysis of classical swine fever virus isolated from Taiwan. *Vet Microbiol.* (2005) 106:187–93. doi: 10.1016/j.vetmic.2004.12.014

47. Lin YJ, Chien MS, Deng MC, Huang CC. Complete sequence of a subgroup 3.4 strain of classical swine fever virus from Taiwan. *Virus Genes*. (2007) 35:737–44. doi: 10.1007/s11262-007-0154-4

48. Ji S, Luo Y, Zhang T, Shao L, Meng XY, Wang Y, et al. An improved indirect ELISA for specific detection of antibodies against classical swine fever virus based on structurally designed E2 protein expressed in suspension mammalian cells. *Arch Virol.* (2018) 163:1831–9. doi: 10.1007/s00705-018-3809-7

49. Li D, Dong H, Li S, Munir M, Chen J, Luo Y, et al. Hemoglobin subunit Beta interacts with the capsid protein and antagonizes the growth of classical swine fever virus. *J Virol.* (2013) 87:5707–17. doi: 10.1128/JVI.03130-12

50. Moser C, Ruggli N, Tratschin JD, Hofmann MA. Detection of antibodies against classical swine fever virus in swine sera by indirect ELISA using recombinant envelope glycoprotein E2. *Vet Microbiol.* (1996) 51:41–53. doi: 10.1016/0378-1135(96)00019-3

51. Luo L, Nishi K, MacLeod E, Sabara MI, Lin M, Handel K, et al. Baculovirus expression and antigenic characterization of classical swine fever virus E2 proteins. *Transbound Emerg Dis.* (2013) 60:143–51. doi: 10.1111/j.1865-1682.2012.01327

52. Li W, Mao L, Yang L, Zhou B, Jiang J. Development and partial validation of a recombinant E2-based indirect ELISA for detection of specific IgM antibody responses against classical swine fever virus. *J Virol Methods.* (2013) 191:63–8. doi: 10.1016/j.jviromet.2013.03.003

53. Parchariyanon S, Inui K, Damrongwatanapokin S, Pinyochon W, Lowings P, Paton D. Sequence analysis of E2 glycoprotein genes of classical swine fever viruses: identification of a novel genogroup in Thailand. *Dtsch Tierarztl Wochenschr*. (2000) 107:236–8.

54. Fatima M, Luo Y, Zhang L, Wang PY, Song H, Fu Y, et al. Genotyping and molecular characterization of classical swine fever virus isolated in China during 2016-2018. *Viruses*. (2021) 13:664. doi: 10.3390/v13040664

55. Zhang H, Leng C, Tian Z, Liu C, Chen J, Bai Y, et al. Complete genomic characteristics and pathogenic analysis of the newly emerged classical swine fever virus in China. *BMC Vet Res.* (2018) 14:204. doi: 10.1186/s12917-018-1504-2

56. Peng WP, Hou Q, Xia ZH, Chen D, Li N, Sun Y, et al. Identification of a conserved linear B-cell epitope at the N-terminus of the E2 glycoprotein of classical swine fever virus by phage-displayed random peptide library. *Virus Res*. (2008) 135:267–72. doi: 10.1016/j.virusres.2008.04.003

57. Vandeputte J, Too HL, Ng FK, Chen C, Chai KK, Liao GA. Adsorption of colostral antibodies against classical swine fever, persistence of maternal antibodies, and effect on response to vaccination in baby pigs. *Am J Vet Res*. (2001) 62:1805–11. doi: 10.2460/ajvr.2001.62.1805

58. Je SH, Kwon T, Yoo SJ, Lee DU, Lee S, Richt JA, et al. Classical swine fever outbreak after modified live LOM strain vaccination in naive pigs, South Korea. *Emerg Infect Dis*. (2018) 24:798–800. doi: 10.3201/eid2404.171319

59. Dewulf H, Laevens FK, Koenen F, Vanderhallen H, Mintiens K, Deluyker H, et al. An experimental infection with classical swine fever in E2 sub-unit marker-vaccine vaccinated and in non-vaccinated pigs. *Vaccine*. (2000) 19:475–82. doi: 10.1016/S0264-410X(00)00189-4

60. Uttenthal Å, Le Potier MF, Romero L, Mario De Mia G, Floegel-Niesmann G. Classical swine fever (CSF) marker vaccine: trial I. Challenge studies in weaner pigs. *Vet Microbiol.* (2001) 83:85–106. doi: 10.1016/S0378-1135(01)00409-6

61. Depner K, Bouma A, Koenen F, Klinkenberg D, Lange E, de Smit H, et al. Classical swine fever (CSF) marker vaccine: trial II. Challenge study in pregnant sows. *Vet Microbiol.* (2001) 83:107–20. doi: 10.1016/S0378-1135(01)00410-2

frontiers | Frontiers in Veterinary Science

TYPE Brief Research Report
PUBLISHED 20 June 2023
DOI 10.3389/fvets.2023.1170499

OPEN ACCESS

EDITED BY
Qi Wang,
Chinese Academy of Agricultural Sciences, China

REVIEWED BY
Eunice M. Machuka,
International Livestock Research Institute (ILRI), Kenya
Anbu K. Karuppannan,
Tamil Nadu Veterinary and Animal Sciences University, India

*CORRESPONDENCE
Roongtham Kedkovid
✉ roongtham.k@chula.ac.th
Roongroje Thanawongnuwech
✉ roongroje.t@chula.ac.th

RECEIVED 21 February 2023
ACCEPTED 05 June 2023
PUBLISHED 20 June 2023

CITATION
Sirisereewan C, Nguyen TC, Janetanakit T, Kedkovid R and Thanawongnuwech R (2023) Emergence of novel porcine circovirus 2d strains in Thailand, 2019–2020.
Front. Vet. Sci. 10:1170499.
doi: 10.3389/fvets.2023.1170499

Emergence of novel porcine circovirus 2d strains in Thailand, 2019–2020

Chaitawat Sirisereewan[1], Thanh Che Nguyen[2], Taveesak Janetanakit[3], Roongtham Kedkovid[4,5]* and Roongroje Thanawongnuwech[1,3]*

[1]Department of Veterinary Pathology, Faculty of Veterinary Science, Chulalongkorn University, Bangkok, Thailand, [2]The International Graduate Program of Veterinary Science and Technology, Faculty of Veterinary Science, Chulalongkorn University, Bangkok, Thailand, [3]Center of Excellence for Emerging and Re-emerging Infectious Diseases in Animals and One Health Research Cluster, Faculty of Veterinary Science, Chulalongkorn University, Bangkok, Thailand, [4]Department of Veterinary Medicine, Faculty of Veterinary Science, Chulalongkorn University, Bangkok, Thailand, [5]Center of Excellence in Swine Reproduction, Chulalongkorn University, Bangkok, Thailand

Porcine circovirus 2 (PCV2) has been recognized as a causative agent of porcine circovirus diseases (PCVDs) affecting the global swine industry. In this study, the genetic diversity of PCV2 strains circulating in Thailand between 2019 and 2020 was investigated using 742 swine clinical samples from 145 farms. The results showed PCV2-positive rates of 54.2% (402/742) and 81.4% (118/145) at the sample and farm levels, respectively. Genetic analysis of 51 Thai PCV2 genomic sequences showed that 84.3% (43/51) was PCV2d, 13.7% (7/51) was PCV2b and 1.9% (1/51) was PCV2b/2d recombinant virus. Surprisingly, the majority of the Thai PCV2d sequences from this study (69.77%, 30/43) formed a novel cluster on a phylogenetic tree and contained a unique ^{133}HDAM^{136} on the ORF2 deduced amino acid sequence, which is in one of the previously identified immunoreactive domains strongly involved in virus neutralization. The PCV2b/2d recombinant virus also carried ^{133}HDAM^{136}. The emergence of the novel PCV2d strains predominating in Thailand was discussed. This study highlights the need for further investigations on the spreading of these PCV2d strains in other regions and the efficacy of current commercial vaccines.

KEYWORDS

porcine circovirus 2, PCV2d, mutation, recombination, pigs, Thailand

1. Introduction

Porcine circovirus (PCV) 2, the causative agent of porcine circovirus diseases (PCVDs) affecting the global swine industry, is a non-enveloped single-stranded DNA virus containing a circular genome of 1766–1768 nucleotides (nt) (1) containing three main open reading frames (ORFs). Replicase protein encoded by ORF1 (*Rep* gene) is essential for viral replication (2). Capsid protein encoded by ORF2 (*Cap* gene) is a viral structural protein playing a significant role in the immunogenicity, virulence, and characteristics of the virus genotypes (3, 4). Finally, an ORF3 protein could induce apoptosis (4). Since its discovery, PCV2 has been recognized as a viral pathogen with a significant economic impact on the pig industry in various regions, particularly in North America, Europe, and Asia (5–7).

To date, PCV2 is classified into eight genotypes, PCV2a–h, based on the ORF2 nucleotide sequence (6). PCV2d is currently the predominant genotype worldwide (8), possibly due to selection pressure from the global PCV2 vaccination or the previously circulating PCV2

strains. In general, mutation at neutralizing epitopes might render the mutant virus less susceptible to the pre-existing antibodies (from vaccination or previously circulating viruses) (9). Hence, a further genetic shift from the current PCV2d strains was not unexpected. In this study, novel variants of PCV2d with a unique mutation at a previously recognized immunoreactive domain on the ORF2 were identified and found to rapidly dominate in Thailand. This finding may raise awareness for further investigations on the spreading of these viruses in other regions and the cross-protection with current commercial vaccines.

2. Materials and methods

2.1. Clinical samples

A set of 742 swine clinical samples, each collected from a different pig, were retrieved from the sample repository of Chulalongkorn University, Veterinary Diagnostic Laboratory (CU-VDL) and Diagnostic Laboratory of Large Animal Hospital and Students Training Center (DLSTC). The samples were originally submitted to CU-VDL and DLSTC as part of routine diagnosis from January 2019 to December 2020. These samples were obtained from 145 swine farms located in 18 provinces across different geographical regions of Thailand, primarily in the high pig-density areas in the Western, Central, and Eastern parts (Supplementary Figure 1). The corresponding data of these samples were also obtained, including sample types, sample collection dates, age groups or statuses of the pigs, clinical signs, and farm locations.

2.2. PCV2 detection and DNA sequencing

Viral DNA was extracted from the clinical samples by using the IndiMag Pathogen kit of viral RNA/DNA (Indical Bioscience, Germany) on the automated extraction platform. The obtained DNA was stored at −80°C until used.

For PCV2 detection, a real-time PCR assay was done using Luna® Universal Probe qPCR master mix (NEB, MA, USA) with previously described protocol (10). The PCV2-PCR positive samples were further systematically selected for genetic characterization.

The sample selection process aimed to fulfill three criteria; (1) obtaining at least one PCV2 sequence from each of the six geographical regions of Thailand (the Northern, Northeastern, Central, Western, Eastern, and Southern regions), (2) including PCV2 sequences from both 2019 and 2020, and (3) acquiring a maximum of one PCV2 sequence from each individual pig. Whenever possible, samples with ct values lower than 30 during the PCV2 detection process were selected, to increase the likelihood of successful whole genome sequencing.

For genome sequencing, PCR amplicons were prepared and then submitted to the third-party sequencing company. The PCR assay was performed as previously described (11, 12). The PCR reactions were done using Onetaq® 2x Master Mix (NEB, MA, USA). The PCR products were examined by 1% agarose gels and purified using NucleoSpin™ Gel and PCR Clean-up (MACHEREY-NAGEL, Germany). The PCR products were then submitted to Celemics, Inc. (Seoul, Korea) for barcode-tagged sequencing. The obtained nucleotide sequences were assembled and validated with SeqMan and EditSeq software v.5.03 (DNASTAR Inc., Madison, Wisconsin, USA) and submitted to GenBank.

2.3. Sequence analysis

Classification of the Thai PCV2 sequences was done using a previously proposed phylogeny-based method (6). The Thai PCV2 sequences ($n = 51$) were aligned with a set of PCV2a-h reference sequences ($n = 266$, Supplementary Table 1) (6). In total, 317 sequences were used for phylogenetic analysis. Phylogenetic trees were constructed based on the Neighbor-Joining (NJ) algorithm using p-distance data. The classification was separately done using the complete sequences of genomic, ORF1, and ORF2 data. The tree was also reconstructed using the Maximum Likelihood method with a sequence of PCV1 (GenBank accession number: KJ408798) as an outgroup to confirm the topology.

For the initial PCV2d sequence analysis, a phylogenetic tree of complete ORF2 sequences of Thai PCV2d from 2010 to 2020 was built ($n = 124$). The data from 2010 to 2015 were retrieved from GenBank ($n = 73$, Supplementary Table 2) and the data from 2019 to 2020 ($n = 51$) were from this study. Nucleotide sequences were aligned and the phylogenetic tree was then constructed based on the NJ algorithm with the Maximum Composite Likelihood model (NJ-MCL method).

NCBI BLAST function (https://blast.ncbi.nlm.nih.gov) was performed using 19RBR58 ORF2 as a query sequence (6th February 2023) to retrieve sequences with high similarity from GenBank database for further PCV2d ORF2 analysis. The dataset was named 19RBR58/BLAST ($n = 440$, Supplementary Table 3). The non-redundant version of 19RBR58/BLAST (19RBR58/BLAST/NR, $n = 158$) was used in phylogenetic analysis. A phylogenetic tree was constructed using NJ-MCL method.

Otherwise stated, all sequence alignment was done using the Clustal W algorithm (13) of BioEdit 7.2.5 (14). Phylogenetic tree construction was done using MEGA version 10.2.6 (15) with bootstrap analysis of 1,000 replications.

Recombination analysis was carried out using Recombination Detection Program (RDP, version 4.22) (16). Seven recombination detection methods were used; i.e., RDP, GENECOV, Bootscan, MaxChi, Chimera, SiScan, and 3Seq. A recombination event was accepted when it was detected by at least five methods with the $p < 0.01$. Bonferroni correction was applied. In the final step, the identified recombinant virus was re-analyzed with SIMPLOT software v. 3.5 by Bootscan methods (17) and a direct PCR sequencing covering the recombination breakpoint.

3. Results

3.1. PCV2d is the major genotype in Thailand

PCV2 screening by real-time PCR was done on 742 pigs from 145 farms. The results are shown in Table 1. Overall, animal-level and farm-level positivity were 54.2% (402/742) and 81.4%

TABLE 1 The prevalence of PCV2 in all tested samples during 2019–2020.

Periods	Group of pigs[†]	Types of samples							Prevalence at sample level	Prevalence at farm level
		Pooled tissues	Serum	Feces	Semen	Oral fluids	Colostrum	Umbilical cords	Positive rate	Positive rate
Jan-Dec 2019	Suckling	16/21	0/7	4/7	-	-	-	-	194/373 (52.0%)	62/81 (76.5%)
	Nursery	66/75	24/98	0/1	-	-	-	-		
	Growers	28/28	15/38	0/1	-	-	-	-		
	Breeders	2/4	14/48	1/1	1/10	-	-	-		
	Fetuses	23/34	-	-	-	-	-	-		
Jan-Dec 2020	Suckling	3/8	2/13	0/1	-	-	-	-	208/369 (56.4%)	66/74 (89.2%)
	Nursery	38/43	23/53	1/4	-	0/2	-	2/2		
	Growers	14/15	90/132	-	-	-	-	-		
	Breeders	0/2	10/38	-	1/12	-	2/2	-		
	Fetuses	22/42	-	-	-	-	-	-		
Jan 2019-Dec 2020		212/272 (77.9%)	178/427 (41.7%)	6/15 (40.0%)	2/22 (9.1%)	0/2 (0%)	2/2 (100%)	2/2 (100%)	402/742 (54.2%)	118/145 (81.4%)[‡]

[†]Suckling: < 4 weeks; Nursery: 5–8 weeks; Growers: 9–20 weeks; Breeders: boars, gilts, and sows.
[‡]The PCV2 positive farms were calculated from Jan 2019 to Dec 2020.

(118/145), respectively. Fifty-one PCV2-positive samples (from 51 pigs) from 48 farms were genetically characterized. The nucleotide sequences were deposited in the NCBI GenBank database under accession no. OL677572–OL677622 (Supplementary Table 4). Phylogeny-based genotyping of the ORF2 data showed that the Thai strains were PCV2b and PCV2d (Figure 1), found at 13.73% (7/51) and 84.31% (43/51), respectively (similar results were observed when ORF1 or genome data were used). However, one strain, 19NPT29, was not grouped within any genotype clusters. At the farm level, PCV2b and PCV2d were found at 14.58% (7/48) and 87.50% (42/48), respectively.

3.2. Novel PCV2d variants were identified and dominated among the PCV2d strains

Due to the high detection rate of PCV2d in this study, a phylogenetic tree was constructed to examine the genetic relationship between the current Thai PCV2d sequences (2019–2020) and the previously identified Thai PCV2d sequences (2010–2015). A cluster of PCV2d strains exclusively from 2019 to 2020 with a high bootstrap support was identified (data not shown). This cluster was named 19RBR58-like cluster, which accounted for 69.77% (30/43) of the PCV2d strains or 58.82% (30/51) of the PCV2 in this study. Percent nucleotide sequence identity of the 19RBR58-like cluster were as follows; genomic: 99.60–100, ORF2: 99.29–100, and ORF1: 99.58–100. Amino acid sequence identity was as follows; capsid: 99.15–100, and replicase: 99.36–100.

ORF2 nucleotide and amino acid sequence alignment were examined to identify a distinctive genetic characteristic of the 19RBR58-like cluster. A unique ^{133}HDAM^{136} and ^{232}K were found in all amino acid sequences from the 19RBR58-like cluster. Other Thai PCV2 sequences (PCV2a, b, d, and h) were ^{133}ANAL^{136} or ^{133}ATAL^{136}. To our knowledge, PCV2 strains with ^{133}HDAM^{136} have not been reported previously.

NCBI BLAST function using 19RBR58 ORF2 (6th February 2023) (https://blast.ncbi.nlm.nih.gov) was used to retrieve sequences with high similarity from GenBank database for further analysis (Supplementary Table 3). From the dataset, PCV2d strains with ^{133}HDAM^{136} from Japan and Taiwan during the period of 2018–2020 were found. However, those sequences were direct submissions. Moreover, PCV2d with amino acid sequences other than HDAM, ANAL, and ATAL at the position 133–136 were also identified (Supplementary Table 3) such as HAAM and HNAM. Clustering of the 19RBR58-like viruses was shown in Figure 2.

3.3. The novel PCV2d variants was a parental strain of a PCV2b/2d recombinant virus

Recombination analysis using seven different methods provided strong statistical support (average $p = 3.84 \times 10^{-9}$) confirming that 19NPT29 is an intergenotypic recombinant virus of PCV2b and PCV2d. The analysis indicated that PCV2b strains (such as South Korea/2016/KU-1605-like viruses) and PCV2d strains (such as Thailand/2019/19RBR10-like viruses) were the potential parental strains involved in the recombination event. Notably, the parental PCV2d strain was also found within the 19RBR58-like cluster, and the presence of ^{133}HDAM^{136} and ^{232}K in the capsid protein was observed in 19NPT29. The putative recombination breakpoints were identified at

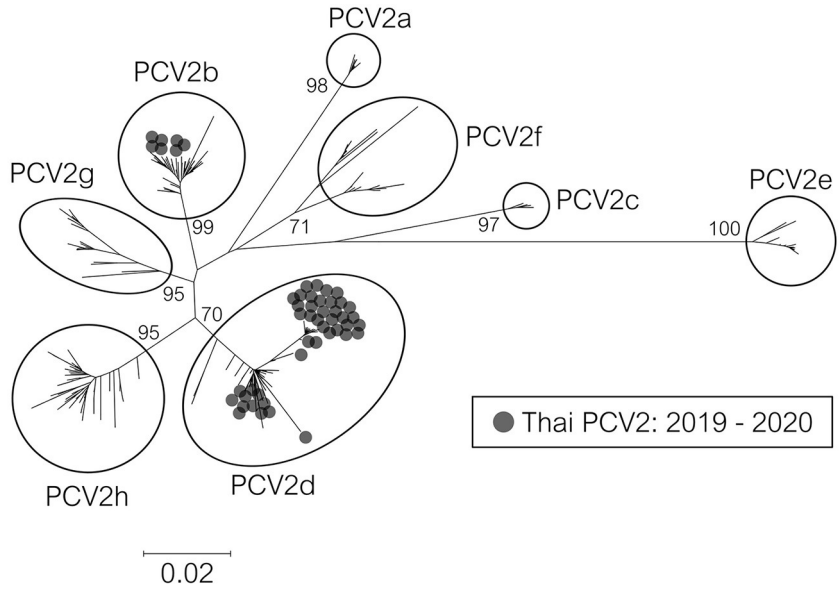

FIGURE 1
Phylogenetic tree of PCV2 ORF2 sequences from Thailand. The 317 complete ORF2 sequences were Thai PCV2 sequences (2019–2020) in this study and reference sequences from an available database (6). The tree was constructed using the Neighbor-Joining method with a p-distance model and bootstrapping at 1,000 replicates. Node labels indicate bootstrap values. The taxon position markers were adjusted to enhance readability.

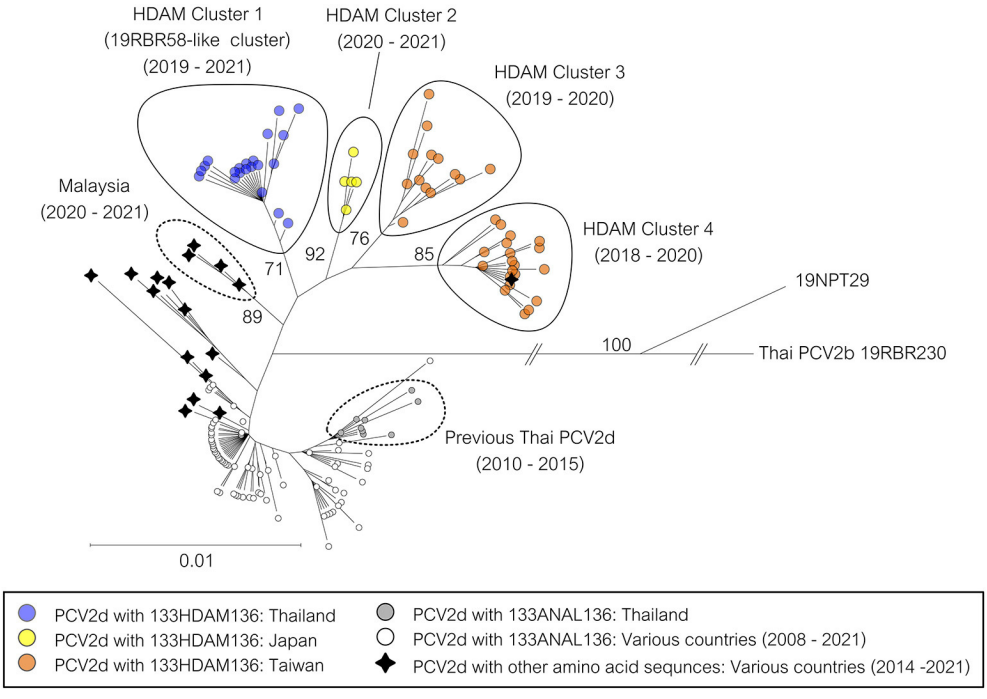

FIGURE 2
Phylogenetic tree of PCV2d ORF2 sequences from Thailand. The 158 complete ORF2 sequences were Thai PCV2d sequences in this study and the related PCV2d sequences from NCBI BLAST. A sequence of Thai PCV2b was used as an outgroup. The tree was constructed using the Neighbor-Joining method with the Maximum Composite Likelihood model and bootstrapping at 1,000 replicates. Node labels indicate bootstrap values. Specific branches were shortened, and the taxon position markers were adjusted to improve readability. A tree with each taxon label indicating the country of origin and the year of sample collection is available as Supplementary Figure 2.

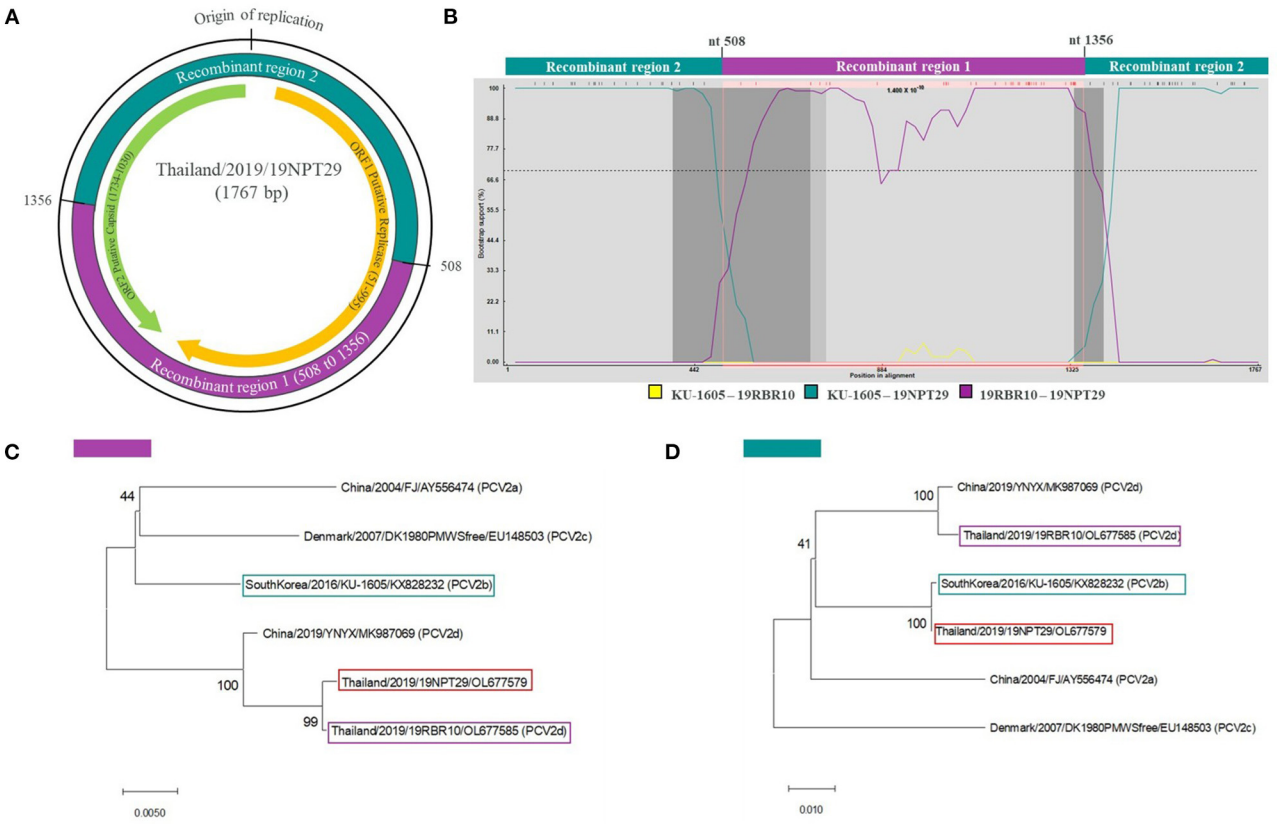

FIGURE 3
Recombination analysis of 19NPT29. Recombination analysis was done using RDP software. Recombination breakpoints were identified in ORF1 and ORF2 regions of the 19NPT29 genome, resulting in recombinant region 1 (purple shaded) and 2 (dark green shaded) **(A)**. Bootscanning analysis shows KU-1605 (South Korea) and 19RBR10 (Thailand, in this study) as parental strains **(B)**. The phylogenetic trees were constructed based on recombinant region 1 **(C)** and 2 **(D)** to confirm recombination event.

nucleotide positions 508 (ORF1) and 1356 (ORF2) (Figure 3). The detection rate of the recombinant strain at the animal and farm levels was found to be 1.96% (1/51) and 2.08% (1/48), respectively.

4. Discussion

PCV2 is a major swine virus causing economic losses. Although vaccines have been widely used, vaccine failures and immune escaping mutation of PCV2 has been proposed (8). In this study, novel variants of PCV2d were identified providing a clue on the PCV2 evolution and epidemiology.

The prevalence of PCV2 in Thailand remained consistently high during the period of 2019–2020 compared to the period of 2009–2015. The prevalence at the animal level from 2009 to 2015 was 44.09% (18). In the current study, the prevalence increased to 54.2%. At the farm level, the prevalence from 2009 to 2015 was 80% (18), and in 2019–2020, it reached 81.4%. These findings suggests that PCV2 was still circulating, despite the implementation of PCV2 vaccines in Thailand. Unfortunately, the PCV2 vaccination status of each farm was not available in this study. Therefore, no conclusion can be made regarding the effect of the PCV2 vaccination and the overall PCV2 prevalence in Thailand.

In recent years, a genotype shift toward PCV2d can be observed in various countries, particularly in Asia. These countries include China (19), South Korea (20), Vietnam (21), Malaysia (22), and Thailand (18). In Thailand, the prevalence of PCV2d has been increasing since 2010, with only PCV2d detected by 2015 (18). However, in this study, a novel strain of PCV2d, which accounted for 69.77% of all the current Thai PCV2d, was identified. Therefore, this novel strain of PCV2d plays a crucial role in the prevailing PCV2d strain in Thailand during 2019–2020. Moreover, this finding suggests that it may serve as the starting point for the next genetic shift within PCV2d.

This study identified the dominance of novel PCV2d strains, the 19RBR58-like cluster, over the previously circulating PCV2 strains in Thailand. At position 133–136 of the capsid protein, the 19RBR58-like cluster was ^{133}HDAM^{136} while other Thai PCV2 strains were ^{133}ANAL^{136} or ^{133}ATAL^{136}. Notably, this region of amino acids resides in one of the antibody recognition domains (domain B) previously described (23, 24), i.e., domain A (aa 51–84), B (aa 113–139), C (aa 161–207), and D (aa 228–233). A single mutation at position 134, 135 or 136 has been shown to strongly reduce the neutralization activity (9). Therefore, the capsid protein with ^{133}HDAM^{136} might render the 19RBR58-like cluster less susceptible to the antibodies from the previously circulating strains and the vaccines. In fact, PCV2 vaccination is widely implemented

in Thailand (personal communication). The observed immune escaping mechanism is further supported by the rapid increase of the 19RBR58-like cluster. Prior to 2015, the 19RBR58-like cluster was not detected in Thailand, and there is a lack of sequence data from 2016 to 2018. Thus, it is possible that the emergence of the 19RBR58-like cluster occurred during the period of 2016–2018.

In addition to Thailand, this study also identified PCV2d sequences with ^{133}HDAM^{136} from Japan and Taiwan (direct submission in GenBank). Interestingly, the strains carrying ^{133}HDAM^{136} from each region formed a distinct cluster on the phylogenetic tree. This suggests that the current situation of these viruses may not be attributed to recent spreading between regions. Phylogenetic analysis further revealed that all the clusters harboring ^{133}HDAM^{136} (Thailand, Japan, and Taiwan) likely share a common ancestor with PCV2d strains from Malaysia. At present, the prevalence of the ^{133}HDAM^{136} PCV2d variants in Japan and Taiwan is unknown. Further investigations are needed to determine whether the prevalence of these PCV2d variants is high, similar to that observed in Thailand.

Recombinant viruses derived from PCV2d strains have been reported in various countries, including China, India, and South Korea (25–27). In this study, a recombinant PCV2d/PCV2b strain, named 19NPT29, was identified. Interestingly, ^{133}HDAM^{136} was also found in the capsid protein of 19NPT29. It would be valuable to conduct further studies to investigate whether the presence of ^{133}HDAM^{136} provides any advantages to the recombinant PCV2 strain, particularly in the case of inter-genotypic recombinants. Unfortunately, conducting further epidemiological studies on the 19NPT29-like viruses from the source farm is not possible as the farm is no longer operational.

The main limitation of this study was the absence of information regarding the vaccination status of the farms, along with the passive surveillance nature of the study. The observed mutation in the antibody recognition domain of the capsid protein within the 19RBR58-like cluster is suspected to have played a role in its emergence. Therefore, the information regarding the vaccination status would have been invaluable for interpreting the data and generating hypotheses for further studies on cross-protection. Furthermore, it is important to note that the samples used in this study were obtained from two diagnostic laboratories (CU-VDL and DLSTC), which may have led to potential underrepresentation of certain geographical regions. However, it is worth mentioning that this study managed to collect samples from all the high-pig-density regions in the country. Conducting active surveillance in the future may provide a more precise assessment of the prevalence of PCV2 and the PCV2d status.

In conclusion, this study reveals the presence of a novel PCV2d strain with ^{133}HDAM^{136} in the capsid protein as the predominant PCV2 strain in Thailand. Additionally, a recombinant virus between PCV2b and the novel PCV2d was identified. The emergence of these novel PCV2d strains might have been influenced by both vaccination and the previously circulating viruses. Conducting active surveillance can provide a comprehensive understanding of PCV2 evolution and facilitate the implementation of early interventions against the emergence of novel strains.

Data availability statement

The datasets presented in this study can be found in online repositories. The names of the repository/repositories and accession number(s) can be found in the article/Supplementary material.

Author contributions

CS, TN, and TJ collected the samples and did the PCR and sequencing. CS, RK, and RT analyzed the data and interpreted the results and prepared the manuscript. All authors helped in designing the research and contributed to the article and approved the submitted version.

Funding

This project was supported by the National Research Council of Thailand (NRCT): RT NRCT Senior scholar 2022 #N42A650553.

Acknowledgments

CS would like to thank the Second Century Fund (C2F), Chulalongkorn University, for providing the scholarship. In addition, we thank the staff of Veterinary Diagnostic Laboratories, Faculty of Veterinary Science, Chulalongkorn University for their technical assistance. We would like to thank Chulalongkorn University for supporting the Center of Excellence for Emerging and Re-emerging Infectious Disease in Animals (CUEIDAs) (GCE6403031002-1) and the One Health Research Cluster (CU-764002-HE02).

Conflict of interest

The authors declare that the research was conducted in the absence of any commercial or financial relationships that could be construed as a potential conflict of interest.

Publisher's note

Supplementary material

The Supplementary Material for this article can be found online at: https://www.frontiersin.org/articles/10.3389/fvets.2023.1170499/full#supplementary-material

References

1. Guo LJ, Lu YH, Wei YW, Huang LP, Liu CM. Porcine circovirus type 2 (Pcv2): genetic variation and newly emerging genotypes in China. *Virol J.* (2010) 7:273. doi: 10.1186/1743-422X-7-273

2. Mankertz J, Buhk HJ, Blaess G, Mankertz A. Transcription analysis of porcine circovirus (Pcv). *Virus Genes.* (1998) 16:267–76. doi: 10.1023/A:1008022521329

3. Nawagitgul P, Morozov I, Bolin SR, Harms PA, Sorden SD, Paul PS. Open reading frame 2 of porcine circovirus type 2 encodes a major capsid protein. *J Gen Virol.* (2000) 81:2281–7. doi: 10.1099/0022-1317-81-9-2281

4. Olvera A, Cortey M, Segales J. Molecular evolution of porcine circovirus type 2 genomes: phylogeny and clonality. *Virology.* (2007) 357:175–85. doi: 10.1016/j.virol.2006.07.047

5. Grau-Roma L, Fraile L, Segales J. Recent advances in the epidemiology, diagnosis and control of diseases caused by porcine circovirus type 2. *Vet J.* (2011) 187:23–32. doi: 10.1016/j.tvjl.2010.01.018

6. Franzo G, Segales J. Porcine circovirus 2 (Pcv-2) genotype update and proposal of a new genotyping methodology. *PLoS ONE.* (2018) 13:e0208585. doi: 10.1371/journal.pone.0208585

7. Afolabi KO, Iweriebor BC, Okoh AI, Obi LC. Global status of porcine circovirus type 2 and its associated diseases in Sub-Saharan Africa. *Adv Virol.* (2017) 2017:6807964. doi: 10.1155/2017/6807964

8. Xiao CT, Halbur PG, Opriessnig T. Global molecular genetic analysis of porcine circovirus type 2 (Pcv2) sequences confirms the presence of four main Pcv2 genotypes and reveals a rapid increase of Pcv2d. *J Gen Virol.* (2015) 96:1830–41. doi: 10.1099/vir.0.000100

9. Huang L, Sun Z, Xia D, Wei Y, Sun E, Liu C, et al. Neutralization mechanism of a monoclonal antibody targeting a porcine circovirus type 2 cap protein conformational epitope. *J Virol.* (2020) 94:e01836–19. doi: 10.1128/JVI.01836-19

10. Wang Y, Feng Y, Zheng W, Noll L, Porter E, Potter M, et al. A multiplex real-time pcr assay for the detection and differentiation of the newly emerged porcine circovirus type 3 and continuously evolving type 2 strains in the United States. *J Virol Methods.* (2019) 269:7–12. doi: 10.1016/j.jviromet.2019.03.011

11. Fenaux M, Halbur PG, Gill M, Toth TE, Meng XJ. Genetic characterization of type 2 porcine circovirus (Pcv-2) from pigs with postweaning multisystemic wasting syndrome in different geographic regions of North America and development of a differential Pcr-restriction fragment length polymorphism assay to detect and differentiate between infections with Pcv-1 and Pcv-2. *J Clin Microbiol.* (2000) 38:2494–503. doi: 10.1128/JCM.38.7.2494-2503.2000

12. An DJ, Roh IS, Song DS, Park CK, Park BK. Phylogenetic characterization of porcine circovirus type 2 in Pmws and Pdns Korean pigs between 1999 and 2006. *Virus Res.* (2007) 129:115–22. doi: 10.1016/j.virusres.2007.06.024

13. Thompson JD, Higgins DG, Gibson TJ. Clustal W: improving the sensitivity of progressive multiple sequence alignment through sequence weighting, position-specific gap penalties and weight matrix choice. *Nucleic Acids Res.* (1994) 22:4673–80. doi: 10.1093/nar/22.22.4673

14. Hall TA. Bioedit: a user-friendly biological sequence alignment editor and analysis program for windows 95/98/Nt. *Nucl Acids Symp Ser.* (1999) 41:95–8.

15. Tamura K, Stecher G, Peterson D, Filipski A, Kumar S. Mega6: molecular evolutionary genetics analysis version 60. *Mol Biol Evol.* (2013) 30:2725–9. doi: 10.1093/molbev/mst197

16. Martin DP, Lemey P, Lott M, Moulton V, Posada D, Lefeuvre P. RDP3: a flexible and fast computer program for analyzing recombination. *Bioinformatics.* (2010) 26:2462–3. doi: 10.1093/bioinformatics/btq467

17. Lole KS, Bollinger RC, Paranjape RS, Gadkari D, Kulkarni SS, Novak NG, et al. Full-length human immunodeficiency virus type 1 genomes from subtype C-infected seroconverters in India, with evidence of intersubtype recombination. *J Virol.* (1999) 73:152–60. doi: 10.1128/JVI.73.1.152-160.1999

18. Thangthamniyom N, Sangthong P, Poolperm P, Thanantong N, Boonsoongnern A, Hansoongnern P, et al. Genetic diversity of porcine circovirus type 2 (Pcv2) in Thailand during 2009–2015. *Vet Microbiol.* (2017) 208:239–46. doi: 10.1016/j.vetmic.2017.08.006

19. Nan W, Wu J, Hu H, Peng G, Tan S, Deng Z. Prevalence and genetic diversity of porcine circovirus type 2 in Northern Guangdong Province during 2016–2021. *Front Vet Sci.* (2022) 9:932612. doi: 10.3389/fvets.2022.932612

20. Kwon T, Lee DU, Yoo SJ, Je SH, Shin JY, Lyoo YS. Genotypic diversity of porcine circovirus type 2 (Pcv2) and genotype shift to Pcv2d in Korean pig population. *Virus Res.* (2017) 228:24–9. doi: 10.1016/j.virusres.2016.11.015

21. Doan HTT, Do RT, Thao PTP, Le XTK, Nguyen KT, Hien NTT, et al. Molecular genotypic analysis of porcine circovirus type 2 reveals the predominance of Pcv2d in Vietnam (2018-2020) and the association between Pcv2h, the recombinant forms, and vietnamese vaccines. *Arch Virol.* (2022) 167:2011–26. doi: 10.1007/s00705-022-05517-4

22. Tan CY, Thanawongnuwech R, Arshad SS, Hassan L, Fong MWC, Ooi PT. Genotype shift of malaysian porcine circovirus 2 (Pcv2) from Pcv2b to Pcv2d within a Decade. *Animals.* (2022) 12:1849. doi: 10.3390/ani12141849

23. Mahe D, Blanchard P, Truong C, Arnauld C, Le Cann P, Cariolet R, et al. Differential recognition of Orf2 protein from type 1 and type 2 porcine circoviruses and identification of immunorelevant epitopes. *J Gen Virol.* (2000) 81:1815–24. doi: 10.1099/0022-1317-81-7-1815

24. Lekcharoensuk P, Morozov I, Paul PS, Thangthumniyom N, Wajjawalku W, Meng XJ. Epitope mapping of the major capsid protein of type 2 porcine circovirus (Pcv2) by using chimeric Pcv1 and Pcv2. *J Virol.* (2004) 78:8135–45. doi: 10.1128/JVI.78.15.8135-8145.2004

25. Wei C, Lin Z, Dai A, Chen H, Ma Y, Li N, et al. Emergence of a novel recombinant porcine circovirus type 2 in China: Pcv2c and Pcv2d recombinant. *Transbound Emerg Dis.* (2019) 66:2496–506. doi: 10.1111/tbed.13307

26. Jang G, Yoo H, Kim Y, Yang K, Lee C. Genetic and phylogenetic analysis of porcine circovirus type 2 on Jeju Island, South Korea, 2019–2020: evidence of a novel intergenotypic recombinant. *Arch Virol.* (2021) 166:1093–102. doi: 10.1007/s00705-020-04948-1

27. Parthiban S, Ramesh A, Karuppannan AK, Dhinakar RG, Johnson RJ, Hemalatha S, et al. Emergence of novel porcine circovirus 2 genotypes in Southern India. *Transbound Emerg Dis.* (2022) 69:1804–12. doi: 10.1111/tbed.14158

frontiers | Frontiers in Veterinary Science

TYPE Original Research
PUBLISHED 29 June 2023
DOI 10.3389/fvets.2023.1158306

OPEN ACCESS

EDITED BY
Tao Lin,
New Hope Group, United States

REVIEWED BY
Eduardo Costa,
Wageningen Bioveterinay Research Institute, Netherlands
Dachrit Nilubol,
Chulalongkorn University, Thailand

*CORRESPONDENCE
Gustavo Machado
✉ gmachad@ncsu.edu

RECEIVED 03 February 2023
ACCEPTED 12 June 2023
PUBLISHED 29 June 2023

CITATION
Sanchez F, Galvis JA, Cardenas NC, Corzo C, Jones C and Machado G (2023) Spatiotemporal relative risk distribution of porcine reproductive and respiratory syndrome virus in the United States.
Front. Vet. Sci. 10:1158306.
doi: 10.3389/fvets.2023.1158306

Spatiotemporal relative risk distribution of porcine reproductive and respiratory syndrome virus in the United States

Felipe Sanchez[1,2], Jason A. Galvis[1], Nicolas C. Cardenas[1], Cesar Corzo[3], Christopher Jones[2] and Gustavo Machado[1,2]*

[1]Department of Population Health and Pathobiology, College of Veterinary Medicine, North Carolina State University, Raleigh, NC, United States, [2]Center for Geospatial Analytics, North Carolina State University, Raleigh, NC, United States, [3]Veterinary Population Medicine Department, College of Veterinary Medicine, University of Minnesota, Saint Paul, MN, United States

Porcine reproductive and respiratory syndrome virus (PRRSV) remains widely distributed across the U.S. swine industry. Between-farm movements of animals and transportation vehicles, along with local transmission are the primary routes by which PRRSV is spread. Given the farm-to-farm proximity in high pig production areas, local transmission is an important pathway in the spread of PRRSV; however, there is limited understanding of the role local transmission plays in the dissemination of PRRSV, specifically, the distance at which there is increased risk for transmission from infected to susceptible farms. We used a spatial and spatiotemporal kernel density approach to estimate PRRSV relative risk and utilized a Bayesian spatiotemporal hierarchical model to assess the effects of environmental variables, between-farm movement data and on-farm biosecurity features on PRRSV outbreaks. The maximum spatial distance calculated through the kernel density approach was 15.3 km in 2018, 17.6 km in 2019, and 18 km in 2020. Spatiotemporal analysis revealed greater variability throughout the study period, with significant differences between the different farm types. We found that downstream farms (i.e., finisher and nursery farms) were located in areas of significant-high relative risk of PRRSV. Factors associated with PRRSV outbreaks were farms with higher number of access points to barns, higher numbers of outgoing movements of pigs, and higher number of days where temperatures were between 4°C and 10°C. Results obtained from this study may be used to guide the reinforcement of biosecurity and surveillance strategies to farms and areas within the distance threshold of PRRSV positive farms.

KEYWORDS

PRRS virus, swine disease dynamics, biosecurity, surveillance, local transmission

1. Introduction

Porcine reproductive and respiratory syndrome virus (PRRSV) remains widely distributed across the United States swine industry (1–3). Disease surveillance, vaccination strategies, and biosecurity protocols have played a key role in curving PRRSV outbreaks; however, variants of the endemic North American (NA-type, type 2) and the European (EU-type, type 1) strain periodically cause outbreaks that lead to significant economic losses (4–9). Outbreaks of PRRSV

in the United States have been shown to exhibit seasonal patterns throughout the country, but vary among swine-producing regions (1, 3, 10–12). In the southeastern United States, PRRSV outbreak patterns are typically characterized by a unimodal peak occurring during the fall and winter months, followed by decreases in incidence during the late spring and summer months (1, 3, 10, 13, 14). Summer outbreaks, while less common, occur sporadically and vary by year (3, 7).

The spread of PRRSV is predominantly governed by direct contacts facilitated by the movement of infected pigs between farms, and indirect contacts also referred to as local transmission or area spread, which encompasses several unmeasured between-farm dynamics occurring at close geographical proximity (1, 15–25). Despite local transmission being the least understood transmission pathway of many infectious diseases in humans and animals (26), several epidemiological processes have been attributed to contributing to the local transmission of PRRSV including, the between-farm movement of contaminated personnel (27, 28), trucks delivering pigs and feed (18, 21), animal by-products delivered via feed (16, 18, 29, 30), equipment (e.g., boots, coveralls, bleeding equipment) (28), and airborne viral particle dispersal (23, 31–35). However, differentiating the contribution of each process remains highly challenging. Moreover, the distance at which each process poses a greater risk to neighboring farms remains poorly understood but is fundamental to the understanding of between-farm transmission dynamics (36). Between-farm transmission mechanisms acting on a local scale may vary in relation to the distance between farms and have been reported to range from 1 km to 35 km (1, 11, 17, 18, 20, 32, 33, 35, 37–39). Some of the local transmission mechanisms are also influenced by local environmental conditions (e.g., temperature, relative humidity, pH), genetic diversity of PRRSV, differences in management and biosecurity levels at different farm types, pig density, and the spatial proximity of susceptible farms to infected farms (farm density) (15, 39–41). Given the high density of farms and pigs in intensive pig production areas across the United States, a better understanding of the distance at which the risk of PRRSV transmission from infected to susceptible farms is increased may support and inform the implementation of targeted biosecurity enhancement and surveillance strategies (42, 43).

In this study, we use an adaptive kernel density approach to derive spatial and spatiotemporal estimates of the variation in PRRSV relative risk. Using the kernel density estimate approach, we (1) define the maximum spatial distance at which farms may spread PRRSV based on the proximity of susceptible farms to infected farms and (2) identify farm types with elevated risk for local transmission of PRRSV. Secondly, we implemented a Bayesian spatiotemporal hierarchical model to account for environmental, on-farm biosecurity features, pig density, farm density, and between-farm contact networks metrics to (3) identify factors associated with the risk of PRRSV local transmission.

2. Materials and methods

2.1. PRRSV data source and processing

PRRSV outbreak data for all production types used in this study were obtained from the Morrison Swine Health Monitoring Project (MSHMP) (2). Outbreak data collection was performed by each production company during outbreak investigations or routine surveillance activities and shared with MSHMP (2). Data obtained includes information on farm-level outbreaks between November 1st, 2017, through December 31st, 2020, from 2,293 farms belonging to three non-commercially related pig production companies in a dense pig production region of the United States Information about each farm includes, pig capacity, a unique farm identification number, geographical coordinates (hereafter geolocations), production type, and date of confirmed PRRSV outbreak via PRRSV positive laboratory results. Additionally, the Euclidean distance between farms was calculated using farm geolocations. Production types in our farm population ($n = 2{,}293$) were classified as finisher ($n = 1{,}458$, premises that raise pigs from approximately 10 weeks of age until reaching market weight at approximately 5–6 months of age and include wean-to-finish, and feeder-to-finish), nursery ($n = 468$, premises that raise piglets from weaning from approximately 3 weeks of age to about 10 weeks of age), isolation ($n = 33$, premises specialized in holding breeding or genetic research animals for a temporary period of time), boar stud ($n = 15$), and sow ($n = 319$, premises with breeding, gestation and/or farrowing rooms and includes farrow-to-wean and farrow-to-feeder farms).

Farms were divided into cases and controls, where cases were defined as any farm that reported an outbreak during the time period of interest, and controls are farms that did not report an outbreak. PRRSV case and control data were split into years (2018, 2019, and 2020) and a seasonal classification (PRRSV season). We defined the PRRSV season as a six-month period from November 1st through May 31st, which represents a time period where increases in farm-level PRRSV incidence have been previously described for the region of the United States considered in this study (3, 14).

2.2. Spatial PRRSV relative risk

Spatial kernel density-ratio, also known as spatial "relative risk" (hereafter risk), is an exploratory approach used to describe the geographical variation in disease risk based on the distribution of PRRSV outbreaks (cases) and the underlying at-risk (controls) population (44–47). PRRSV risk (x) was estimated for each farm ($x = \{x_1, \ldots, x_n, n = 2{,}293\ farms\}$) in each year and PRRSV season. Farms can report several PRRSV outbreaks in a given year or PRRSV season; however, for the spatial risk analysis, we defined cases as farms that reported at least one PRRSV outbreak, and controls as the remaining farms that did not report an outbreak for a given year and PRRSV season (46). We identified a total of 245 cases in 2018, 190 cases in 2019, and 165 cases in 2020. For the PRRSV seasons, a total of 227 cases in the 2017–2018 PRRSV season, 167 cases in the 2018–2019 PRRSV season, and 148 cases in the 2019–2020 PRRSV season were used. A nonparametric kernel density-ratio approach was used to estimate the risk $\mathrm{p}(x)$ for each farm location (x) in each year and PRRSV season as follows:

$$\hat{\mathrm{p}}(x) = \log \hat{f}(x) - \log \hat{g}(x) \quad (1)$$

where $\hat{f}(x)$ represents the log density estimates of cases and $\hat{g}(x)$ represents the log density estimates of controls. The natural log is used to symmetrize the treatment of the density estimate ratios, with $\mathrm{p}(x) > 0$, representing areas of medium to high PRRSV risk (high concentrations of cases relative to controls), and $\hat{\mathrm{p}}(x) < 0$, representing areas of low PRRSV risk (low concentration of cases relative to controls) (45–48). Calculating spatial risk relies on the selection of an optimal bandwidth

(the maximum distance at which local transmission is unlikely to occur) which directly drives the decline of the risk probability (kernel) given the geolocation of a farm (45, 46, 87). Given the heterogeneous distribution of farm density in our study area, we used an adaptive smoothing approach that allows the bandwidth of each kernel to vary depending on the density of farms (cases and controls) at a given farm geolocation (49). This method reduces smoothing at locations where the density of farms is high (e.g., 10–20 farms per 5 km^2), and increases the amount of smoothing in areas where farm density is low (e.g., 1–5 farms per 5 km^2) (49). Adaptive smoothing requires the selection of pilot and global bandwidths, where the pilot bandwidths (i.e., cases and controls have a separate fixed distance), and the global bandwidth (i.e., cases and controls have a shared fixed distance), which is a smoothing parameter that adjusts the pilot bandwidth in areas where case and control densities are similarly distributed (45). Here, we compared two different approaches–asymmetric and symmetric adaptive smoothing–for the selection of the pilot bandwidths (Supplementary material S1; Supplementary Figures S1–S6). Pilot and global bandwidths were then used to calculate $\hat{f}(x)$ and $\hat{g}(x)$. Spatial risk (Equation 1) was then calculated by using $\hat{f}(x)$ and $\hat{g}(x)$, and applying a uniform edge-correction, which accounts for the probability loss of farm geolocations close to the boundary of the study region (45, 46). Lastly, we used 1,000 iterations of Monte Carlo simulations to delineate areas of significant spatial risk ($p < 0.05$) (50). Farms within areas of significant risk were quantified as the count of case or control farms falling within areas of significant spatial risk by farm type.

2.3. Spatiotemporal PRRSV relative risk

The spatiotemporal risk of PRRSV was estimated in weekly time steps of cases for each year and PRRSV season, thus cases were defined as farms with at least one outbreak per week and controls as farms that did not report outbreaks for a given week. The entire farm population (n = 2,293) is considered in each weekly time step. A total of 438 cases with an average of 8.76 cases/week were used in 2018, 279 cases with an average of 5.47 cases/week in 2019, and 238 cases with an average of 4.67 cases/week in 2020. Similarly, a total of 382 cases with an average of 12.7 cases/week were used for the 2017–2018 PRRSV season, 231 with an average of 7.45 cases/week in the 2018–2019 PRRSV season, and 190 with an average of 6.33 cases/week in the 2019–2020 PRRSV season. In contrast to the spatial risk, the spatiotemporal risk uses spatial and temporal bandwidths derived from farm geolocations of cases to generate density estimates of cases, while density estimates for controls were generated using only the spatial bandwidth previously calculated for cases since we assume the farm population to be static between November 1st, 2017 and December 31st, 2020 (48, 51, 52). Thus, conditional spatiotemporal risk surfaces were derived as:

$$\hat{p}(x|t) = \log \hat{f}(x,t) - \log \hat{f}(t) - \log \hat{g}(x) \quad (2)$$

where $\hat{p}(x|t)$ is the conditional risk, $\hat{f}(x,t)$ is the log density estimates of cases at a given time step t = (t1,..., t_w, w = 52 weeks per year; w = 30 weeks per PRRSV season), $\hat{f}(t)$ is an estimator for the marginal temporal case density, and $\hat{g}(x)$ is the static spatial log density of the controls (48). One thousand iterations of Monte Carlo simulations were used to delineate areas of significant spatiotemporal risk ($p < 0.05$) (50).

Spatiotemporal risk values generated for the entire farm population at each time step (t) were extracted to individual farm geolocations (x). Farms were then classified as low, medium, and high risk based on quantiles of the spatiotemporal risk distribution of all the farms in each year and PRRSV season. Spatiotemporal risk above 60% of the risk distribution was considered as the exceedance risk threshold (53) since it represented a midpoint between lower (negative) and higher (positive) risk values for the years and PRRSV season. Thus, farms with risk below 60% of the risk distribution were categorized as low risk, 61 to 80% quantile as medium risk, and 81 to 100% quantile as high risk for each year and PRRSV season (Supplementary Figures S7–S12).

2.4. Priority index

The priority index (PI) is a metric that has been used to facilitate the communication of spatiotemporal risk (54). The aim of the PI is to provide an easily interpretable metric, represented as an ordered percentage that indicates the level of prioritization that should be given to a farm based on the estimated risk. The priority index was calculated from the spatiotemporal risk weekly estimates as:

$$PI = \hat{p}(x|t) / \max\left(\hat{p}(x|t)\right) * 100 \quad (3)$$

where the PI of a farm is a percentage based on the risk $\hat{p}(x|t)$ of a farm in reference to the maximum risk value of the farm population. Priority indices calculated for each farm were further reclassified as low (0–30%), medium (31–60%), and high (61–100%) priority classifications based on quantiles. Priority index classifications were then summarized by farm types for each year and PRRSV season time periods and used to set the priority risk order of each farm type.

2.5. Bayesian spatiotemporal hierarchical model framework

We fit a Bayesian spatiotemporal hierarchical model of PRRSV weekly outbreak data to account for three on-farm biosecurity features, six between-farm contact network metrics, six environmental variables, farm density, and pig density (Figure 1; Supplementary material Table S1). A total of 1,948 farms out of our 2,293 farms were used in the Bayesian spatiotemporal hierarchical model, since 217 farms lacked between-farm contact data, 124 lacked on-farm biosecurity features, and four lacked environmental data. Additionally, between-farm contact data was not available for the entire study period; therefore, the Bayesian spatiotemporal hierarchical model was implemented for the year 2020. Farm geolocations i $(i = i_1, \ldots, i_n, n = 1{,}948$ *farms in the year* $2020)$ were defined as $Y_i = 1$ when a PRRSV outbreak was reported, and $Y_i = 0$ for farms with no reported outbreaks of each week in the year 2020. The generalized hierarchical spatiotemporal model was implemented as a logistic regression, where Y_i follows a binomial distribution:

$$Y_i \sim Bernouilli(\mu_i) \quad (4)$$

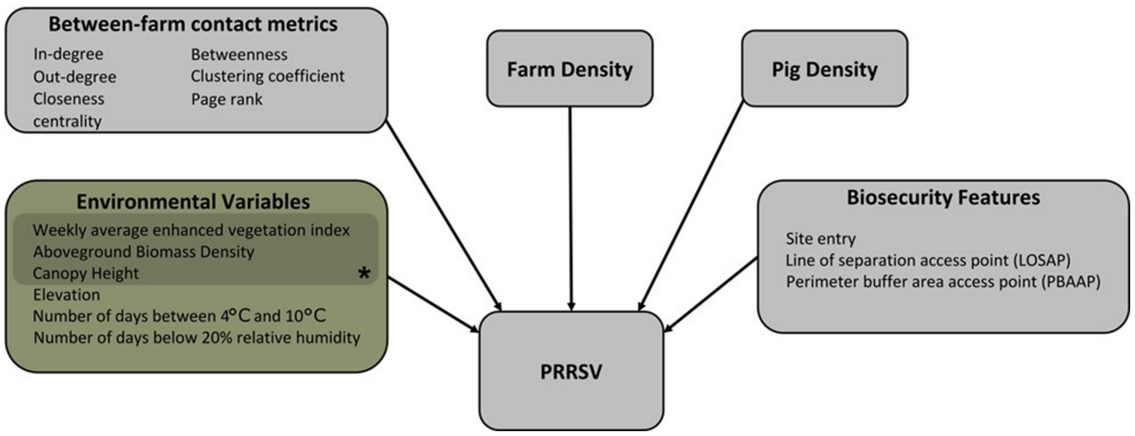

FIGURE 1
The conceptual model framework of the Bayesian spatiotemporal hierarchical model showing the directional relationship between variables and PRRSV outbreaks. *Variables representing vegetation buffers around farms.

and linear predictors were constructed as:

$$Logit\left(\mu_i\right) = \alpha + X\beta + \upsilon\left(i\right) + week\left(w\right) + \omega\left(i\right) \quad (5)$$

where $\propto$ represents the probability of a PRRSV outbreak, α the model intercept, $\boldsymbol{X}\beta$ describes the matrix of covariates, $\upsilon\left(i\right)$ is an independent and identically distributed (iid) random effect to account for variation between individual farms, $week\left(w\right)$ is an *iid* random effect to account for variation between weeks, and $\omega\left(i\right)$ represents a spatial random field (Gaussian field) to account for spatial errors (55).

Briefly, the regression analysis was implemented with a stochastic partial differential equation (SPDE) model using integrated nested Laplace approximations (INLA) (56–60). The process first requires the creation of a mesh of Delaunay triangulations, which includes the specification of the maximum triangle edge length, and the model domain boundary. The resulting mesh (Supplementary Figure S13) consisted of 4,504 triangle vertices, where the model domain boundary was defined by a polygon representative of our study area in which the maximum triangle edge length was specified as 10 km within the inner domain and 20 km in the outer domain (55).

The INLA default priors were used; therefore, the penalized complexity (PC) priors [(1, 0.01), (0.32, 0.01)] were used for the spatial random fields where the spatial range and standard deviation quantile and probability tailored to be higher than 1 is 0.01 (59, 61, 62). Model fixed effect outputs were exponentiated and presented as odds ratio (63, 64). The sensitivity of priors to the posterior random field values was examined by comparing the random posterior mean distribution values of PC priors against log-gamma priors [(1, 0.05), (1, 0.001)] (Supplementary Figure S14).

2.6. Bayesian spatiotemporal hierarchical model data preparation

Variables considered in our Bayesian spatiotemporal hierarchical model framework focus on local transmission mechanisms, and environmental or anthropogenically mediated factors that may contribute to increases or decreases in risk of PRRSV outbreaks (Figure 1; Supplementary material Table S1) (1, 3, 19, 20, 23, 25, 65–67). On-farm biosecurity feature data were extracted for each farm from a database of Secure Pork Supply (SPS) biosecurity plans assembled by the Rapid Access Biosecurity app (RABapp™) (68) and included: the count of site entries, count of perimeter buffer area access points (PBAAP), and count of lines of separation access points (LOSAP) (Supplementary Figure S16; Supplementary material Table S1). In addition to on-farm biosecurity features, we included pig capacity, and farm density, which was calculated by creating a spatial buffer of 17 km around each farm location and counting the number of farms within the buffer. A spatial buffer of 17 km was used based on findings from the spatiotemporal kernel density approach discussed in further detail in section 3.2.

A directed and static network was reconstructed from between-farm pig movement data between January 1st, 2020, and December 31st, 2020, and represented as a graph g = (V, E), where V represents the nodes (farm) of the network and E represents the contact between two nodes or edges of the network. The unique farm identification number in each origin and destination movement record was used to form the edges of the network (69). Between-farm contact network metrics: in-degree, out-degree, PageRank, clustering coefficient, closeness centrality, and betweenness were calculated to characterize node and network-level features of the directed, static network and are described in Supplementary material Table S1. A total of 217 farms were missing pig movement data in 2020, and thus were excluded from this dataset. Therefore, between-farm pig movement data belonging to 1,948 farms was used to calculate between-farm contact network metrics considered in the Bayesian spatiotemporal hierarchical model framework (Figure 1).

Individual farm geolocations were used to extract environmental variables: weekly enhanced vegetation index (EVI), downloaded from the National Aeronautics and Space Administration (NASA), Moderate Resolution Imaging Spectroradiometer (MODIS) Land Products (70), and yearly averages of aboveground biomass density (AGBD), canopy

height, and land surface elevation, downloaded from the Oak Ridge National Laboratory, Distributed Active Archive Center for Biogeochemical Dynamics website (ORNL DAAC) (71). These variables are meant to represent topographical or vegetative buffers around farms that reduce or facilitate the spread of airborne particulate matter and PRRS virus (1, 72–75). Similarly, farm geolocations were used to extract daily average land surface temperature, and relative humidity data from Daymet: Daily Surface Weather Data (76). Temperature and relative humidity have been shown to impact the infectivity and stability of PRRSV (41, 65, 67), and were included in our model as the count of days a farm geolocation *i* was associated with temperatures between 4°C and 10°C [T(4°C,10°C)] [e.g., farm geolocation *i* had 20 days of T(4°C,10°C) over the studied period], and the count of days a farm geolocation *i* was associated with relative humidity below 20% (RH < 20%) (e.g., farm geolocation *i* was 30 days on RH < 20% over the studied period). All variables listed above were downloaded at a 1 km x 1 km spatial resolution and are described in further detail in Supplementary material Table S1. A total of 71 farm geolocations were outside the data availability range of the AGBD, canopy height, or land surface elevation data products; therefore, data from the nearest farm [average = 5 km (min = 446 m; max = 9.8 km)] within a 10 km radius with complete data were used. Four farms were beyond the 10 km threshold and were excluded from the analysis (Supplementary Figure S15).

2.7. Bayesian spatiotemporal hierarchical model variable selection and model comparison

All variables considered in our model framework (Figure 1) were first examined via univariate analysis following the model established in Equation 5, and significance was determined by the 95% credible intervals (CI) in which estimates did not cross one, and the model fit was evaluated using the Watanabe-Akaike information criteria (WAIC). Before selecting variables for the multivariate model, multicollinearity between variables was examined by calculating Pearson's correlation coefficient (r), where significant ($p < 0.05$) correlations above 0.6 were considered highly correlated and would limit our ability to determine individual effects on PRRSV outbreaks. The variables T[4°C,10°C] and RH < 20% ($r = 0.98$), biosecurity features LOSAP and PBAAP ($r = 0.79$), and network metrics, page rank and in-degree ($r = 0.69$) were highly correlated. All other variables were below 0.6 or had insignificant correlations. Among highly correlated variables, the variable yielding a lower WAIC in the univariate analysis was selected for the multivariate model variable selection process. A backward elimination process was carried out starting with all significant variables retained from the univariate analysis. Insignificant variables from the multivariable model were removed one-by-one the and the best-fitting model was selected based on the WAIC. Given the high density of farms in our study area, farm density was included in the multivariate analysis as a confounding factor.

All data extraction, processing, and analyzes presented in this work were performed in the R (4.2.1) programming language (77) using the packages: tidyverse (78), sf (79), sp. (80), spatstat (81), sparr (82), raster (83), igraph (84), MODIStsp (70), daymetr (85), INLA (56), inlabru (86), and INLAoutputs (64).

3. Results

3.1. Spatial PRRSV relative risk

The median distance between farms reporting PRRSV outbreaks was 66.7 km (interquartile range (IQR): 39.4 km - 109.3 km) for 2018, 70 km (IQR: 40.4 km - 114 km) for 2019, 61.4 km (IQR: 36.6 km - 98 km) for 2020, and 66 km (IQR: 39 km - 106.4 km) for all years combined. For the PRRSV seasons, the distance between PRRSV cases was 64.6 km (IQR: 38 km - 107.5 km) for the 2017–2018 PRRSV season, 70.7 km (IQR: 40.2 km - 120.5 km) for the 2018–2019 PRRSV season, and 63.4 km (IQR: 37.3 km - 102 km) for the 2019–2020 PRRSV season. The maximum distance the spatial PRRSV risk extended to was, on average, 14.8 km for both the annual and PRRSV seasons. A total of 377 farms in 2018, 91 in 2019, and 321 in 2020 were within high risk areas ($p < 0.05$) (Table 1). Among the different farm types, sow farms consistently had a higher number of infected farms within areas of significant high risk in both the annual and PRRSV season time periods, while finisher and nursery farms had more control farms (Table 1; Supplementary material Tables S2–S4). Comparison among years, 2018 ($n = 85$) had the greatest number of PRRSV infected farms within significant high risk areas compared to 2019 ($n = 21$) and 2020 ($n = 57$; Table 1).

3.2. Spatiotemporal PRRSV relative risk

The spatiotemporal analysis revealed that the maximum distance PRRSV risk extended to was 15.3 km in 2018, 17.6 km in 2019, and 18 km in 2020, and for the PRRSV seasons, 13.6 km in the PRRSV 2017–2018, 19.2 km in the PRRSV 2018–2019, and 18.9 km in the PRRSV 2019–2020. Spatiotemporal risk estimates for the entire farm population in each time step were classified as high, medium, and low risk based on a 60% exceedance threshold where, on average, 20% of the farms were classified as high risk, 20.1% as medium risk, and 59.9% as low risk for all farm types and years combined (Supplementary Figures S7–S12). Among farm types, boar stud farms were more frequently located in areas of high risk (30% IQR: 27–38%), followed by sow (29% IQR: 27–34%), nursery (19% IQR: 18–22%), finisher (14% IQR: 13–19%) and isolation farms (12% IQR: 9–24%) (Table 2). However, it is important to note that the higher percentages seen for boar stud farms may be driven by the fewer number of boar stud farms (n = 15) in the farm population. Spatiotemporal risk estimates for the PRRSV seasons revealed sow farms we more frequently classified to be in high risk areas (29% IQR: 24–36%) during this time period, followed by boar studs (27% IQR: 20–33%), nursery (21% IQR: 18–24%), isolation farms (12% IQR: 12–30%), and finisher (18% IQR: 16–25%; Supplementary material Table S5). Among all farm types, finisher farms (63% IQR: 54–74%) and nursery farms (57% IQR: 52–67%) were consistently classified to be in areas of low risk for both the yearly (Table 2) and PRRSV season time periods (Supplementary material Table S5).

Our spatiotemporal analysis revealed a seasonal signal, marked by an increase in farms classified as being in high and medium PRRSV risk areas during the fall, winter, and spring months, with varying intensity between farm types, and years 2018 to 2019, and 2019 to 2020 (Figure 2; Supplementary Figure S8). The signal onset of the seasonal pattern appears to begin at an earlier date [mid-summer (Week 28) to

10.3389/fvets.2023.1158306

TABLE 1 Yearly count of cases and controls by farm type within significant ($p<0.05$) high risk areas estimated using a spatial asymmetric adaptive smoothing approach for 2,293 farms (n=number of farms per farm type) in a dense pig production region of the United States.

Year	Sow (n=319)		Nursery (n=468)		Finisher (n=1,458)		Isolation (n=33)		Boar Stud (n=15)	
	Cases	Controls	Cases	Controls	Cases	Controls	Cases	Controls	Cases	Controls
2018	34	49	13	79	21	126	0	2	0	4
2019	27	21	6	52	5	85	0	1	0	2
2020	44	43	7	81	6	135	0	3	0	3

TABLE 2 Percent of high, medium, and low PRRSV risk levels [median and interquartile range (IQR)] based on weekly risk estimates obtained from the spatiotemporal analysis by farm type for each year and for the entire study period.

Period	Sow			Nursery			Finisher			Isolation			Boar Stud		
	High	Med.	Low	High	Med.	Low	High	Med.	Low	High	Med.	Low	High	Med.	Low
2018	24 (24–29)	22 (17–31)	51 (40–57)	18 (16–21)	21 (15–30)	56 (50–73)	17 (13–25)	20 (10–28)	59 (49–77)	12 (9–19)	39 (19–45)	45 (39–75)	27 (20–27)	27 (20–27)	53 (47–60)
2019	33 (29–37)	16 (14–21)	49 (45–53)	18 (17–20)	16 (11–23)	65 (55–71)	14 (14–20)	17 (6–21)	71 (55–79)	12 (12–48)	21 (12–33)	33 (27–88)	40 (33–40)	13 (7–20)	47 (47–47)
2020	30 (28–35)	27 (16–29)	44 (42–48)	20 (19–25)	22 (20–28)	53 (51–59)	15 (13–16)	25 (21–28)	61 (58–64)	18 (6–29)	42 (24–48)	39 (33–73)	27 (27–33)	20 (13–27)	53 (40–60)
2018–2020*	29 (27–34)	21 (14–28)	48 (43–53)	19 (18–22)	21 (15–26)	57 (52–67)	14 (13–19)	21 (13–26)	63 (54–74)	12 (9–24)	35 (18–45)	42 (33–82)	30 (27–38)	20 (13–27)	47 (47–53)

*Median and IQR for all years combined.

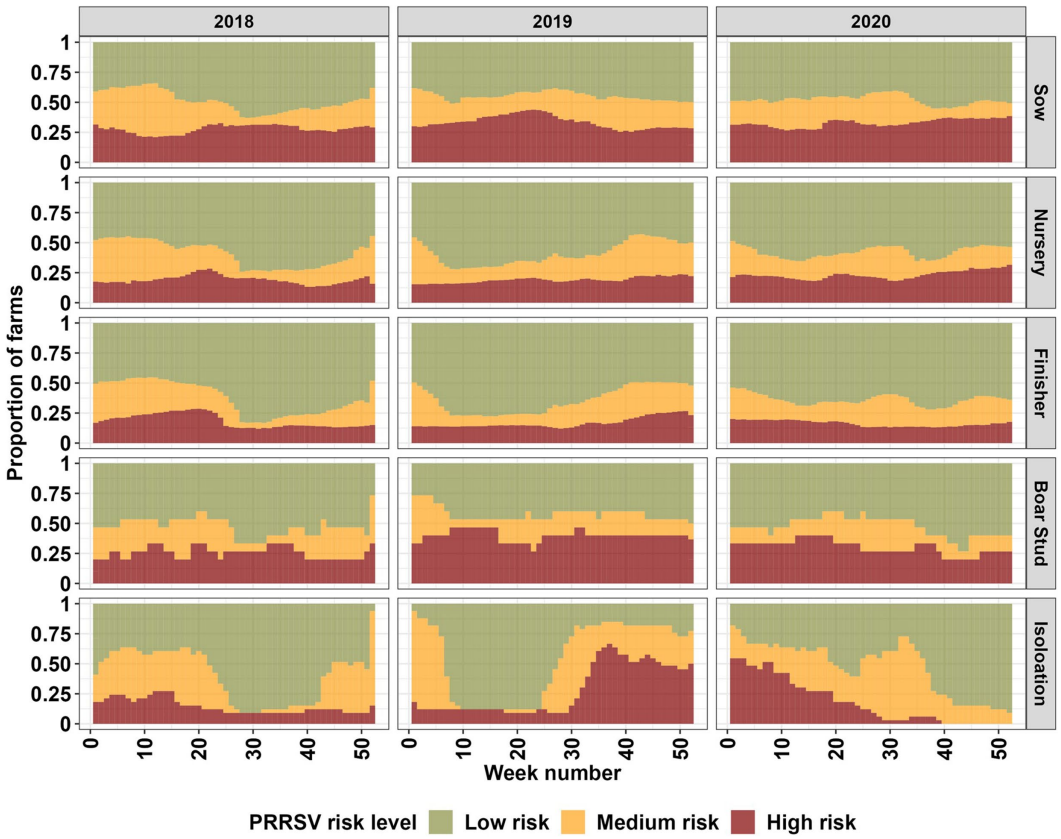

FIGURE 2
Farm type breakdown of high, medium, and low PRRSV risk levels for the entire farm population (2,293) based on a 60% exceedance relative risk threshold for each week (from 1 to 52 weeks) in the years 2018 through 2020.

early fall (Week 35)] for the year 2019; however, it is not consistent among all farm types. Sow farms displayed an interesting pattern among farm types, with increases in risk during summer months (Week 20–35) (Figure 2; Supplementary Figure S17). Nursery, finisher, boar stud, and isolation farms appear to show a similar summer increase in the year 2020, but it is not present for other years. Among all farm types, sow, finisher and nursery farms appear to more closely resemble each other in terms of seasonal risk. Boar stud and isolation show more erratic changes in risk, however, the large shifts in risk levels are related to the small number of farms for these farm types.

Results obtained from calculating the PI, which may be used to order farms in risk priority, revealed that 79.4% of the farms in 2018 were in the low PI category, 16.1% were in the medium PI, and 4.5% were in the high PI category (Supplementary material Table S6). Similarly, 63.7% in 2019 and 67.9% in 2020 were in the low PI category, 28% in 2019 and 23.9% in 2020 were in the medium PI category, and 8.35% in 2019 and 8.28% in 2020 were in the high PI category. Among the different farm types, sow farms consistently had the most farms in the high and medium risk category except boar stud farms in 2019 and 2020; however, as noted before, there are fewer boar stud farms as compared to sow farms in the study population. A similar proportion of farms with high, medium, and low PI overall and by farm type were observed for the PRRSV seasons (Supplementary material Table S7).

3.3. Bayesian spatiotemporal hierarchical model

Results from the univariate analysis revealed that the animal movement network metric, out-degree, the number of LOSAP, number of days the temperature was between T [4°C,10°C], and relative humidity <20% were significantly associated with PRRSV outbreaks (Table 3). The best fitting multivariate model (WAIC = 2,620) obtained through backward variable selection included the following variables: out-degree, LOSAP, T [4°C, 10°C], and farm density (Table 3). The strongest association was related to out-going movements, which resulted in an increase in the odds of PRRSV outbreaks by 1.11 times (Table 3). The second most associated variable was LOSAP, with an increase of 1.04 times the odds of PRRSV outbreaks for every additional LOSAP. Lastly, T [4°C, 10°C] resulted in a 1.01 increase in odds for every one unit increase in T [4°C, 10°C].

TABLE 3 Summary statistics of the fixed effects of the Bayesian spatiotemporal hierarchical models, showing odds ratio (OR), 2.5%–97.5% credible intervals, and WAIC.

	Univariate			
		CI		
Covariate	**OR**	**2.5%**	**97.5%**	**WAIC**
Pig capacity	1	1	1	2,456.06
Farm density	1	0.99	1	2,462.08
EVI	1.04	0.07	4.65	2,445.97
T[4°C,10°C]	**1.02**	**1.01**	**1.03**	**2,421.68**
RH < 20%	**1.01**	**1.01**	**1.02**	**2,425.71**
Aboveground biomass density	1	0.97	1.03	2,449.03
Canopy height	0.96	0.69	1.30	2,459.40
Elevation	1	0.99	1.01	2,457.84
In-degree	1	0.95	1.01	2,456.86
Out-degree	**1.11**	**1.08**	**1.14**	**2,397.36**
Closeness centrality	−0.14	37.44	229.68	2,448.63
Betweenness	1	1	1	2,454.07
Clustering coefficient	0.28	0.07	1.31	2,451.75
Page rank	0	0	0	2,451.87
Site entry	4.102065×10^{4}	7.698183×10^{14}	12.97760×10^{10}	13,045.11
PBAAP	1.03	0.98	1.07	2,448.90
LOSAP	**1.05**	**1.02**	**1.08**	**2,423.73**

	Multivariate			
		CI		
Covariate	**OR**	**2.5%**	**97.5%**	**WAIC**
Out-degree	**1.08**	**1.11**	**1.14**	
LOSAP	**1.01**	**1.04**	**1.07**	
T[4°C,10°C]	**1.01**	**1.01**	**1.02**	
Farm density	1	1	1.01	
				2,374.83

Bold values correspond to variables that were significant in our analysis.

4. Discussion

We estimated the maximum distance at which the risk of PRRSV is significantly high given the spatial proximity of farms reporting PRRSV outbreaks. Through our spatial and spatiotemporal analysis, we demonstrated that farms within an 11.9 km to 17 km radius of PRRSV positive farms were at greater risk of being infected due to proximity. PRRSV risk was higher during fall winter and early spring months with variation among the different farm types and years (Figure 2), which is consistent with seasonal patterns previously described for this region of the United States (1, 3, 10, 11, 14). Spatiotemporal risk estimates revealed that approximately 29% of sow farms were consistently located in areas of high risk. We also show that outgoing animal movements (out-degree), the number of barn access points (LOSAP), and the number of days where temperatures were between 4°C and 10°C [T(4°C,10°C)] were risk factors for PRRSV outbreaks (Table 3).

Given the temporal dynamics of PRRSV, and in comparison to the spatial analysis which is a time-static representation of farms reporting PRRSV outbreaks for an entire year and/or PRRSV season, weekly PRRSV outbreak reports were used in our spatiotemporal analysis. Our spatiotemporal analysis showed that the risk of PRRSV transmission from infected farms was significant up to 17 km compared to 11.9 km in our spatial analysis. We attribute the increase in distance calculated in our spatiotemporal analysis to the density of cases to controls considered in each weekly time step, since we expect that the farm density modulates the size of the bandwidth radius, thus increasing the radius distance to compensate for the low density of cases (46, 87). We remark that the spatial distribution of cases and controls alone may not be sufficient to fully explain PRRSV risk dynamics; therefore, we consider that the maximum distance of 17 km calculated in our spatiotemporal analysis reflects a close representation of PRRSV spatial risk in our study region, since risk estimates consider temporal patterns associated with PRRRV (3, 10, 11).

Our spatiotemporal analysis showed increases in PRRSV risk during the fall, winter, and early spring months, which aligns with previous findings for the dense pig production region considered in this study (3, 10, 11, 14). The seasonal effect was consistently detected throughout the study period, but varied in intensity between years and

farm types. In contrast to the typical seasonal patterns previously reported for the dense pig production region considered in this study and continued to be observed in this study, an increase in risk during the summer (Week 20–35) months was detected in sow farms for all years in our study period, with nursery and finisher farms displaying a similar pattern for the years 2018 and 2020, and boar stud and isolation farms only in 2020 (Figure 2). Summer PRRSV outbreaks in breeding and finisher farms have been previously reported (3, 7); however, we show that given the spatial proximity of farms in dense pig production areas, the risk for a PRRSV outbreak may propagate to different farm types. This information supports previous findings and highlights the importance of considering transmission dynamics between farm types during months outside the typical PRRSV season to help farm managers and veterinarians plan for enhanced biosecurity and surveillance (2, 3, 10, 12, 13).

Transmission dynamics of PRRSV involve two main transmission pathways: direct contacts mediated by the movement of infected pigs between farms (18, 20, 25, 66), and indirect contacts referred to as local transmission (1, 11, 15, 16, 18, 19, 23, 33, 66). Local transmission encompasses several mechanisms of spread and is typically used to explain processes that occur over short geographical distances and cannot be attributed to direct contacts caused by live animal shipments among farms (16, 18, 19, 27, 28, 31, 88). Airborne transmission of PRRSV has been suggested as a possible source of local transmission, especially in areas of high farm density; however, evidence has been inconsistent (31). Experimental studies conducted to examine the distance airborne between-farm transmission of PRRSV may occur showed that PRRSV was recovered at a distance of 9.2 km (23, 32). In a recent study, an atmospheric dispersion model was used to determine that farms within a distance of 25 km distance from a PRRSV positive farm were at high PRRSV risk (33). Dispersion models, such as the one developed by (33) may be invaluable tools when conducting outbreak investigations; however, as noted by the authors, further refinement to include environmental factors (e.g., temperature and humidity) and seasonal differences may yield more accurate estimates. In our study, both the spatial (11.9 km - 14.8 km) and spatiotemporal (17 km) distances calculated are within the distances proposed in (23, 33), and given the high density (e.g., 10–20 farms per 5 km^2) of farms in our study area, the potential for airborne transmission occurring in our study area cannot be ruled out. However, given the additional mechanisms (e.g., movement of contaminated transportation vehicles, equipment, and personnel) involved in local transmission that have been shown to contribute to the between-farm transmission of PRRSV (18, 28, 89), the small number of samples recovered through airborne transmission (23, 32), and consideration of mechanical (presence of air filtration systems) or environmental factors (e.g., temperature, humidity, vegetation and slope) that may impact the survivability or infectivity of PRRSV, we agree with previous conclusions that airborne transmission is an infrequent or unlikely event (31).

Breeding farms have been the center of most swine disease transmission studies (3, 38, 39, 43, 90–92). In this study, we have shown that the number of sow farms in high-risk areas was larger than all other farm types. A potential explanation as to why sow farms were consistently categorized as high risk may be due to the higher level of systematic testing performed at sow farms as compared to other farm types (2, 18, 19). Higher levels of surveillance in sow farms increase the detection rate of PRRSV outbreaks, consequently increasing the number of analyzed PRRSV outbreaks in our study. Conversely, the underdetection of downstream farms, which has been noted in previous studies as a limitation to understanding PRRSV transmission dynamics (18, 19, 42, 91, 93), is consistent with our findings in the spatial analysis where large numbers of PRRSV negative farms were within areas of significant high risk. A recent work investigated the association between PPRSV outbreaks and farm proximity to areas of high commingling (slaughterhouses) and found no association; however, the study only considered breeding herds, which highlights the need to consider other farm types that may contribute to disease circulation (43). Our study showed both upstream and downstream farm types within areas of significant risk, and until systematic testing occurs in all farm types, estimations of PRRSV spatial risk will remain a challenge, especially for the estimations for growing pigs. We encourage future research to incorporate parameters that evaluate the sensitivity of the model on the basis of a distribution of possible surveillance levels among the different farm types.

The most important risk factor associated with PRRSV outbreaks in this study was the movement of animals, which has been shown to be the dominant PRRSV transmission route (17, 18, 25, 90, 91, 94, 95–97). Specifically, the effect was related to the out-going movements of animals, which is usually associated with farm types that have large and consistent outgoing shipments of pigs, such as sow and nursery farms. Such farms may usually take on the role of "movement hubs" in a network, thus facilitating the spread of diseases (38, 90, 91, 98). The high number of out-going movements is supported in our findings, where the largest out-degree values were associated with infected nursery farms with a median value of 9 (IQR: 7–11), and 8 (IQR: 6–11) for controls (Supplementary material S2; Supplementary material Table S8). Similarly, positive sow farms had out-degree median values of 6 (IQR: 4–10), and 6 (IQR: 3–10) for controls (Supplementary material Table S8).

The second important variable was LOSAP, which can serve as potential entry pathway for the introduction of pathogens (42, 94). Entry or exit through a LOSAP may involve several risk events such as garbage collection, equipment repair, and removal of cull sows that have been identified as relevant risk events associated with the introduction of diseases (18, 27, 28, 97, 99). Among the different farm types, sow farms had the highest median LOSAP values with control farms having a median value of 5 (IQR: 1–16) LOSAP, and cases having a median value of 3 (IQR: 1–12) LOSAP.

Temperature and relative humidity have been shown to influence the survivability and optimal preservation of infectivity of PPRSV (65, 67). Here, we showed that the increased number of days between 4°C and 10°C and the number of days a farm experienced relative humidity values below 20% increased the probability of PRRSV outbreaks. This is consistent with the seasonal signal of increased risk during the fall and winter months seen in our data and reported in previous research (3, 14). Lastly, we sought to expand on the investigation of the use of vegetation buffers as possible means to mitigate PRRSV transmission. EVI values between 41 and 45, which correspond to dense tree coverage that is consistent with evergreen broadleaf forests were shown to prevent the spread of PRRSV (1). We included EVI, AGB, and canopy height data to capture the structure of the vegetation around the farms; however, these variables were not significant. Given the coarse spatial resolution used in this study, and the benefits of using vegetation buffers to mitigate odor and pathogen emission and introduction (1, 72, 74), we remark that further exploration into the use of remotely sensed data to delineate vegetation buffers is warranted since the availability of imagery from satellites with high temporal and

spatial resolution continues to become more accessible. Lastly, a previous study found the slope of the terrain to be associated with lower PRRSV incidence, with an elevation of 61 meters from sea level determined to be a safe range (1). We did not find a significant correlation between PRRSV outbreaks and land slope in our model; however, we remark that our results may in-part be related to the 1 km x 1 km spatial resolution of our data, and a finer spatial resolution should be explored.

4.1. Limitations and further remarks

The present study has limitations. Firstly, swine production is dynamic in nature, with farms being active and inactive throughout the years. During the time period considered in this study, 34/2,293 farms (1.5%) changed from active to inactive between Nov 1st, 2017 through December 31st 2020, thus we consider our results closely reflect the current status of the swine industry in our study region given the high level of participation of the swine production companies in our study. Another limitation in our study relates to how PRRSV surveillance systems differ between farm types, with sow farms usually conducting routine testing while downstream farm testing is not always performed systematically (39, 42, 93). Differences in systematic testing between the different farm types could have affected our risk estimations; however, we believe that the PRRSV database captured by MSHMP is still the best alternative to the currently available PRRSV datasets (2). For our spatiotemporal analysis, we arbitrarily chose the exceedance risk threshold to be at 60% since it aligned with the interpretation described in (46), where $\hat{p}(x) > 0$ represent areas of higher risk, and $\hat{p}(x) < 0$ areas of low risk. In future studies, other cutoff values should be explored. Additionally, given that a farm may continue to be reported as having an outbreak for multiple weeks, this may potentially influence our spatiotemporal relative risk estimates by increasing the number of cases in a given week. However, since we are interested in quantifying the risk for the potential transmission of PRRSV, it is important we do not omit farms that could contribute to the dissemination of PRRSV. A future study should consider an approach that considers observation autocorrelated in time.

Even though we had to restrict our risk factor analysis to 2020 due to limitations of the between-farm movement data, our results would likely be similar for other years, given how animal movements are vertically integrated in the United States (18, 2, 66, 91, 100). Environmental factors that are known to vary through time were averaged for an entire year, which might dilute the temporal differences in environmental conditions that may influence PRRSV transmission dynamics (3, 13, 14). However, results obtained from this study provide the important groundwork for further exploration of temporal differences related to factors associated with PRRSV local spread. Despite the limitations present in this study, here, we address an important gap related to the spatial range associated with the risk of PRRSV local transmission and estimate the maximum distance to which farms may become exposed and or infected from nearby infected farms. Both results could potentially be used to inform swine producers within areas of elevated risk to consider enhancing surveillance, sampling and disease control strategies (2, 96, 101). In addition, information gathered from this study may be used to calibrate future PRRSV transmission models by considering the calculated spatial bandwidths as the maximum transmission distance (18–20, 66).

The results of this study suggest that farms within a 17 km radius of farms reporting PRRSV outbreaks are at greater risk of infection. We demonstrated that PRRSV outbreaks remain mostly seasonal, with differences in risk intensity between farm types. Our analysis also captured sporadic summer increases in risk, with differences between years and farm types. We found that sow farms had the highest number of cases within areas of significant high risk and were collocated with at-risk finisher and nursery farms. These findings suggest that downstream farms (i.e., finisher farms) may play an important role in maintaining the circulation of PRRSV within the farm population, and support the need for systematic testing among the different farm types. Lastly, out-going movement of pigs, the number of access points and temperature were significant risk factors of PRRSV outbreaks. Ultimately, we provide insights into PRRSV risk dynamics among farm types and establish a maximum distance for the risk of PPRSV local transmission, which could be used to inform targeted surveillance and disease control strategies and calibrate future PRRSV transmission models.

Data availability statement

The datasets presented in this article are not readily available because the data that support the findings of this study are not publicly available and are protected by confidential agreements, therefore, are not available. Requests to access the datasets should be directed to GM, gmachad@ncsu.edu.

Author contributions

FS, CJ, JG, and GM conceived the study. FS, GM, CJ, NC, and JG participated in the design of the study and model formulation. CC coordinated the disease data collection by the Morrison Swine Health Monitoring Program (MSHMP). FS and JG conducted the data processing, cleaning, designed the model, and simulated the scenarios with the assistance of CJ, NC, and GM. FS, JG, NC, GM, and CJ wrote and edited the manuscript. All authors discussed the results and critically reviewed the manuscript.

Funding

This project was funded by the Center for Geospatial Analytics and the College of Veterinary Medicine at North Carolina State University. The Morrison Swine Health Monitoring Project is a Swine Health Information Center (SHIC) funded project. This work was also supported by Food and Agriculture Cyber informatics and Tools, 2020-67021-32462, proposal number 2019-07452 from the USDA National Institute of Food and Agriculture.

Acknowledgments

The authors would like to acknowledge participating companies and veterinarians and the Morrison Swine Health Monitoring Project funded by the Swine Health Information Center.

Conflict of interest

The authors declare that the research was conducted in the absence of any commercial or financial relationships that could be construed as a potential conflict of interest.

Publisher's note

All claims expressed in this article are solely those of the authors and do not necessarily represent those of their affiliated organizations, or those of the publisher, the editors and the reviewers. Any product that may be evaluated in this article, or claim that may be made by its manufacturer, is not guaranteed or endorsed by the publisher.

Supplementary material

The Supplementary material for this article can be found online at: https://www.frontiersin.org/articles/10.3389/fvets.2023.1158306/full#supplementary-material

References

1. Jara M, Rasmussen DA, Corzo CA, Machado G. Porcine reproductive and respiratory syndrome virus dissemination across pig production systems in the United States. *Transbound Emerg Dis*. (2021) 68:667–83. doi: 10.1111/tbed.13728

2. Perez AM, Linhares DCL, Arruda AG, Van Der Waal K, Machado G, Vilalta C, et al. Individual or common good? Voluntary data sharing to inform disease surveillance systems in food animals. *Front Vet Sci*. (2019) 6:194. doi: 10.3389/fvets.2019.00194

3. Sanhueza JM, Stevenson MA, Vilalta C, Kikuti M, Corzo CA. Spatial relative risk and factors associated with porcine reproductive and respiratory syndrome outbreaks in United States breeding herds. *Prev Vet Med*. (2020) 183:105128. doi: 10.1016/j.prevetmed.2020.105128

4. Benfield DA, Nelson E, Collins JE, Harris L, Goyal SM, Robison D, et al. Characterization of swine infertility and respiratory syndrome (SIRS) virus (isolate ATCC VR-2332). *J Vet Diagn Investig*. (1992) 4:127–33. doi: 10.1177/104063879200400202

5. Holtkamp DJ, Kliebenstein JB, Neumann EJ, Zimmerman JJ, Rotto HF, Yoder TK, et al. Assessment of the economic impact of porcine reproductive and respiratory syndrome virus on United States pork producers. *J Swine Health Prod*. (2013) 21:72–84.

6. Jiang Y, Li G, Yu L, Li L, Zhang Y, Zhou Y, et al. Genetic diversity of porcine reproductive and respiratory syndrome virus (PRRSV) from 1996 to 2017 in China. *Front Microbiol*. (2020) 11:618. doi: 10.3389/fmicb.2020.00618

7. Kikuti M, Paploski IAD, Pamornchainavakul N, Picasso-Risso C, Schwartz M, Yeske P, et al. Emergence of a new lineage 1C variant of porcine reproductive and respiratory syndrome virus 2 in the United States. *Front Vet Sci*. (2021) 8:752938. doi: 10.3389/fvets.2021.752938

8. Valdes-Donoso P, Alvarez J, Jarvis LS, Morrison RB, Perez AM. Production losses from an endemic animal disease: porcine reproductive and respiratory syndrome (PRRS) in selected Midwest US sow farms. *Front Vet Sci*. (2018) 5:102. doi: 10.3389/fvets.2018.00102

9. van Geelen AGM, Anderson TK, Lager KM, Das PB, Otis NJ, Montiel NA, et al. Porcine reproductive and respiratory disease virus: evolution and recombination yields distinct ORF5 RFLP 1-7-4 viruses with individual pathogenicity. *Virology*. (2018) 513:168–79. doi: 10.1016/j.virol.2017.10.002

10. Alkhamis MA, Arruda AG, Vilalta C, Morrison RB, Perez AM. Surveillance of porcine reproductive and respiratory syndrome virus in the United States using risk mapping and species distribution modeling. *Prev Vet Med*. (2018) 150:135–42. doi: 10.1016/j.prevetmed.2017.11.011

11. Arruda AG, Sanhueza J, Corzo C, Vilalta C. Assessment of area spread of porcine reproductive and respiratory syndrome (PRRS) virus in three clusters of swine farms. *Transbound Emerg Dis*. (2018) 65:1282–9. doi: 10.1111/tbed.12875

12. Sanhueza JM, Vilalta C, Corzo C, Arruda AG. Factors affecting porcine reproductive and respiratory syndrome virus time-to-stability in breeding herds in the Midwestern United States. *Transbound Emerg Dis*. (2019) 66:823–30. doi: 10.1111/tbed.13091

13. Arruda C, Vilalta P, Puig AP, Alba A. Time-series analysis for porcine reproductive and respiratory syndrome in the United States. (Yongchang Cao, Ed.). *PLoS One*. (2018) 13:e0195282. doi: 10.1371/journal.pone.0195282

14. Tousignant SJP, Perez AM, Lowe JF, Yeske PE, Morrison RB. Temporal and spatial dynamics of porcine reproductive and respiratory syndrome virus infection in the United States. *Am J Vet Res*. (2015) 76:70–6. doi: 10.2460/ajvr.76.1.70

15. Dee J, Deen K, Rossow C, Weise R, Eliason S, Otake HS, et al. Mechanical transmission of porcine reproductive and respiratory syndrome virus throughout a coordinated sequence of events during warm weather. *Can J Vet Res*. (2003) 67:12–9.

16. Dee MC, Niederwerder G, Patterson R, Cochrane C, Jones D, Diel E, et al. The risk of viral transmission in feed: what do we know, what do we do? *Transbound Emerg Dis*. (2020) 67:2365–71. doi: 10.1111/tbed.13606

17. Galvis JA, Corzo C, Machado G. Modelling porcine reproductive and respiratory syndrome virus dynamics to quantify the contribution of multiple modes of transmission: between-farm animal and vehicle movements, farm-to-farm proximity, feed ingredients, and re-break (preprint). *Ecology*. (2021) 2021:453902. doi: 10.1101/2021.07.26.453902

18. Galvis JA, Corzo CA, Machado G. Modelling and assessing additional transmission routes for porcine reproductive and respiratory syndrome virus: vehicle movements and feed ingredients. *Transbound Emerg Dis*. (2022) 69:e1549–60. doi: 10.1111/tbed.14488

19. Galvis JA, Jones CM, Prada JM, Corzo CA, Machado G. The between-farm transmission dynamics of porcine epidemic diarrhoea virus: a short-term forecast modelling comparison and the effectiveness of control strategies. *Transbound Emerg Dis*. (2021) 69:396–412. doi: 10.1111/tbed.13997

20. Machado G, Galvis JA, Lopes FPN, Voges J, Medeiros AAR, Cárdenas NC. Quantifying the dynamics of pig movements improves targeted disease surveillance and control plans. *Transbound Emerg Dis*. (2020) 68:1663–75. doi: 10.1111/tbed.13841

21. Makau DN, Paploski IAD, Corzo CA, VanderWaal K. Dynamic network connectivity influences the spread of a sub-lineage of porcine reproductive and respiratory syndrome virus. *Transbound Emerg Dis*. (2021) 69:524–37. doi: 10.1111/tbed.14016

22. Makau DN, Paploski IAD, VanderWaal K. Temporal stability of swine movement networks in the U.S. *Prev Vet Med*. (2021) 191:105369. doi: 10.1016/j.prevetmed.2021.105369

23. Otake S, Dee C, Corzo SO, Deen J. Long-distance airborne transport of infectious PRRSV and *Mycoplasma hyopneumoniae* from a swine population infected with multiple viral variants. *Vet Microbiol*. (2010) 145:198–208. doi: 10.1016/j.vetmic.2010.03.028

24. VanderWaal K, Perez A, Torremorrell M, Morrison RM, Craft M. Role of animal movement and indirect contact among farms in transmission of porcine epidemic diarrhea virus. *Epidemics*. (2018) 24:67–75. doi: 10.1016/j.epidem.2018.04.001

25. VanderWaal K, Paploski IAD, Makau DN, Corzo CA. Contrasting animal movement and spatial connectivity networks in shaping transmission pathways of a genetically diverse virus. *Prev Vet Med*. (2020) 178:104977. doi: 10.1016/j.prevetmed.2020.104977

26. Benincà E, Hagenaars T, Boender GJ, van de Kassteele J, van Boven M. Trade-off between local transmission and long-range dispersal drives infectious disease outbreak size in spatially structured populations. (Matthew (Matt) Ferrari, Ed.). *PLoS Comput Biol*. (2020) 16, 16:e1008009:e1008009. doi: 10.1371/journal.pcbi.1008009

27. Galli F, Friker B, Bearth A, Dürr S. Direct and indirect pathways for the spread of African swine fever and other porcine infectious diseases: an application of the mental models approach. *Transbound Emerg Dis*. (2022) 69:e2602–16. doi: 10.1111/tbed.14605

28. Pitkin A, Deen J, Dee S. Further assessment of fomites and personnel as vehicles for the mechanical transport and transmission of porcine reproductive and respiratory syndrome virus. *Can J Vet Res*. (2009) 73:298–302.

29. Niederwerder M. Risk and mitigation of African swine fever virus in feed. *Animals*. (2021) 11:792. doi: 10.3390/ani11030792

30. Ochoa L, Greiner L, Pacion T. Feed as a vehicle for Prrs virus transmission and the effects of formaldehyde on porcine reproductive and respiratory virus in feed: proof of concept. *J Anim Sci*. (2018) 96:63–3. doi: 10.1093/jas/sky073.117

31. Arruda S, Tousignant J, Sanhueza C, Vilalta Z, Poljak M, Torremorell CA, et al. Aerosol detection and transmission of porcine reproductive and respiratory syndrome virus (PRRSV): what is the evidence, and what are the knowledge gaps? *Viruses*. (2019) 11:712. doi: 10.3390/v11080712

32. Dee S, Otake S, Oliveira S, Deen J. Evidence of long distance airborne transport of porcine reproductive and respiratory syndrome virus and *Mycoplasma hyopneumoniae*. *Vet Res*. (2009) 40:39. doi: 10.1051/vetres/2009022

33. Kanankege KST, Graham K, Corzo CA, VanderWaal K, Perez AM, Durr PA. Adapting an atmospheric dispersion model to assess the risk of windborne transmission of porcine reproductive and respiratory syndrome virus between swine farms. *Viruses*. (2022) 14:1658. doi: 10.3390/v14081658

34. Li P, Koziel JA, Zimmerman JJ, Hoff SJ, Zhang J, Cheng T-Y, et al. Designing and testing of a system for Aerosolization and recovery of viable porcine reproductive and respiratory syndrome virus (PRRSV): theoretical and engineering considerations. *Front Bioeng Biotechnol*. (2021) 9:659609. doi: 10.3389/fbioe.2021.659609

35. Otake S, Dee SA, Jacobson L, Pijoan C, Torremorell M. Evaluation of aerosol transmission of porcine reproductive and respiratory syndrome virus under controlled field conditions. *Vet Rec*. (2002) 150:804–8. doi: 10.1136/vr.150.26.804

36. Shea K, Runge MC, Pannell D, Probert WJM, Li S-L, Tildesley M, et al. Harnessing multiple models for outbreak management. *Science*. (2020) 368:577–9. doi: 10.1126/science.abb9934

37. Christianson WT, Joo HS. *Porcine reproductive and respiratory syndrome: A review*. United States: Swine Health Production (1994).

38. Lee K, Polson D, Lowe E, Main R, Holtkamp D, Martínez-López B. Unraveling the contact patterns and network structure of pig shipments in the United States and its association with porcine reproductive and respiratory syndrome virus (PRRSV) outbreaks. *Prev Vet Med*. (2017) 138:113–23. doi: 10.1016/j.prevetmed.2017.02.001

39. Pileri E, Mateu E. Review on the transmission porcine reproductive and respiratory syndrome virus between pigs and farms and impact on vaccination. *Vet Res*. (2016) 47:108. doi: 10.1186/s13567-016-0391-4

40. Dee S, Deen J, Rossow K, Wiese C, Otake S, Joo HS, et al. Mechanical transmission of porcine reproductive and respiratory syndrome virus throughout a coordinated sequence of events during cold weather. *Can J Vet Res*. (2002) 66:232–9.

41. Jacobs AC, Hermann JR, Muñoz-Zanzi C, Prickett JR, Roof MB, Yoon K-J, et al. Stability of porcine reproductive and respiratory syndrome virus at ambient temperatures. *J Vet Diagn Investig*. (2010) 22:257–60. doi: 10.1177/104063871002200216

42. Lambert M-È, Poljak Z, Arsenault J, D'Allaire S. Epidemiological investigations in regard to porcine reproductive and respiratory syndrome (PRRS) in Quebec, Canada. Part 1: biosecurity practices and their geographical distribution in two areas of different swine density. *Prev Vet Med*. (2012) 104:74–83. doi: 10.1016/j.prevetmed.2011.12.004

43. Moeller J, Mount J, Geary E, Campler MR, Corzo CA, Morrison RB, et al. Investigation of the distance to slaughterhouses and weather parameters in the occurrence of porcine reproductive and respiratory syndrome outbreaks in U.S. swine breeding herds. *Can Vet J*. (2022) 63:528–34.

44. Bithell JF. An application of density estimation to geographical epidemiology. *Stat Med*. (1990) 9:691–701. doi: 10.1002/sim.4780090616

45. Davies TM, Hazelton ML. Adaptive kernel estimation of spatial relative risk. *Stat Med*. (2010) 29:2423–37. doi: 10.1002/sim.3995

46. Davies TM, Marshall JC, Hazelton ML. Tutorial on kernel estimation of continuous spatial and spatiotemporal relative risk: spatial and spatiotemporal relative risk. *Stat Med*. (2018) 37:1191–221. doi: 10.1002/sim.7577

47. Kelsall JE, Diggle PJ. Non-parametric estimation of spatial variation in relative risk. *Stat Med*. (1995) 14:2335–42. doi: 10.1002/sim.4780142106

48. Fernando WTP, Hazelton ML. Generalizing the spatial relative risk function. *Spat Spatio Temporal Epidemiol*. (2014) 8:1–10. doi: 10.1016/j.sste.2013.12.002

49. Abramson IS. On bandwidth variation in kernel estimates-a square root law. *Ann Stat*. (1982) 10:1217–23. doi: 10.1214/aos/1176345986

50. Hazelton ML, Davies TM. Inference based on kernel estimates of the relative risk function in geographical epidemiology. *Biom J*. (2009) 51:98–109. doi: 10.1002/bimj.200810495

51. Davies TM, Lawson AB. An evaluation of likelihood-based bandwidth selectors for spatial and spatiotemporal kernel estimates. *J Stat Comput Simul*. (2019) 89:1131–52. doi: 10.1080/00949655.2019.1575066

52. Terrell GR. The maximal smoothing principle in density estimation. *J Am Stat Assoc*. (1990) 85:470–7. doi: 10.1080/01621459.1990.10476223

53. Richardson S, Thomson A, Best N, Elliott P. Interpreting posterior relative risk estimates in disease-mapping studies. *Environ Health Perspect*. (2004) 112:1016–25. doi: 10.1289/ehp.6740

54. Baquero OS, Machado G. Spatiotemporal dynamics and risk factors for human leptospirosis in Brazil. *Sci Rep*. (2018) 8:15170. doi: 10.1038/s41598-018-33381-3

55. Krainski E, Gómez-Rubio V, Bakka H, Lenzi A, Castro-Camilo D, Simpson D, et al. *Advanced spatial modeling with stochastic partial differential equations using R and INLA*. Boca Raton, FL: Chapman and Hall/CRC (2018).

56. Bakka H, Rue H, Fuglstad G, Riebler A, Bolin D, Illian J, et al. Spatial modeling with R-INLA: a review. *WIREs Comput Stat*. (2018) 10:e1443. doi: 10.1002/wics.1443

57. Elias TK, Virgilio GR, Haakon B, Amanda L, Daniela CC, Daniel S, et al. *Advanced spatial modeling with stochastic partial differential equations using R and INLA*. Boca Raton, FL, United States: Chapman & Hall/CRC Press (2019).

58. Lindgren F, Rue H, Lindström J. An explicit link between Gaussian fields and Gaussian Markov random fields: the stochastic partial differential equation approach. J. R. *Stat Soc Ser B Stat Methodol*. (2011) 73:423–98. doi: 10.1111/j.1467-9868.2011.00777.x

59. Rue H, Martino S, Chopin N. Approximate Bayesian inference for latent Gaussian models by using integrated nested Laplace approximations. J. R. *Stat Soc Ser B Stat Methodol*. (2009) 71:319–92. doi: 10.1111/j.1467-9868.2008.00700.x

60. van Niekerk J, Bakka H, Rue H, Schenk O. New Frontiers in Bayesian modeling using the INLA package in R. *J Stat Softw*. (2021) 100:2–10. doi: 10.18637/jss.v100.i02

61. Fuglstad G-A, Simpson D, Lindgren F, Rue H. Constructing priors that penalize the complexity of Gaussian random fields. *J Am Stat Assoc*. (2019) 114:445–52. doi: 10.1080/01621459.2017.1415907

62. Simpson D, Rue H, Riebler A, Martins TG, Sørbye SH. Penalising model component complexity: a principled, practical approach to constructing priors. *Stat Sci*. (2017) 32:576. doi: 10.1214/16-STS576

63. Blangiardo M, Cameletti M. *Spatial and Spatio-temporal Bayesian models with R-INLA*. Chichester, West Sussex: John Wiley and Sons, Inc (2015).

64. Santos Baquero O. *INLAOutputs: Process selected outputs from the "INLA" package*. CRAN (2018).

65. Cutler TD, Wang C, Hoff SJ, Zimmerman JJ. Effect of temperature and relative humidity on ultraviolet (UV254) inactivation of airborne porcine respiratory and reproductive syndrome virus. *Vet Microbiol*. (2012) 159:47–52. doi: 10.1016/j.vetmic.2012.03.044

66. Galvis JA, Corzo CA, Prada JM, Machado G. Modelling the transmission and vaccination strategy for porcine reproductive and respiratory syndrome virus. *Transbound Emerg Dis*. (2021) 69:485–500. doi: 10.1111/tbed.14007

67. Hermann J, Hoff S, Muñoz-Zanzi C, Yoon K-J, Roof M, Burkhardt A, et al. Effect of temperature and relative humidity on the stability of infectious porcine reproductive and respiratory syndrome virus in aerosols. *Vet Res*. (2007) 38:81–93. doi: 10.1051/vetres:2006044

68. Machado G, Galvis JOA, Cardenas NC, Ebling DDS, Freeman A, Hong X, et al. *The rapid access biosecurity (RAB) appTM handbook (preprint)*. Open Science Framework (2023).

69. Brandes U, Erlebach T. *Network analysis*, vol. *3418*. Berlin, Heidelberg: Springer Berlin Heidelberg (2005).

70. Busetto L, Ranghetti L. MODIStsp: an R package for automatic preprocessing of MODIS land products time series. *Comput Geosci*. (2016) 97:40–8. doi: 10.1016/j.cageo.2016.08.020

71. ORNL DAAC. *ORNL DAAC for biogeochemical dynamics*. (2022). Available at: https://daac.ornl.gov/ (Accessed June 11, 2022).

72. Adrizal A, Patterson PH, Hulet RM, Bates RM, Myers CAB, Martin GP, et al. Vegetative buffers for fan emissions from poultry farms: 2. ammonia, dust and foliar nitrogen. *J Environ Sci Health Part B*. (2008) 43:96–103. doi: 10.1080/03601230701735078

73. Arruda C, Vilalta AP, Morrison R. Land altitude, slope, and coverage as risk factors for porcine reproductive and respiratory syndrome (PRRS) outbreaks in the United States. (ram K. Raghavan, Ed.). *PLoS One*. (2017) 12:e0172638. doi: 10.1371/journal.pone.0172638

74. Guo L, Ma S, Zhao D, Zhao B, Xu B, Wu J, et al. Experimental investigation of vegetative environment buffers in reducing particulate matters emitted from ventilated poultry house. *J Air Waste Manag Assoc*. (2019) 69:934–43. doi: 10.1080/10962247.2019.1598518

75. Tyndall J, Colletti J. Mitigating swine odor with strategically designed shelterbelt systems: a review. *Agrofor Syst*. (2006) 69:45–65. doi: 10.1007/s10457-006-9017-6

76. Thornton MM, Shrestha R, Wei Y, Thornton PE, Kao S, Wilson BE. *Daymet: Daily surface weather data on a 1-km grid for North America, Version 4*. (2020).

77. Core Team R. *R: A language and environment for statistical computing*. Vienna, Austria: CRAN (2021).

78. Wickham H, Averick M, Bryan J, Chang W, McGowan L, François R, et al. Welcome to the Tidyverse. *J Open Source Softw*. (2019) 4:1686. doi: 10.21105/joss.01686

79. Pebesma E. Simple features for R: standardized support for spatial vector data. *R J*. (2018) 10:439. doi: 10.32614/RJ-2018-009

80. Bivand R, Pebesma EJ, Gómez-Rubio V. *Applied spatial data analysis with. 2nd* ed. New York: Springer (2013).

81. Baddeley A, Rubak E, Turner R. *Spatial point patterns: Methodology and applications with R*. Boca Raton, London, New York: CRC Press, Taylor and Francis Group (2016).

82. Davies TM, Hazelton ML, Marshall JC. Sparr: analyzing spatial relative risk using fixed and adaptive kernel density estimation in R. *J Stat Softw*. (2011) 39:1–14. doi: 10.18637/jss.v039.i01

83. Hijmans E, Sumner C, Baston D, Bevan A, Bivand R, Busetto L, et al. Raster: *Geographic data analysis and modeling*. (2022).

84. Csárdi G, Nepusz T, Airoldi EM. *Statistical network analysis with Igraph*. New York: Springer (2016).

85. Hufkens K, Basler D, Milliman T, Melaas EK, Richardson AD. An integrated phenology modelling framework in r. (Sarah Goslee, Ed.) methods Ecol. *Evolution*. (2018) 9:1276–85. doi: 10.1111/2041-210X.12970

86. Bachl FE, Lindgren F, Borchers DL, Illian JB. Inlabru: an R package for Bayesian spatial modelling from ecological survey data. (Robert Freckleton, Ed.). *Methods Ecol Evol*. (2019) 10:760–6. doi: 10.1111/2041-210X.13168

87. Davies TM, Jones K, Hazelton ML. Symmetric adaptive smoothing regimens for estimation of the spatial relative risk function. *Comput Stat Data Anal*. (2016) 101:12–28. doi: 10.1016/j.csda.2016.02.008

88. Ruston CR. Evaluation of a staged loadout procedure for market swine to prevent transfer of pathogen contaminated particles from livestock trailers to the barn. *J Swine Health Prod*. (2021) 29:234–43.

89. Thakur KK, Revie CW, Hurnik D, Poljak Z, Sanchez J. Analysis of swine movement in four Canadian regions: network structure and implications for disease spread. *Transbound Emerg Dis*. (2016) 63:e14–26. doi: 10.1111/tbed.12225

90. Kinsley AC, Perez AM, Craft ME, Vanderwaal KL. Characterization of swine movements in the United States and implications for disease control. *Prev Vet Med*. (2019) 164:1–9. doi: 10.1016/j.prevetmed.2019.01.001

91. Passafaro TL, Fernandes AFA, Valente BD, Williams NH, Rosa GJM. Network analysis of swine movements in a multi-site pig production system in Iowa, USA. *Prev Vet Med*. (2020) 174:104856. doi: 10.1016/j.prevetmed.2019.104856

92. Paploski IAD, Corzo C, Rovira A, Murtaugh MP, Sanhueza JM, Vilalta C, et al. Temporal dynamics of co-circulating lineages of porcine reproductive and respiratory syndrome virus. *Front Microbiol*. (2019) 10:2486. doi: 10.3389/fmicb.2019.02486

93. Velasova M, Alarcon P, Williamson S, Wieland B. Risk factors for porcine reproductive and respiratory syndrome virus infection and resulting challenges for effective disease surveillance. *BMC Vet Res*. (2012) 8:184. doi: 10.1186/1746-6148-8-184

94. Black NJ, Cheng T-Y, Arruda AG. Characterizing the connection between swine production sites by personnel movements using a mobile application-based geofencing platform. *Prev Vet Med*. (2022) 208:105753. doi: 10.1016/j.prevetmed.2022.105753

95. Haredasht D, Polson R, Main K, Lee DH, Martínez-López B. Modeling the spatio-temporal dynamics of porcine reproductive & respiratory syndrome cases at farm level using geographical distance and pig trade network matrices. *BMC Vet Res*. (2017) 13:163. doi: 10.1186/s12917-017-1076-6

96. Perez AM, Davies PR, Goodell CK, Holtkamp DJ, Mondaca-Fernández E, Poljak Z, et al. Lessons learned and knowledge gaps about the epidemiology and control of porcine reproductive and respiratory syndrome virus in North America. *J Am Vet Med Assoc*. (2015) 246:1304–17. doi: 10.2460/javma.246.12.1304

97. Silva GS, Machado G, Baker KL, Holtkamp DJ, Linhares DCL. Machine-learning algorithms to identify key biosecurity practices and factors associated with breeding herds reporting PRRS outbreak. *Prev Vet Med*. (2019) 171:104749. doi: 10.1016/j.prevetmed.2019.104749

98. Dorjee S, Revie CW, Poljak Z, McNab WB, Sanchez J. Network analysis of swine shipments in Ontario, Canada, to support disease spread modelling and risk-based disease management. *Prev Vet Med*. (2013) 112:118–27. doi: 10.1016/j.prevetmed.2013.06.008

99. Silva GS, Corbellini LG, Linhares DLC, Baker KL, Holtkamp DJ. Development and validation of a scoring system to assess the relative vulnerability of swine breeding herds to the introduction of PRRS virus. *Prev Vet Med*. (2018) 160:116–22. doi: 10.1016/j.prevetmed.2018.10.004

100. Sellman S, Beck-Johnson LM, Hallman C, Miller RS, Owers Bonner KA, Portacci K, et al. Modeling nation-wide U.S. swine movement networks at the resolution of the individual premises. *Epidemics*. (2022) 41:100636. doi: 10.1016/j.epidem.2022.100636

101. Alarcón LV, Allepuz A, Mateu E. Biosecurity in pig farms: a review. *Porc Health Manag*. (2021) 7:5. doi: 10.1186/s40813-020-00181-z

Frontiers in Veterinary Science

Transforms how we investigate and improve animal health

The third most-cited veterinary science journal, bridging animal and human health with a comparative approach to medical challenges. It explores innovative biotechnology and therapy for improved health outcomes.

Discover the latest Research Topics

See more →

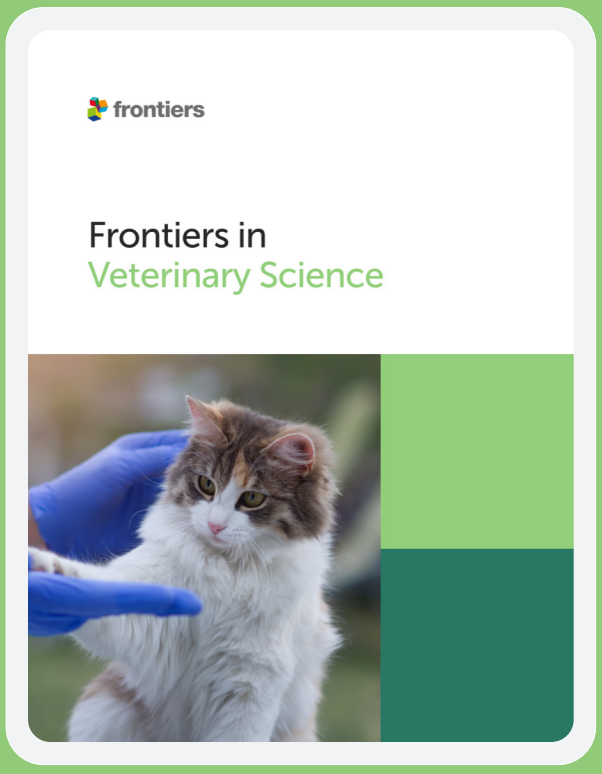

Frontiers

Avenue du Tribunal-Fédéral 34
1005 Lausanne, Switzerland
frontiersin.org

Contact us

+41 (0)21 510 17 00
frontiersin.org/about/contact